

**A COMPARISON OF THE VULCANISATION OF POLYISOPRENE BY A RANGE OF  
THIURAM DIULFIDES**

BY

**JASON VAN ROOYEN**

THESIS SUBMITTED IN FULFILMENT OF THE REQUIREMENTS

FOR THE DEGREE OF

**MAGISTER SCIENTIAE**

IN THE FACULTY OF SCIENCE AT THE  
UNIVERSITY OF PORT ELIZABETH SOUTH AFRICA

DECEMBER 2007

SUPERVISOR: Dr C. D. WOOLARD

In memory of  
Colleen Jennifer van Rooyen

## Acknowledgements

---

The author would like to thank all the people that were actively involved in the fulfilment of this project.

In particular the author would like to thank:

- God and the memories of his mother Colleen Jennifer van Rooyen
- Christian Science, and Mary Baker Eddy for her teachings and inspirational works
- Talana and Marissa Louw for their support and assistance throughout this project
- His family and friends without all of them none of this would be possible
- Mr H. J. Schalekamp for his technical assistance
- Margaret Matthews for her guidance
- The National Research Foundation, UPE research committee and Dow (Karbochem) for their financial support

## 1 Table of contents

---

	Summary	i
	List of Abbreviations	iv
<b>Chapter 1</b>	Introduction	1
<b>Chapter 2</b>	Experimental	53
<b>Chapter 3</b>	N,N'-diphenylthiuram disulfide rate study	67
<b>Chapter 4</b>	Tetramethylthiuram disulfide rate study	90
<b>Chapter 5</b>	Tetraethylthiuram disulfide rate study	104
<b>Chapter 6</b>	N,N'-dicyclopentamethylenethiuram disulfide rate study	116
<b>Chapter 7</b>	N,N'-Bis(ortho-methoxyphenyl)thiuram disulfide rate study	130
<b>Chapter 8</b>	N,N'-Bis(4-sec-butylphenyl)thiuram disulfide rate study	141
<b>Chapter 9</b>	N,N'-dimorpholinethiuram disulfide rate study	153
<b>Chapter 10</b>	Discussion	167
<b>Chapter 11</b>	Conclusions	195
<b>Appendix A</b>	N,N'-dianilinethiuram disulfide rate study	199
<b>Appendix B</b>	Tetramethylthiuram disulfide rate study	205
<b>Appendix C</b>	Tetraethylthiuram disulfide rate study	212
<b>Appendix D</b>	N,N'-dicyclopentamethylenethiuram disulfide rate study	218
<b>Appendix E</b>	N,N'-Bis( $\sigma$ -anisidine)thiuram disulfide rate study	225
<b>Appendix F</b>	N,N'-Bis(4-sec-butylaniline)thiuram disulfide rate study	232
<b>Appendix G</b>	N,N'-dimorpholinethiuram disulfide rate study	239



## Summary

---

This study was initiated in an attempt to investigate dithiocarbamic acid accelerated sulfur vulcanisation. This was, however, found impossible due to the innate instability of dithiocarbamic acids. The focus of the study was then shifted toward thiuram disulfide accelerated sulfur vulcanisation, with emphasis being placed on a rate comparison. Three groups of accelerators were investigated, namely the aromatic, linear aliphatic and cyclic aliphatic thiuram disulfide adducts. The analysis methods that were employed were conventional rubber (cis-1,4-polyisoprene) techniques coupled to model (squalene) compound investigations. The data that was collected consisted of rheometrical torque vs. time data in the rubber system while the data obtained in the model compound study consisted of sulfur and accelerator concentration data as determined by means of high performance liquid chromatography (HPLC).

The aromatic accelerators were synthesised in our labs by means of an addition reaction between the aromatic amine and  $\text{CS}_2$  in basic medium and subsequent oxidation with  $\text{K}_3\text{Fe}(\text{CN})_6$ , all in a 1:1 molar ratio. The reaction yield was low due to the instability of the dithiocarbamate intermediates and a sluggish oxidation reaction.

In the rate constant determination a first order mathematical approach was used for the rubber system as crosslinking is considered to roughly obey first order kinetics. The model compound data was also found to more accurately fit the first order rate law, with an initial slopes method also being applied to the system to determine secondary rate constants and relative rates for the system. The determination of vulcanisation rate constants in the cis-1,4-polyisoprene system was a success, while the rate data determined by means of the squalene model was more related to the rate of accelerator and sulfur consumption as opposed to the rate of crosslinking as is the case with the rubber rate data. The sulfur first order rate data mirrored the rate data derived from the rubber system more closely than the corresponding accelerator rate data, the relative rate data determined by means of initial slopes method, proved that the homolytic cleavage of thiuram disulfides and the subsequent formation of accelerator polysulfides were not limiting steps. This is seen in the similar relative rate data derived from both the

raw sulfur and accelerator data in systems that exhibit vastly different vulcanisation rates.

Squalene was deemed a suitable model for the cis-1,4-polyisoprene system, although one should consider the extent of charring and solution effects in the individual systems to account for possible incongruities that may be observed between the rubber and simulated system. The lack of agreement between the rubber and model compound rate constant data lies in the fact that the rate of crosslinking is not simplistically related to the rate at which accelerator and sulfur is consumed, this being especially true for the rate at which the accelerator is consumed. Thus the discussion over the acceleratory rates in the various accelerator systems was limited to observations made in the rubber system, with the model compound data was used exclusively to elucidate mechanistic processes.

It was discovered that the groups of accelerators examined, namely linear, cyclic and aromatic thiuram disulfide adducts, produced vastly varied rate data. The aromatic thiuram disulfide adducts had only a slight acceleratory effect on the rate of vulcanisation as compared to the unaccelerated sulfur system. The morpholine adduct had a moderately larger rate of acceleration followed by tetramethyl and tetrethylthiuram disulfide, with N,N-dicyclopentamethylenethiuram disulfide having the fastest rate of acceleration.

Part of the rate data was found to be relatable to Taft substitution constants and other physical properties. It was found that thiuram disulfide accelerators with small to negative Taft substitution constants had an increased ability to accelerate the rate of rubber vulcanisation and cause an increase in crosslink density. That is thiuram disulfides with substituents that had an increased ability to donate electron density had a greater rate acceleratory effect and crosslinking efficiency. It should be noted though, that this is a broad generalisation since the aromatic adducts did not follow the relation closely. This was ascribed to resonance effects. This tied up with similar spectroscopic data, notably  $^{13}\text{C}$  NMR data. Even though a linear relationship could not be found between the rate of cure in the rubber system and thione carbon chemical shifts, a limiting threshold value was discovered. Accelerators with deshielded thione carbon atoms caused an increased rate of vulcanisation with optimum  $^{13}\text{C}$  chemical shifts

occurring between 190-193 ppm. It was also discovered with the aid of computational chemistry, that an increase in the negative charge found on the nitrogen atom was associated with an increased rate of vulcanisation in the rubber system.

Even though the aromatics presented marching cures, scorch times (relying on the  $\tau_5$  times) were found to be loosely related to Taft substitution constants. Generally as the electron donating ability of the substituents increases, that is the Taft substitution constant becomes smaller to negative, we find an increase in vulcanisation scorch times was found. Tetraethylthiuram disulfide was, however, found not to obey this generalisation.

Thus  $^{13}\text{C}$  NMR, computer modelling and Taft substitution constant may be used as a qualitative guide to approximate thiuram disulfide reactivity. This would make the preliminary choice of accelerators easier after which experimental data should be sort to conclusively prove that particular curative systems crosslinking efficiency, taking into consideration end product requirements.

Keywords: vulcanisation, sulfur, squalene, cis-1,4-polyisoprene, first order rate constants, Taft substitution constants.

## List of abbreviations

---

AUFS	Absorbance units full scale
BR	Polybutadiene rubber
CBS	N-Cyclohexyl-2-benzothiazole sulfenamide
CPTD	N,N'-dicyclopentamethylenethiuram disulfide
CPTM	N,N'-Dicyclopentamethylenethiuram monosulfide
CPTU	Cyclopentamethylenethiourea
CTP	N-(Cyclohexylthio)phthalimide
Dma.dmtc	Dimethylammonium dimethyldithiocarbamate
DPG	Diphenyl guanidine
DSC	Differential scanning calorimetry
ENBH	2-Ethylidene norbornane
EPDM	Ethylene-Propylene-Diene Rubber
ESR	Electron spin resonance
GC	Gas chromatography
GPC	Gel permeation chromatography
Hdmtc	Dimethyldithiocarbamic acid
HPLC	High performance liquid chromatography
Hpmtc	Dicyclopentamethylenedithiocarbamic acid
ID	Internal diameter
IR	Synthetic polyisoprene rubber
MBT	2-Mercaptobenzothiazole
MBTM	2-Bisbenzothiazole-2,2'-monosulfide
MBTS	2-Bisbenzothiazole-2,2'-disulfide
MM	Molecular mass
NMR	Nuclear magnetic resonance
$\rho$	Hammett reaction constant
RP-HPLC	Reverse performance high phase liquid chromatography
SBR	Styrene-butadiene rubber
$\sigma$	Hammett substitution constant
$\sigma^*$ and $\sigma_R^*$	Taft substitution constant
TA	Thermal analysis

TBBS	2-t-Butylbenzothiazole sulfenamide
TBSI	N-t-Butyl-2-benzothiazole sulfenimide
TETD	Tetraethylthiuram disulfide
TETM	Tetraethylthiuram monosulfide
TGA	Thermogravimetric analysis
THF	Tetrahydrofuran
TLC	Thin layer chromatography
TME	2,3-Dimethyl-2-butene
TMTD	Tetramethylthiuram disulfide
TMTM	Tetramethylthiuram monosulfide
TMTP	Tetramethylthiuram polysulfides
TMTU	Tetramethylthiourea
UV/Vis	Ultra-violet/visible
ZBPD	Zn-O,O-dibutylphosphorodithioate
ZDMC	Bis(dimethyldithiocarbamate)zinc(II)

# 1 Introduction

---

1.1 Brief overview of vulcanisation .....	2
1.2 Vulcanisation by thiuram disulfides.....	7
1.3 Vulcanisation by dithiocarbamic acids .....	10
1.4 Preparation and the instability of dithiocarbamates.....	13
1.4.1 Preparation of dithiocarbamates.....	13
1.4.2 Reasons for low compound stability of dithiocarbamates .....	14
1.4.3 Attempts at synthesising stable dithiocarbamic acids and methods to reduce the extent of decomposition .....	15
1.5 The preparation of thiuram disulfides.....	18
1.6 Model compounds.....	19
1.6.1. Techniques available for rubber and mechanistic analyses .....	19
1.6.2. Model compounds for mechanistic studies.....	21
1.6.3. Choosing a model compound.....	23
1.7 Studies of the rate of vulcanisation.....	24
1.7.1. Background to rate analyses .....	24
1.7.3. Methods for determining cure rates .....	33
1.8 Hammett Plots.....	36
1.8.1 Introduction.....	36
1.8.2 Hammett Equations and Linear Free Energy Relationships .....	37
1.8.3 Application .....	39
1.8.4 Overcoming non-rigidity in molecules.....	40
1.8.5 Application to vulcanisation .....	42
1.9 Computational chemistry .....	43
1.10 Objectives of this study.....	46
1.11 References.....	47

## 1.1 Brief overview of vulcanisation

Vulcanisation is a process that converts an uncrosslinked material or rubber into a crosslinked more durable material called an elastomer. The process introduces covalent crosslinks between the polymer chains resulting in increased elasticity, decreased plasticity, and the elimination of thermoplasticity and solubility.<sup>1</sup>

Unvulcanised rubbers have poor physical and chemical properties. Their polymeric networks are randomly arranged and held together by their entangled convoluted state and by weak electrostatic London and van der Waals forces.

When a stress in the form of a load is applied to an uncrosslinked material, it undergoes plastic deformation. Here chain segments may align, giving rise to stress crystallisation, while other regions undergo chain slippage. When the stress is removed, the rubber undergoes only a finite amount of elastic recovery; thus the material has been permanently deformed.

An example of such a deformation would be creep. This is typically observed in natural rubber which appears to behave similar to a viscous liquid over time, moving down the potential energy gradient imparted to it by gravity.<sup>1</sup>

With the discovery of vulcanisation in 1839 by Charles Goodyear,<sup>1</sup> vulcanised rubber became as important an engineering material as wood, glass and steel. Initially only sulfur was used as a crosslinking agent. It should be noted that Goodyear's recipe that was used commercially in the earlier years did not make use of sulphur as the only crosslinking agent. Large quantities of litharge, PbO, were also used. Later amines were introduced as accelerators such as aniline and guanidines. Today a variety of methods are available, chemical as well as physical, to introduce crosslinks into a material. These comprise the use of sulfur, peroxides, special vulcanising agents as well as high-energy irradiation.<sup>2</sup>

Accelerated sulfur vulcanisation is the most widely employed method. It is, however, limited to rubbers having unsaturated carbon backbones, such as diene rubbers or rubbers that have unsaturation in their side groups such as ethylene propylene co-diene monomer rubbers (EPDM).<sup>2</sup> The unsaturation is derived in part or totally from diene monomers as seen in synthetic elastomers like cis-1,4-polyisoprene (IR), polybutadiene (BR), and styrene butadiene rubber (SBR) to name but a few.

The chief competitor to accelerated sulfur vulcanisation in these diene systems is peroxide induced crosslinking. Peroxide cured systems display limited reversion and improved thermal stability. Sulfur vulcanisation, however, has been maintained as it is economically feasible, and more importantly these systems display better mechanical properties.

As the name implies, accelerated sulfur vulcanisation involves the addition of organic compounds called accelerators to vulcanisation systems. These accelerators make the process more efficient by increasing the rate of vulcanisation. Initially it was found that amines such as piperidine and aniline were potent accelerators.<sup>1</sup>

A wide variety of accelerators have since been discovered. The most important groups of accelerators employed today are the benzothiazoles, sulfenamides, guanidines, thiuram disulfides and the dithiocarbamates (see figure 1.1).

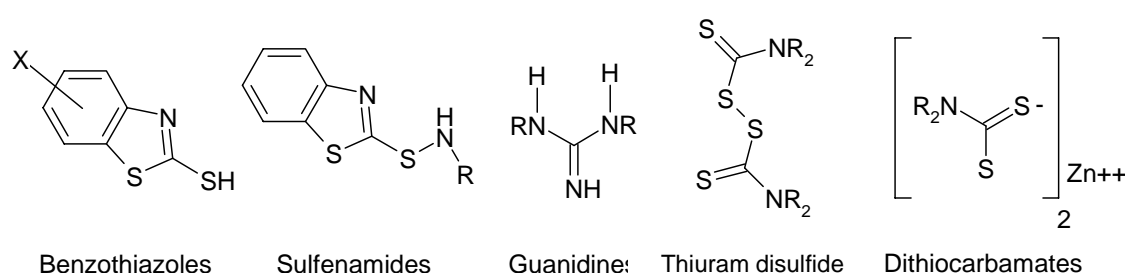


**Figure 1.1: Structures of the most common vulcanisation accelerators**

The thiuram disulfide vulcanisation accelerators based on the thiazoles, thiuram and morpholine groups are extremely convenient accelerators. They introduce specific favourable properties to the vulcanisate as do the other accelerators, but owing to the fast rate at which they accelerate vulcanisation, they may be used in smaller amounts. They are also very diverse as they can be used to produce rubber vulcanisates that contain little elemental sulfur, and thus their vulcanisates exhibit the important property of thermal stability as displayed by peroxide cured systems.<sup>3</sup>

In their pure form though, disulfide crosslink effectiveness is lower than that of peroxide cured systems owing to the increased resonance stabilization found in their sulfur intermediates,<sup>4</sup> typically polysulfidic species.<sup>3</sup>



Table 1.1: Classes of vulcanisation accelerators

Class	Speed	Acronyms*
Amines	Slow	
Guanidines	Medium	DPG
Benzothiazoles	Semi-fast	MBT, MBTS
Sulfenamides and sulfenimides	Fast, delayed action	CBS, TBBS, TBSI
Dithiophosphates and xanthates	Fast	ZDBP
Thiurams	Very fast	TMTD, TETD, CPTD
Dithiocarbamates	Very fast	ZDMC

\* for full names, please consult the table of abbreviations

The vulcanisation process may be divided into three distinct phases, which are evident when viewing a typical oscillating disk rheometer trace as shown in Figure 1.2.

The three stages as seen in Figure 1.2 are: the induction or scorch period, curing or crosslinking period and the maturation or overcure period. First the interpretation of the rheometer trace may be made easier if one understands how an oscillating disk rheometer works.

An oscillating disk rheometer works by measuring the amount of torque required to move a disk, which is enveloped in rubber, through a small angle while the rubber is maintained at a prescribed temperature.

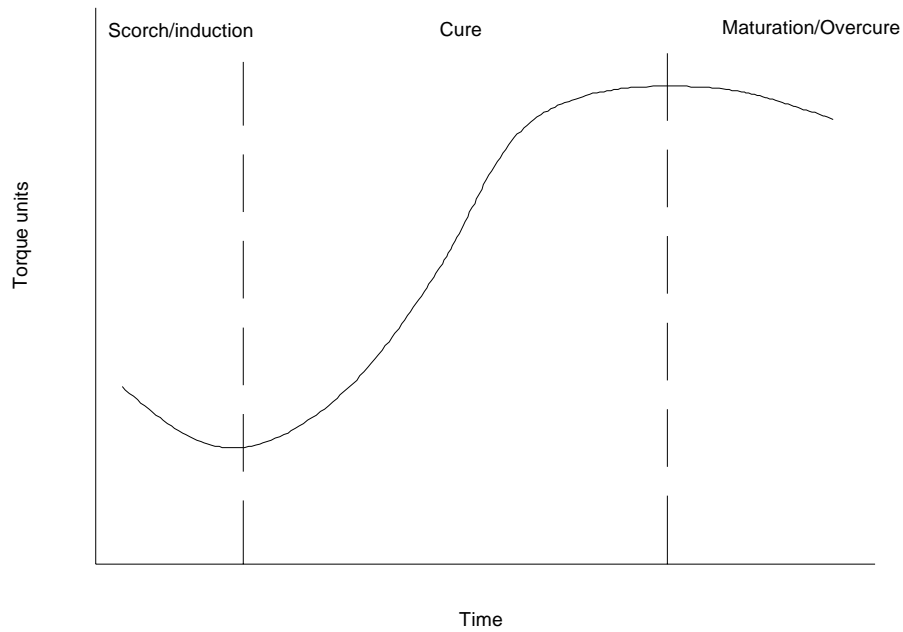


Figure 1.2: A generalised rheometer trace depicting the three stages of vulcanisation

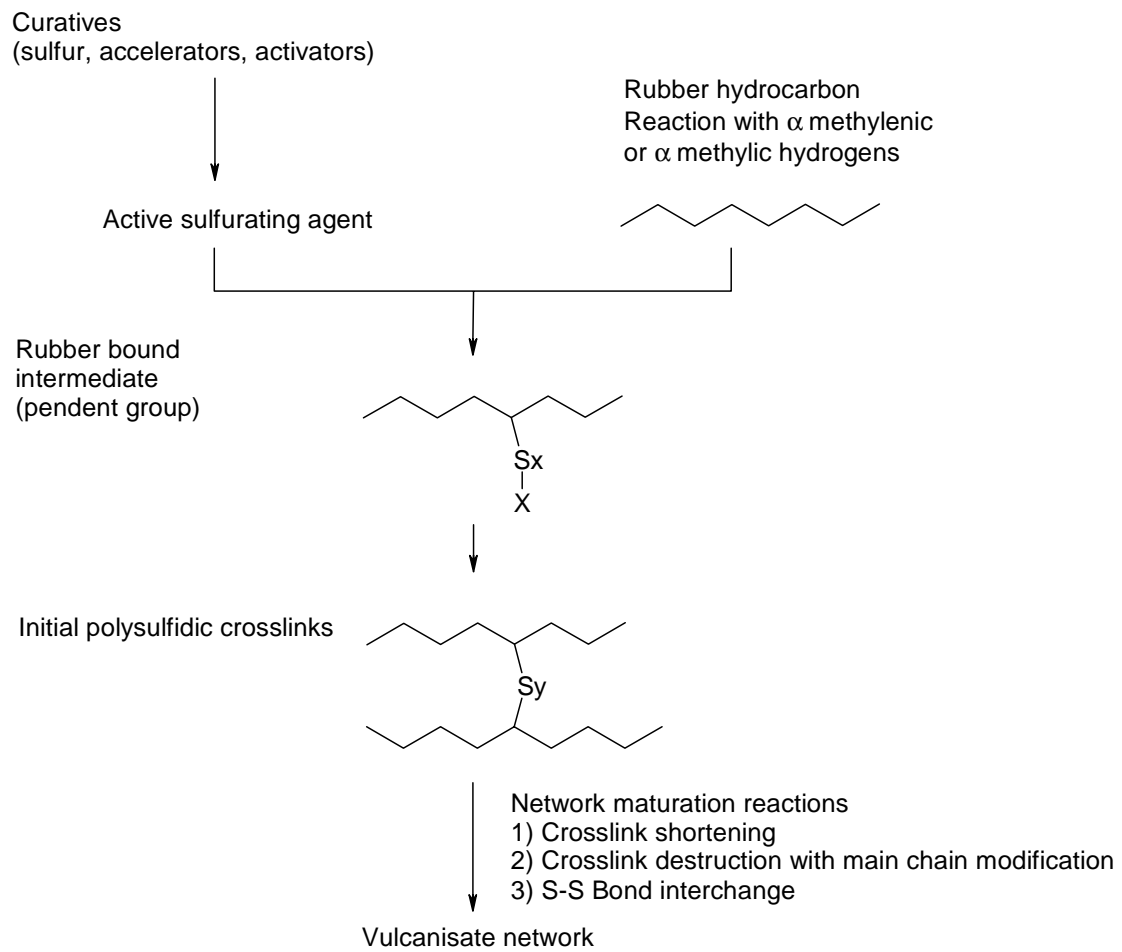


Figure 1.3: Simplified reaction scheme for accelerated sulfur vulcanisation<sup>5,6</sup>

A schematic representation of the mechanism of vulcanisation is shown in Figure 1.3. The vulcanisation process will be described physically and chemically with Figures 1.2 and 1.3 in mind, following the schemes from left to right and top to bottom respectively. First is the scorch or the induction period where the formation of the active sulfurating agent occurs. This is often a polysulfidic accelerator species. This may also be formed during the mixing process where energy is imparted to the system. A reduction in torque results from a lubrication effect as the sample reaches cure temperature. The active sulfurating agent then reacts with the  $\alpha$ -methyl or the  $\alpha$ -methylene hydrogens on the rubber hydrocarbon to form pendent groups (rubber bound polysulfidic species).

In some vulcanisation systems thiol pendent groups are formed together with polysulfidic accelerator pendent groups, an example of such a system would be the tetramethylthiuram disulfide (TMTD) system.<sup>7</sup> This is the most important period when moulding a crosslinkable material.

Next is the cure region where the torque increases as result of the oscillating disk experiencing more resistance to its movement. As the material becomes more rigid during crosslinking, polymer chains can no longer slip over each other. Pendent groups react with adjacent pendent groups to produce crosslinks. At this point the material can no longer be moulded as this would require the rupture of covalent bonds.

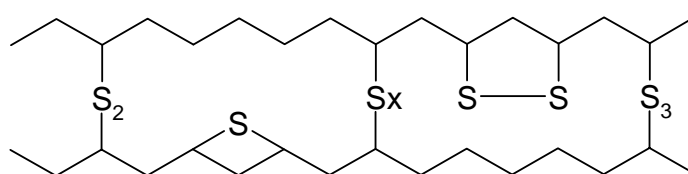


Figure 1.4: A diagrammatic representation of a typical sulfur vulcanisate network<sup>5</sup>

Finally network maturation occurs. Figure 1.4 depicts a typical vulcanisate network. The polysulfidic crosslinks that are formed are thermally unstable and undergo a number of side reactions ranging from crosslink shortening, main chain modification and sulfur bond interchange.<sup>8</sup> The torque may begin to reduce as a result of reversion where the number of sulfur atoms in each crosslink is reduced. There may be a reduction in the number of crosslinks and thus a reduction in the rigidity of the

material. This also results in the production of cyclic sulfides. After a certain time period there is inevitably a reduction in torque as a result of the destruction of the vulcanisation network by the oscillating disk as the process is not unobtrusive and results in the shearing of the polymer chains and bonds.

## 1.2 Vulcanisation by thiuram disulfides

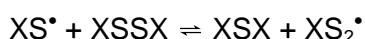
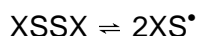
Complexity is an unavoidable problem which must be addressed when one develops a plausible reaction mechanism for a process that consist of interconnected steps and reactions that depend on the flux of compounds and the production of intermediates that supply subsequent reactions. There are a number of thiuram disulfides that have been used commercially as vulcanisation accelerators, of these tetramethylthiuram disulfide (TMTD) has been the most studied.

There are essentially three routes that may be employed to produce crosslinks via tetramethylthiuram disulfide (TMTD) accelerated vulcanisation in the absence of ZnO. The first step involves the disproportionation of two pendent groups on neighbouring rubber chains to form a crosslink and tetramethylthiuram monosulfide (TMTM), tetramethylthiuram polysulfide (TMTP) or tetramethylthiuram disulfide. The second route is via the reaction of a thiuram pendent group with a polythiol pendent group on a neighbouring chain to produce a crosslink and dithiocarbamic acid while the third is considered the reaction of a dimethylammonium polysulfide pendent group with a thiuram polysulfide pendent group on a neighbouring chain to produce a crosslink and an tetramethylthiourea.<sup>9,10,11</sup>

It is generally accepted that TMTD accelerated sulfur vulcanisation in the absence of ZnO is a free radical process. The first reaction is believed to be the homolysis of the S-S bond in TMTD to produce a thiuram persulfenyl radical ( $XS_x^*$ ) or thiuram sulfenyl radicals ( $XS^*$ ).<sup>9,12,13</sup>

These radicals could interact with one another to form accelerator polysulfides, ultimately forming polysulfidic crosslinks and TMTD or TMTPs.<sup>9</sup> It has been shown that when TMTD is heated above its melting point (145°C) there are a large number of higher order sulfur species, TMTPs formed. Researchers have suggested that this process is also radical in nature.<sup>14</sup>

Coleman *et al.*<sup>15</sup> suggested that TMTPs were formed via the symmetrical and unsymmetrical radical dissociation of TMTD followed by recombination. Geysler and McGill<sup>16</sup> pointed out that the radical scission of tri- and tetrasulfides would lead to polysulfides of higher sulfur rank but could not explain the presence of high concentrations of TMTM. TMTM formation would require the scission of the more stable C-S bond. They suggested that TMTM was formed by the interaction of a thiuram sulfenyl radical with undissociated TMTD.

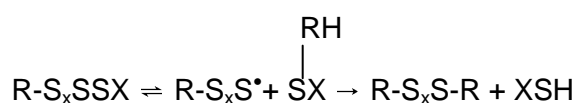


Crosslinking thus also explains the small amount of residual TMTD seen in all TMTD vulcanisates.



where  $X = (CH_3)_2NC=S$

Another route for crosslinking involves the abstraction of an allylic hydrogen atom from the polyisoprene chain by a sulfenyl radical. This is then followed by the combination of the remaining thiuram persulfenyl and polyisoprene radicals to generate a crosslink and a dithiocarbamic acid. This can be viewed as a concerted reaction without the formation of a true alkenyl radical intermediates.<sup>9</sup>

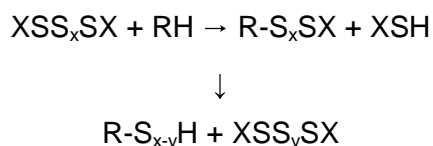


where RH = rubber chain

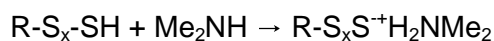
XSH = dithiocarbamic acid (dimethyldithiocarbamic acid, Hdmtc, in the case of TMTD)

Thus TMTPs are the active sulfurating agents in TMTD based cures, producing thiuram terminated polysulfidic pendent groups. Coleman *et al.*<sup>15</sup> postulated a free radical mechanism for pendent group formation on observing singlets assigned to various free radicals by means of electron spin resonance (ESR). This, however, did

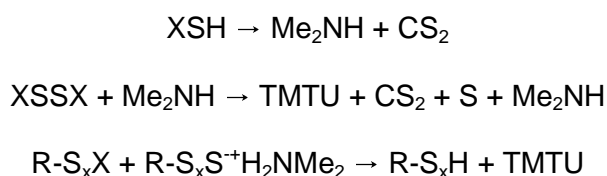
not present conclusive proof as the radicals were detected as copper derivatives. The derivatisation process may possibly alter the nature of the reactions involved. Geysler and McGill<sup>16</sup> disagree with the free radical mechanism postulating a concerted reaction mechanism where S-S bonds are broken producing C-S bonds by means of hydrogen abstraction to produce dimethyldithiocarbamic acid (Hdmtc). In the absence of ZnO these thiuram terminated polysulfidic pendent groups then undergo exchange reactions with Hdmtc to form thiol pendent groups and TMTD.



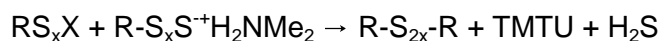
As the TMTD concentration decreases, the thiuram sulfenyl and persulfenyl radicals increasingly decompose to form dimethylamino radicals ( $\text{Me}_2\text{N}^\bullet$ ), recombination of radicals being less favourable. The highly electronegative nitrogen atom on the  $\text{Me}_2\text{N}^\bullet$  radical may abstract hydrogen from the rubber alkene to form  $\text{Me}_2\text{NH}$  that reacts with the thiol pendent groups to form amine terminated pendent groups (dimethylammonium pendent groups).<sup>6</sup>



Thiol pendent groups are relatively unreactive compared to dimethylammonium pendent groups. Where tetramethylthiourea (TMTU) is formed during the crosslinking process, TMTU formation has been attributed to the attack of  $\text{Me}_2\text{NH}$ , originally formed from the decomposition of Hdmtc from TMTD.<sup>17,18,19</sup>



$\text{Me}_2\text{NH}$  adds preferentially to thiol pendent groups as noted by the absence of TMTU prior to crosslinking. It is proposed that crosslinks are formed via rapid reaction between dimethylammonium pendent groups and newly formed thiuram pendent groups, before the later can exchange with Hdmtc. TMTD will be liberated in such a reaction.<sup>7</sup>



### 1.3 Vulcanisation by dithiocarbamic acids

Much is known about thiuram disulfide, zinc dimethyldithiocarbamate (ZDMC), 2-mercaptobenzothiazole (MBT) and 2-bisbenzothiazole-2,2'-disulfide (MBTS) vulcanisation and their dependence on various additives such as ZnO. This study was initiated in an attempt to investigate the role dithiocarbamic acids play in vulcanisation. It has been shown by Shumane<sup>20</sup> that the removal of dimethyldithiocarbamic acid (Hdmtc) impedes the crosslinking process in the polyisoprene/TMTD/sulphur system. It is known that polysulfidic terminated thiuram pendant groups are formed in part by the interaction of polysulfidic TMTD accelerator species with the polymer chain, but they are predominantly formed by an exchange reaction that occurs between Hdmtc and polysulfidic thiol pendant groups.<sup>21</sup> They may also be formed by polysulfidic Hdmtc interacting with the polymer chain.<sup>22</sup>

Polysulfidic thiol pendant groups are speculated to be formed by the interaction of polysulfidic Hdmtc with the polymer chain. Crosslinking in the absence of ZnO is likely a result of the reaction between polysulfidic thiuram pendant groups and polysulfidic thiols. Crosslinking is delayed until the majority of the thiuram groups are bonded to the polymer chain. At this point the Hdmtc concentration is low reducing the frequency of the exchange reaction between Hdmtc and the polysulfidic thiols, allowing the crosslinking reaction to dominate.<sup>16</sup> Hdmtc as an accelerator in sulphur vulcanisation acts as a catalyst for the reaction as it is regenerated during the crosslinking process. The mechanism of its action as an accelerator is still rather illusive.<sup>21</sup>

Hdmtc is of paramount importance to the crosslinking reaction. It has been shown that IR/TMTD/S<sub>8</sub> systems release a volatile component that can be used to accelerate vulcanization in IR/S<sub>8</sub> samples. This was achieved by separating 2 samples of unvulcanised IR/TMTD/S<sub>8</sub> and IR/S<sub>8</sub> by a metal ring (the IR/S<sub>8</sub> being on top). When heated in a vulcanisation press, the IR/S<sub>8</sub> was found to have been vulcanised to a greater extent than when the IR/TMTD/S<sub>8</sub> sample was replaced by IR/S<sub>8</sub>. This indicated that a volatile species was formed in the IR/TMTD/S<sub>8</sub> which then migrated across the space between the rubber samples to accelerate vulcanisation in

the upper sample. When IR/S<sub>8</sub> was replaced by IR/TMTD/S<sub>8</sub> no volatile component was formed and no acceleration in the upper sample could be observed.<sup>21</sup>

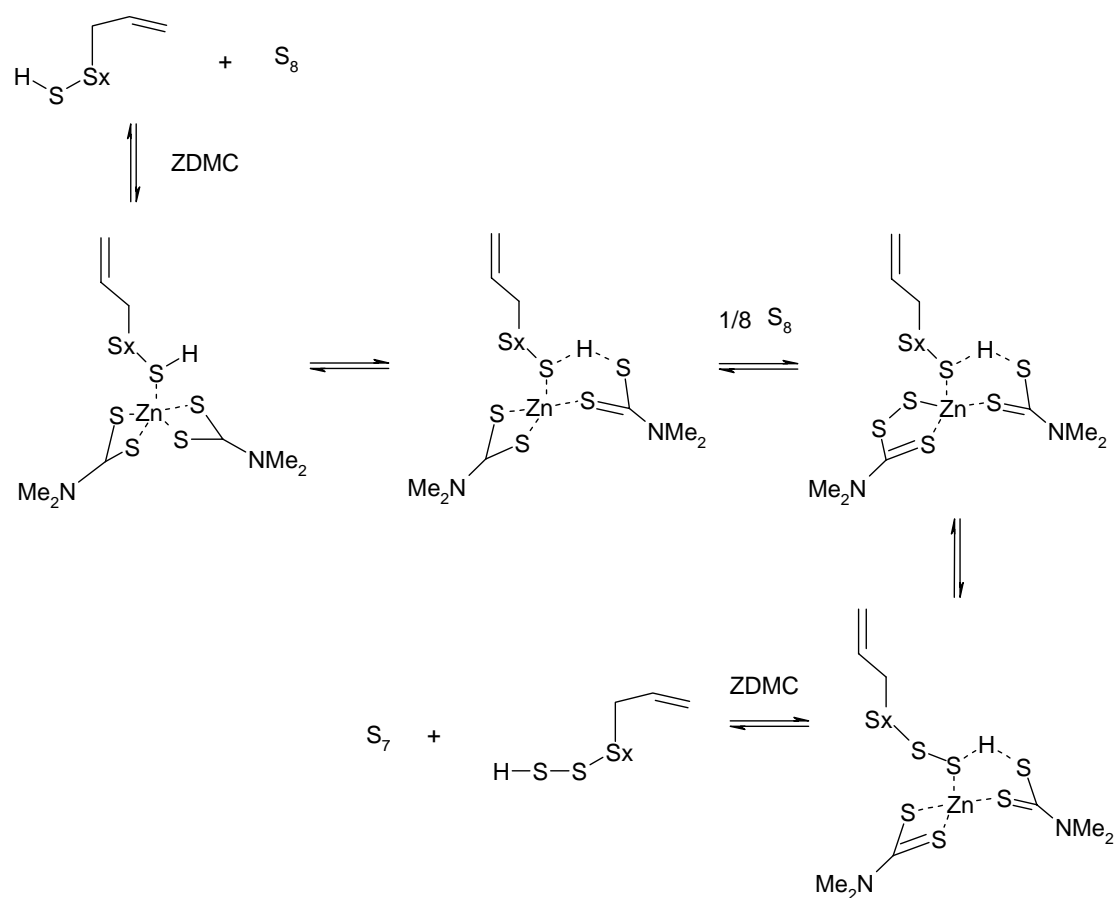


**Figure 1.5: Mechanism for the formation of thiol polysulfides in ZDMC/S<sub>8</sub> cured systems<sup>23</sup>**

Furthermore it is known that the crosslink density of the IR/TMTD/S<sub>8</sub> vulcanisate is not as great as the corresponding IR/TMTD/S<sub>8</sub>/ZnO system. The reason for the latter having an increased crosslink density is possibly that  $\text{Zn}^{2+}$  traps the volatile unstable Hdmtc in the form of zinc dimethyldithiocarbamate (ZDMC), which is no-longer volatile. It is then more stable and available for further crosslinking reactions. The mechanism of ZDMC vulcanisation<sup>20,21,23</sup> as seen in Figure 1.5 will be briefly considered as it is quite different from that of thiuram vulcanisation.

The first step consists of sulfurating the rubber backbone by ZDMC incorporating sulphur into the zinc dithiocarbamate ring as shown by Figure 1.5. This brings about the insertion of sulphur into the allylic H bond. Secondly the resulting polysulfidic species, crosslink intermediates, react via a metathesis reaction to produce crosslinks (see Figure 1.6).



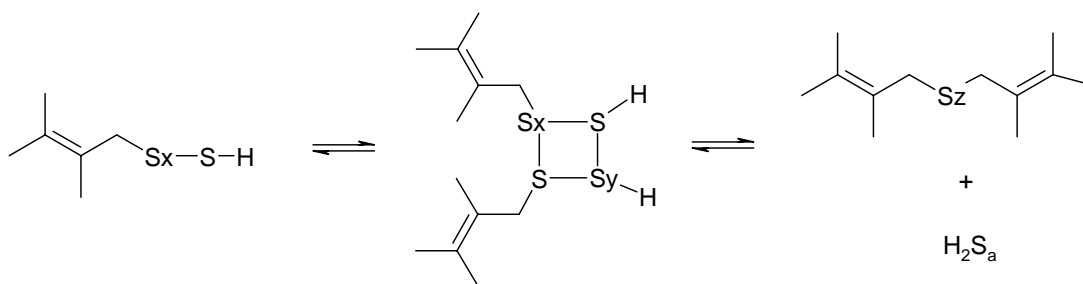


Figure 1.6: Metathesis reaction for the formation of crosslinks in the ZDMC/S<sub>8</sub> system<sup>23</sup>

The metathesis reactions are in equilibrium and never go to completion. The final step is the removal of unreacted polysulfides by reaction with ZDMC to produce H<sub>2</sub>S<sub>n</sub> and consequently desulfurating the polysulfides.<sup>23</sup>

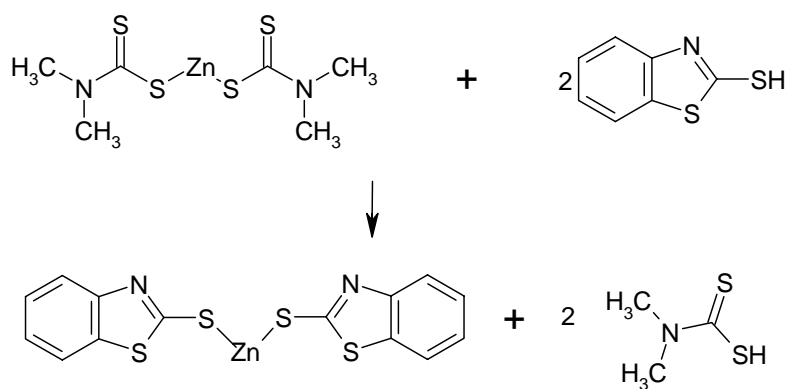


Figure 1.7: Reaction scheme for the production of Hdmtc<sup>20</sup>

The mechanism of Hdmtc vulcanisation, on the other hand, is poorly understood, primarily as a result of the problem associated with the production of pure dithiocarbamic acids. It is thus not possible to use Hdmtc as an accelerator on its own to try to elucidate the dithiocarbamic acid vulcanisation mechanism. It is possible, as seen in Figure 1.7, to produce small quantities of Hdmtc from an exchange reaction between MBT and zinc dimethyldithiocarbamate in a 2:1 ratio, heated at 150°C for 15 min in a glass vessel connected to a cold trap.<sup>20</sup>

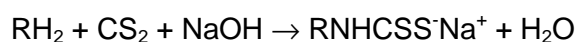
Hdmtc purification and synthesis always results in the formation of residual quantities of dimethylammonium dimethyldithiocarbamate (dma-dmtc).<sup>20</sup> It has been well established that in most cases one of the decomposition products is the parent amine.<sup>20</sup>

The above procedure fails to introduce pure dithiocarbamic acid into a vulcanisate as both may introduce agents which are capable of accelerating sulphur vulcanisation, i.e. dma-dmtc and MBT. These agents would introduce reaction pathways that are not ascribed to the action of Hdmtc. Due to these difficulties, experimental investigations thus far have involved monitoring the crosslink density of isolated IR/S<sub>8</sub> rubber pads placed in close proximity (above) to a IR/TMTD/S<sub>8</sub> vulcanising pad as explained above. The volatile Hdmtc evolved from the latter is absorbed into the IR/S<sub>8</sub> pad and accelerates the rate of crosslinking.<sup>20</sup> Wet mixtures of Hdmtc have also been investigated because of the instability of the pure dry Hdmtc. It has already been established that dma-dmtc is formed in solution thus complicating the investigation of dithiocarbamic acid vulcanisation. Both these systems of analysis have proved Hdmtc to be an active crosslinking agent, but the mechanism remains undetermined.<sup>20</sup>

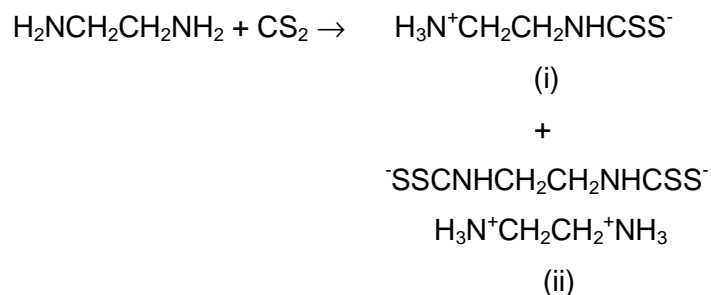
## 1.4 Preparation and the instability of dithiocarbamates

### 1.4.1 Preparation of dithiocarbamates

Nitrogen substituted dithiocarbamates may be formed (RNHCSSH or R<sub>2</sub>NCSSH) by the reaction of CS<sub>2</sub> with either a primary or secondary amine, usually in an alcoholic<sup>24</sup> or aqueous medium.<sup>25</sup> To conserve the more valuable amine the reaction is generally performed in basic medium.



When diamines are reacted with a chemically equivalent amount of CS<sub>2</sub>, two products are formed: the expected inner salt and a considerable amount of the bisdithiocarbamate. For example if aqueous ethylenediamine is reacted with CS<sub>2</sub>, the inner salt (i) is obtained with up to 30% of the bisdithiocarbamate (ii).<sup>26</sup>



Dithiocarbamates may also be prepared by the conversion of carbamates into dithiocarbamates. Holland<sup>27</sup> observed that CS<sub>2</sub> reacted with carbamylmethylammonium carbamylmethylcarbamate at room temperature in aqueous alcohol, to yield the corresponding dithiocarbamate.

In this study we were initially interested in making the dithiocarbamic acid but the lability of the salt and the acid prevented the isolation and purification of these compounds.

#### 1.4.2 Reasons for low compound stability of dithiocarbamates

Compound stability is governed by a large number of effects such as resonance, inductive effects, hyperconjugation etc. Even though three different canonical forms are associated with the dithiocarbamate metal salts (M<sub>2</sub>S<sub>2</sub>CNR<sub>2</sub>) (see Figure 1.8), they are relatively unstable.

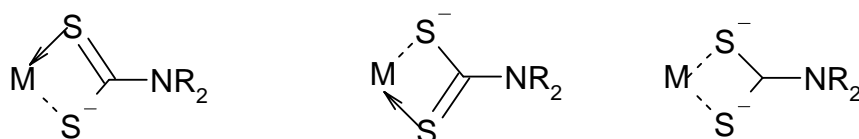
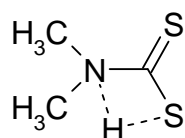


Figure 1.8: Different resonance forms found in metal dithiocarbamates<sup>28</sup>

The dithiocarbamic acids are even more labile as result of intramolecular hydrogen bonding between the nitrogen and the hydrogen on the sulfur atom.



The fractional charges that result from the intramolecular hydrogen bond introduce a high internal energy in the dithiocarbamic acid molecules that is responsible for their great instability.<sup>29</sup>

### 1.4.3 Attempts at synthesising stable dithiocarbamic acids and methods to reduce the extent of decomposition

The parent compound dithiocarbamic acid (ammonium dithiocarbamate, see Figure below) may be obtained as colourless needles from its ammonium salt by treatment with cold acid. It is unstable and readily decomposes to thiocyanic acid and  $\text{H}_2\text{S}$ .<sup>30</sup> Thermal decomposition starts at  $20^\circ\text{C}$ . It has been reported that dithiocarbamic acids may be formed from their corresponding salts by the addition of strong mineral acids at low temperature ( $\pm 5^\circ\text{C}$ ). For example ethylenebisdithiocarbamic acid has been obtained in this way from its sodium salt.<sup>31</sup>

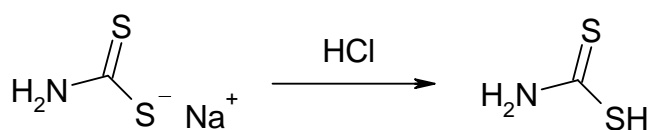
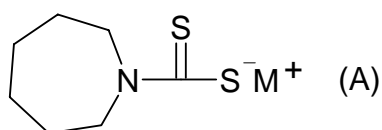


Figure 1.9: The formation of ammonium dithiocarbamic acid from its salt

Diphenyldithiocarbamic acid ( $147^\circ\text{C}$  mp), unlike other dithiocarbamic acids is reported as being sufficiently stable to be recrystallised from benzene.<sup>32</sup> In this laboratory the compound was produced by the first synthetic method listed in the previous section. The presence of the dithiocarbamate was validated by the addition of  $\text{CuSO}_4 \cdot 5\text{H}_2\text{O}$ <sup>33</sup> which forms a red precipitate from the interaction of Cu (II) with dithiocarbamate. Attempts to recrystallise the salt in hexane yielded the parent amine. Efforts to acidify the impure salt at various pH's to produce the acid and the subsequent recrystallisation of the solid from benzene also yielded the parent amine (diphenylamine mp  $52^\circ\text{C}$ ) as determined by HPLC and NMR analysis.

Various methods have been employed to increase the stability and subsequently the life span of dithiocarbamates. Williams<sup>34</sup> discovered that various salts and esters of hexamethylenedithiocarbamate (A) were stable for extended periods and at elevated temperatures.



Heavy metal salts of the dithiocarbamates have proved to be more stable and/or provide less phytotoxic decomposition products.<sup>34</sup> In the production of water insoluble heavy metal dithiocarbamates, chemically equivalent quantities of water-soluble dithiocarbamate salt and water-soluble heavy metal salt are usually added. It has, however, been discovered that if slightly less water-soluble heavy metal salt is added such that an oxidation potential does not persist at the end of the reaction, the compound's stability is increased. Johnson<sup>35</sup> circumvented an oxidation potential in the final product by the addition of an inorganic sulfite, thus showing an increase in the stability of the dithiocarbamate.

Manganous dimethyldithiocarbamate<sup>36</sup> may be stabilized by the addition of zinc dimethyldithiocarbamate. It has been discovered generally though that the zinc dithiocarbamate salts have greater stability.

The pH of the reaction mixture is also critical to the production of dithiocarbamates. For example, Lunginbuhl<sup>37,38</sup> showed that in the preparation of zinc ethylenedithiocarbamate, the pH should be maintained between 2.5 and 5 during the addition of  $ZnCl_2$  to an aqueous solution of the disodium ethylenedithiocarbamate. Neal and Sturgis<sup>39</sup> in the preparation of Zn, Cd, Hg, Pb and Fe salts of dialkyldithiocarbamates employed higher pH's making use of a sodium acetate buffer system.

The pH of the initial reaction has also been monitored as a means of stabilising the dithiocarbamate. Gobel<sup>40</sup> suggested the pH of the ethylenediamine,  $CS_2$  and NaOH reaction mixture should be maintained at a pH of 9.3 by the gradual addition of alkali.

Two methods for the stabilization of dithiocarbamates, for which no chemically plausible reason can be seen, are the use of salts such as  $CaHPO_4$ ,  $Ca(NO_3)_2$  and  $Ba(NO_3)_2$  by Drexel<sup>41</sup> for the stabilization of aqueous solutions of N-alkyldithiocarbamates, Beauchamp<sup>42</sup> who added 1-2% by weight of thiourea to suspensions of manganous dimethyldithiocarbamate to inhibit decomposition.

Many authors have reportedly formed the free acid, although doubt exists because of the age of the articles and the method of analysis. The need to purify the compounds and to remove solvent so that uncontaminated spectral studies may be performed has always resulted in an increased amount of decomposition. For example in this study it was noted how recrystallisation from solvents caused an increase in the rate

of decomposition especially in solvents that had high boiling points. Recrystallisation and extraction from solvents that weren't degassed led to increased decomposition. Compounds exposed to air and moisture also decomposed. A large amount of decomposition was observed on acidification even though various attempts and methods were employed. Various pH's, buffers and extraction experiments were performed but RP-HPLC analysis always yielded multiple components, either as a result of decomposition and/or poor selectivity in the extraction experiments.

Most dithiocarbamic acids have never been isolated, but rather their existence has been inferred by the analysis of solutions of their compounds. As has been mentioned they are extremely unstable even in solution although their life spans may be increased by subtle manipulation of the system. Methods of stabilization include pH adjustments, use of buffers, altering the ionic strength of the media and using mixtures of solvents to achieve stabilization by altering the degree of solvation of the molecule. The compound's presence in solution may be verified by various methods for example dithiocarbamic acids have characteristic absorption bands at 1542-1480  $\text{cm}^{-1}$  (partial double bond character between N-C), 550-700  $\text{cm}^{-1}$  (a C-S stretch) and a weak band at 2560-2590  $\text{cm}^{-1}$  (S-H stretch).<sup>43,44</sup>

Methods of purification and isolation have generally only gone as far as solvent extraction and solutions containing these solutes. For example, Oktavec *et al.*<sup>45</sup> used chloroform extraction to extract dithiocarbamic acids from aqueous solutions and then analysed the extracts spectrophotometrically in the range 200-310 nm. They proceeded to analyse the efficiency of dithiocarbamic acid extraction into chloroform at various pH's and the time dependence of dithiocarbamic acid decomposition in chloroform.

Jansen and Mathes<sup>46</sup> reported the possible synthesis of dithiocarbamic acid as one of the intermediary products in the production of thiazinethiols (see Figure 1.10). Here the dithiocarbamic acid was formed by reacting diacetoneamine (4-amino-4-methyl-pentanone) with  $\text{CS}_2$ . The intermediate was, however, mostly in the cyclical form as seen in Figure 1.10, thus preventing the successful isolation and purification of the dithiocarbamic acid.

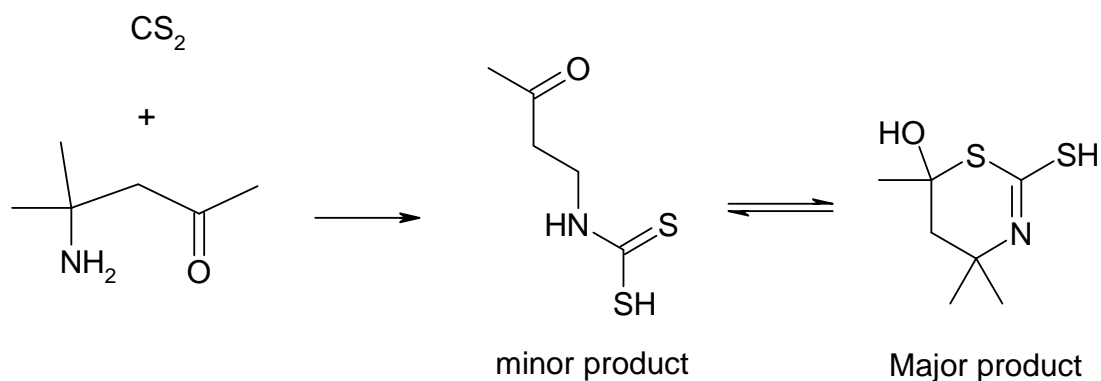
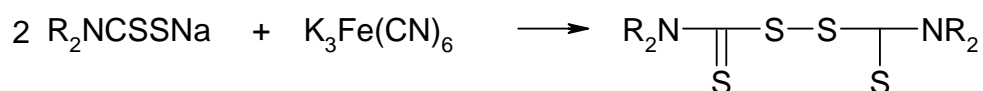


Figure 1.10: Synthesis of intermediary products for thiazinethiol formation.

### 1.5 The preparation of thiuram disulfides

As the production of pure dithiocarbamates proved to be difficult and the production of pure dithiocarbamic acids proved impossible, it was decided to rather look at the linear free energy relationship between a series of thiuram disulfide accelerators.

Thiuram disulfides may be produced by the oxidation of alkyl and dialkyldithiocarbamates, usually in the form of water soluble salts, by a variety of mild oxidizing agents, such as iodine, hydrogen peroxide, ammonium persulfate and potassium ferricyanide.<sup>47</sup>



Both  $\text{I}_2$  and potassium ferricyanide were experimented with, and it was decided to use the latter.  $\text{I}_2$  solutions have to be made by the addition of the iodide salt to produce  $\text{I}_3^-$ , consequently limiting the maximum concentration attainable. The iodide solutions were also unstable and the purity of the iodine was questionable. These problems were not experienced with potassium ferricyanide, although fresh solutions had to be prepared for each synthesis.

## 1.6 Model compounds

### 1.6.1. Techniques available for rubber and mechanistic analyses

The crosslinked structure of elastomers renders them insoluble to conventional analytical solvents which makes the analysis of the rubber compound both quantitatively and qualitatively extremely difficult. Swelling and extraction experiments may be performed whereby crosslink density and the concentrations of various species may be determined respectively. The extraction technique is limited though since the intermediates are in lower concentrations, generally rubber bound and at times labile thus converting to other products as time progresses. These problems have led to a wide variety of other methods being introduced to investigate the reactions that occur during the vulcanisation process.

The use of chemical probes is the oldest technique<sup>8</sup> dating back to the 1950s and has been comprehensively reviewed by Saville and Watson<sup>8</sup> and successfully applied in a study by Cunneen and Russel.<sup>48</sup> Here all polysulfide crosslinks may be broken by propane-2-thiol, disulfide crosslinks with hexane-1-thiol and all carbon sulfur crosslinks with methyl iodide. This allows one with the aid of crosslink density swelling experiments to determine the contribution that the different crosslinks; mono-, di- and polysulfide, make to the overall crosslink density. However, this method does not determine the number of crosslinks that are present since in general, the chemical probes do not react stoichiometrically.

Spectroscopic methods may be employed for example to elucidate the vulcanisation mechanism. Non-conventional nuclear magnetic resonance (NMR), electron spin resonance (ESR) may be used to determine whether a polar (ionic) or radical reaction mechanism may apply. Coleman *et al.*<sup>15</sup> observed thiuram, thiocarbonyl and persulfenyl radicals when examining TMTD accelerated vulcanisation and concluded that a radical mechanism played an important role in that accelerator's mode of action or at least initiation.<sup>8</sup>

Ultra-violet/visible (UV/Vis) spectroscopy may be used to determine crosslink distribution in thiuram vulcanised rubber systems. This method is, however, not specific as many compounds show absorption bands in the region of interest for crosslinks (200-260 nm).<sup>49</sup>



Infrared and Raman spectroscopy<sup>50</sup> are handy complementary techniques for the analysis of vulcanised elastomers. When used in combination they supply data on both polar species (Infrared) and polarizable as well as non-polarizable species (Raman spectroscopy). Raman spectroscopy is important in detecting sulfur compounds since these have only very weak infrared absorptions. The draw back with Raman spectroscopy though is that it is primarily a surface technique and where a visible light laser source is used fluorescence as well as coloured samples hinder the effectiveness of the technique.

Solid state carbon 13 (<sup>13</sup>C) nuclear magnetic resonance (NMR) methods in combination with solubilisation techniques have been applied to overcome the disadvantages encountered with Raman and infrared spectroscopy.<sup>51</sup> However, the solubilisation technique was not quantitative and lacked primary standards with which to assign the <sup>13</sup>C resonances.

Many groups have been claimed to be detected via this technique such as cyclic sulfides,<sup>52,53</sup> cis-trans isomerism<sup>54,55</sup> and polysulfides<sup>56</sup> in different systems. The technique is flawed in that it doesn't allow one to distinguish between polysulfidic crosslinks having the same number of sulfur atoms<sup>57</sup> but different molecular structures. The signal overlap may thus be subject to spurious interpretations.

Alternate NMR nuclei may also be applied in the study of rubber other than the conventional <sup>1</sup>H and <sup>13</sup>C nuclei. Phosphorous containing zinc complexes were studied by McCleverty *et al.*<sup>58</sup> by means of <sup>31</sup>P NMR. They showed the chemistry of these complexes to be quite similar to their dithiocarbamate analogues, but no reference was made as to whether these complexes could be applied as accelerators in real vulcanisation systems.

McCleverty<sup>59</sup> also employed a different approach in his use of <sup>111</sup>Cd and <sup>113</sup>Cd NMR. The molecular structure of cadmium dithiocarbamate complexes was shown to be comparable to that of their zinc analogues<sup>2</sup> and in vulcanisation technology the cadmium derivatives are good substitutes for the zinc dithiocarbamates.

Thus the cadmium dithiocarbamate derivatives may be used as realistic model compounds for their zinc analogues and have the advantage of being detectable by NMR as apposed to their zinc counterparts. Fluorine labelled thiuram disulfides have also been investigated, making use of <sup>19</sup>F NMR.<sup>60</sup>

Unfortunately NMR observation of the only magneto-active sulfur isotope  $^{33}\text{S}$  presents difficulties as a result of its low natural abundance, low susceptibility and high quadrupole moment, which results in very broad  $^{33}\text{S}$  signals. Therefore the method is not regarded as a suitable tool for studying vulcanisation chemistry.<sup>61</sup>

Another technique that may be used to analyse rubber compounds is X-ray diffraction. It is the ultimate characterisation technique for an unknown compound and the bond distances and angles that are observed may give invaluable information on bond orders and molecular strain. The crystal structures of both tetramethylthiuram<sup>62</sup> disulfide and tetraethylthiuram<sup>63</sup> disulfide have both been published.

### 1.6.2. Model compounds for mechanistic studies

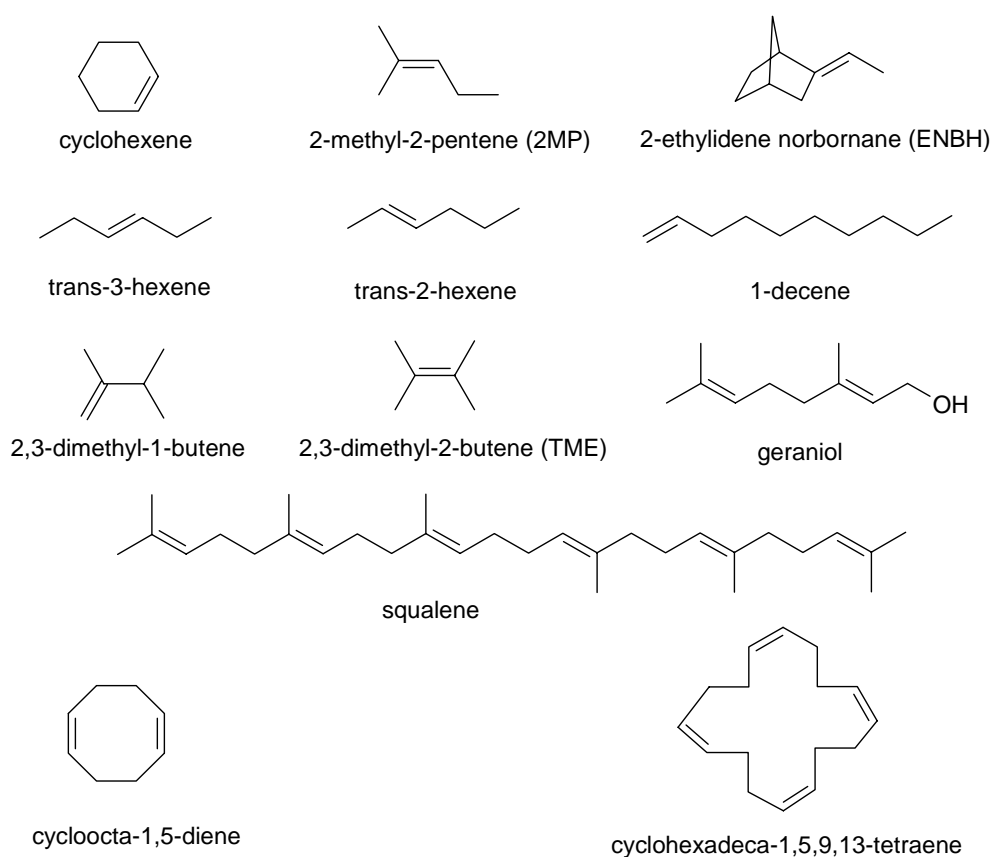


Figure 1.11: Compounds that have been successfully used as models for various Rubbers<sup>73</sup>

The importance of model compound analysis is the ease with which the experiments may be analysed, because of the lower molecular mass and the simplified structure.

Chromatographic as well as processes that determine the molecular structure may be employed.

Duynstee and co-workers<sup>64,65,66</sup> were the first to employ low temperature techniques in the analysis of the model compound vulcanisation products of ethylidene norbornane (ENBH) that has been used as the model compound for EPDM. They made use of thin layer chromatography (TLC), high performance liquid chromatography (HPLC), preparative HPLC and nuclear magnetic resonance to separate and identify the norbornane vulcanisation product.

Versloot<sup>67</sup> applied the same low temperature HPLC technique for the separation and identification of the vulcanisation products for the 2,3-dimethyl-2-butene (TME) a model compound used for polyisoprene. Van der Horst *et al.*<sup>22</sup> used the same model compound in their work to introduce a thiol detection system. They separated and resolved his products via HPLC, making use of post column derivatisation to detect the various thiols via spectroscopy.

Wolfe<sup>68</sup> employed gas-chromatography (GC) to investigate ZnO activated thiuram vulcanisation of cyclohexene, where he analysed the amount of cyclohexene reacted as well as the amount of thiol products formed by the reduction of the vulcanisation products with Li AlH<sub>4</sub>.

GC was also used by Lautenschlaeger and coworkers,<sup>69,70,71</sup> to separate and identify the products obtained from the model compound vulcanisation of 2-methyl-2-pentene which was used as a model for natural rubber. But as seen previously GC has the disadvantage of requiring high temperatures to introduce the samples into the gas phase. These high temperatures may cause isomerism and/or degradation of the sulfidic products. It has already been mentioned that polysulfidic linkages are thermally unstable and readily convert to lower sulfur rank linkages and cyclic sulfur structures. Thus the data obtained from GC analysis should be treated with caution.

When polyfunctional model compounds such as squalene, geraniol, cis-1,5-cyclooctadiene and cyclohexadectetraene are used, different of analysis methods are required as the spectrum of products derived are far more complex, as a result of the introduction of non-equivalent reaction sites; which introducing the possibility of isomerism. Gregg and Latimer<sup>72</sup> investigated the model compound vulcanisation of cyclohexadecatetraene and analysed the products by a combination

of gel permeation chromatography (GPC), NMR and Infrared spectroscopy. Squalene was used in a study by Boretti<sup>73</sup> which investigated the N-(cyclohexylthio)phthalimide inhibition of benzothiazole accelerated vulcanisation. He made use of HPLC to separate and quantify curatives and GPC to detect cross-linked products that were formed as a result of vulcanisation.

### 1.6.3. Choosing a model compound

As can be seen from the preceding paragraphs, the choice of model compound used in an investigation is crucial to obtain results that are easy to analyse, as well as molecule that can be considered an effective model for the system under investigation. As has been seen that simple models such as TME may be used but they don't allow for complex reactions such as cyclization, main chain modification and double bond migration, nor reactions that involve vicinal methylenic carbons. These models may be used successfully if only the simple interactions are monitored. Since the molecule is symmetrical it has one equivalent allylic hydrogen position resulting in simplified reaction products. TME has a similar structure to a monomeric unit found in polyisoprene (see Figure 1.12) and thus may be used as model for this polymer.

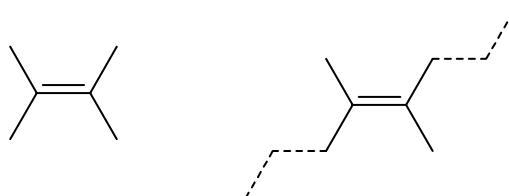


Figure 1.12: The similarity of TME to polyisoprene.

In certain systems model compounds give spurious results, Boretti<sup>73</sup> found that 2,3-dimethyl-2-butene and 2-methyl-2-pentene were ineffective models for MBTS accelerated sulfur vulcanisation of polyisoprene. He discovered that both these model compounds lead to MBT formation prior to crosslinking, which does not occur in polyisoprene. The result would be the premature reaction of MBT with N-(cyclohexylthiol)phthalimide (CTP) and thus alter the true course of prevulcanisation inhibition. He subsequently found squalene to be a more effective model for polyisoprene.

Reactions requiring more than one double bond cannot be followed with monofunctional model compounds like TME, and require more complex model compounds like squalene and geraniol. Furthermore there may be differences in the manner similar monofunctional model compounds react. Nieuwenhuizen<sup>74</sup> reported that thiuram disulfide vulcanisation of the model compounds cyclohexene and TME gave different results. The difference in results was attributed to the relative immobility of the double bond in cyclohexene as compared with TME.

It was decided that squalene would be the best model for studying the rate of thiuram disulfide vulcanisation. It would allow for all the possible reactions to occur as in rubber due to its complex nature. It also mimics the structure of polyisoprene well, consisting of six isoprene units. A concern, however, would be that squalene is the trans conformer as opposed to the cis, as seen in cis-1,4-polyisoprene.

## **1.7 Studies of the rate of vulcanisation**

### **1.7.1. Background to rate analyses**

The kinetic analysis of vulcanisation is important and is as well studied as the reaction pathways that are operating during the process. Kinetics gives insight into the time, temperature and concentration dependence for the reactions that occur. The temperature gradients as well as the extent of cure in a rubber mass can be investigated if the thermal properties and the kinetics of vulcanisation are known. Temperature gradients within a sample are governed by and generated by the cure reaction, heat conduction through the rubber and mould as well as heat exchange by convection to the surrounds. The kinetics may also be used to give insight into the vulcanisation process during the cooling period when the article is removed from the mould.<sup>75</sup>

The evaluation of order with respect to time and or concentration is an integral part in evaluating kinetics even though it is not always easy. Here we will introduce some brief concepts that relate to reaction rates that will lay the foundation for the proceeding work.

The rate of a reaction with order  $n$  can be expressed as follows:

$$\frac{dx}{dt} = k(a - x)^n \quad (1)$$

a = initial concentration

x = quantity of starting material reacted

t = time

k = rate constant

n = order of the reaction

For n = 0, that is a zero order reaction we get dx/dt = constant

Depending on whether n = 1 or some whole number or fractional number, the integration of Equation 1 gives us two different answers. For n = 1 we get

$$\ln(a - x) = -kt + \ln a \quad (2)$$

Here the half life time is constant. When n ≠ 1, the integration of Equation 1 gives

$$\left(\frac{1}{1-n}\right)(a-x)^{1-n} = -kt + \left(\frac{1}{1-n}\right)a^{1-n} \quad (3)$$

and the half life becomes a function of initial concentration.

If n has been accurately determined, plots of 1/(1 - n)(a - x) for when n ≠ 1 or log(a<sup>0</sup> - x) for when n = 1, against time of reaction must give straight lines. The slope of the curves will be equal to the rate constant. In a zero order reaction, the reaction curves themselves are straight lines.

It is sometimes expedient to plot the results of experiments for which only fractional parts of the reactions occur. If one used (a-x) = c and a = c<sub>0</sub> in Equation 3 the following expression is obtained:

$$\frac{1}{n}(C^{1-n} - C_0^{1-n}) = kt \quad (4)$$

With a single transformation the following is obtained

$$\left(\frac{C}{C_0}\right)^{1-n} - 1 = (n-1)C_0^{n-1}kt \quad (5)$$

If  $C/C_0 = \alpha$ , we obtain the important expression below

$$\alpha^{1-n} - 1 = (n-1)C_0^{n-1}kt \quad (6)$$

Substituting the dimensionless parameter  $kC_0^{n-1}t \equiv \tau$ , one obtains

$$\alpha^{1-n} - 1 = (n-1)\tau \quad (7)$$

It is readily seen that since  $\log \tau = \log t + \log kC_0^{n-1}$ , a simple plot of  $\alpha$  against  $\log t$  must give a characteristic curve for each value of  $n$  and the same value for  $n$  can be made to coincide by shifting the curve along the abscissa.

There are a large number of chemical reactions that take place during vulcanisation and it is thus difficult to systematically classify all of them. The reactions, however, may broadly be divided into 'direct' and indirect' crosslinking reactions. Direct crosslinking reactions are considered to occur when the chemical agent reacts directly with the hydrocarbon in the formation of bridge bonds. Whereas indirect vulcanisation occurs when the chemical agents are used in the presence of activators and other chemicals that would serve to increase the rate of the reaction.

Compounds that bring about direct crosslinking are the tetrasubstituted thiuram disulfides and monosulfides in the presence of ZnO and peroxides such as dicumyl peroxide etc. The accelerated vulcanisation of rubber by sulfur is considered to be an indirect process.

When determining the rate of a reaction and attempting to evaluate the order of the reaction, it is important to understand that the rate of any process will be determined by the slowest step that is the rate limiting process. As already mentioned, Coleman *et al.*<sup>15</sup> observed thiuram persulfenyl radicals by means of ESR when examining TMTD accelerated vulcanisation and concluded that a radical mechanism played an important role in that accelerator's mode of action or at least initiation. It was thus

suggested, to try estimate the activation energy for the homolytic cleavage of the thiuram disulfides by computer modelling and attempt to relate the obtained values to the vulcanisation rates observed. The homolytic cleavage, however, proved impossible as the dynamic computer simulation proved tedious. Once molecular cleavage was achieved, it was uncertain whether a homo- or heterolytic process was operational.

Thiuram disulfide vulcanisation is a complicated set of chemical reactions with at least three well characterised partial reactions with varying orders. The thiuram disulfide vulcanisation of rubber in the presence of sulfur is distinguished by a change in the reaction order with time and is dependent on the sulfur concentration. Individual processes indicate a time law of zero order with respect to sulfur and a concentration dependence order of between 0.8 and 1.0.<sup>76</sup> Thiuram disulfide decrease and dithiocarbamate formation has been determined to be a first order process. Crosslinking itself has been determined to follow first order reaction kinetics. It is thus noted that the application of rate laws to vulcanisation will never give a complete holistic fit, but rather would be found to be an approximation obeying the rate law in different regions of the reactions progress. It is therefore necessary to restrict the rate constant determinations to the same regions throughout the analysis for comparable results.

### **1.7.2. The use of vulcanisation reaction mechanisms in pursuit of a holistic kinetic model**

A large number of authors have considered order determinations and the type of rate theories that may best describe vulcanisation. Scheele<sup>76</sup> worked extensively on determining the over-all order in relation to sulfur and accelerator concentrations for many different types of accelerated vulcanisation systems. These orders enabled crude fits, being limited in their ability to predict scorch times specifically those presented during prevulcanisation inhibition. His work was also unable to account for reversion, but he did lay the foundation for the optimisation of both accelerator and sulfur loadings.<sup>12</sup>



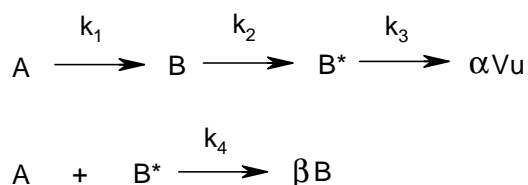
Table 1.2: Examples of some empirical kinetic models for cure kinetics ( $\alpha$  = degree of cure,  $n$  = order)<sup>77</sup>

Model	Solution characteristics
$\frac{d\alpha}{dt} = k(1 - \alpha)^n, n \geq 1$	$\alpha = 1 - e^{-kt}, (n=1);$ $\alpha = 1 - \frac{1}{[1 + kt(n-1)]^{1/(n-1)}}, (n > 1)$
$\frac{d\alpha}{dt} = \frac{n}{k} t^{-(n+1)} \alpha^2, n \geq 1$	$\alpha = \frac{kt^n}{1 + kt^n}$

Empirical models were also employed as shown in Table 1.2. These models may be described as being regression models that fit data assuming a particular functional form, where parameters are estimated from the experimental data using non-linear parameter estimation procedures.<sup>77</sup> The only value of these models is their ability to describe the shape of the torque vs. time curves produced by an oscillating disc rheometer. These models are unable to predict induction periods or the occurrence of reversion. They also do not acknowledge mechanistic constraints and are unable to predict the effect a change in composition will have on the system.<sup>77</sup>

Coran<sup>12,13,14</sup> improved the understanding of the kinetics of scorch delay vulcanisation by breaking the kinetic evaluation up into individual reactions. His scheme was based on the chemical analysis performed by Campbell and co-workers on natural rubber sulfur vulcanisates accelerated by means of 2-(morpholinothio)benzothiazole.<sup>78,79</sup> From the data he was able to deduce that once all the accelerator and accelerator sulfur reaction products were consumed, the crosslinking reaction followed first order kinetics. He concluded that the accelerator and accelerator sulfur reaction products served to inhibit the crosslinking reactions. This is reasonable since it is known that in the initially stages of vulcanisation, when the accelerator and accelerator polysulfide concentrations are high, the rate of exchange between thiol pendent groups and accelerator pendent groups is fast. This would allow for a high concentration of accelerator polysulfide pendent groups thus only allowing slow second order crosslinking involving the disproportionation of these accelerator polysulfide pendent groups. He thus postulated that the extent of delay depends on the rate at which accelerator and free accelerator polysulfides are removed.

Coran's<sup>12</sup> reaction scheme may be represented as follows:



where A is the concentration of the accelerator and all its by-products with sulfur, zinc oxide, amines and carboxylates; B is the polymeric sulfur precursor to crosslinking and B\* is the activated form of B. The activated form of B for thiuram systems is radical in nature when ZnO is absent and polar in the presence of ZnO. Vu is a crosslink while  $\alpha$  and  $\beta$  are constants that adjust the stoichiometry. Rubber is not accounted for in this system as it is considered to be in excess.

The model is able to explain the long delay periods associated with the thiazole sulfenamide accelerators. If the reaction through  $k_4$  is considered to be much faster than through  $k_3$  very little crosslink formation is able to occur. Only once all the accelerator and the free accelerator by-products are completely consumed can crosslinking commence at an appreciable rate. Thus the reaction through  $k_2$  is considered rate controlling once all the accelerator and its by-products are consumed. The constant  $k_2$  may be derived from data obtained by means of an Agfa Vulkometer or a Monsanto oscillating disk rheometer. The rate constant  $k_2$  is defined as the maximum slope of the curve derived from the plot of  $\ln(R_\infty - R_t)$  vs. t, where  $R_\infty$  and  $R_t$  are defined as the tightness of cure at infinite time and time t respectively.<sup>12</sup> A relative value for  $k_2$  may be obtained from the maximum slope of the torque vs. time curve obtained from the rheometer trace. These maximum slopes have been determined and used in this thesis to investigate any relationships that may exist in relation to substitution effects and cure characteristics.

Coran<sup>12</sup> makes a number of assumptions that place limitations on his theory. Before discussing the limitations of his theory it may prove useful to evaluate his mathematical approach. Using the proposed reaction scheme he makes use of the steady state assumption:

$$d[B^*]/dt = k_2[B] - k_3[B^*] - k_4[A][B^*] = 0 \quad (i)$$

and

$$[B^*] = k_2[B]/(k_4[A] + k_3). \quad (\text{ii})$$

In the initial stages of vulcanisation  $k_4[A] \gg k_3$  thus equation (ii) simplifies to:

$$[B^*] \approx k_2[B]/k_4[A] \quad (\text{iii})$$

Thus for the disappearance of A one obtains:

$$-d[A]/dt = k_1[A] + k_4[A][B^*] \quad (\text{iv})$$

Assuming:

$$[B] = [A]_0 - [A] \quad (\text{v})$$

And substituting equation (iii) and (v) into equation (iv) one obtains:

$$-d[A]/dt = k_1[A] + k_2([A]_0 - [A]) \quad (\text{vi})$$

Which integrates to:

$$[A]/[A]_0 = \{k_2 - k_1^{(k_2 - k_1)t_{dis}}\}/(k_2 - k_1) \quad (\text{vii})$$

Making the assumption that  $[A] = 0$  at  $t_{dis}$  the time when the reaction governed by  $k_2$  becomes an unperturbed first order reaction (plot of  $\ln(R_\infty - Rt)$  vs.  $t$  becomes a straight line) allows for equation (vii) to be written as follows:

$$k_1 t_{dis} - \ln k_1 = k_2 t_{dis} - \ln k_2 \quad (\text{viii})$$

If  $k_1/k_2 = Z$  then the solution to the above equation may be represented as follows:

$$k_2 t_{dis} = -\ln Z / (1 - Z) \quad (\text{ix})$$

As seen earlier  $k_2$  may be determined from the plot of  $\ln(R_\infty - Rt)$  vs.  $t$ , which corresponds to the slope of the curve after the induction period. The value  $t_{dis}$  is considered to be the time where curvature in the plot of  $\ln(R_\infty - Rt)$  vs.  $t$  after the induction period desists to produce a linear region which would correspond to the reaction governed by the rate constant  $k_2$ , an unperturbed first order reaction. The rate constant  $k_1$  may then be determined from the log plot of equation (ix) while the

disappearance of A may be calculated from equation (vii). Limited by the assumptions that were made Coran's theory is only able to determine the concentration of crosslinks during the initial stages of vulcanisation. From the model:

$$d[V_u]/dt = \alpha k_3[B^*] \quad (x)$$

Substituting in equation (iii) one obtains:

$$d[V_u]/dt = \alpha k_2 k_3 [B]/k_4 [A] \quad (xi)$$

Substituting in equation (v) and (vii) one derives the following:

$$dV_u/dt = (\alpha k_1 k_2 k_3 / k_4)^{[(k_2 - k_1)^t]} - 1 \{k_2 - k_1^{[(k_2 - k_1)^t]}\} \quad (xii)$$

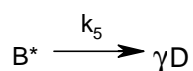
Which upon integration gives:

$$V_u = -(\alpha k_3 / k_4) \ln \{ [k_2^{(k_1)^t} - k_1^{(k_2)^t}] / (k_2 - k_1) \} \quad (xiii)$$

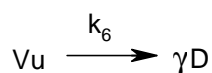
The theory does have a few shortcomings as is clearly depicted from his mathematical approach. Firstly he doesn't explicitly include sulfur into the theory, being unable to predict the effect a change in sulfur concentration has on the final vulcanisate. The model was found to be inconsistent in its ability to predict the dependence of crosslink concentration relative to the initial loading of accelerator. He does not discretely handle polysulfide formation rather choosing to rely heavily on the generalised reaction scheme.<sup>77</sup> The species A is supposed to include the concentrations of both accelerator and all its derivatives with sulfur and the other additives. Experimentally he only investigated the concentration of the accelerator and the monosulfidic species.<sup>12</sup> This may compromise the relevance of his theory due to the prominence of accelerator polysulfides as the active sulfurating agents in vulcanisation theory. His assumption that accelerator is consumed in the initial stages is not completely applicable to thiuram disulfide systems since it is known that accelerator may be liberated in the advanced stages of crosslinking as is seen for tetramethylthiuram disulfide accelerated sulfur vulcanisation. The kinetics of reversion is not accounted for in this theory.<sup>77</sup> Even with these limitations the theory has made a significant advancement in the utilisation of kinetics based on a

mechanistic understanding of the benzothiazole system and may be found to be generally applicable.

Ding and co-workers<sup>80,81</sup> then added two more reactions to Coran's reaction scheme. The first reaction takes into consideration the variation of equilibrium modulus with cure temperature:



Where D is a dead end species and  $\gamma$  is a stoichiometric coefficient. The second is a side reaction that takes into consideration reversion:



Chapman<sup>82</sup> introduced an alternative kinetic model to explain the cure behaviour of efficient sulfenamide systems. The model was based on the analysis of isotopically labelled benzothiazole accelerates in accelerated sulfur vulcanisation. The nature of the experiments gave insight as to the type of intermediates that were formed. He thus took into consideration accelerator pendent groups and a crosslink that was derived from the reaction of two accelerator pendent groups. He developed empirical equations that were guided by the experimental results to determine the concentrations of accelerator pendent groups and crosslinks. Once again as with Coran's<sup>12</sup> kinetic model Chapman's<sup>82</sup> model is unable to predict reversion and the concentration of free accelerator polysulfides.

More recently Gosh *et al.*<sup>77</sup> developed a comprehensive kinetic model for benzothiazole accelerated sulfur vulcanisation. Their model makes use of a population balance method in which all known reactions and their mass actions are accounted for. The model is, however, limited to the benzothiazole system as a result of the types of reactions that have been considered. Certain reactions that are prominent in thiuram disulfide systems are not crucial to benzothiazole systems and are subsequently not considered. These reactions include dithiocarbamic acid formation and its pseudo catalytic effects, the production of thiourea, free amine and the relevance of dimethylammonium pendent groups in crosslinking. Interestingly, their model considers thiol pendent groups to be dead end species. This is not

considered to be the case for thiuram disulfide systems. Their method does, however, predict the concentration profiles for most of the intermediates found in the benzothiazole system and is thus of crucial importance in elucidating the effect the intermediates have on the system.

Duchacek<sup>83,84,85</sup> performed kinetic studies to elucidate the cure reactions present in the thiuram disulfide accelerated sulfur vulcanisation system. A single first order reaction was found to be operational for the crosslinking of natural rubber by means of TMTD in the presence of sulfur. The crosslinking of cis-1,4-polybutadiene by means of TMTD in the presence of sulfur was found to be governed by the sum of three independent first order reactions. The first being a fast crosslinking reaction, the second is a slow crosslinking reaction that is limited by the formation of a zinc dimethyldithiocarbamate intermediate, while the third is a decomposition reaction governed by an induction period. Taylor *et al.*<sup>86</sup> also worked on the vulcanisation of poly-1,4-butadiene by tetramethylthiuram disulfide. Monte-Carlo simulations were used in their investigation to determine possible reactions in a sphere around the crosslinking site. They were able to predict the elastic moduli and aspects concerning the nature of the network. They were, however, unable to predict the effect a change in the loadings of accelerator and sulfur would have on the crosslink density.

The investigations in this dissertation rely primarily on simple kinetic evaluations based on the rate at which accelerator and sulfur is depleted. In the rheology the rate of crosslinking is the prime concern. The crosslinking region has been shown to approximate first order kinetics. It should be noted that the complex investigations expounded upon above are crucial to a complete understanding of vulcanisation systems.

### **1.7.3. Methods for determining cure rates**

Vulcanisation kinetics is an important field of study that allows one to establish processes and adjust them such that they operate at maximum efficiency. Rates may be determined from cure times that may be determined from measurements made with a Monsanto Rheometer, as was the case in this study, or a Wallace Shawburg Curemeter as well as by means of isothermal experiments.<sup>87</sup>

The data obtained has to be treated with care since each method that is employed to determine the rate of cure presents certain limitations. Rheometers give longer cure

times than curemeters and both instruments give longer cure times than the isothermal experiments. The reasons for the differences are as follows: in the rheometer heat is continually being lost to the rotor during the measurement thus the core temperature is less than the platen's temperature therefore the average temperature is always less than the set temperature. On the other hand curemeter samples take longer to heat up since they are thicker than the samples used in the isothermal experiments. Thus both the instruments introduce temperature anomalies to the analysis. The use of isothermal experiments is, however, tedious as it takes weeks to determine cure time curves for a complete set of samples in a study, as each point has to be obtained separately by correlating the temperature time history of the samples with swelling experiments in toluene.

Kinetic analysis may also be performed by studying the enthalpy profiles obtained by isothermal studies using a DSC.<sup>87</sup> Both the DSC and rheometrical methods were initially considered in the determination of the rate of vulcanisation as both methods were available in our laboratories and both had easy mathematical calculations.

In the DSC method using enthalpies the equation to consider follows:

$$\frac{dQ}{dt} = k_0 (Q_\infty - Q_t)^n \cdot \exp \frac{-E}{Rt}$$

Where  $Q_t$  is the heat of cure evolved up to time  $t$ , and  $Q_\infty$  is the total heat for the rubber mass unit.<sup>75</sup>

It was, however, decided to obtain cure rates from data obtained from torque vs. time graphs as produced by a Monsanto Rheometer, as the instrument was found to be far more reliable than the DSC which was found to be subject to many environmental factors. Assuming first order kinetics the following relation is obtained:

$$\frac{dx}{dt} = k(a - x)$$

Where  $a$  = initial concentration of linear material and  
 $x$  = the amount of linear material at time  $t$ .

Integrating one obtains:

$$\ln \frac{(a - x)}{a} = -kt$$

Or from the data obtained from the torque vs. time graphs the following is derived:

$$\ln \frac{(M_{\infty} - M_t)}{(M_{\infty} - M_0)} = -kt_r$$

Where  $M_{\infty}$  = maximum modulus

$M_0$  = initial modulus

$M_t$  = modulus at time t

$t_r$  = reduced time  $(t - t_0)$ , where  $t_0$  is the time when the above equation becomes linear

It is assumed that  $M_{\infty} - M_t = a$

$$M_{\infty} - M_0 = b$$

Then

$$a = be^{-kt}$$

Therefore a plot of  $\ln(a/b)$  vs. t will give a slope of -kt.

Since the experimental evaluation is limited to the rate at which crosslinking occurs, the rate in the linear acceleratory region of the rheometer curve needs to be determined. The data analysis was set up in a way such that the initial time at which crosslinking commenced could be varied. This would allow for the determination of the best straight line with which to determine the rate constant. The assumption of first order kinetics is a generalisation with the system only obeying a pseudo-first order law in relation to the torque vs. time data. This is in line with the more complex models such as that of Coran<sup>12</sup> which reduce the crosslinking step to a pseudo-first order process. In this study rate data pertaining to a pseudo first order crosslinking reaction, the Coran<sup>12</sup> rate constant ( $k_2$ ) and maximum slope are investigated.



## 1.8 Hammett Plots

### 1.8.1 Introduction

Polar and radical reactions are strongly dependent on the structure of the organic molecules involved, primarily on the positions of substituents relative to the reaction site, be it cationic, anionic or radical. This may, however, reduce the favourability of a reaction since the intermediary product may be too stable to promote the forward reaction.

The main stabilizing factors for reaction intermediates are:

- hyperconjugation
- inductive effects
- resonance stabilization and

The action of a substituent on reaction rates and equilibria is primarily due to the displacement of electrons within a molecule. Inductive effect, a broad description of many individual fundamental processes, generally considered to be the inductive transmission of charge through a chain of atoms; is considered to be a localized effect. Wheland and Pauling's<sup>88</sup> quantum mechanical description hypothesises that the average electron density in every part of a molecule is affected by substituents. This may be due either to the substituent's ability to attract or repels electrons, or because the substituent permits the construction of alternative electron distributions of a highly polar nature which may resonate with less polar forms.

Inductive effects as mentioned earlier, consist of a variety of fundamentally separate concepts yet are closely related and may be bound together in a loosely conceptualised word – “field” effects. For example within this grouping one encounters “static” effects which depend on the ground state electron configuration. Methoxy and hydroxyl groups interact strongly with benzene in its ground state electron configuration, activating the ring towards electrophilic substitution.<sup>89</sup>

There are direct effects, which are not transmitted through atoms but rather the electrical field produced by the substituent at a point is considered to be a function of

the distribution of matter both in the molecule and in its environment (electrostatic effects). These effects are considered to travel through space and thought to be negligible at distances greater than 2Å.<sup>89</sup>

These effects can be used to explain why a reaction will take place or not. However, a factor which is often crucially overlooked is steric hindrance. Is the theorized reactive center accessible to attack by substituting side groups or molecules that may serve as activators? When considering how reactions take place it is often easiest to consider whether an atom or group removes electron density from a bond thus promoting its cleavage or if the group is electron rich whether it donates electron density onto an atom which has lone pairs thus making these lone pairs (Lewis base) more reactive (electron cloud expansion-orbital synergistic effects). These considerations are both important when considering thiuram disulfide accelerators as both nitrogen atoms and persulfide bonds are present.

### 1.8.2 Hammett Equations and Linear Free Energy Relationships

In 1937 Louis Hammett<sup>90,91,92,93</sup> suggested that the effects that meta and para substituents have on the ionization constants of benzoic acid could be used as a general predictor of the electronic influences that substituents may have on a variety of reactions. His choice of molecule was crucial though. Benzoic acid is a rigid molecule because of the benzene ring which prevents free movement of substituents relative to the carboxylic acid group. The presence of resonance forms also introduces rigidity. Mesomeric conformers destroy the freedom of rotation around a bond, whenever a single link resonates with a configuration that contains a double link in the same position. For example in phenol there is no freedom of rotation between the carbon and oxygen atom (see Figure 1.13).

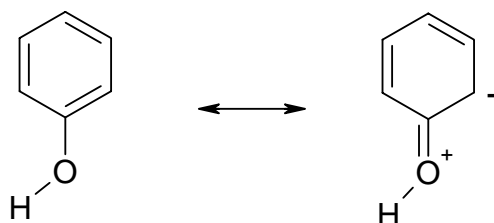


Figure 1.13: Resonance structures of phenol, depicting rigid geometry

Hammett didn't consider ortho substituents in an attempt to simplify his study by eliminating any possibility of steric hindrance of the reaction site, steric inhibition of resonance, the possibility of hydrogen bonding as well as the possibility of the ortho substituent participating in the reaction. Hammett introduced an equation defining a substitution constant  $\sigma$  as the logarithm of the ratio of the ionization constant of the substituted benzoic acid to that of the benzoic acid itself in an aqueous solution at 25°C.

$$\rho\sigma = \log \frac{K}{K_H}$$

$K$  and  $K_H$  are ionization constants of the substituted and the non-substituted benzoic acids respectively. The substitution constant  $\sigma$  is a good measure of the groups electron donating or attracting ability and since there are two sites to be occupied each group has two  $\sigma$  values, a para and a meta value. For example electron attracting groups such as  $\text{NO}_2$  and  $\text{CF}_3$  have large positive  $\sigma$  values while electron donating groups have large negative values. For some groups the  $\sigma_{\text{para}}$  is much greater than the  $\sigma_{\text{meta}}$  values. This is because resonance stabilization has a greater effect in the para region, where appropriate than in the meta region (see Figure 1.14).

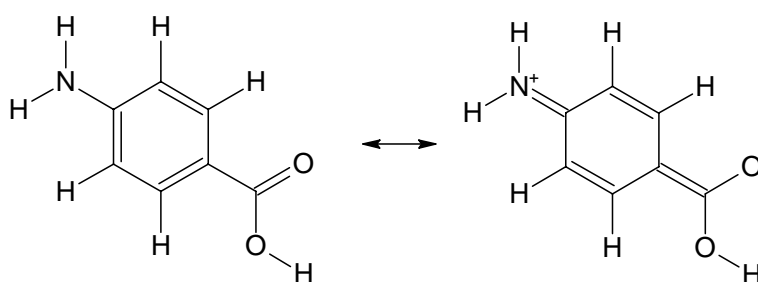


Figure 1.14: Resonance structure for p-amino benzoic acid, no such stabilizing structure exists in the meta position

The constant  $\rho$  (reaction constant) is the slope of the Hammett plot ( $\log K/K_H$  vs.  $\sigma$ ). When  $\rho$  is positive the reaction is promoted by electron attracting substituents. By making the necessary substitutions one may derive a free energy relationship as well as a rate constant relationship between two reactions, thus the following two equations are obtained.

$$\rho\sigma = \frac{\Delta G}{-2.33RT} - \frac{\Delta G_H}{-2.303RT} \quad \log \frac{k}{k_H} = \rho\sigma$$

It was decided to produce various substituted aromatic thiuram disulfide accelerators, determine the rates of vulcanization and then establish a correlation between rate and substituents effects.

### 1.8.3 Application

Since Hammett<sup>93</sup> first applied his theory to various substituted benzoic acids, these principals have extensively been used to determine the linear free energy relationships of many systems. He has done further work on the effect of structure on the rates of aromatic organic reaction.<sup>93</sup> The subsequent information is included in an attempt to show, even though only slightly, the diversity on the applications that may be entered into when examining free energy relations.

The kinetics of the reaction of aromatic aldehydes with ammonia have been followed and reactivity constants ( $\rho$ ) determined, as well as the effect of temperature and hydroxide concentration on the rate. Ogata and co-workers<sup>94</sup> discovered that positive  $\rho$  were obtained from electron-releasing para substituents in benzaldehyde and a negative  $\rho$  for electron attracting substituents in the same position, this differs from the theory that has been previously considered and may be a resonance effect.

The rate of solvolysis of substituted phenyldimethylcarbinyl chlorides in a variety of isopropyl alcohols has been examined. Discovering that the rate of solvolysis of t-cumyl chloride decreases with increasing molecular weight of the alcohol.<sup>95</sup>

An interesting investigation by Dektar and Hacker<sup>96</sup> indirectly proves Pauling's theory that inductive effects operate over long distances.<sup>88</sup> They examined the modulation of the  $\pi$ -facial selectivity in Diels-alder cycloaddition to isodicyclopentafulvene, by remote para substitution of an exocyclic phenol ring. Choosing groups that didn't sterically hinder the reaction centre, and making use of dual substitution parameter (DSP) to introduce separate substitution constants for the inductive and the resonance effect that a group may attribute, ( $\sigma_I$  &  $\sigma_R$ ). It was found that long range

inductive effects significantly effected selectivity, noting that  $\pi$ -facial attack is preferred when the substituent is an electron releasing group.<sup>96</sup>

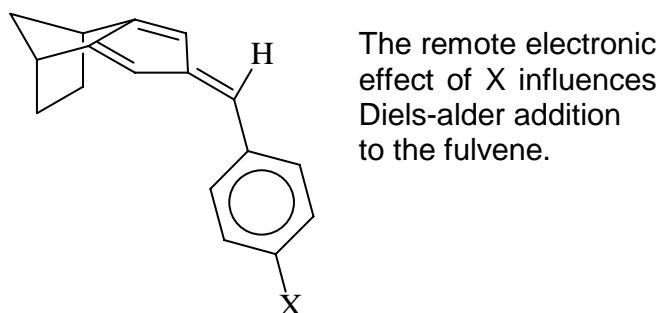


Figure 1.15:  $\pi$ -facial selectivity in Diels-alder cycloaddition modulated by long range inductive effects in various isodicyclopentafulvene adducts<sup>96</sup>

Problems experienced as a result of deviations from the Hammett relation are primarily as a result of non-rigidity in molecules.<sup>97</sup> All the applications thus far have involved aromatic, cyclic, bicyclic and small unsaturated molecules which all have a fair amount of rigidity. Hammett did not include ortho benzoic acids in his study, because of problems associated with steric hindrance and chelation. Ortho substituents did not obey the relation. This has since become known as the ortho effect. The ortho effect has since been observed in the dissociation constants of cis-3-acrylic acid, where no relation between Hammett parameters and equilibrium constants could be found. This was attributed to the ortho effect acting by means of chelation between the substituents and the reaction site.

#### 1.8.4 Overcoming non-rigidity in molecules

Various methods have been employed to overcome non-rigidity in molecules and the subsequent deviation from the Hammett relation. Robert and Moreland<sup>98</sup> introduced a substitution constant  $\sigma'$ , that took into consideration solely the inductive affect attributed by a group on aliphatic molecules with fixed geometries (see Figure 1.16 for examples of molecules which contain rigidity).

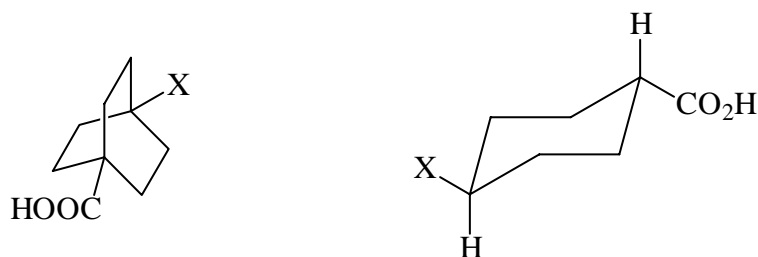


Figure 1.16: Examples of molecules with rigid structures

Taft analysed the effect substituents had on the reaction rates of a series of esters,  $XCO_2R$ . If R was kept constant he assumed that the resonance, inductive as well steric effects could all be attribute to the group X. He was able to eliminate the resonance contribution the carboxylic acid may have with group X, by bonding the two groups together via and intermediary aliphatic group thus effectively eliminating resonance interaction. Taft,<sup>99</sup> applying an earlier suggestion by Ingold, defined the rate of basic hydrolysis of esters as

$$\log \left[ \frac{k}{k_H} \right]_{\text{in base}} = \rho^* \sigma^* + E_s$$

where  $\rho^*$  ( $\rho^*=2.48$ ) is a scaling parameter to bring values of  $\sigma^*$  onto a scale comparable to those of Hammett  $\sigma$  values, while  $\sigma^*$  and  $E_s$  constants that reflect the inductive and steric effects of X respectively.<sup>99</sup> He was able to determine the steric effect constant ( $E_s$ ) by measuring the rates of acid hydrolysis of aromatic esters, as their rates of hydrolysis are not strongly influenced by polar substituents as demonstrated by small reactivity constants  $\rho$ .

Even though large assumptions were made in the determination of the constants in Taft's equation, many authors have proved their validity. The steric constant,  $E_s$  furthermore has proved to reflect the size of groups with accuracy and is thus useful for that purpose, while  $\sigma^*$  has proved to be a useful measure of inductive effect.<sup>100</sup> In this study the Taft relation has been used to take into account electronic effects, as they are more broadly applicable than the corresponding Hammett parameters. Where the Taft constants were not available the equivalent Hammett parameters were converted (see experimental section for conversion).

### 1.8.5 Application to vulcanisation

Hammett plots have been applied to the linear free energy relationship (LFER) that occurs in prevulcanisation inhibition. The effect of substituents on the cure rate and scorch delay have been examined primarily with regard to sulfonamides inhibitors in MBT accelerated sulfur vulcanisation systems by Morita.<sup>101</sup> Vulcanisation inhibitors include the group of compounds thioimides, sulfenamides, thioketal and polysulfides.

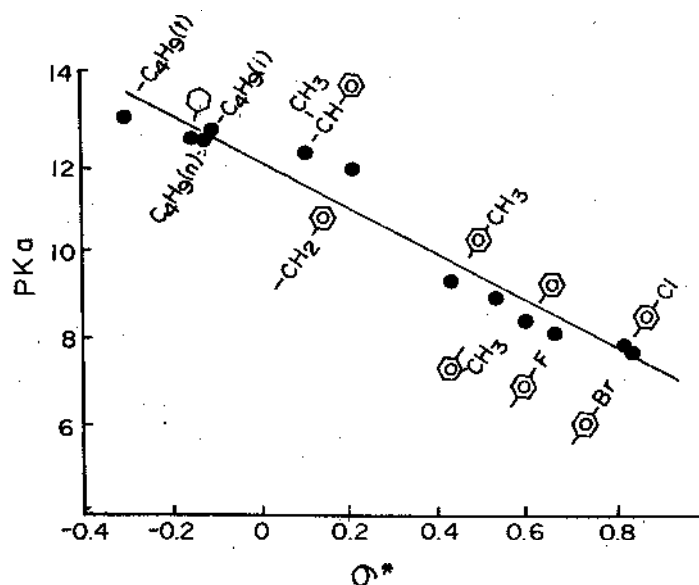


Figure 1.17: Relationship of the pKa of the substituted thiols and the  $\sigma^*$  of these substituents<sup>101</sup>

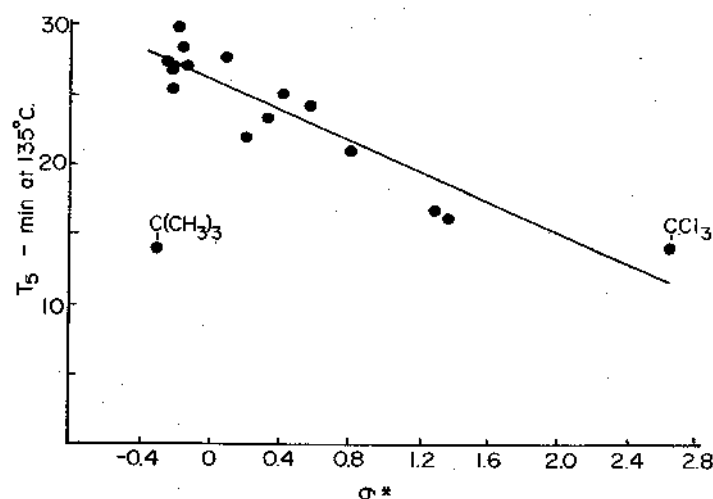


Figure 1.18: Relationship of scorch time of the substituted thiols to the  $\sigma^*$  of these substituents<sup>101</sup>

In stocks accelerated by MBT, it is generally accepted that inhibitors retard the rate of vulcanisation by scavenging 2-mercaptobenzothiazole (BtSH) liberated during cure to produce asymmetric disulfides, BtSSR. The scorch delay is related to the rate of reaction between BtSH and the inhibitor (LSR), which is subsequently influenced by the electronic nature of the groups L and R.<sup>102</sup>

The significance of thiosubstituents (R) in inhibitors (LSR) can be seen in the following figures. Figure 1.17 shows a good linear correlation between  $pK_a$  and  $\sigma^*$  constant (Taft's substituents inductive effect constant).

The negative slope observed in Figure 1.17 is analogous to that seen in Figure 1.18, of scorch delay time vs.  $\sigma^*$ . This means the scorch delay time is shorter when the thiosubstituent is electron withdrawing. It has been noted in similar papers that plots of decomposition temperature vs. scorch delay show that compounds with increased decomposition temperatures generally show increased scorch delay times.<sup>102</sup> It should be noted that Morita's work, out of which Figures 1.17 and 1.18 are extracted, has been comprehensively reviewed by Ignatz-Hoover *et al.*<sup>103</sup>

Thus it can be seen that the Hammett free energy relation is invaluable in its wide application to very varied systems. This enables chemists to establish trends in reactivity within a group of specific molecules, and monitoring the effect the group has on the specific measure parameter being investigated.

## 1.9 Computational chemistry

Computational chemistry is the use of computer software to gain insight into chemical processes, predicting the geometry of molecules, stability of chemical systems, determining the energy difference between different states, as well as the investigation of mechanistic pathways on the atomic level. Computational chemistry relies heavily on potential energy surfaces, being examined by single point calculations geometry optimisations and molecular dynamic simulations. Energies and derivatives of energies, such as the forces on atoms, are necessary to "construct" a potential energy surface. This concept unites molecular and quantum mechanics generating the potential energy surfaces required for molecular optimisations.<sup>104</sup> Both molecular and quantum mechanics rely on the



Born-Oppenheimer approximation. In quantum mechanics the Schrödinger equation (1) gives the wave functions and the energies of molecules.

$$H\psi = E\psi \quad (1)$$

Where H is the molecular Hamiltonian,  $\psi$  is the wave function, and E is the energy. The molecular Hamiltonian is composed of these operations: the kinetic energy of the nucleus and the electrons and their attractive and repulsive operations.<sup>104</sup>

$$H = (\text{kinetic energy})_N + (\text{kinetic energy})_E + (\text{repulsion})_{NN} + (\text{repulsion})_{EE} + (\text{attraction})_{NE}$$

If one assumes that because the nucleus is many times heavier than an electron, the movement of an electron relative to the nucleus is negligible (Born-Oppenheimer approximation). Thus electron distribution is limited to the fixed position of nuclei and not their velocities and since nuclear-nuclear repulsion may be ignored since it is constant for a specific conformation one obtains.

$$H_{\text{electronic}} = (\text{kinetic energy})_E + (\text{repulsion})_{EE} + (\text{attraction})_{NE}$$

Once the Schrödinger equation has been solved the term for nuclear repulsion needs to be included.

$$H_{\text{electronic}}\psi_{\text{electronic}} = E_{\text{electronic}}\psi_{\text{electronic}}$$

$$V_{\text{PES}} = E_{\text{electronic}} + (\text{repulsion})_N$$

Generating potential energy surfaces using this equation requires solutions for many configurations. This would take a large amount of computational time. Thus electronic energies are not examined explicitly but rather implicitly by the introduction of force field equations which examine the electronic energies implicitly via parameterisation.<sup>105</sup>

The types of calculations that may be entered into are:

- Single point calculations giving the static properties of molecules such as potential energy and electrostatic potentials etc.;
- Geometry optimisation which is a process that finds the set of molecular coordinates with the minimum potential energy;

- Molecular dynamic takes into consideration thermal motion, giving information on thermodynamic properties and the dynamic behaviour of molecules.<sup>105</sup>

The computer software employed for these studies was Hyperchem (fourth edition). This software employs two methods to computer structural and molecular properties, namely molecular mechanics and semi empirical quantum mechanics. Empirical methods have several advantages over ab-initio (from the beginning) methods. One it performs calculations much faster, especially when macromolecules are considered, and secondly much greater accuracy may be achieved when well parameterised systems are considered.<sup>105</sup> The disadvantages are that parameters for a specific class of molecule must be available and if not the development of such parameters is time consuming.

These two empirical methods will be briefly discussed: Molecular mechanics force fields use the equations of classical mechanics to describe the potential energy surface and physical properties of molecules. A molecule is described as a collection of atoms that interact with each other over a simple analytical function. This description is called a force field. One component of a force field is the energy arising from the stretching and compressing of bonds. This component is approximated as a harmonic oscillator using Hooke's law

$$V_{\text{spring}} = 1/2K_f(r - r_0)^2.$$

This gives the potential energy of a system  $V_{\text{spring}}$ , while  $r$  and  $r_0$  are the displaced and equilibrium bond distances and  $K_f$  is an interaction constant for a specific set of atoms considered.<sup>106</sup>

The potential energy of a molecular system in a force field is the sum of the individual components of the potential such as bond angles, and van der Waals potentials. The functions of these potentials are deviations of a molecule from a hypothetical molecule that has bonded interactions at minimum values. The absolute energy as calculated by molecular mechanics (MM) has no intrinsic physical meaning, and is thus only useful for comparison between molecules. The energies from single point calculations are related to enthalpies, but are not true enthalpies since they don't take into consideration thermal motion and temperature contributions.

Molecular mechanics does not treat electrons explicitly therefore it cannot describe bond breaking forming and systems that rely on electron delocalisation or orbital interactions. Quantum mechanics would be more useful in solving these problems. Semi-empirical methods<sup>106</sup> may be used to produce meaningful often quantitative results for large molecular systems. The roots of this method lie in the theory of  $\pi$  electrons, now largely superseded by all valence electron theories. Molecules consist of electrons and nuclei. Most applications separate the movement of electron and nuclei, this is known as the Born-Oppenheimer approximation. This model results in nuclei moving along a potential energy surface, with the electrons adjusting instantaneously.

Semi-empirical methods have the advantage of requiring no information about the location or geometry of bonds in molecule. Parameters for elements, usually derived from experimental data, are independent of the chemical environment. In contrast parameters used in molecular mechanics are often dependent on the molecular environment. With simple precautions semi-empirical methods can describe bond breaking. Semi-empirical calculations may be performed on over a 100 atoms without excessive computing time.

The theory behind computer modelling involves the concepts of potential energy surfaces and the distinction between classical and quantum treatments. Quantum mechanics finds the overall energy of a molecule by solving the Schrödinger equation for an electronic Hamiltonian.<sup>106</sup> Repeated solutions for different nuclear configurations, lead to some approximate potential energy surface. This procedure requires a solution albeit an approximate solution, for every Schrödinger equation associated with each of the varied conformations. This can be very time consuming and impractical especially when very large molecules are considered.

Molecular mechanics and semi-empirical methods were considered in this study as they were user friendly and gave more reliable results at a faster rate.

### **1.10 Objectives of this study**

It was hoped to establish a relationship between reaction rate and molecular properties for thiuram disulfides. It was decided to examine the linear free energy relationship of groups of thiuram disulfide accelerators, the objectives of the study were as follows:

- I. obtain a suitable method for the synthesis of thiuram disulfides;
- II. determine the rate of vulcanisation of the chosen thiuram disulfides in the particular model compound in the presence of sulphur;
- III. determine the rate of vulcanisation of the chosen thiuram disulfides in cis-1,4-polyisoprene in the presence of sulphur;
- IV. establish a relation between rate constants and various substituent constants;
- V. investigate whether the data obtained from the model compound experiments are in agreement with those obtained in the rubber system.

### 1.11 References

- 
- 1) E. W. Duck, Plastic and Rubbers, Philosophical Library Inc., New York, Chapter 5, (1971)
  - 2) W. Hofmann, Rubber Technology Handbook, Carl Hanser, Munich, (1989)
  - 3) V. A. Shershev, Rubber Chem. Technol. 55, 537 (1982)
  - 4) A.S. Kuz'minsky, C.M. Kavum, and V.P. Kirpichev, Physico-Chemical Foundations of Obtaining Processing and Application of Elastomers, Khimya, Moscow, 1976
  - 5) M. Porter, The Chemistry of Sulfides, Ed. A.V. Tobolsky, Interscience Publishers, New York, 165 (1968)
  - 6) F. W. H. Kruger and W. J. McGill, J. Appl. Polym. Sci., 42, 2669 (1991)
  - 7) M. Geysler and W. J. McGill, J. Appl. Polym. Sci., 60, 439 (1996)
  - 8) L. Bateman, C. G. Moore, M. Porter, B. Saville, Chemistry of Vulcanization; The Chemistry and Physics of Rubber-like Substances, Ed. L. Bateman, Chapter 15, McLaren, London (1963)
  - 9) F. W. H. Kruger and W. J. McGill, J. Appl. Polym. Sci., 45, 563 (1992)
  - 10) S. R. Shelver, M. Shumane, M. H. S. Gradwell, W. J. McGill, J. Appl. Polym. Sci., 74, 1371 (1999)
  - 11) C. P. Reyneke-Barnard, M. H. S. Gradwell, W. J. McGill, J. Appl. Polym. Sci., 78, 1100 (2000)
  - 12) A. Y. Coran, Rubber Chem. Technol., 37, 689 (1964)
  - 13) A. Y. Coran, Rubber Chem. Technol., 38, 1 (1965)
  - 14) A. Y. Coran, Rubber Chem. Technol., 38, 1 (1965)
  - 15) M. M Coleman, J. R. Shelton and J. L. Koenig, Rubber Chem. Technol., 46, 957 (1973)

- 
- 16) M. Geysler and W.J. McGill, *J Appl. Polym. Sci.*, 60, 431 (1996)
  - 17) B. A. Dogadkin and V. A. Shershnev, *Rubber Chem. Technol.*, 33, 401 (1960)
  - 18) B. A. Dogadkin and V. A. Shershnev, *Chem. Abstr.*, 52, 10626c (1958)
  - 19) B. A. Dogadkin, V. A. Shershnev and A. V. Dobromyslova, *Chem. Abstr.*, 55, 5006c (1961)
  - 20) M. Shumane, *The Role of Dimethyldithiocarbamic acid in Accelerated Sulfur Vulcanization of Diene Rubbers*, PhD Thesis, University of Port Elizabeth, Port Elizabeth, South Africa (2001)
  - 21) S. R. Shelver, M. Shumane, M. S. H Gradwell and W. J. McGill, *J. Appl. Polym. Sci.*, 74, 1371-1379 (1999)
  - 22) M. Van der Horst, K. G. Hendrikse and C. D. Woolard, *J. Appl. Polym. Sci.*, 89, 47 (2003)
  - 23) P. J. Nieuwenhuizen, A. W. Ehlers, J. G Haasnoot, S. R. Janse, J Reedijk and E. J. Baerends, *J. Am. Chem. Soc.*, 121, 163 (1999)
  - 24) A. W. Hofmann, *The esters of thiocyanic acid isomers with mustard oils*. *Ber.*, 1, 169 (1868)
  - 25) W. F. Hester, to Rohm and Haas Co. Fungicidal composition, U.S.P. 2,317,765, Apr. 27, 1943. Re-issue No. 23,742, Nov. 24 (1953)
  - 26) A. W. Hofmann, *On ethylenediamine*, *Ber.*, 5, 241A (1872)
  - 27) D. O. Holland, *J. Chem. Soc.*, 2134 (1950)
  - 28) M. Remko and B. M. Robe, *J. Mol. Struct.*, 339, 125 (1995)
  - 29) S. J. Joris, K. I. Aspila and C. L. Chakrabarti, *J. Phys. Chem.*, 74, 860 (1970)
  - 30) G. Gattow, *Angew. Chem. Internal. Edit.* 5, 316 (1966)
  - 31) A. Ya. Yakubovitch and V. A. Klimova., *J. Gen. Chem. U.S.S.R., Eng. Transl.*, 9, 1777 (1939)
  - 32) D. Graig, A. E. Juve, W. L. Davidson, W. L. Semon and D. C. Hay, *J. Polym. Sci.*, 8, 321 (1952)
  - 33) W. Scheele and O. Lorenz, *Rubber Chem. Technol.*, 29, 894, (1956)
  - 34) I. Williams, E. I. duPont de Nemours & Co., *Derivatives of hexamethylenedithiocarbamic acid*. U.S. PATENT 2,187,719, Jan. 23 (1940)
  - 35) R. S. Johnson, to E. I. duPont de Nemours & Co., *Stabilization of derivatives of dithiocarbamic acids*. U.S. PATENT 2,665,285, Jan, 5 (1954)
  - 36) R. O. Jr. Beauchamp and T. P. Johnston, to Tennessee Corp. *Manganous dimethyldithiocarbamate stabilised with Zn dimethyldithiocarbamate*. U.S. PATENT 2,861,091, Nov, 18 (1958)

- 
- 37) C. B. Lunginbuhl, to E. I. Dupont de Nemours & Co., Process for improving the stability of Zn ethylenebisdithiocarbamate. U.S. PATENT 2,690,447, Sept. 28 (1954)
  - 38) C. B. Lunginbuhl, to E. I. Dupont de Nemours & Co., Process for the manufacture of Zn ethylenebisdithiocarbamate. U.S. PATENT. 2,690,448, Sept. 28 (1954)
  - 39) A. M. Nealand B. M. Sturgis, to E. I. duPont de Nemours & Co. Heavy metal salts of dithiocarbamate acids. U.S. PATENT 2,406,960, Aug. 22 (1942)
  - 40) R. J. Gobiell, to E. I. duPont de Nemours & Co. Process of producing metal salts of alkylene bisdithiocarbamic acids. U.S. PATENT 2,693,485, Nov. 2 (1954)
  - 41) R. L. Drexel, to E. I. duPont de Nemours & Co. Stabilized dithiocarbamate pesticidal composition. U.S. PATENT 2,797,881, June 25 (1957)
  - 42) R. O. Jr. Beauchamp, to Tennessee Corp. Stabilization of the Manganous salts of dimethyldithiocarbamic acid. U.S. PATENT 2,806,870, Sept. 17 (1957)
  - 43) G. D. Thorn and R. A. Ludwig, The Dithiocarbamates and Related Compounds. Elsevier Publishing Co., Amsterdam (1962)
  - 44) M. St. Flett, Characteristic Frequencies of Chemical Groups in the Infra-red, Elsevier Publishing Co., Amsterdam (1963)
  - 45) D. Oktavec, B. Siles, J. Remen, V. Konecny, G. J. Vaclav, Collect. Czech. Chem. Commun., 47, 112876-2881 (1982)
  - 46) J. E. Jansen and R. A. Mathes, J. Am. Chem. Soc. 77, 3431 (1955)
  - 47) M. Bentov, Synthesis of tetramethylthiuram disulfide-S<sup>35</sup>, Rapt. No. 832, Comm. Energie atomique (France), R., (1958)
  - 48) J. L. Cunneen and R. M. Russel, Rubber Chem. Technol., 43, 1215, (1970)
  - 49) A. J. Aarts and K. M. Baker, Kautsch. Gummi Kunstst., 37, 497 (1984)
  - 50) G. Ellis, P. J. Hendra, C. H. Jones and K. D. O. Jackson, Kautsch. Gummi Kunstst., 43, 118 (1990)
  - 51) D. D. Westler, Rubber Chem. Technol., 53, 1191 (1980)
  - 52) A. M. Zaper and K. J. L., Rubber Chem. Technol., 60, 252 (1987)
  - 53) A. M. Zaper and J. L. Koenig, Rubber Chem. Technol., 1987, 278 (1987)
  - 54) R. S. Clough and J. L. Koenig, Rubber Chem. Technol., 62, 908 (1978)
  - 55) S. R. Smith and J. L. Koenig, Rubber Chem. Technol., 65, 82 (1992)
  - 56) M. Andreis, J. Lui and J. L. Koenig, Rubber Chem. Technol., 62, 82 (1989)
  - 57) M. R. Krejsa and J. L. Koenig, Rubber Chem. Technol., 65, 956 (1992)

- 
- 58) J. A. McCleverty, S. Gill, R. S. Z. Kowalski, N. A. Bailey, R. Mulvaney and D. A. O'Cleirigh, *J. Chem. Soc., Dalton Trans* 627 (1983)
- 59) J. A. McCleverty, in *Sulfur, its Significance for Chemistry, for the Geo-, Bio-, and Cosmosphere and Tehnology, Studies in Inorganic Chemistry*, (Ed.:A. Muller and B. Krebs), Elsevier Science Publishers B.V., Amsterdam, p. 311 (1984)
- 60) J. Kelm and D. Gross, *Rubber Chem. Technol.*, 58, 37 (1985)
- 61) V. M. Bzhezovsky and G. A. Kalabin, in *Chemistry of Organosulfur Compounds. General Problems*, (Ed. L. I. Belen'kii), Ellis Horwood Limited, Chichester, p. 266 (1990)
- 62) Y. Wang, J. -H. Liao and C. -H. Ueng, *Acta Cryst.*, c42, 1420 (1986)
- 63) I. L. Karle, J. A. Estlin and K. Britts, *Acta Cryst.*, 22, 273 (1967)
- 64) J. H. M. V. d. Berg; E. F. J. Duynstee, P. J. D Maas, *Rubber Chem. Technol.*, 58, 58 (1985)
- 65) J. H. M. V. d. Berg, J. W. Beulen, J. M. H. Hacking, E. F. J. Duynstee, *Rubber Chem Technol.*, 57, 725 (1984)
- 66) E. F. J. Duynstee, *Kautschuk Gummi Kunstst.*, 40, 205 (1987)
- 67) P. Versloot, J. G. Haasnoot, J. Reedijk, M. van Duin, E. F. J. Duynstee, *J. Put, Rubber Chem. Technol.*, 65, 343 (1992)
- 68) J. R. Wolfe Jr., *Rubber Chem. Technol.*, 41, 1339 (1968)
- 69) F. K. Lautenschlaenger, *Rubber Chem. Technol.*, 53, 27 (1979)
- 70) F. K. Lautenschlaenger, P. Zeeman, *Rubber Chem. Technol.*, 52, 1030 (1979)
- 71) F. K. Lautenschlaenger, K. Edwards, *Rubber Chem. Technol.*, 53, 27 (1980)
- 72) E. C. Gregg, R. J. Latimer, *Rubber Chem. Technol.*, 57, 1056 (1984)
- 73) L. G. Boretti, C.D. Woolard, *Rubber Chem. Technol.*, 79, 135 (2006)
- 74) P. J. Nieuwenhuizen, *New Perspectives on Sulfur Vulcanisation*, PhD. Thesis, Rijks University, Leiden (1998)
- 75) B. Rochette, A. Sadr, M. Abdul and J. M. Vergnaud, *Thermochimica Acta*, 85, 415 (1985)
- 76) W. Scheele, *Rubber Chem. Technol.*, 34, 1306 (1964)
- 77) P. Gosh, S. Kantare, P. Patkar, J.M. Caruthers, V. Venkatasubramanian, *Rubber Chem. Technol.*, 76, 592 (2003)
- 78) R. H Campbell, R. W. Wise, *Rubber Chem. Technol.*, 37, 635 (1964)
- 79) R. H Campbell, R. W. Wise, *Rubber Chem. Technol.*, 37, 650 (1964)
- 80) R. Ding, A. I. Leonov, A. Y. Coran, *Rubber Chem. Technol.*, 69, 81 (1996)

- 
- 81) R. Ding, A. I. Leonov, *J Appl. Poly. Sci.*, 61, 455 (1996)
  - 82) D. Chapman, *J. Elast. Plastics*, 10, 129 (1978)
  - 83) V. Duchacek, *J Appl. Poly. Sci.*, 15, 2079 (1971)
  - 84) V. Duchacek, *J Appl. Poly. Sci.*, 18, 125 (1974)
  - 85) V. Duchacek, *J Appl. Poly. Sci.*, 19, 1617 (1975)
  - 86) G. K. Taylor, E. S. Castner, V. Gallatsatos, *J. Chem. Soc. Faraday Trans.*, 91, 2655 (1995)
  - 87) A. P. Le Parlouer and J. M. Vergnaud, 3<sup>rd</sup>. *Internat. Conf. "Computers and Chemical Engineering"*, Paris April 19-21 (1983)
  - 88) Wheland and Pauling, *J. Am. Chem. Soc.*, 57, 2086 (1935)
  - 89) S. Siegel and J. M. Komarmy, *J. Am. Chem. Soc.*, 82 (1959)
  - 90) B. Miller, *Advanced Organic Chemistry Reaction Mechanisms*, Prentice Hall, New Jersey (1998)
  - 91) N. B. Chapman and J. Shorter Ed., *Correlation Analysis in Chemistry*, Plenum Press, New York, p. 87 (1978)
  - 92) C. D. Johnson, *The Hammett Equation*, Cambridge University Press, Cambridge, 1 (1973)
  - 93) L. P. Hammett, *J. Am. Chem. Soc.*, 59, 96 (1937)
  - 94) Y. Ogata, A. Kawasaki and N. Okumura, *J. Org. Chem.*, 29, 1985, (1964)
  - 95) Y. Okamoto, T. Inukai and H.C. Brown, *J. Am. Chem. Soc.*, 80, 4972 (1958)
  - 96) J. L. Dektar and N. P. Hacker, *J. Org. Chem.*, 53, 1935 (1988)
  - 97) M. Charton and H. Meislich, *J. Am. Chem. Soc.*, 80, 5940 (1958)
  - 98) J. D. Roberts and W. T. Moreland, Jr., *J. Am. Chem. Soc.*, 75, 2167, (1953)
  - 99) R. W. Taft, Jr. in *Steric Effects in Organic Chemistry*, M. S. Newman, ed, John Wiley, New York (1956)
  - 100) J. Shorter, in *Advances in Linear Free Energy Relationships*, N.B. Chapman and J. Shorter, eds., Plenum Press, New York 71-118 (1972)
  - 101) E. Morita, *Rubber Chem. Technol.*, 57, 746 (1984)
  - 102) A. B. Sullivan, L. H. Davis and O. W. Maender, *Rubber Chem. Technol.*, 56, 1061 (1983)
  - 103) F. Ignatz-Hoover, A. R. Katritzky, V. S. Lobanov and M Karelson, *Rubber Chem. Technol.*, 72, 318 (1999)
  - 104) G. H. Grant and W. G. Richards, *Computational Chemistry*, Oxford University Press, Oxford (1996)
  - 105) F. Jansen, *Introduction to Computer Modelling*, John Wiley and Sons, New York (1999)



---

106) C. J. Cramer, Essentials of Computational Chemistry, John Wiley and Sons, Ltd., England (2002)

## 2 Experimental

---

2.1	Materials.....	54
2.2	Purification of industrial chemicals.....	56
2.2.1	Purification of 2-mercaptobenzothiazole (MBT).....	56
2.2.2	Purification of 2-bismercaptobenzothiazole-2,2'-disulfide (MBTS).....	56
2.3	Instrumentation.....	56
2.3.1	Balances.....	56
2.3.2	Differential scanning calorimetry (DSC).....	57
2.3.3	Thermogravimetric analysis (TGA).....	57
2.3.4	Nuclear magnetic resonance (NMR) spectrometry.....	58
2.3.5	Infra-red (IR) spectroscopy.....	59
2.3.6	Brabender plasticorder.....	59
2.3.7	Mill.....	59
2.3.8	Rheometer.....	59
2.3.9	Press.....	60
2.3.10	Chromatography.....	60
2.4	Experimental Procedure.....	60
2.4.1	Sample preparation and reaction.....	60
2.4.2	Model compound vulcanisation.....	61
2.4.3	Compounding.....	61
2.4.4	Peroxide detection.....	63
2.4.5	Hammett plot substituent constant ( $\sigma$ ) conversion.....	63
2.4.6	Computer Modelling.....	65
2.4.7	Data presentation.....	65
2.5	References.....	66

## 2.1 Materials

The chemicals used in this study are listed below in Table 2.1. The industrial grade materials found in the table below, were purified according to section 2.2.

Table 2.1: Materials used in this study

Acetone	SMM Instruments, Vorna Valley, South Africa, AG
3-Aminophenol	Fluka, Buchs, Switzerland, 98%
$\sigma$ -Anisidine	Hopkin & Williams, Chadwell Heath, England, AG
Benzene	SMM Instruments, Vorna Valley, South Africa, AG
2-bisbenzothiazole-2,2'-disulfide (MBTS)	Bayer, Leverkusen, Germany
Carbon disulfide	Saarchem, Midrand, South Africa, 99.5%
Carbazole	Hopkin & Williams Ltd, Chadwell Heath, England
Chloroform	Saarchem, Midrand, South Africa, AG
cis-1,4-polyisoprene (IR)	Dunlop Tyres, Durban, South Africa
Copper (II) sulfate	Merck, Midrand, South Africa, 99%
Deuterated chloroform	Merck, Darmstadt, Germany, 99.8%
Deuterated dimethyl sulfoxide	Merck, Darmstadt, Germany, 99.8%
Diacetonamine hydrogenoxalate	Aldrich Chemical Company, Inc, Milwaukee, USA, 98%
Dibenzylamine	Fluka, Buchs, Switzerland, 95%
Dichloromethane	SMM Instruments, Vorna Valley, South Africa, AG
Diethyl ether	SMM Instruments, Vorna Valley, South Africa, 95%
Dimethyl aniline	May & Baker Ltd, Dagenham, England, 95%
$p$ -(2,4-Dinitroanilino)phenol	Janssen Chimica, Beerse, Belgium
Dicyclopentamethylenethiuram disulfide	Robinson Brothers Ltd, West Bromwich, England
Ethanol	SMM Instruments, Vorna Valley, South

	Africa, 99.9%
Filter Paper Whatman 40	Ashless, Clifton, USA(12.5 cm)
Hexane	Saarchem, Midrand, South Africa, AG
2-Mercaptobenzothiazole	Bayer, Leverkusen, Germany
Methanol HPLC Grade	Fluka, Buchs, Switzerland, 99.9%
Morpholine (MBT)	Saarchem, Midrand, South Africa, 99%
Petroleum ether (60-80°C)	SMM Instruments, Vorna Valley, South Africa, 90%
Phosphorous (V) oxide	Riedel-de-Haen, Seelze, Germany, AG
Piperidine	Saarchem, Midrand, South Africa, 98%
Potassium hexacyanoferate (iii)	Saarchem, Midrand South Africa, 99%
Potassium hydrogen phthalate	Riedel-de-Haen, Seelze, Germany , 99.5%
Quinoline	Hopkin & Williams Ltd, Chadwell Heath, England, 97%
4-sec-butylaniline	Aldrich Chemical Company, Inc, Milwaukee, USA, 98%
Silica gel 60	Merck, Wadeville, South Africa, Particle size 0.063-0.200 nm
Sodium diethyldithiocarbamate	Aldrich Chemical Company, Inc, Milwaukee, USA, 98%
Sodium dimethyldithiocarbamate hydrate	Aldrich Chemical Company, Inc, Milwaukee, USA, 98%
Sodium hydroxide	SMM Instruments, Vorna Valley, South Africa, AG
Sulfur	AECI, Modderfontein, South Africa
Squalene	Aldrich Chemical Company, Inc, Milwaukee, USA, AG
Tetraethyl thiuram disulfide (TETD)	Fluka, Buchs, Switzerland, 98%
Tetrahydrofuran	Saarchem, Midrand, South Africa, AG
Tetramethyl thiuram disulfide (TMTD)	Bayer, Leverkusen, Germany
TLC Aluminium Sheets Silica Gel 60	Merck, Darmstadt, Germany
Toluene	SMM Instruments, Vorna Valley, South Africa, 92%
p-Toluidine	Riedel-de-Haen, Seelze, Germany, AG
Zinc dibenzylthiocarbamate	Flexsys, St Stevens, Belgium

## 2.2 Purification of industrial chemicals

### 2.2.1 Purification of 2-mercaptobenzothiazole (MBT)

MBT was recrystallised from boiling benzene (b.p 80.1°C).<sup>1</sup> The recrystallisation was performed in a fume hood with the aid of protective eye wear and nitrile gloves, due to the carcinogenic nature of benzene. The boiling benzene was saturated with MBT and then filtered while hot to remove any solid impurities. The solution was then cooled, accompanied by the crystallisation of MBT. The MBT was then filtered. The MBT was then rinsed with cold benzene. The MBT was then dried in a vacuum desiccator containing P<sub>2</sub>O<sub>5</sub>. Purity was established by reverse phase high performance liquid chromatography (RP-HPLC), nuclear magnetic resonance (NMR) and differential scanning calorimetry (DSC).

### 2.2.2 Purification of 2-bismercaptobenzothiazole-2,2'-disulfide (MBTS)

MBTS was purified in an analogous manner to MBT. The purity was established by means of RP-HPLC, NMR and DSC.

## 2.3 Instrumentation

### 2.3.1 Balances

Three balances (Table 2.2) were used to weigh off reaction starting materials, curatives and rubber.

Table 2.2: Balances used in this study

Analytical balance	Sartorius BP 110S	(± 1×10 <sup>-4</sup> g)
Microbalance	Mettler MX 5	(± 1×10 <sup>-6</sup> g)
Top pan balance	Mettler BB 240	(± 1×10 <sup>-3</sup> g)

### 2.3.2 Differential scanning calorimetry (DSC)

Differential scanning calorimetry was used in conjunction with thermogravimetric analysis to investigate the reactions occurring between curatives used in this study. DSC was also used to determine the melting points of compounds and gave a good indication of compound purity<sup>2</sup>.

The DSC experiments were run in a TA Instruments Q100 DSC, connected to TA Q series software while the data analysis was performed using the Thermal Advantage Software. High purity nitrogen gas with a constant flow rate of 50 mL/min was used as the purge gas. Samples of approximately 15 mg were sealed in aluminium pans and run at 5°C/min for the dynamic studies where curative interactions were monitored, and 10°C/min for the melting point determinations. An empty sealed aluminium pan served as the reference in all the experiments.

The DSC was calibrated for heat capacity using a sapphire disc and temperature was calibrated for against the melting points of the metals in Table 2.3.

Table 2.3: Temperature calibration metals

Mercury	-38.83°C
Indium	156.61°C
Tin	231.88°C

### 2.3.3 Thermogravimetric analysis (TGA)

Mass loss determinations were conducted in a TA Instruments TG 2050 thermogravimetric analyser connected to a TA Instruments Thermal Analysis 2000 system. The dynamic studies involving the curatives were performed in a 100 µL Pt cradle with the instrument set at a 5°C/min heating rate.

High purity nitrogen at a flow rate of approximately 100 mL/min was used as the purge gas. This method of analysis also proved useful in determining the amount of inorganic

oxidant present in the synthesised accelerators; thus providing a useful technique to monitor compound purity after different purification steps. Samples with a mass of approximately 20 mg were used throughout this study.

The internal temperature calibration of the TGA furnace was performed by Curie point temperature ( $T_c$ ) calibration method. The metals used to include all useful experimental ranges are listed in Table 2.4.

Table 2.4: TGA Curie point calibration standards<sup>2,3</sup>

Metal	Curie temperature
Alumel	154.2°C
Nickel	355.3°C
Perkalloy	596°C
Iron	780°C

The mass was calibrated with accurately pre-weighed 100 mg and 1000 mg calibration pieces.

#### **2.3.4 Nuclear magnetic resonance (NMR) spectrometry**

300MHz proton ( $^1\text{H}$ ) and carbon ( $^{13}\text{C}$ ) spectra were recorded on a Bruker Spectrospin NMR spectrometer using either  $\text{CDCl}_3$  or  $\text{DMSO-d}_{6-x}$  as solvent. Recorded spectra were obtained from samples prepared by purification and synthesis. It should be noted that for both the  $^1\text{H}$  and  $^{13}\text{C}$  spectral assignments, symmetry needs to be taken into consideration with only half the number of protons being reported as a result of symmetry. It is noted that the  $^{13}\text{C}$  spectra introduce complexities where more carbon peaks are observed than one might expect, if a molecule were perfectly symmetrical in structure. These differences are elucidated by molecular modelling and interpreted in the relevant sections. Sample spectra are shown in the appendices.

### **2.3.5 Infra-red (IR) spectroscopy**

Infrared spectra of the compounds were determined on a Perkin Elmer 1600 series FTIR instrument. All samples were run with  $\text{CHCl}_3$  as the solvent, with the solutions having concentrations in the range of 5-7% (Mass/Volume). IR cells that had NaCl windows and path length of 1 cm were used.

### **2.3.6 Brabender plasticorder**

The rubber compounds were compounded on a Brabender Plasticorder, which was fitted with a W30 type mixing head with a 30 mL mixing capacity. The mixing head which was attached to the Brabender Plasticorder was connected to a PL2200 interface which allowed the mixes torque time profiles to be monitored via a Brabender Winmix programme.

### **2.3.7 Mill**

The rubber compounds prepared on the Brabender Plasticorder were milled on a Schwabenthan mill with the roller speeds set at 13.1 rpm and 11.6 rpm and approximate mill nip size of 4 mm.

### **2.3.8 Rheometer**

The cure characteristics of the compounds prepared on the Brabender Plasticorder and mill were determined on a Monsanto 100 Rheometer. The cure characteristics were determined at 150°C and the cure time for 95% cure ( $\tau_{95}$ ) recorded.

The data is presented by means of relative torque vs. time curves. The use of “relative torque” is essential since the instrument that was used was not calibrated for torque thus absolute readings in N.m could not be stated. It should be noted that reproducible changes in torque are observed. Even when instruments are calibrated a comparison of results obtained between different instruments seldom coincide. This variation may be further exacerbated by using instruments that employ different experimental set ups to obtain the torque vs. time curves. This problem is experienced when comparing the



torque vs. time data obtained from a Monsanto rheometer with that derived from an Agfa Vulkameter.

### **2.3.9 Press**

The samples prepared on the Brabender Plasticorder and mill were placed in small rubber moulds and pressed isothermally at 150°C for the desired length of time as determined by rheometry ( $\tau_{95}$  time). At the end of each press the samples were removed from the mould and placed in cold water to quench any further reaction.

### **2.3.10 Chromatography**

Reverse phase high performance liquid chromatography (RP-HPLC) was performed with a Waters HPLC system comprising of a Waters 510 and 515 pumps and a Model 2487 dual wavelength ultraviolet detector. A Model 660 solvent programmer controlled the pumps. Gradient and isocratic elution methods were both employed in this study. The gradient programmer allowed for the possible implementation of 10 different gradients<sup>4</sup>. The steeper the slope the faster the rate of change from a methanol water composite mobile phase to a 100% methanol mobile phase.

The type of elution system employed in each of the systems under consideration will be mentioned in the relevant chapters to follow. A constant flow rate of 1 mL/min was programmed for both the isocratic and gradient elution methods. Samples to be analysed were separated on a Waters Symmetry Column (particle size = 5  $\mu\text{m}$ , 250 nm  $\times$  4.6 mm ID) stainless steel column and the detector's wavelength set at 260 nm with the sensitive set at 1 AUFS (absorbance units full scale). Data from the UV detector was captured, analysed and stored using Peak Simple Software.

## **2.4 Experimental Procedure**

### **2.4.1 Sample preparation and reaction**

Curatives were accurately weighed on a microbalance and ground together with a mortar and pestle to obtain a master batch. A 1:1 molar ratio of accelerator to sulfur was used in each of the experiments. Samples were removed from the master batch and weighed in pre-weighed DSC pans, which were then encapsulated and sealed. The pans were placed in the DSC and then heated for various time periods at 150°C. In the text this is referred to as an isothermal study.

For the dynamic studies curative interactions were monitored at a heating rate of 5°C/min for both DSC and TGA. For the DSC experiments the samples were prepared as above. The samples for the TGA were removed from the master batch and placed directly on the platinum cradle of the TGA.

#### **2.4.2 Model compound vulcanisation**

The model compound vulcanisation studies were performed in evacuated sealed glass ampoules. A model compound based on isoprene units / accelerator / sulfur molar ratio of 33.9:1.1:1 was used. The molar ratios were equated for use with 0.5 mL of the respective model compound, squalene. The molar ratio of squalene was, however, adjusted to 5.65:1.1:1 as squalene consists of 6 isoprene units.

The sealed ampoules containing the curatives were placed in a silicone oil bath at the required temperature (150°C) and agitated for the duration of the experiment. The ampoules were then immediately placed in liquid nitrogen to quench the reaction. The ampoules were then broken open and their contents dissolved with 50 mL tetrahydrofuran (THF). The solution was then transferred to a 100 mL volumetric flask and made up to the required volume with THF. The samples used for RP-HPLC analysis were prepared by transferring 5 mL of the above solution to a 25 mL volumetric flask and then made up to the required volume with methanol. All calibration curves required for the analysis were prepared by weighing the samples in an aluminium DSC pans which were then placed in respective 25 mL volumetric flasks. The standard samples were then dissolved in 10 mL dichloromethane and made to the required volume with methanol.

#### **2.4.3 Compounding**

The compounding of the rubber with various curatives was carried out using a Brabender Plasticorder fitted with a 30 mL mixing head, using a fill factor of 0.80. The ratio of curatives used was a 1:1 molar ratio of accelerator to sulfur. The rubber used was Nipol polyisoprene (IR) 2200, having a cis 1,4 content of 96%. Where the densities of the accelerators were unknown they were assumed to be 1.42 g/mL, which is the density of tetramethylthiuram disulfide (TMTD). The effect of any difference from 1.42 g/mL on the fill factor is negligible. This is primarily due to the fact that the mass of the curatives is low. The slight error in density allows for a minimal error in the calculated volume. Thus the approximate amount of polyisoprene required was determined by the equation below

$$m_r = \frac{V_h F_f}{\left( \frac{1}{\rho_r} + \frac{1}{100} \sum_{i=1}^n \left( \frac{phr_i}{\rho_i} \right) \right)}$$

$$m_i = \frac{phr_i m_r}{100}$$

where  $m_r$  = mass of polyisoprene (g)

$v_r$  = volume of mixing head (30 mL)

$F_f$  = fill factor (0.80)

$\rho_r$  = density of rubber (0.91 g/mL)

$\rho_i$  = density of ingredient (g/mL)

$phr_i$  = parts per hundred rubber for the ingredients

$m_i$  = mass of ingredient (g)

#### *Polyisoprene mixing procedure*

The mixing procedure for the various compounds prepared was as follows

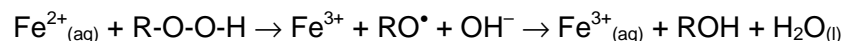
- I.  $T_{0-0.5 \text{ min}}$  added  $\frac{3}{4}$  polyisoprene at 60 rpm
- II.  $T_{0.5-1 \text{ min}}$  allowed polyisoprene to masticate
- III.  $T_{1-3 \text{ min}}$  added curatives
- IV.  $T_{3 \text{ min}}$  added remainder of polyisoprene

- V.  $T_{3-5 \text{ min}}$  mix at 60 rpm
- VI. Removed the compound from the mixing head and sheeted 10× on the mill

#### 2.4.4 Peroxide detection

Morgan and McGill<sup>5</sup> reported that methylenic model compounds reacted with oxygen at room temperature to produce hydroperoxide. 3-Hydroxyperoxide-2,3-dimethyl-1-butene was produced from 2,3-dimethyl-2-butene (TME). Morgan<sup>3</sup> noted that if the peroxides were not removed 2-mercaptobenzothiazole (MBT) and 2-bisbenzothiazole-2,2'-disulfide (MBTS) vulcanisation of TME did not correspond to the same system in polyisoprene. Therefore Morgan and McGill<sup>5</sup> indicated the need for peroxide removal or conversion of the peroxide to the alcohol to avoid interference with the MBT and MBTS vulcanisation. It has been shown that the alcohol that is formed doesn't interfere with MBT and MBTS accelerated sulfur vulcanisation of TME.

Peroxides may be removed from methylenic model compounds by reacting the model compound with aqueous ferrous sulfate.



Squalene was tested for the presence of peroxides using a Merckoquant® 1011 peroxidase enzyme test kit, with detectable concentrations ranging between 1 mg/mL and 25 mg/mL. No peroxides were detected in the squalene used for the experiments.

#### 2.4.5 Hammett plot substituent constant ( $\sigma$ ) conversion

The Hammett Equation (1) chiefly concerns aromatic substituents and the Taft (2) concerns mainly allylic groups taking into account a steric factor ( $E_s$ ).<sup>6</sup>

$$\log \frac{k}{k_0} = \rho \sigma \tag{1}$$

$$\log \frac{k}{k_0} = \rho^* \sigma^* + E_s \tag{2}$$

Aromatic and allylic groups may both be considered by Taft substitution constants ( $\sigma^*$ ). Where  $\sigma^*$  was not available, Hammett substituents constants were converted to  $\sigma^*$  constants. The  $\sigma^*$  constant of a polysubstituted phenyl group is the sum of the individual  $\sigma$  constants. The meta and para substituents on anilino groups are considered to have a negligible steric effect.

The  $\sigma^*$  constants of a substituted phenyl may thus be derived from  $\sigma$  constants by the following derived equation.<sup>7</sup>

Let (R) be a substituted phenyl and ( $\phi$ ) a phenyl group

$$\log \frac{k_R}{k_0} = \log \left( \frac{k_R}{k_\phi} \right) + \log \left( \frac{k_\phi}{k_0} \right) \quad (3)$$

by substituting in  $\log(k/k_0) = \rho\sigma$  and  $\log(k/k_0) = \rho^*\sigma^* + E_s$ , since  $\sigma_\phi = 0$  one obtains

$$\rho^*\sigma^*_R + E_{s,r} = \rho\sigma_R + (\rho^*\sigma^*_\phi + E_{s,\phi})$$

since the steric effect is negligible, assuming

$$E_{s,r} = E_{s,\phi}, \rho = \rho^*$$

And substituting  $\sigma_\phi^* = 0.6$ , which is the substitution constant for a phenyl<sup>8</sup> group one obtains

$$\begin{aligned} \sigma_R^* &= \sigma_R + \sigma_\phi^* \\ &= \sigma_R + 0.6 \end{aligned}$$

In the case of polysubstituted phenyl groups (R') with substituents  $R_1$ ,  $R_2$  and  $R_3$  one obtains

$$\sigma_{R'}^* = \sigma_{R1} + \sigma_{R2} + \sigma_{R3} + 0.6$$

#### 2.4.6 Computer Modelling

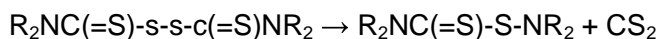
Computer modelling was performed using HyperChem™ (ed 4) from Hypercube, Inc. Parameters that were needed for this study were selected bond lengths and atomic charges specifically for the thiuram moiety. Energies of optimised geometries were also calculated. Geometry optimisation was performed using a molecular mechanics operation, making use of the Polak-Ribiere algorithm, with termination conditions for the RMS and maximum number of cycles set at 0.01 kcal/[Å mol] and 32000 respectively. This geometry optimisation protocol was employed for the determination of bond lengths and total energy. The atomic charges for the various molecules were determined by semi-empirical calculations, both CNDO and AM1 methods were employed. The calculation options were set so that the molecule's total charge was zero with a spin multiplicity of 1. The calculation made use of a Restricted Hartree-Fock (RHF) calculation with a convergence limit of 0.0001 and an interaction limit of 50. A single point calculation using this method was then ensued.

Where S-S dihedral angles are known due to the availability of crystal structure data, higher level computer modeling calculations were performed by Prof C McClelland using the computational chemistry program Spartan produced by Wavefunction Inc. (v1.0.1). This has specifically been done to determine whether computational molecular models are able to accurately predict thiuram disulfide dihedral angles. Prof C McClelland first ran a conformational search at the semi-empirical MO level (PM3), producing a list of conformers. The lowest energy structures were then refined at the DFT level.

#### 2.4.7 Data presentation

The concentration of reactants used in the reverse phase analysis has been quoted in molar units in all the diagrams. Polysulfide concentrations were not determined directly, but rather their peak areas were used as a rough indication of the relative amounts of total polysulfides present at each reaction interval. The polysulfide peaks were determined by a method used by Möckel<sup>9</sup> and Snow<sup>10</sup>, which states that log retention (Rt) time verses sulfur rank (i.e. number of sulfur atoms in a polysulfide) give a straight

line. This method is, however, limited to isocratic systems. When gradient separation was required for complete resolution of the desired products, the total polysulfide peak area was assumed to be the sum of all the peak areas between the accelerator and sulfur peaks. This is a large assumption, based on the assumption that the decomposition products, such as the amine would elute before the accelerator peak due to hydrogen bonding. Thioureas are often seen and are formed at elevated temperatures. However, they are much more polar than the thiuram disulfides and are found to elute even before the thiuram monosulfide very near the void volume for RP-HPLC. Some of the products may also be sulfenamides and polysulfide thereof as shown in the reaction below.



Graphs depicting reaction profiles, take into consideration the final concentration versus time.

## 2.5 References

- 1) R.C. Weast, Ed., CRC Handbook of Chemistry and Physics, 51<sup>st</sup> Ed., The Chemical Rubber Co. Publishers, Cleveland (1970)
- 2) P.K Gallagher, Handbook of Thermal Analysis and Calorimetry, Ed. M Brown, Chapter 4, Elsevier, USA (1998)
- 3) W.W.M. Wendlandt, Thermal Analysis, 3<sup>rd</sup> Ed., Wiley-Interscience Publishing, New York (1974)
- 4) Automated Gradient Operators Manual 660, Waters, 34 Maple Street, Millford, Massachusetts, 01757 (1983)
- 5) B. Morgan and W.J. McGill, J. Appl. Polym. Sci., 76, 1377, (2000)
- 6) R.W. Taft. Jr in "Steric Effects in Organic Chemistry", M.S. Newman, Ed., John Wiley & Sons, Inc., New York, 1956.
- 7) E. Morita, Rubber Chem. Technol., 57, 744, (1984)
- 8) E. Morita, Rubber Chem. Technol., 55, 352, (1982)
- 9) H.J. Möckel, J. Chromatogr. 317, 589 (1984)
- 10) N.H. Snow, J. Chem. Ed., 73, 592 (1996)

# 3 N,N'-diphenylthiuram disulfide

## rate study

---

3.1	Introduction.....	68
3.2	A synthetic approach for the production aromatic thiuram disulfides.....	73
3.2.1	Problems associated with the synthesis.....	73
3.2.2	Synthesis and purification of N,N'-diphenylthiuram disulfide.....	73
3.3	Reaction rate analysis .....	75
3.3.1	RP-HPLC analysis for the isothermal curative interactions and model compound study.....	75
3.3.2	Dynamic study of N,N'-diphenylthiuram disulfide sulfur interactions via thermal analysis .....	75
3.3.3	Curative interactions .....	78
3.3.4	Model compound reactions and rate analysis .....	78
3.3.5	Rate analysis of cis-1,4-polyisoprene, N,N'-diphenylthiuram disulfide and sulfur cured system .....	83
3.4	Computer modelling.....	86
3.5	References .....	88



### 3.1 Introduction

The synthesis of a variety of thiuram disulfide accelerators was attempted so that a correlation might be derived between molecular structure and free energy. The synthesis is a two step process. Firstly there is an addition reaction of an amine with carbon disulfide in basic medium to form the dithiocarbamate<sup>1,2</sup>. This is then followed by an oxidation reaction to produce the thiuram disulfide. The additions of both CS<sub>2</sub> and the oxidizing agent, K<sub>3</sub>Fe(CN)<sub>6</sub>, is performed over an hour in each of the steps, while the reaction mixture is maintained at approximately 5°C in an ice bath<sup>3</sup>.

It was initially decided to produce a series of aromatic thiuram disulfide accelerators from the aromatic dithiocarbamate derivative because substituted aromatics were readily available in these laboratories. It did, however, prove useful in the interim to introduce two other types of thiuram disulfide accelerators, cyclic aliphatics, to bridge the gap between linear aliphatics and the aromatic compounds.

There was concern expressed as to whether the phenyldithiocarbamate could be produced by this procedure, since Kelly in 1927 synthesised 2-mercaptobenzothiazole (MBT) by a similar reaction<sup>4</sup>.

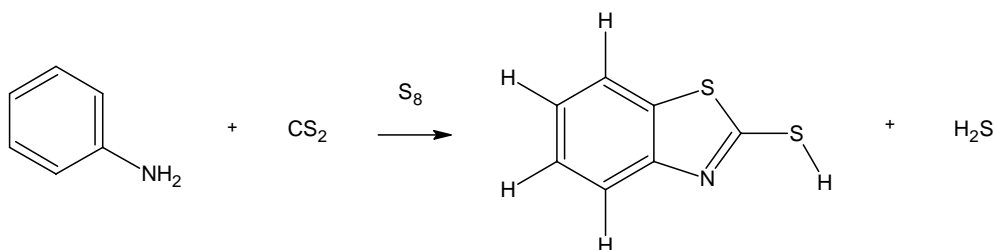


**Figure 3.1:** Synthesis of MBT at 250°C and 450 Psi

Kelly<sup>4</sup> performed the reaction at 250°C and 3102.6 kPa. One equivalent of sulfur was added. This is in contrast to the method used here: where the reaction was performed at ambient temperature and pressure and in a basic medium in the absence of sulfur.

The first step of the synthesis was performed (as shown in Figure 3.2) in an attempt to produce the dithiocarbamate. The product that was produced was white in colour. A non-destructive method, frontal analysis on a reverse phase C-18 column, was

used to purify the phenyldithiocarbamate salt, but owing to the compound instability, purification was incomplete. Dithiocarbamates are as unstable if not more unstable than their thiuram disulfide counter parts therefore a mild purification technique had to be employed. Marginal purification was achieved by means of frontal analysis making use of reversed phase C-18 silica column, in which all the silanol groups were end-capped with methyl groups. The crude sodium salt of the phenyldithiocarbamate was dissolved in degassed diethyl ether and applied to a 10 cm (2 mm diameter) reversed phase and eluted with the same degassed diethyl ether. The 10 mL of the eluent was collected and the solvent then evaporated off at room temperature and then analyzed.

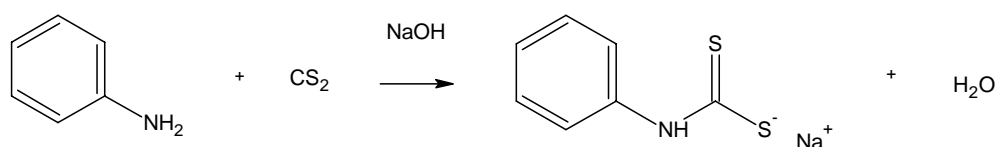


**Figure 3.2:** Synthesis of the sodium salt of phenyldithiocarbamate

A DSC scan showed the synthesized compound to differ from both MBT and MBTS.

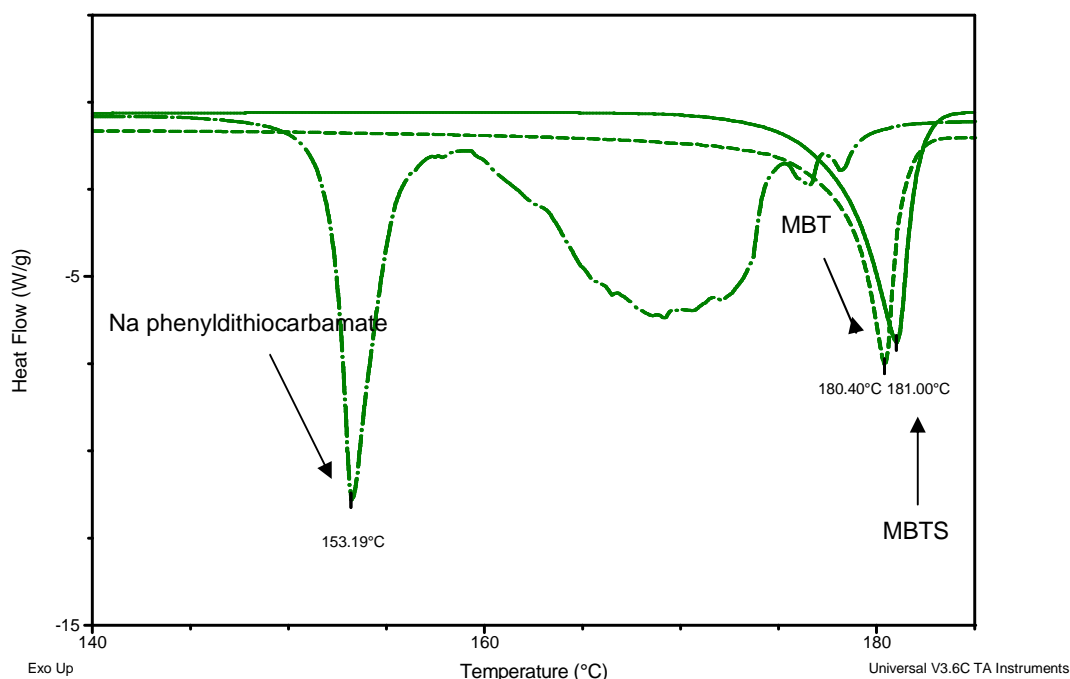


**Figure 3.3:** Comparison of the melts of the synthesized sodium salt of the phenyldithiocarbamate with MBT and MBTS

The sodium salt of the phenyldithiocarbamate melted at 145°C ( $T_{\text{onset}}$ ) with  $T_{\text{max}}$  occurring at 153°C while the MBT and MBTS melted within 2°C of one another at 178.54°C ( $T_{\text{onset}}$ ) with  $T_{\text{max}}$  occurring at 180°C and 178.54°C ( $T_{\text{onset}}$ ) with  $T_{\text{max}}$  occurring at 181°C respectively. Aldrich reports the melts as between 170 and 180°C<sup>5</sup>. A qualitative test was performed by means of the addition of  $\text{CuSO}_4 \cdot 7\text{H}_2\text{O}$ , which forms a red precipitate in the presence of a dithiocarbamate<sup>6</sup>. The red precipitate was observed for the sodium phenyldithiocarbamate that was produced. No such interaction was observed for MBT or MBTS.

NMR analysis proved very difficult as a result of impurities. It was possible, however, to observe that both compounds, MBT and the sodium salt of the phenyldithiocarbamate gave very different spectra. MBT's S-H was observed at a chemical shift ( $\delta$ ) of 11.2 ppm while the N-H for the sodium salt of phenyldithiocarbamate was observed at a  $\delta$  7.95 ppm (see Figures 3.4 and 3.5). MBTS's  $^1\text{H-NMR}$  was also run to eliminate speculation that it too may be formed during the synthesis, especially during the oxidation process to form the thiuram disulfide.

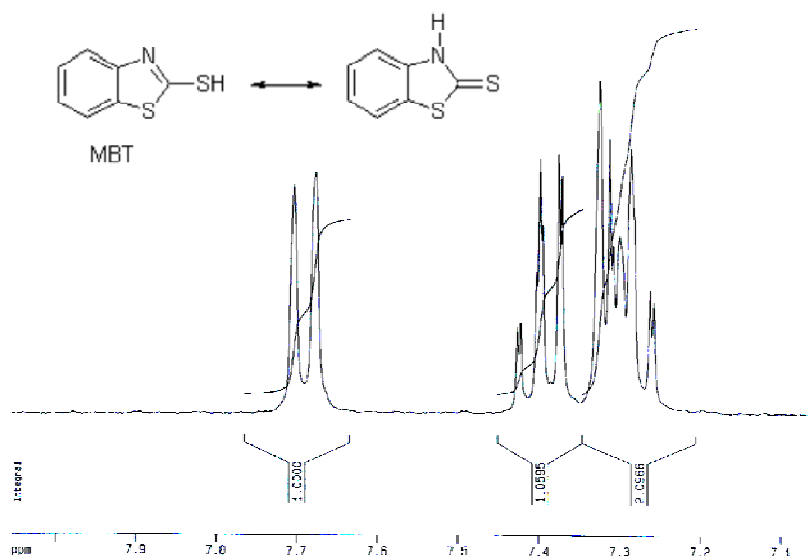


**Figure 3.4:**  $^1\text{H-NMR}$  of MBT with deuterated DMSO as solvent

Figure 3.5 depicts the complex  $^1\text{H-NMR}$  spectrum of MBT, which is further complicated by tautomerism as shown by the inset.

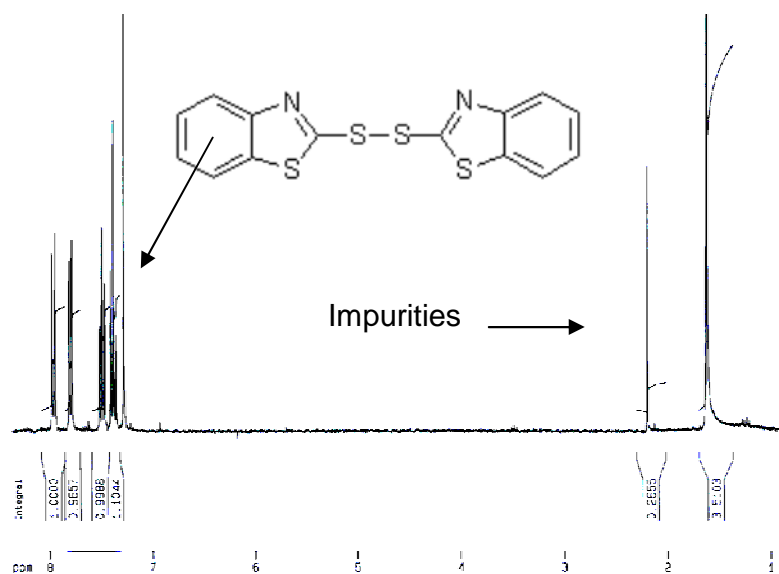


Figure 3.5:  $^1\text{H-NMR}$  spectrum of MBTS in  $\text{CDCl}_3$

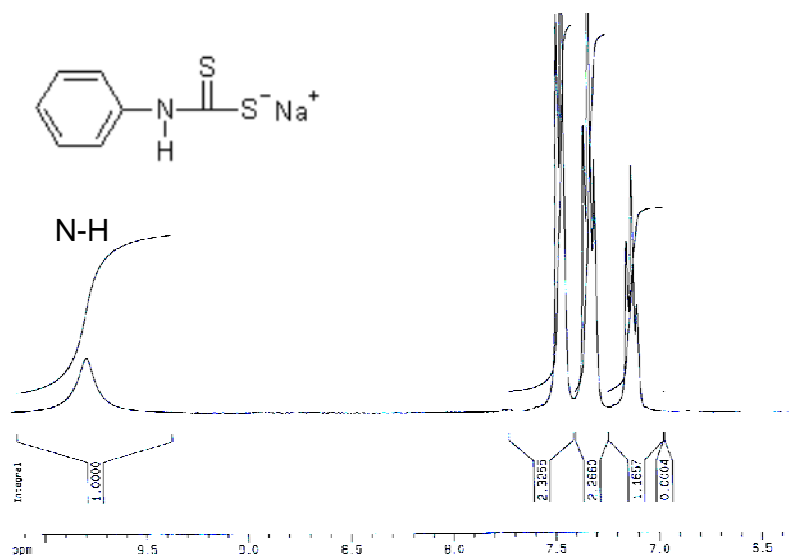


Figure 3.6:  $^1\text{H-NMR}$  for sodium phenyldithiocarbamate in DMSO

The IR's gave conclusive proof for the production of the sodium salt of the phenyldithiocarbamate, as signals were observed at  $4213.1\text{ cm}^{-1}$  and  $928.6\text{ cm}^{-1}$  for a N-H stretch and a C-N partially double bond character associated with all dithiocarbamates.<sup>7,8</sup>

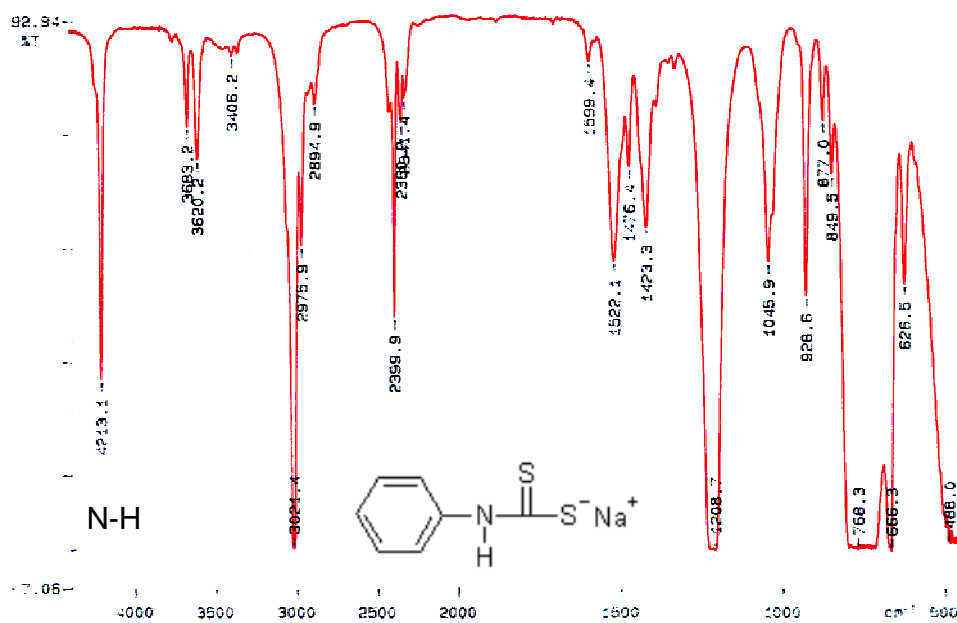


Figure 3.7: IR for sodium phenyldithiocarbamate in  $\text{CHCl}_3$

MBT showed a S-H stretch at  $3393.1 \text{ cm}^{-1}$  with no N-H stretches being observed.<sup>7,8</sup>

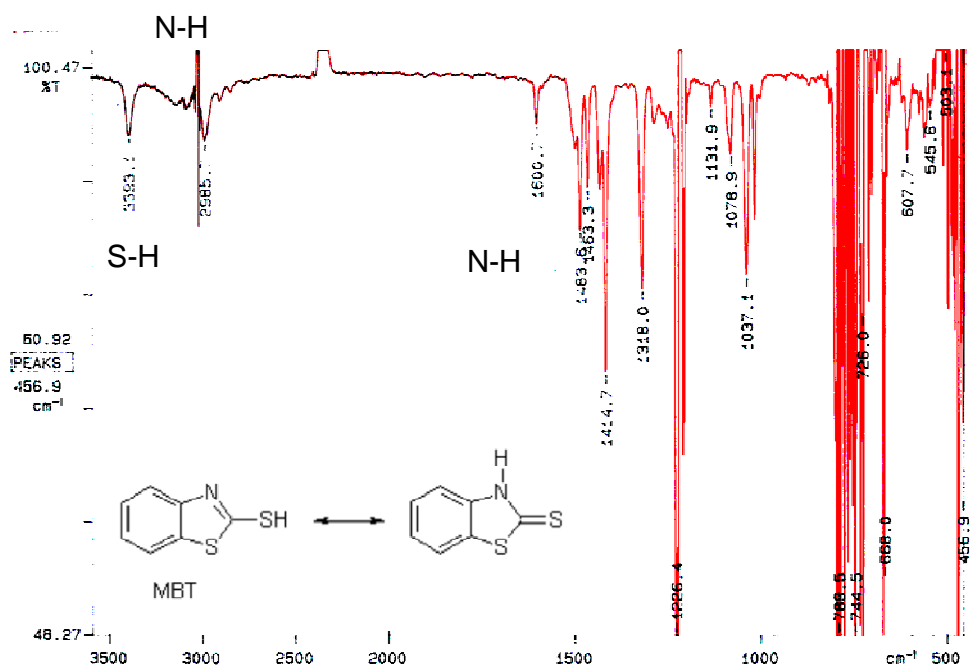


Figure 3.8: IR for MBT in  $\text{CHCl}_3$

The spectral differences are clearly depicted in the above figures, with the sodium phenyldithiocarbamate spectra being considerably different to those of MBT and MBTS.

## **3.2 A synthetic approach for the production aromatic thiuram disulfides**

### **3.2.1 Problems associated with the synthesis**

Numerous problems were associated with the synthetic process. A number of compounds could not be used as starting materials in the synthesis. It was discovered that *p*-(2,4-dinitroanilino)phenol could not be used to produce the dithiocarbamate. An appropriate solvent could not be found to successfully purify the product that formed. The melt was determined to be in the range of 170-190°C, while the starting material is known to melt at 191°C.

The synthesis of the diphenyldithiocarbamate was also unsuccessful. The product readily decomposed to diphenylaniline. The crude synthetic product was tested for the presence of dithiocarbamates by the addition of  $\text{CuSO}_4 \cdot 7\text{H}_2\text{O}$ <sup>6</sup>. This yielded a negative result.

The oxidation of the dithiocarbamates to produce the thiuram disulfide also proved to be difficult in some cases. 2,6-dimethylaniline as well as 3-aminophenol did react to produce the dithiocarbamate but oxidation to the thiuram disulfide did not occur. Most of the reactions that did occur, however, exhibited extremely low yields.

### **3.2.2 Synthesis and purification of N,N'-diphenylthiuram disulfide**

Distilled water (70 mL) was placed into a 250 mL double necked round bottomed flask. The reaction vessel was kept at approximately 5°C throughout the synthesis, while the reaction mixture was stirred continuously to prevent local excesses. NaOH (0.12023 mol, 4.8090 g) was added to the solution followed by aniline (0.05964 mol, 5.5541 g) which was redistilled under vacuum to yield a transparent liquid (b.p. 184°C<sup>9</sup>).  $\text{CS}_2$  (0.05966 mol, 3.6 mL) was then added drop wise over a period of an hour. The reaction mixture went from a light transparent homogenous mixture to a milky orange liquid. After the addition of all the  $\text{CS}_2$  the reaction mixture was stirred for a further hour with a steady  $\text{N}_2$  purge to remove any unreacted  $\text{CS}_2$ .  $\text{K}_3\text{Fe}(\text{CN})_6$

(0.05966 mol, 59.6285 mL of a 1.0001 M solution) was then added to the reaction mixture over a two hour period, the reaction mixture then went yellow with a brown precipitate.

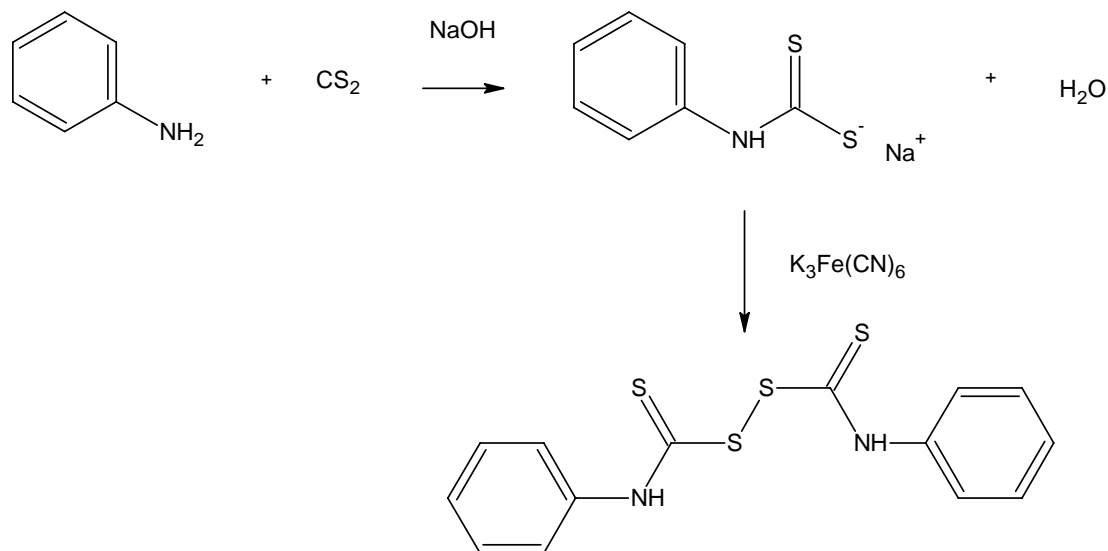


**Figure 3.9:** Synthetic scheme for the synthesis of N,N'-diphenylthiuram disulfide

The compound was filtered and then rinsed in the filter paper with cold water. A 30 cm silica gel column was prepared in a 50:50 (volume ratio), dichloromethane:diethyl ether. The crude compound was then dissolved in a 90:10 dichloromethane:diethyl ether solvent and applied to the column. 50:50 dichloromethane:diethyl ether was used as the mobile phase, requiring 700 mL to elute all the compound from the column. The eluent that remained was a transparent orange colour. This solution was then evaporated off to leave an orange compound. This compound was then recrystallised by means of a miscible solvent method. A minimum amount of dichloromethane was added to the compound to dissolve it and crystallization was achieved by the addition of toluene. This was performed five times. Purity was established via RP-HPLC, DSC, TLC (80:20 dichloromethane:diethyl ether) and NMR. NMR did, however, show the presence of solvent peaks. The reaction yield was 14.54% (1.4591 g) and the melting point was determined to be in the range 149.3°C-155.1°C. IR (CHCl<sub>3</sub> cm<sup>-1</sup>) 4211.3, 3695.2, 3069.1, 2400.0, 1597.6, 1520.1, 1349.0, 926.0, 814.3. <sup>1</sup>H-NMR (CDCl<sub>3</sub>) 7.85 (1H, s, NH), 7.42 (4H, m, ArH), 7.28 (1H, m, ArH). <sup>13</sup>C-NMR (CDCl<sub>3</sub>) 180.41, 137.49, 130.02, 127.53, 125.67.

### 3.3 Reaction rate analysis

#### 3.3.1 RP-HPLC analysis for the isothermal curative interactions and model compound study

HPLC samples for the isothermal curative interactions were initially prepared by dissolving the reaction mixture prepared in the opened DSC pans, in a 25 mL volumetric flask by means of the addition of 5 mL dichloromethane followed by the addition to the mark of HPLC grade methanol. It was, however, discovered that product solubilisation was not completely achieved. This was overcome by increasing the amount of dichloromethane added to 10 mL. For the model compound reactions products solubilisation was achieved by the addition of 100 mL tetrahydrofuran in a 100 mL volumetric flask.

Compound separation for the isothermal study was achieved using a C-18 reverse phase column with pure methanol as the mobile phase. Model compound reaction product separation was achieved using a 90:10 (vol:vol) methanol:water mobile phase. In both cases the detector was set at a wavelength of 260 nm.

#### 3.3.2 Dynamic study of N,N'-diphenylthiuram disulfide sulfur interactions via thermal analysis

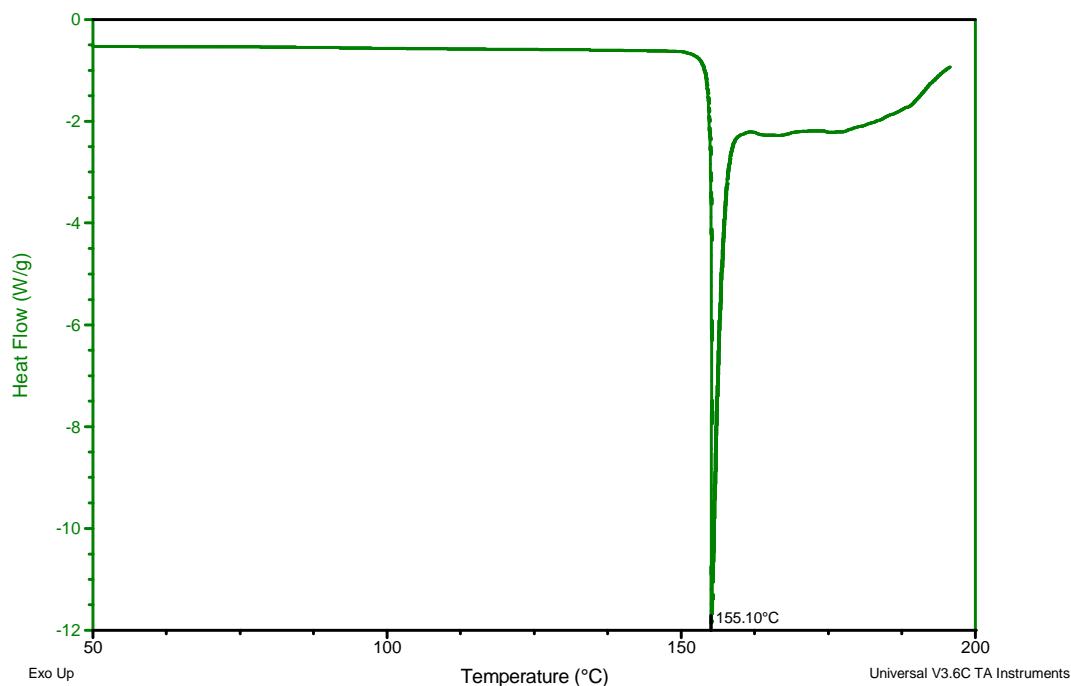
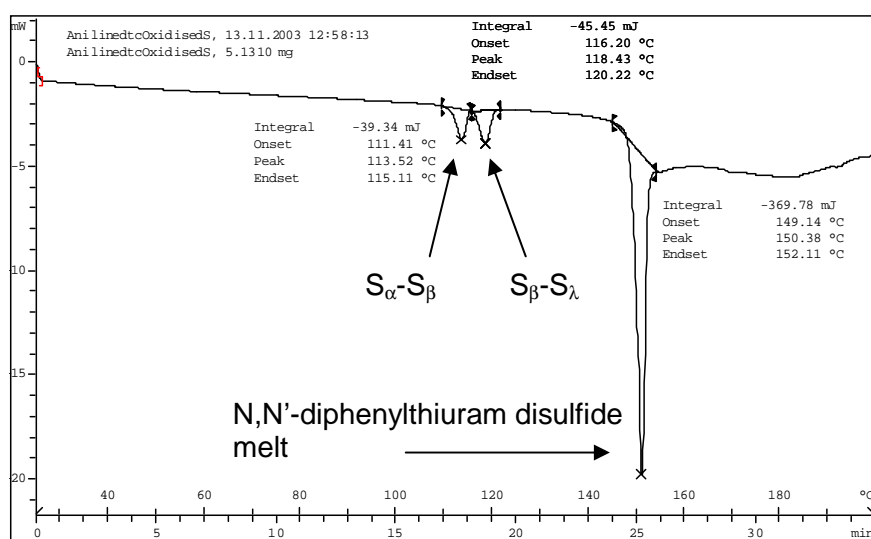


Figure 3.10: Thermogram depicting the melt of N,N'-diphenylthiuram disulfide



The N,N'-diphenylthiuram disulfide that was synthesised was determined to have a melt onset of 149.3°C with the peak maximum occurring at 155.1°C. The melt was then followed by a decomposition from just before 161.4°C to 195.1°C which was accompanied by gas evolution. This is indicated by the wider endotherm superimposed on the sharp melting endotherm.

It can be seen from the thermogram in Figure 3.11 that the degree of interaction between that accelerator and sulfur is minimal, as seen by the maintenance of the discrete sulfur and accelerator transitions and melt respectively. This would indicate a low tendency to form polysulfidic species which are the active sulfurating agents in thiuram disulfide vulcanisation. This would thus hint at the N,N'-diphenylthiuram disulfide being a poor accelerator as was seen with the model compound reaction studies (see Section 3.3.4). The transitions seen between 100 and 120°C are associated with sulfur transitions. The transition of  $S_{\alpha} - S_{\beta}$  occurring at 107.0°C, while the natural melting point that results from autodissociation resulting from solvent effects occurs at approximately 114.6°C.<sup>10,11</sup>



**Figure 3.11: A DSC Thermogram depicting the heat of N,N'-diphenylthiuram disulfide with sulfur**

The accelerator is seen to melt at 150.4°C. This is 5°C lower than expected, but this may be ascribed to a drift in the temperature calibration of the instrument or the existence of a simple freezing point depression when the sulfur and accelerator are mixed (as in the formation of a simple eutectic system). These samples were run on

a Mettler Toledo DSC 820 at the then Port Elizabeth Technikon (Nelson Mandela Metropolitan University North Campus).

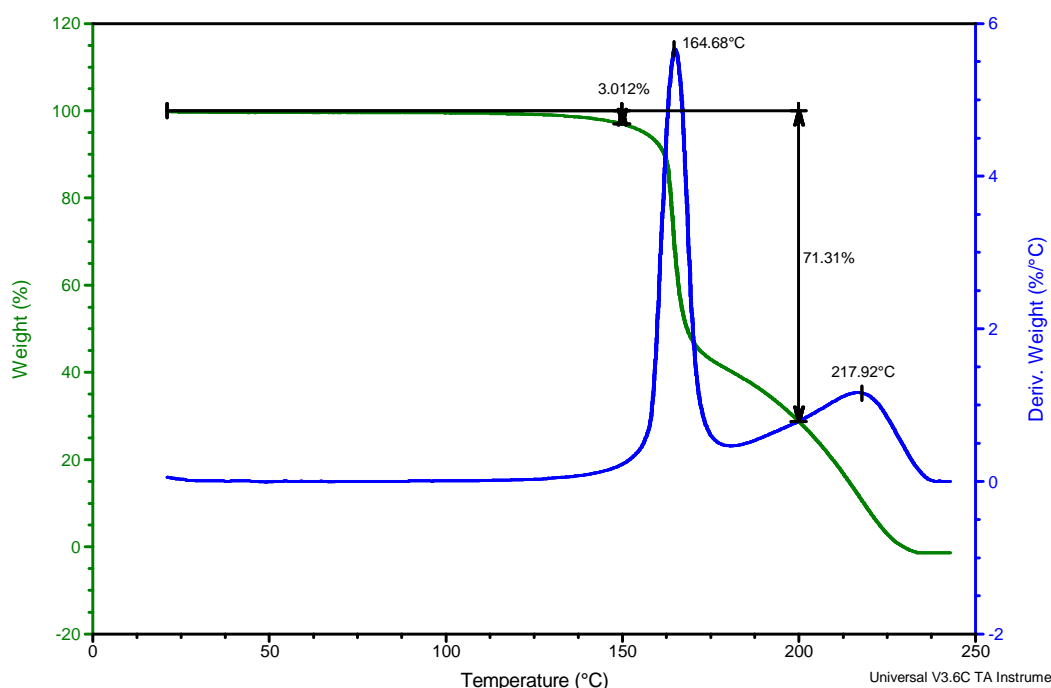


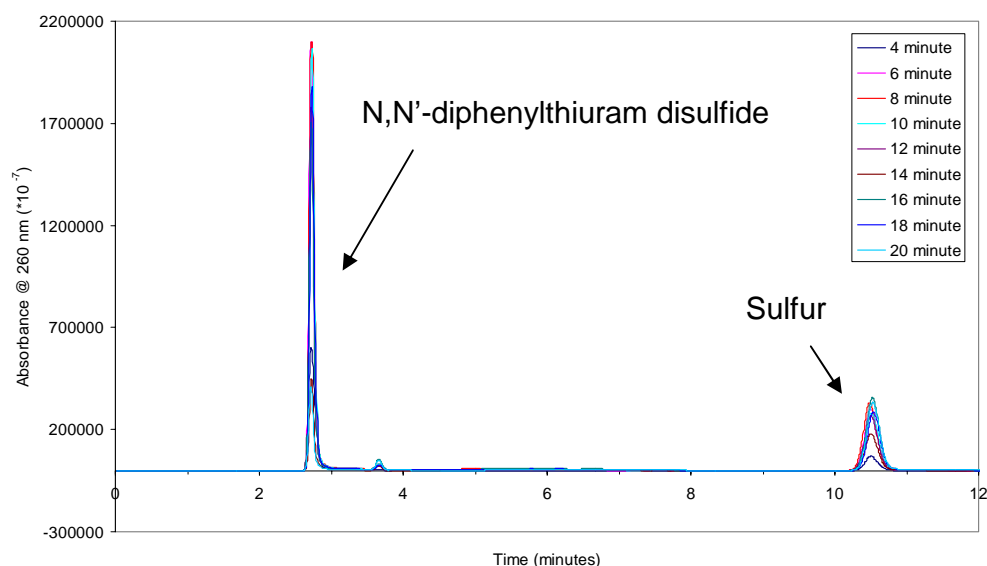
Figure 3.12: A TGA Thermogram depicting the heating of N,N'-diphenylthiuram disulfide with sulfur

Figure 3.11 depicts the well-defined melts of the two components with little or no interaction between them. It is likely that mutual solubilisation of the sulfur and accelerator occurs to a very small extent as both compounds display melting behaviour typical of the separate pure compounds. A mass loss of 71% at 200°C is depicted in Figure 3.12, for the heating of accelerator with sulfur. A mass loss approximately 3% is seen at 150°C, the temperature at which the vulcanisation was performed in this study. This is primarily due to the decomposition of the accelerator to volatile by-products accompanied by the evaporation of molten sulfur and accelerator. Since sulfur boils at 444.6°C,<sup>12</sup> one may assume that the mass loss due to the evaporation of sulfur would be low. This would, however, be erroneous. Figure 3.12 depicts a 100% mass loss at 240°C, a temperature well below the boiling point of sulfur. Sulfur may readily evaporate at a temperature above the sulfur melt (114.6°C)<sup>10,11</sup> when the sample mass is low. The Derivative curve of the mass loss in Figure 3.12 clearly depicts the first mass loss to be that of the accelerator associated with a peak maximum at 164.68°C while the second may be due to the loss of

sulphur and residual accelerator and/or its derivatives with the corresponding peak maximum at 217.9°C.

### 3.3.3 Curative interactions

The low reactivity of N,N'-diphenylthiuram disulfide may be seen in the isothermal curative interaction studies. The chromatograms shown in Figure 3.13 depict the presence of three different compounds: two of which are the expected N,N'-dianilinthiuram disulfide and sulfur peaks at 3.1 and 26.3 minutes respectively. The accelerator does not exhibit the prolific tendency of common accelerators (such as TMTD and TETD) to produce a large number and varied spectrum of polysulfides which would elute between the disulfide and the sulfur.



**Figure 3.13:** Chromatogram depicting the isothermal curative interactions of N,N'-diphenylthiuram disulfide with sulfur

This may be as a result of more energy required for the homolytic cleavage of the disulfide linkage. One may also interpret the homolytic product to be less stable as result of greater resonance stabilization in the undissociated structure, which contains two aromatic rings.

### 3.3.4 Model compound reactions and rate analysis

RP-HPLC of the squalene reactions yielded a larger number of products than was observed for the isothermal curative interactions (see Figure 3.14).

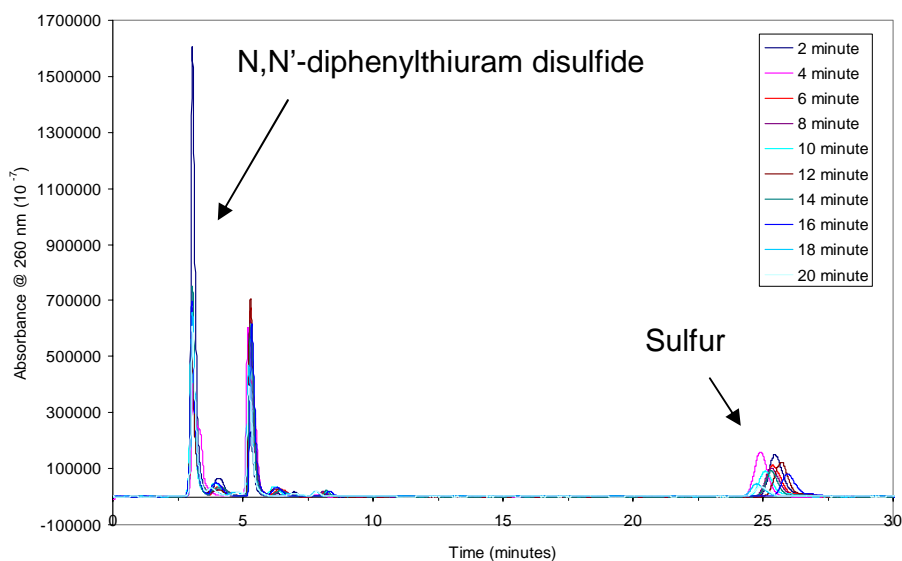


**Figure 3.14:** Chromatogram depicting the model compound interactions of N,N'-diphenylthiuram disulfide with sulfur and squalene

This would tend to indicate that more reactions are able to occur in the presence of squalene. It squalene may facilitate sulfur S<sub>8</sub> ring opening similar to the generally accepted amine facilitated<sup>13</sup> S<sub>8</sub> ring opening shown in Figure 3.15. The actual process, however, may be far more complicated.

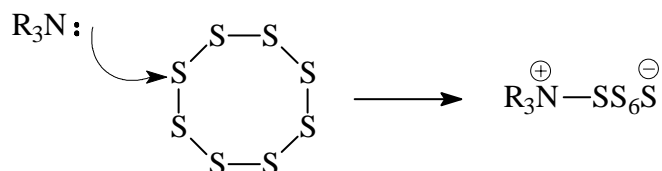


**Figure 3.15:** Amine facilitated ring opening of S<sub>8</sub> sulfur<sup>13</sup>

Differences, however, would be expected. The amine facilitation is considered to follow a polar mechanism while the squalene facilitation may be more radical in nature involving the homolysis of double bonds. This is a reasonable consideration since sulfur is able to react with the squalene at vulcanisation temperatures to produce crosslinks. This is clearly depicted in Figure 3.16, where sulfur was allowed to react with squalene in the absence of accelerator at 150°C. One may suggest that thermolytic cleavage of the S<sub>8</sub> rings should be sufficient to promote the reaction of accelerator and sulfur. It should, however, be noted that S<sub>8</sub> ring opening only starts to occur at 180-190°C,<sup>12</sup> thus not affording a high enough specific abundance to promote the reaction at a temperature of 150°C. The accelerator has almost all decomposed at temperatures that surpass 150°C. In this system, however, it may be

more likely that the thiuram polysulfides react with the squalene to produce thiuram polysulfide pendent groups which decompose to produce polythiol pendent groups and dithiocarbamic acid with the latter decomposing to an amine to promote S<sub>8</sub> ring opening as seen in Figure 3.15.

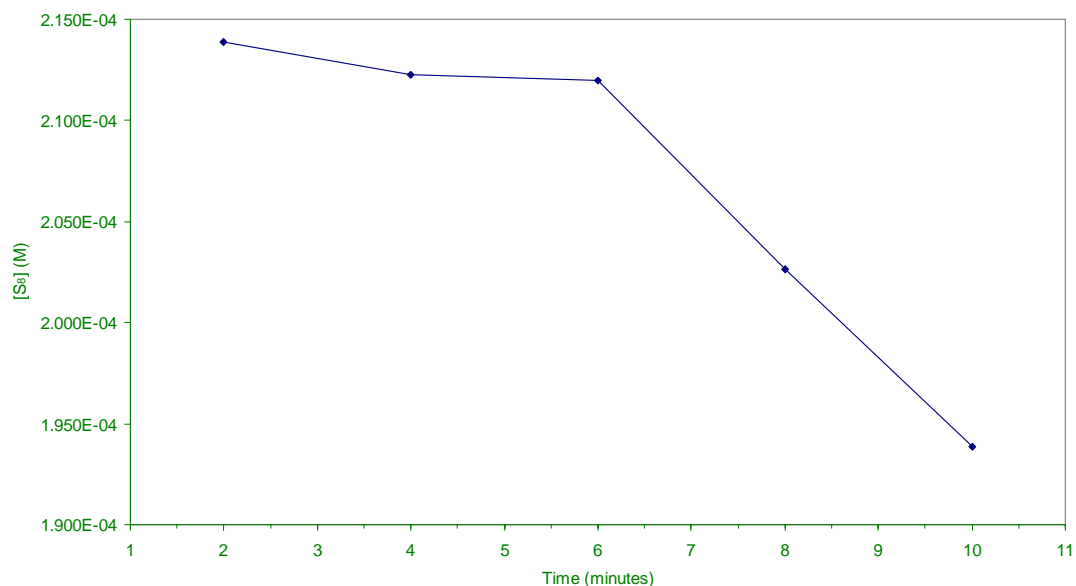


**Figure 3.16:** Consumption of sulfur at various time intervals during the unaccelerated vulcanisation of squalene

Since polysulfidic accelerator species are considered to be the active sulfurating agents, the total concentration of these species is important. Figure 3.17 was therefore produced to depict how the accelerator polysulfide concentration changes along the reaction co-ordinate. The concentration of polysulfidic accelerator species is considered to be directly related to the peak area and has been used as a relative representation in this study. This holds true if one notes that any change in the number of sulfur atoms included in an accelerator polysulfidic species has a negligible effect on the molar extinction coefficient as observed in the original thiuram disulfide. Figure 3.17 depicts a low but relative constant amount of polysulfidic species present throughout the reaction times considered. The amount of N,N'-diphenylthiuram disulfide consumed in the first 6 minutes is large, thereafter it appears to reach a steady state concentration. Initially there is a slight increase in the sulfur concentration, indicating that more sulfur was present than was initially added. It is known that some accelerators release sulfur on decomposition, an example of such an accelerator would be TMTD which decomposes to produce sulfur, TMTU, to mention but a few.<sup>14,15,16,17</sup>



The equation above and similar equations throughout this dissertation depict sulfur in its elemental form. The reason for this is primarily that industry make use of polymeric sulfur (non-stoichiometric sulphur being of undefined chain length) as opposed to elemental,  $\text{S}_8$ , sulfur. This is primarily due to uncertainties with regards to the true nature of sulfur at the level of these reactions. It is not likely that free sulfur will occur in its elemental form at the temperatures used during this investigation. It has been shown that rhombic ( $\text{S}_8$ ) sulfur decomposes to elemental sulfur via a disulfide ( $\text{S}_2$ ) intermediate at a temperature of  $2000^\circ\text{C}$ . There are, however, appreciable amounts of  $\text{S}_2$  present at a temperature of  $193^\circ\text{C}$  with traces of  $\text{S}_4$  being found at  $80^\circ\text{C}$ .<sup>18</sup> Smaller sulfur rings made up of  $\text{S}_6$  and  $\text{S}_7$  have also been shown to exist and found to be stable at temperatures below  $160^\circ\text{C}$ .<sup>19</sup>

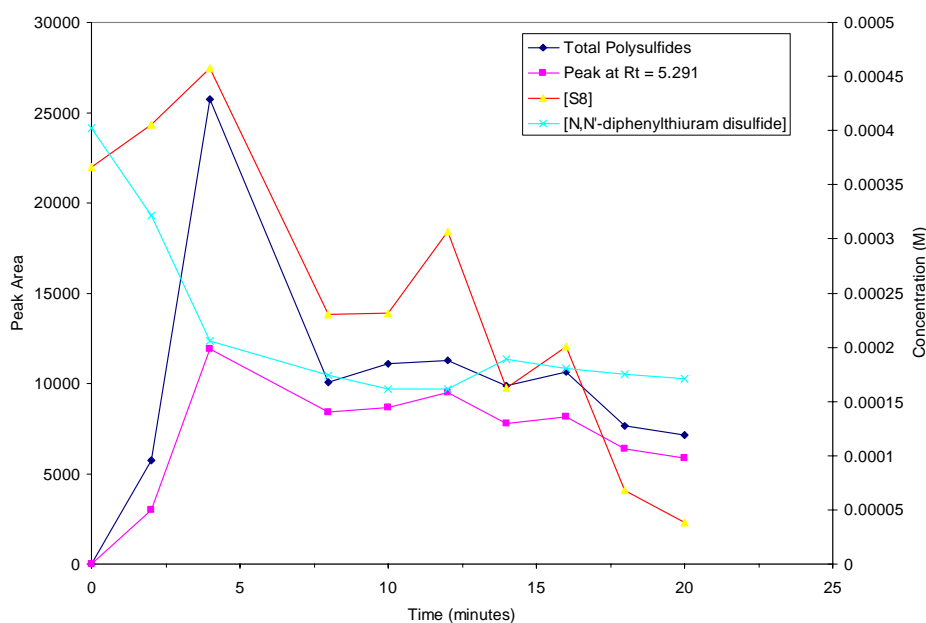


**Figure 3.17:** Reaction profile depicting the consumption of N,N'-diphenylthiuram disulfide and sulfur and the relative amounts of polysulfides at different time intervals

S is used for sulfur in the vulcanisation equations as a mere simplification due to the large variety of species that may actually arise. It is considered to be unlikely that the vulcanisation reactions can work co-operatively producing discrete sulfur moieties. This is further supported by the large spectrum of polysulfidic species that may

actually abound in the vulcanisate network. Species contain one to a maximum of twelve sulfur atoms have been noted in thiuram systems.<sup>20</sup>

The peak at 5.3 minutes and the total polysulfides are presented i.t.o. peak area in Figure 3.17 since no pure compounds exist and so no accurate concentrations could be determined. Nevertheless the shape of the curve indicates the timing of polysulfidic formation. Because polysulfides elute in order of sulfur rank, the peak at 5.3 minutes is possibly the trisulfide.

It is evident from the previous discussions that even though accelerator is consumed, the amount of polysulfidic species produced is limited (very few species are observed between the peak for the disulfide and sulfur). However, one also needs to consider that the rates of polysulfide production and consumption. As the polysulfidic species are generally considered to be the active sulfurating agent in vulcanisation, and as crosslinking does occur, while the polysulfide concentration remains relatively constant, it may occur via a different mechanism. This is seen in the table below (for graphs please consult appendices). It should be noted that Table 3.1 contains three sets of rate data for both the sulfur and the accelerator experimental data. The first two columns contain results that relate to the initial rate of change of accelerator and sulfur consumption, where the slope of the tangent and the initial slope make use of the tangent drawn to the curve and a best fit line to the initial few experimental data points respectively. The third set of data applies a first order rate law to the data.

Table 3.1: Rate data for the N,N'-diphenylthiuram disulfide model compound reactions

Data used	Rate and statistical data						
	Tangent slope (/mol L <sup>-1</sup> min <sup>-1</sup> )	Initial slope (/mol L <sup>-1</sup> min <sup>-1</sup> )	R <sup>2</sup>	N*	First order	R <sup>2</sup>	N*
Sulfur	1.30 x 10 <sup>-5</sup>	1.39 x 10 <sup>-5</sup>	0.974	8	2.62 x 10 <sup>-3</sup>	0.984	5
N,N'-diphenylthiuram disulfide	4.20 x 10 <sup>-5</sup>	3.83 x 10 <sup>-5</sup>	0.962	4	7.46 x 10 <sup>-4</sup>	0.863	4

\* N denotes the number of points used in the plot.

In order to obtain a semi-quantitative measure of reaction rates, the model compound reaction data were treated in two ways. Firstly the slope of the tangent and the initial slope method was used to obtain an indication of the initial rate of consumption of both sulfur and the thiuram disulfide. Secondly, because the consumption of disulfide and consequent reaction with sulfur to form polysulfides is believed to be rate-limited by the homolytic scission of the disulfide and the opening of the sulfur ring, and both processes are first order, the data for sulfur and disulfide consumption were treated as first order processes.

The slope of the tangent and the initial slope method has been used to determine the rate of vulcanisation for all the accelerators considered. It should be noted though, that the first order plots seemed only to produce valid results when the sulfur data was considered. It is seen that when the N,N'-diphenylthiuram disulfide data is considered, various linear regions exist within the concentration verses time curves. The rate constant was determined from the first order plot using the data up to 6 minutes. Because polysulfide formation actually involves a whole series of equilibrium reactions, it would be invalid to treat the decomposition of the disulfide as first order once the reverse reactions start to become significant. Furthermore subsequent reactions that make use of the product produced by this initial reaction are limiting producing a bottle neck.

### **3.3.5 Rate analysis of cis-1,4-polyisoprene, N,N'-diphenylthiuram disulfide and sulfur cured system**

As can be seen from the rheometer trace in Figure 3.18, very little or no induction time is required for the accelerator to actively start crosslinking the rubber. This is, however, not directly apparent in this figure since the scale is so large. It seems to be a marching cure, taking a considerable period to obtain a maximum torque, albeit a rather inferior value compared to other accelerators. The fact that the cure presents a marching curve seems to suggest a different vulcanisation mechanism, one that is not highly dependent on the polysulfidic accelerator species. This is especially significant in light of the low initial accelerator polysulfide concentration.



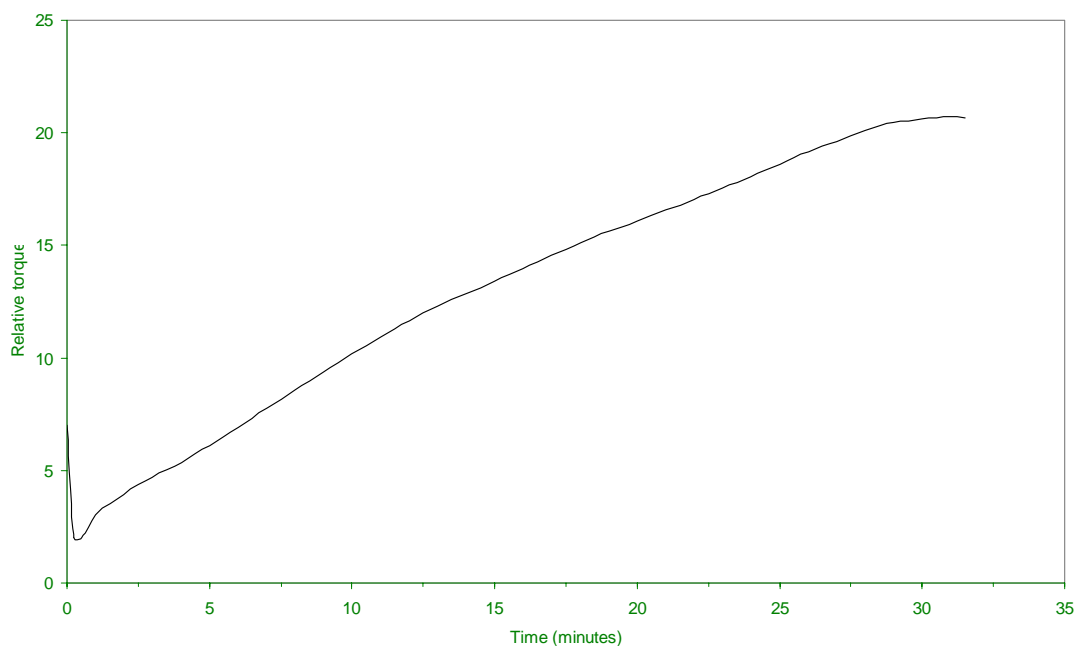


**Figure 3.18:** The rheometer curve depicting the cure of the N,N'-diphenylthiuram disulfide/S<sub>8</sub>/IR system

Unaccelerated sulfur vulcanisation is also considered to be a marching cure, obtaining an apparent maximum torque after 45 minutes. Thus some acceleration although small does occur with N,N'-diphenylthiuram disulfide. The torque increase for the N,N'-diphenylthiuram disulfide accelerated system is also greater than for unaccelerated sulfur vulcanization, again indicating a small degree of acceleration.

Deviations from linearity are primarily due to instrument malfunction during the analysis (electronic noise was observed in sudden jumps and given the low rate of vulcanization such jumps are more significant than with other accelerators). Rheometry is also a destructive technique with the sample continually experiencing shearing forces, thus data in the advanced stages of cure may become unreliable. A first order crosslinking rate constant of  $0.237 \text{ minute}^{-1}$  ( $R^2 = 0.942$ ) was observed for the N,N'-diphenylthiuram disulfide vulcanisation of polyisoprene as determined in Figure 3.19. Only data between the 17<sup>th</sup> to 27<sup>th</sup> minute of reaction which corresponds with a region of inflection could be used for this first order rate constant determination (see Figure 3.19). The maximum slope for the relative torque vs. time curve of Figure 3.18 for this system was found to be 0.863 (relative torque/time in minutes) while the Coran<sup>21</sup> rate constant ( $k_2$ ) was found to be  $0.023 \text{ minute}^{-1}$  (see Section 1.7.2 in the Introduction and Figure 3.20 below).

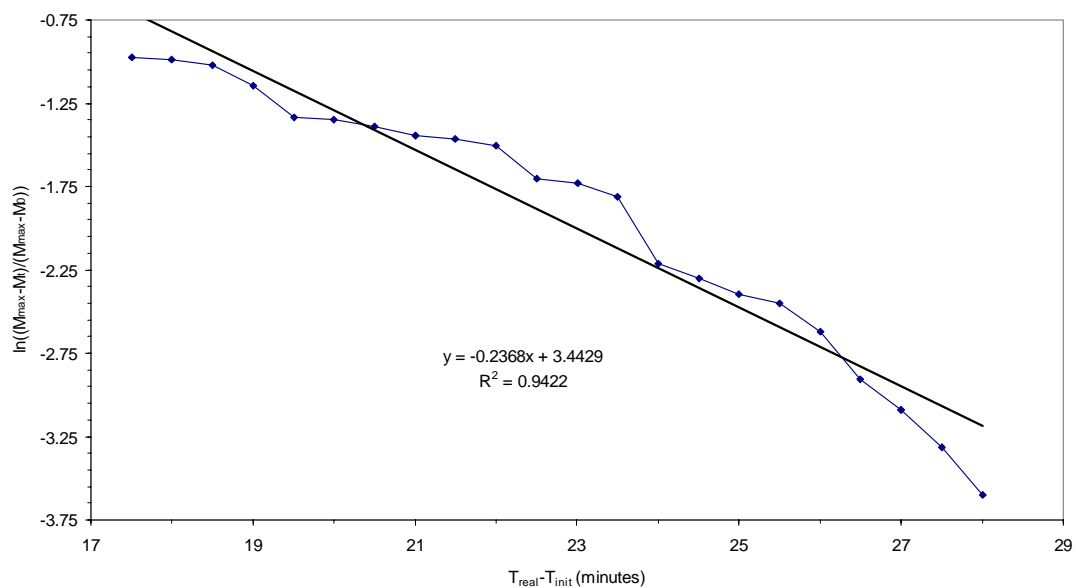


**Figure 3.19:** Determination of the first order rate constant from the rheometer data derived from the cure of N,N'-diphenylthiuram disulfide/S<sub>8</sub>/IR system

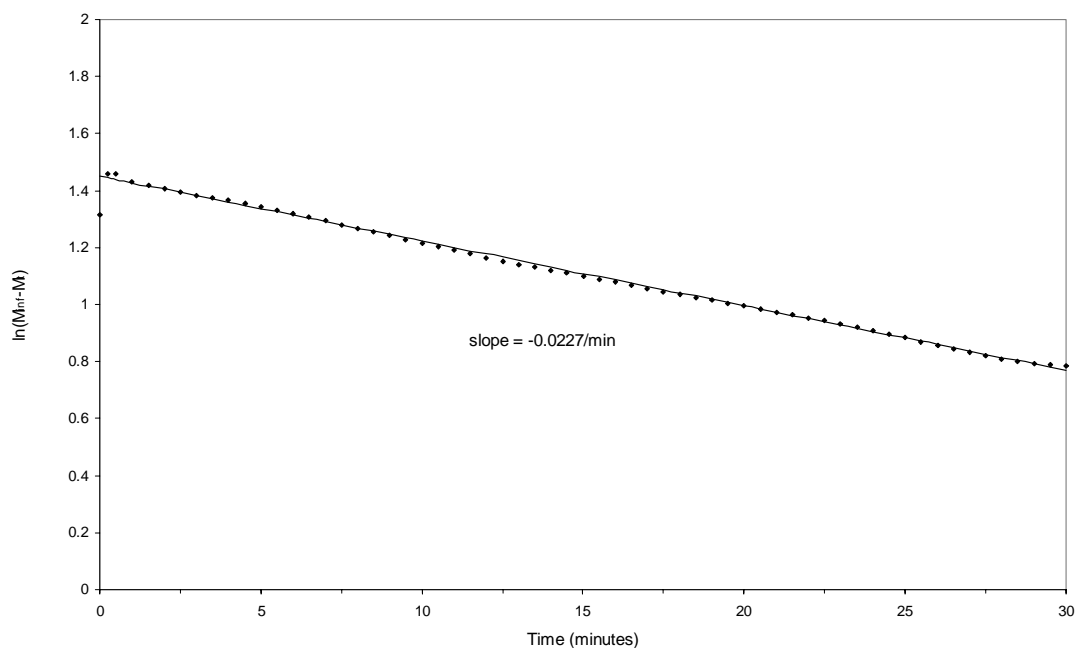


**Figure 3.20:** Determination of the Coran<sup>21</sup> rate constant (k<sub>2</sub>) constant from the rheometer data derived from the cure of N,N'-diphenylthiuram disulfide/S<sub>8</sub>/IR system

Table 3.2 contains all the rate data that can be derived from the rheometry data for the vulcanisation of cis-1,4-polyisoprene by means of N,N'-diphenylthiuram disulfide in the presence of sulphur.

Table 3.2: Summary of the rate data obtained for the vulcanisation of cis-1,4-polyisoprene by N,N'-diphenylthiuram disulfide in the presence of sulfur

<b>Rate and statistical data</b>			
<i>First order crosslinking (/min<sup>-1</sup>)</i>	<i>R<sup>2</sup></i>	<i>Maximum slope (/relative torque.min<sup>-1</sup>)</i>	<i>Coran's<sup>21</sup> rate constant (/min<sup>-1</sup>)</i>
0.2370	0.942	0.863	0.0230

The low rate of vulcanisation and the consequent marching cure observed is not unexpected given the low degree of polysulfide formation observed in the model compound studies. Since polysulfides are generally considered to be the active sulfurating agents we can expect low concentrations of pendent groups and consequently a slow rate of vulcanisation.

### 3.4 Computer modelling

Computer modelling was performed using the methods described in the Experimental Chapter.

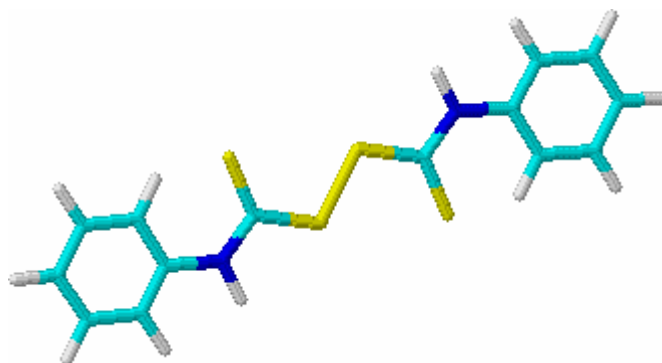
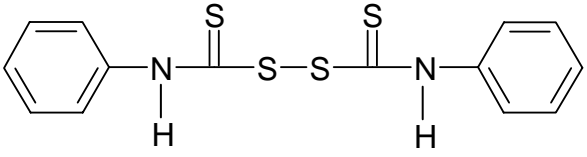



Figure 3.21: Geometry optimised structure for N,N'-diphenylthiuram disulfide

As can be seen from Figure 3.21, the trans structure (about the sulfur atoms) is preferred with the molecule being nearly planar. This is different to what is seen in tetramethylthiuram (TMTD) and tetraethylthiuram disulfide (TETD) which have dihedral angles of approximately 93°<sup>22,23</sup> while N,N'-dicyclopentamethylenethiuram<sup>24</sup> disulfide and N,N'-dimorpholinethiuram<sup>25</sup> disulfide have dihedral angles of 90° and 99° respectively. The lack of agreement may arise from the different structure or from the fact that computational calculations consider the molecule to be in the gas phase

in an equilibrium bond state.<sup>26</sup> It should also be noted that low level computational calculations were considered in this work which may at times present unreliable data. These structural characteristics may be exhibited in the crystalline product which forms the fine needle and plate like structures which are associated with aromatic and rigid molecules.

**Table 3.3:** Computer modelled parameters for N,N'-diphenylthiuram disulfide

N,N'-diphenylthiuram disulfide Energy = 99.884 kJ/mol Gradient = 0.000893							
Bond distance Å	Ar-N	N-C	C-S	S-S	S-C	C-N	N-Ar
		1.348	1.346	1.812	2.023	1.813	1.346
Charge (Mulliken)							
		-0.384				-0.331	
	-0.092	0.244	-0.071	-0.009	0.248	-0.086	

Taft constant 0.6<sup>27</sup>

It can be seen from Table 3.3, that even though N,N'-diphenylthiuram disulfide is a symmetrical molecule, variations in both bond distance and charge (Mulliken symbols) occur across the molecule. This results from subtle differences in electrostatic potential across the molecule which exist from differing angular structural relations through the molecule.

All bond distances are of the correct order while the charges correspond to what one would expect, that is negative charges on the more electronegative atoms. It should be noted that the bond distances observed in Table 3.3 are comparable and of the same order to similar atomic linkages that have been determined experimentally. The disulfide bond distance was found to be 2.02 Å (see Table 3.3) while S-S bond distances are known to be approximately 2.04 Å thus there was good agreement.<sup>9</sup> It was, however, seen by Wang and co-workers that TMTD and TETD presented some of the shortest S-S single bonds observed being 1.99 Å and 1.99 Å for TMTD and

TETD respectively.<sup>22,23</sup> Crystal data for N,N'-dicyclopentamethylenethiuram disulfide and N,N'-dimorpholinethiuram disulfide present the varied S-S single bond distances of 1.65 Å and 2.01 Å.<sup>24,25</sup> All the carbon nitrogen bonds have partial double bond character with bond distances of approximately 1.348 Å being observed. These bond distances correspond closely to molecules which contain partial double bond character in their C-N bonds, with the bond distances being in the region of 1.35 Å. The C-S bond distances are found to be in the order of normal C-S paraffinic linkages which are found to be in the region of 1.81 Å.<sup>9</sup> The computer modelled C-N and C-S bond distances for N,N'-diphenylthiuram disulfide correspond well with the generally applicable literature values as well as the values obtained from the crystal data for TMTD, TETD, N,N'-dicyclopentamethylenethiuram disulfide and N,N'-dimorpholinethiuram disulfide.<sup>22,23,24,25</sup>

The low gradient obtained indicates that a local minimum was obtained for the geometry optimisation. <sup>13</sup>C spectra detect two axes of symmetry one being about the disulfide linkage and the other is parallel and co-linear with the nitrogen aromatic carbon bond. Thus only five carbon peaks are observed.

### 3.5 References

- 1) A. W. Hofmann, The Esters of Thiocyanic Acid Isomeris with the mustard oils. Ber., 1, 169 (1868)
- 2) W. F. Hester, to Rohm and Haas Co. Fungicidal composition, U.S. PATENT 2,317,765, Apr. 27, 1943. Re-issue No. 23,742, Nov. 24, 1953
- 3) M. Bentov, Synthesis of tetramethylthiuram disulfide-S<sup>35</sup>, Rapt. No. 832, Comm. Energie Atomique (France), 1958, R.
- 4) C. D. Trivette, E. Morita and E. J. Young, Rubb. Chem. Technol., 36, 1360 (1962)
- 5) Aldrich Handbook of Fine Chemicals and Laboratory Equipemnt, Sigma-Aldrich(Pty) Ltd, PO Box 10434, Aston Manor 1630, South Africa (2003)
- 6) W. Scheele and O. Lorenz, Rubb. Chem. Technol., 29, 894 (1956)
- 7) D. Thorn and R. A. Ludwig, The Dithiocarbamates and Related Compounds. Elsevier Publishing Co., Amsterdam (1962)
- 8) M. St. Flett, Characteristic Frequencies of Chemical Groups in the Infra-red, Elsevier Publishing Co., Amsterdam (1963)
- 9) R. C. Weast, Ed., CRC Handbook of Chemistry and Physics, 51<sup>st</sup> Ed., The Chemical Rubber Co. Publishers, Cleveland (1970)

- 10) B. Meyer, Elemental Sulfur, Interscience Publishers, New York (1965)
- 11) G. Nickless, Inorganic Sulfur Chemistry, Elsevier Publishing Company, Amsterdam (1968)
- 12) F. R. Partington and K. Stratton, A Text Book of Inorganic Chemistry, 6<sup>th</sup> Ed., Macmillan and Co. Ltd., New York (1953)
- 13) H. Krebs, Rubb. Chem. and Technol., 30, 962, (1957)
- 14) C. W. Bedford and L. B. Sebrell, Ind. Eng. Chem., 14, 25 (1922)
- 15) B. A. Dogadkin and V. A. Shershnev, Rubb. Chem. Technol., 33, 401 (1960)
- 16) D. Craig, Rubb. Chem. Technol., 29, 994 (1956)
- 17) G. A. Blokh, Organic Accelerators in the Vulcanisation of Rubber, Israel Program for Scientific Translations Ltd., 1968
- 18) F. R. Parangton, K. Stratton, A Text Book of Inorganic Chemistry, 6<sup>th</sup> Ed., Macmillan and Co. LTD., (1953)
- 19) P. Gosh, S. Kantare, P. Patkar, J. M. Caruthers, V. Venkatasubramanian, Rubber Chem. Technol., 76, 592 (2003)
- 20) M. Geysler and W. J. McGill. J. Appl. Polym. Sci., 55, 215 (1995)
- 21) A. Y. Coran, Rubber Chem. Technol., 37, 689 (1964)
- 22) Y. Wang, J. -H. Liao and C. -H. Ueng, Acta Cryst., c42, 1420 (1986)
- 23) I. L. Karle, J. A. Estlin and K. Britts, Acta Cryst., 22, 273 (1967)
- 24) M. F. Dix, A. D. Rae, Cryst. Struct. Commun., 29, 159 (1973)
- 25) G. C. Rout, M. Seshanyee, G. Aravamudan, Cryst. Struct. Commun., 38, 1389 (1982)
- 26) HyperChem, 3ed manual (1994), Hypercube, Inc (
- 27) E. Morita, Rubb. Chem. Technol., 57, 746 (1984)

# **Tetramethylthiuram disulfide**

## **rate study**

---

4.1	Purification of tetramethylthiuram disulfide (TMTD).....	91
4.2	Reaction rate analysis .....	91
4.2.1	RP-HPLC analysis of the isothermal curative interactions and model compound study.....	91
4.2.2	Dynamic study of TMTD and sulfur interactions via thermal analysis	92
4.2.3	Curative interactions .....	94
4.2.4	Model compound reactions .....	96
4.2.5	Rate analysis of cis-1,4-polyisoprene, tetramethylthiuram disulfide...	99
4.3	Computer modelling.....	101
4.4	References .....	102

#### 4.1 Purification of tetramethylthiuram disulfide (TMTD)

The TMTD obtained for this study was of industrial grade, manufactured by Bayer. It was therefore necessary to purify the compound. Purification was performed via recrystallisation using the miscible solvent method in which the compound to be purified is soluble in one solvent and not the other. The compound was dissolved in a minimum amount of dichloromethane and then recrystallised by the addition of methanol. The mother liquid was then placed on ice for half an hour to ensure complete crystallisation. The mixture was then filtered using Whatman 42 filter paper and the compound dried in a vacuum desiccator containing P<sub>2</sub>O<sub>5</sub>. The purity of the compound was confirmed via RP-HPLC, NMR, thin layer chromatography (dichloromethane/chloroform 1:1) and DSC analysis. The melting point was found to be 145.9°C T<sub>onset</sub> (onset temperature) with a peak maximum temperature (T<sub>max</sub>) occurring at 154.7°C. IR (CHCl<sub>3</sub> cm<sup>-1</sup>) 2981.5, 2933.0, 1503.0, 1408.7, 1381.5, 1246.5, 1203.8, 1153.0, 976.2, 855.1. <sup>1</sup>H-NMR (CDCl<sub>3</sub>) 3.64 (6H, m, 2CH<sub>3</sub>). <sup>13</sup>C-NMR (CDCl<sub>3</sub>) 194.15, 47.98, 42.45.

#### 4.2 Reaction rate analysis

##### 4.2.1 RP-HPLC analysis of the isothermal curative interactions and model compound study

Separation of the products produced in the isothermal curative interaction study were achieved via RP-HPLC with a gradient elution<sup>1</sup> system. The gradient programme employed may be viewed in Table 4.1.

Table 4.1: Gradient elution profile<sup>1</sup> employed for the separation of the isothermal curative interaction products

Time (min)	Flow rate (mL/min)	% MeOH	% H <sub>2</sub> O	Elution profile <sup>1</sup>
	1	85	15	
15	1	100		10

This gradient allows for the best possible separation of the compounds produced even though resolution of certain unimportant peaks was not possible. It was also decided to change the wavelength at which the detector was set from the commonly



used 280 nm to 260 nm. This resulted in the loss of peaks in the chromatograms for compounds that did not present chromophores that would absorb light at this wavelength. The TMTD and sulfur were thus resolved into well defined separate peaks having retention times of 4.3 and 23.2 minutes respectively.

The model compound reaction products were separated via a simple isocratic elution system employing a 90:10 (vol:vol) methanol/water mobile phase with the TMTD and sulfur peaks being observed at 3.60 and 21.14 minutes respectively.

#### 4.2.2 Dynamic study of TMTD and sulfur interactions via thermal analysis

TMTD was found to melt at  $T_{\max}=154.7^{\circ}\text{C}$ ,  $T_{\text{onset}} = 145.9^{\circ}\text{C}$  (literature values:  $138.9^{\circ}\text{C}^2$ ;  $142\text{-}156^{\circ}\text{C}^3$ ;  $146\text{-}148^{\circ}\text{C}^4$ ). It is, however, important to note that since TMTD decomposes on melting, the endotherm that is seen in Figure 4.1 is not purely due to fusion. This is illustrated by the baseline shift on melting. It is known that many intermediary products are formed during the heating process, such as TMTM, TMTP's and TMTU,<sup>5,6,7,8</sup> although the later is only formed at temperatures above  $190^{\circ}\text{C}$ .<sup>9</sup>

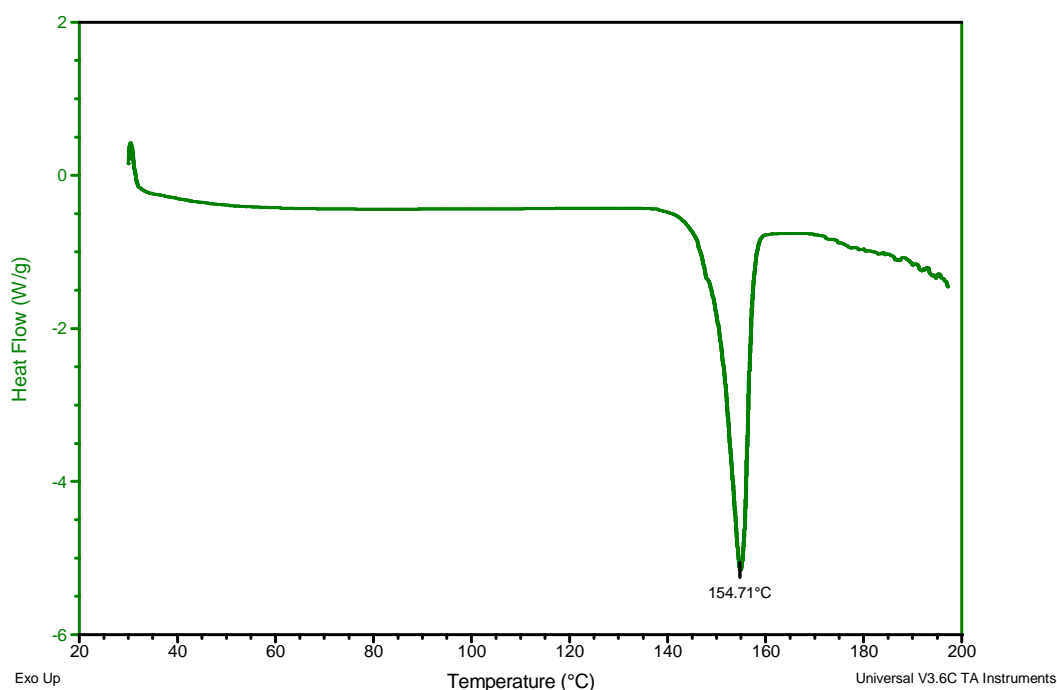
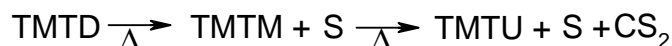


Figure 4.1: DSC thermogram depicting the tetramethylthiuram disulfide melt

These derivatives may have lower melting points therefore an increased volatility. The resulting mass loss due to volatilisation could be responsible for the baseline shift before and after the melt.

The thermogram shown in Figure 4.2 represents the dynamic interactions occurring between sulfur and tetramethylthiuram disulfide. Distinct and discrete transitions may be observed. The transitions that are seen between 100-125°C may be attributed to sulfur. The  $S_{\alpha}$ - $S_{\beta}$  sulfur transition is known to occur at 107.0°C<sup>9</sup>, while the endothermic peak at 118°C may correspond to the  $S_{\beta}$ - $S_{\lambda}$  transition that is seen at 113°C<sup>9</sup>. The last endotherm corresponds to the TMTD melt. Some degree of mutual solubilisation of the accelerator in the sulfur melt was observed, with the large endotherm associated with the melt and decomposition of TMTD occurring at 130°C (cf. Figures 4.1 and 4.2).

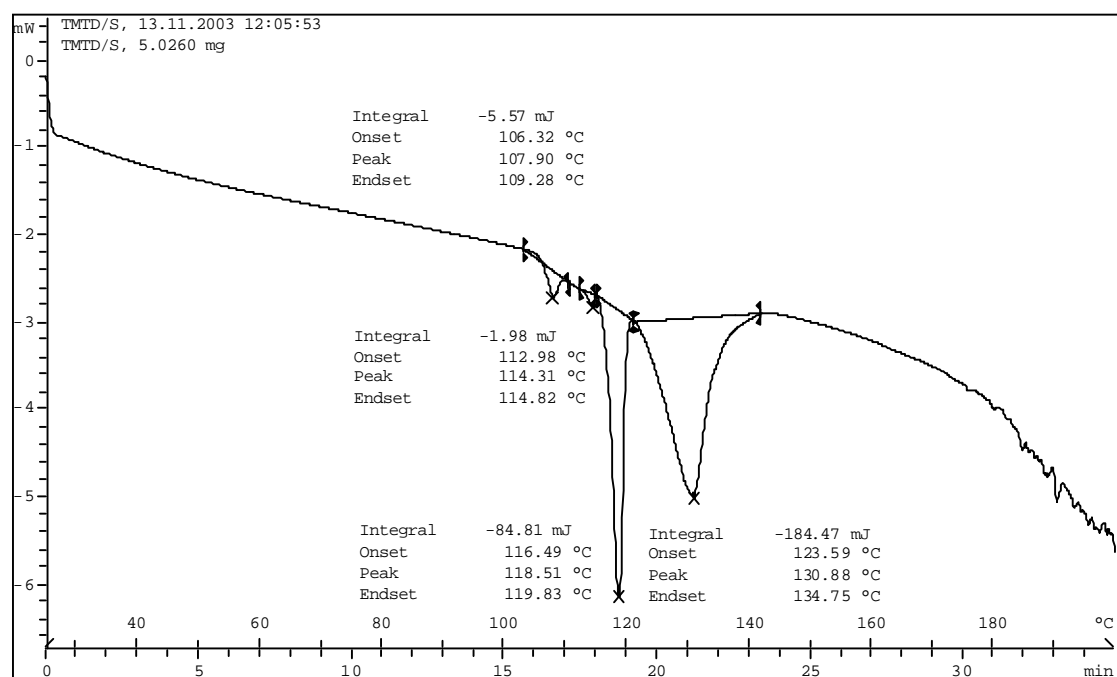
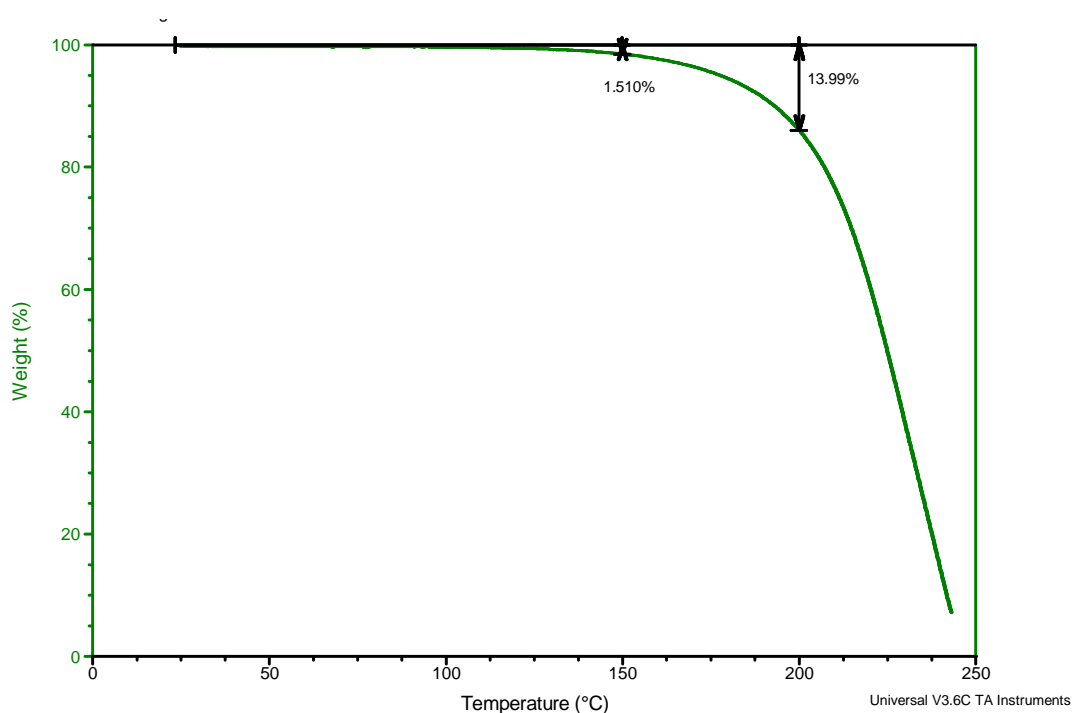


Figure 4.2: DSC thermogram of tetramethylthiuram disulfide with sulfur

The mass loss associated with this dynamic study is approximately 14% as shown in Figure 4.3. This is quite low in comparison to the 71% which was seen in the N,N'-diphenylthiuram disulfide sulfur heat. The mass loss for this system at the temperature employed to perform the vulcanisation (150°C) was found to be 1.5%. The rapid decomposition of the N,N'-diphenylthiuram disulfide may be a factor that lends to its poor properties as an accelerator in sulfur vulcanisation. One may tend to

find the low mass loss in the TMTD sulfur heat unusual, especially if one equates mass loss with the level of decomposition of the accelerator. This parallel, however, is erroneous. It will be shown later that the TMTD, in the TMTD accelerated sulfur vulcanisation of squalene, is almost all consumed by the 6<sup>th</sup> minute (shown in Figure 4.7). This is not the case for N,N'-diphenylthiuram disulfide accelerated sulfur vulcanisation of squalene. This would tend to indicate that even though the TMTD has not decomposed to volatile by-products, it has reacted rapidly in the melt to form a large variety of accelerator polysulfides of low volatility. This is also readily shown in Figure 4.4 which represents the products obtained after the isothermal heat of TMTD with sulfur at different time intervals.



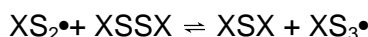
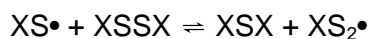
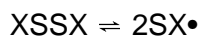
**Figure 4.3:** TGA thermogram depicting the heat of tetramethylthiuram disulfide with sulfur

This should not, however, be used on its own to establish the apparent reactivity of an accelerator. It is known that TMTD is a very good vulcanisation accelerator producing vulcanisates of high crosslink density at an efficient rate.

### 4.2.3 Curative interactions

TMTD is very reactive in the presence of sulfur producing a large number of polysulfidic species as can be seen from Figure 4.4 which depicts the products

formed during the isothermal curative study. It has been proposed that the polysulfidic species are formed as a result of the homolysis of TMTD and the homogenic interaction of the formed radical with either symmetrical or asymmetrically cleaved accelerator species as seen below<sup>10,11</sup>.



As many as 12 sulfur atoms may be incorporated into the polysulfidic accelerator species, but it is more likely that these higher order polysulfides undergo radical cleavage of the sulfur-sulfur bond to produce lower order polysulfides, as opposed to the homolytic cleavage of TMTD. Sulfur abstraction is also more likely to occur from higher order polysulfides by the action of sulfenyl and thiuram persulfenyl radicals, as opposed to the addition of sulfur to these TMTPs<sup>10</sup>.

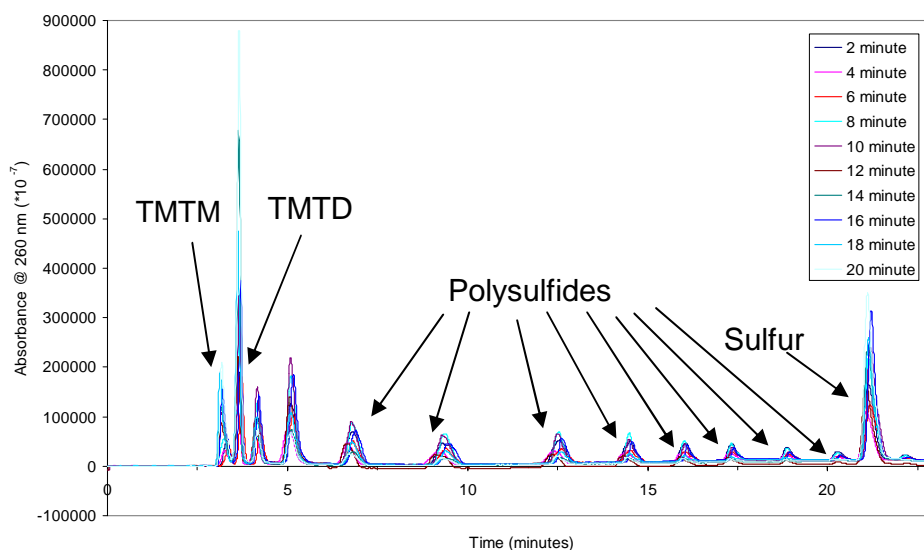


**Figure 4.4:** TMTD/S<sub>8</sub> (1:1 molar ratio) isothermal interactions

Other products may be formed via homolytic reactions. TMTM as well as TMTU have been observed by other researchers. It should be noted though that TMTU is formed from the amine liberated during dimethyldithiocarbamic acid (Hdmtc) decomposition, which in turn is liberated during pendent groups formation (see Figure 4.5). TMTU is only found to form a at high temperatures though.<sup>10,12</sup>

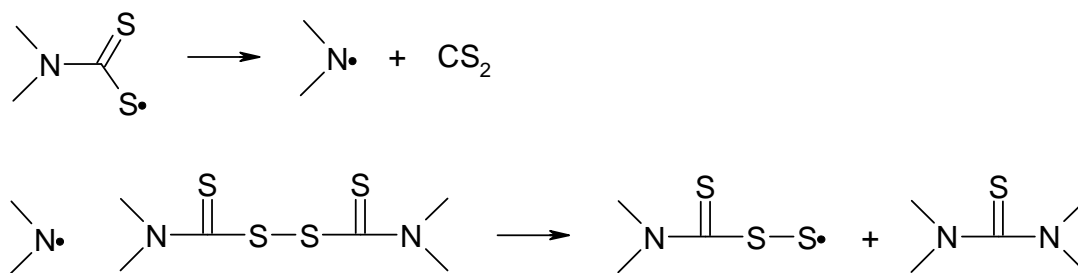


Figure 4.5: TMTU formation by the action of free amines on TMTD<sup>12</sup>

The large number of polysulfidic species present thus make TMTD an extremely effective crosslinking agent, producing a large number of thiuram terminated pendent groups which are in turn able to undergo the menagerie of reactions found in vulcanisation.

#### 4.2.4 Model compound reactions

In the presence of a crosslinkable olefin such as squalene, the amount of polysulfidic species (as well as the maximum sulfur rank observed) is drastically reduced (cf. Figures 4.4 and 4.6). It should be noted that since thiuram disulfides are able to crosslink olefins in the absence of sulfur, the rate of crosslink formation and sulfur consumption may not be related by a simple empirical formula. It is seen in Figure 4.7, that TMTD is consumed fast to reach a pseudo-equilibrium value, while the decrease in the amount of sulfur is more gradual. As indicated previously crosslinking results in the formation of small amounts of TMTD; thus the final concentration is not zero.

RH



In over-cured systems the TMTD concentration may be substantially reduced, tending to zero concentration values.

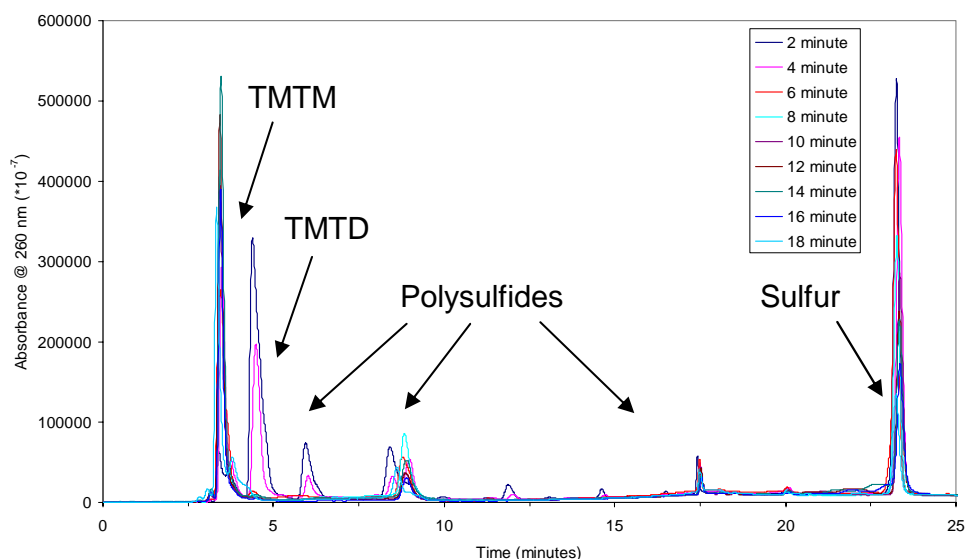


**Figure 4.6:** Chromatogram depicting the model compound interactions of tetramethylthiuram disulfide with sulfur and squalene

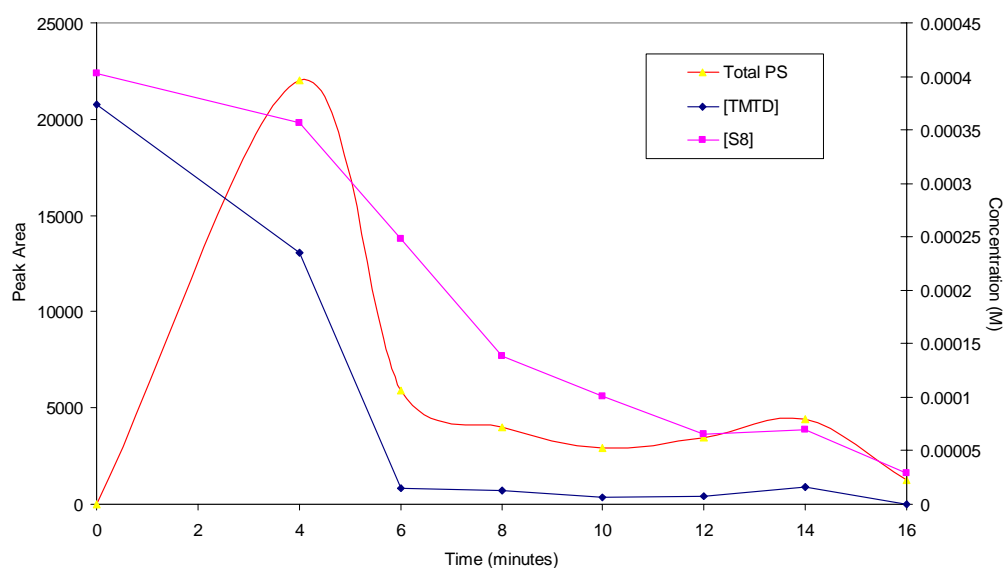


**Figure 4.7:** Reaction profile depicting the consumption of tetramethylthiuram disulfide and sulfur (measured on the concentration axis) and the relative amounts of polysulfides (measured on the peak area axis) at different time intervals

As indicated earlier polysulfides are illustrated i.t.o. total peak area. It may be seen in Figure 4.7 that polysulfide abundance reaches a maximum at 4 minutes. This is because vulcanisation is a series of consecutive reactions with the concentration of the polysulfides peaking when the rate of pendent group formation is at its maximum.

It has been previously noted that the homolytic cleavage of thiuram disulfides is considered to be a limiting step in the process of thiuram disulfide vulcanisation.

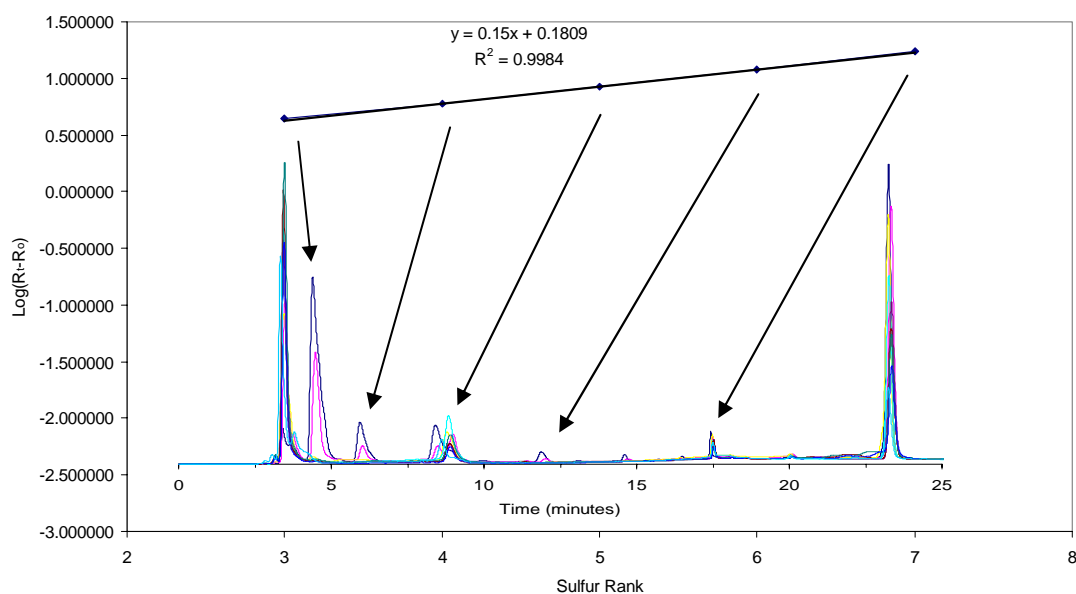


**Figure 4.8:** Thiuram polysulfide determinations for the isocratic separation of the model compound interaction products between tetramethylthiuram disulfide, sulfur and squalene

The thiuram polysulfide peaks have been determined by a method introduced by Möckel<sup>13</sup> and Snow<sup>14</sup> as mentioned in Section 2.4.7 of the Experimental. In their method all the peaks after the thiuram disulfide are considered, with the logarithm of the difference between the retention times of the peak and the thiuram disulfide peak being calculated. When these calculated values fall on a straight line when plotted against counting numbers from three (number of sulphur atoms in thiuram polysulfide) are considered to be polysulfidic thiuram species. The plot is depicted in Figure 4.8. This method has been employed throughout this work to determine the presence of thiuram polysulfides in isocratic chromatographic separations.

The slope of the tangent and the initial slope method proved to be more accurate in determining the rate constant, especially when the sulfur data was considered, while the rate of reaction proved too fast to yield enough points for an accurate determination of the first order rate constant using the TMTD data.

**Table 4.2:** Rate data for the tetramethylthiuram disulfide model compound reactions

Data used	Rate and statistical data						
	Tangent slope (/mol L <sup>-1</sup> min <sup>-1</sup> )	Initial slope (/mol L <sup>-1</sup> min <sup>-1</sup> )	R <sup>2</sup>	N*	First order	R <sup>2</sup>	N*
Sulfur	5.80x10 <sup>-5</sup>	2.56x10 <sup>-5</sup>	0.958	5	8.62x10 <sup>-3</sup>	0.981	6
Tetramethylthiuram disulfide	9.00x10 <sup>-5</sup>	6.46 x10 <sup>-5</sup>	0.901	4	3.47 x10 <sup>-3</sup>	0.897	5

\* N denotes the number of points used in the plot.

A second order plot showed the data to vastly deviate from linearity and was consequently ignored. It is seen in Table 4.2, that the first order constants for the consumption of sulfur and TMTD have different values, indicating the likelihood of different rate determining steps for their consumption.

#### 4.2.5 Rate analysis of cis-1,4-polyisoprene, tetramethylthiuram disulfide and sulfur cured system

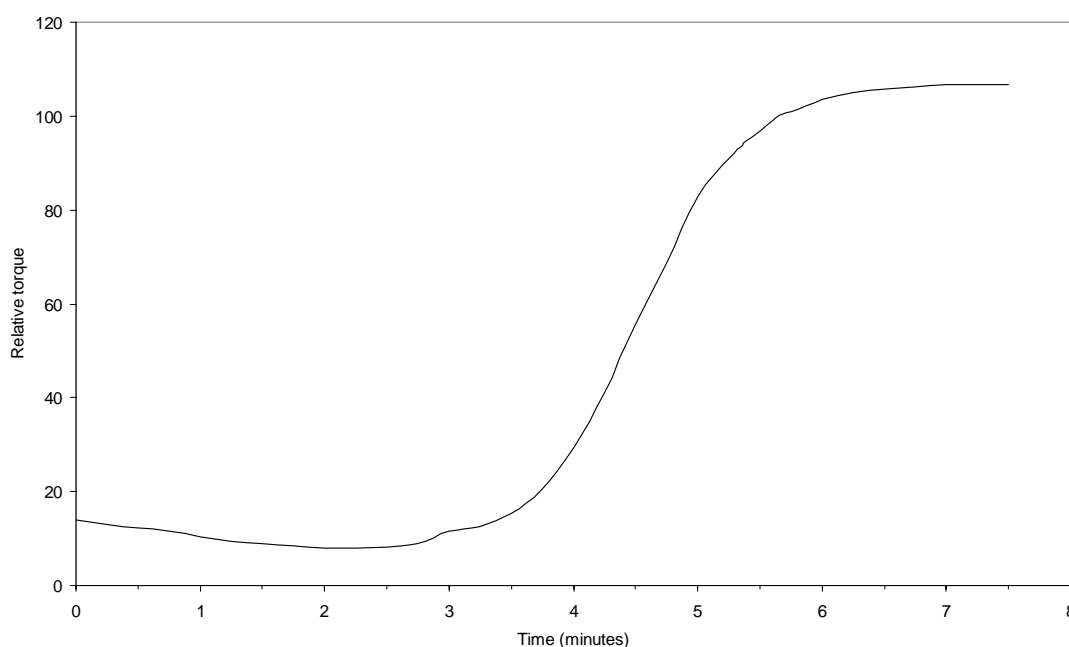


**Figure 4.9:** The rheometer curve depicting the cure of the tetramethylthiuram disulfide/S<sub>8</sub>/IR system

Figure 4.9 illustrates the rheometer cure obtained for the TMTD/sulfur/polyisoprene vulcanised system. The cure is a good example for a general vulcanisation system



having well defined induction, acceleratory and maturation regions. The maximum slope as determined from Figure 4.9 was found to be 55.8 (relative torque/time in minutes) while the first order crosslinking rate constant determined from the torque data in Figure 4.9 was found to be 2.589 minute<sup>-1</sup> ( $R^2=0.983$ ) (see Figure 4.10).

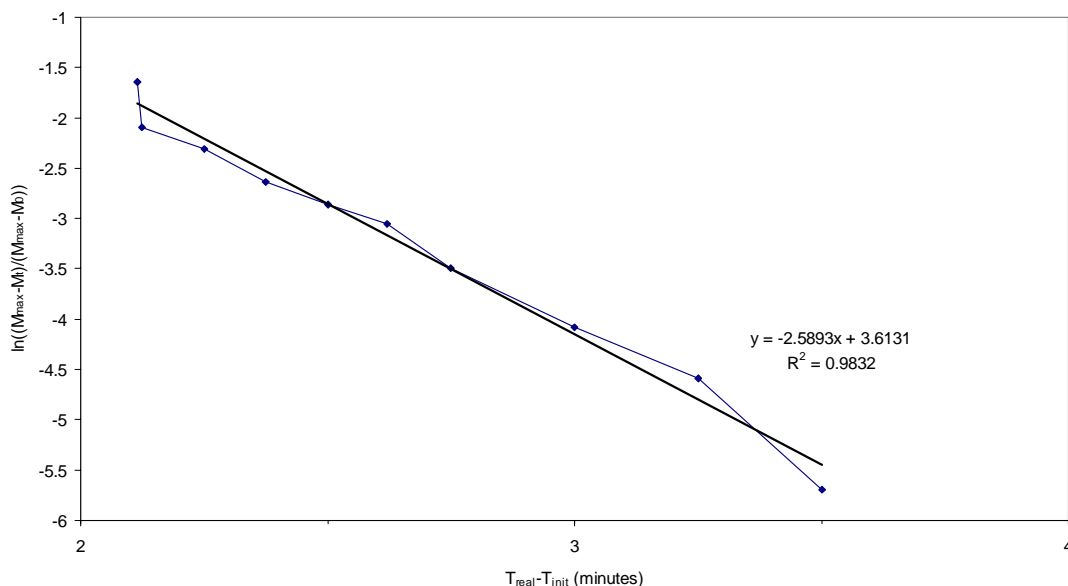


**Figure 4.10:** Determination of the first order rate constant from rheometer data derived from the cure of tetramethylthiuram disulfide/S<sub>8</sub>/IR system

A large number of data points could be employed in the determination of the first order rate constant for the crosslinking reaction thus increasing the accuracy at which the value was determined (shown in Figure 4.10).

**Table 4.3:** Summary of the rate data obtained for the vulcanisation of cis-1,4-polyisoprene by tetramethylthiuram disulfide in the presence of sulfur

<b>Rate and statistical data</b>			
<i>First order crosslinking (/min<sup>-1</sup>)</i>	<i>R<sup>2</sup></i>	<i>Maximum slope (/relative torque.min<sup>-1</sup>)</i>	<i>Coran's<sup>15</sup> rate constant (/min<sup>-1</sup>)</i>
2.5890	0.983	55.8	2.4640

Table 4.3 is a summary of the rate data obtained from the vulcanisation of cis-1,4-polyisoprene by means of tetramethylthiuram disulfide in the presence of sulphur, the Coran<sup>15</sup> plot may be seen in Appendix B.

### 4.3 Computer modelling

As can be seen from Figure 4.11 the trans configuration about the disulfide linkage is the most stable structural form. It is noted that the molecule goes into and out of the plane about the disulfide linkage. The trans configuration (dihedral angle of  $180^\circ$ ) is unusual since crystal structure data for TMTD depicts a dihedral angle of approximately  $93^\circ$ .<sup>16,17</sup> This may be explained by the fact that computer modelling geometry optimisations are considered to be performed in the gas phase making use of equilibrium bond distances.<sup>18</sup> It should also be noted that simple computer modelling calculation algorithms are path dependent and rely to some extent on the initial input. This is especially true in the case of empirical and semi-empirical calculations. Here minimum potential energy wells are obtained that cause the geometric optimisation function to converge at a potential which may not be the absolute minimum for the molecule being considered. Crystal structures constrain molecules in unit cell packings which may perturb equilibrium bond distance and equilibrium angular relationships as the lattice energy gained may outweigh the unfavourable perturbations. In light of what is depicted by the crystal structure data, the trans configuration that was obtained for tetramethylthiuram disulfide in this study by means of computer modelling must have been a local potential energy minimum and not a global potential energy minimum.

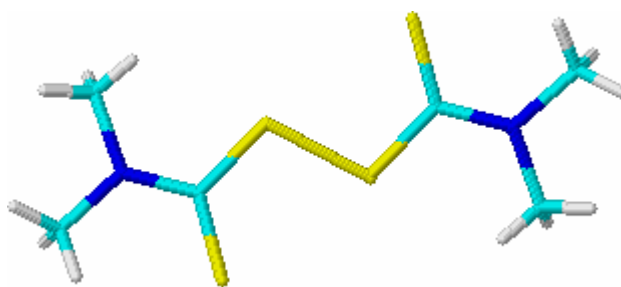
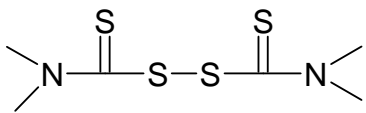
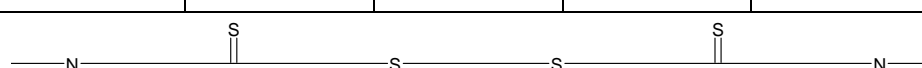


Figure 4.11: Geometry optimised structure for N,N'-tetramethylthiuram disulfide

Table 4.4 depicts the calculated bond distances and charges (Mulliken symbols). As expected from the non-planar nature of the molecule, there are variations in both charge and bond distance across the molecule. This will limit the number of possible free energy relations that may be derived from this data as only the disulfide bond distance would be comparable across the groups of accelerators examined. It is, however, possible to take averages of the structural data obtained for the same moieties across the molecule and compare these values. It should be noted that

variation in both bond distance and charge are small within molecules but variation across the series are substantial.

Table 4.4: Computer modelled parameters for tetramethylthiuram disulfide

Tetramethylthiuram disulfide Energy = 56.628 kJ/mol Gradient = 0.000764						
Bond distance Å	N-C	C-S	S-S	S-C	C-N	
		1.362	1.819	2.023	1.818	1.360
Charge (Mulliken)						
		-0.267			-0.256	
	-0.208	-0.153	0.221	0.229	-0.166	-0.210

Taft constant = 0.0<sup>20</sup>

It is noted from Table 4.4 that the C-N bond has a partial double bond character being close to the expected 1.35 Å which may be attributed to  $\pi$  delocalisation. The C-S bond distances are of the order of paraffinic species, with expected values in the region of 1.81 Å.<sup>19</sup> The disulfide linkage is close to the expected 2.04 Å<sup>19</sup> for similar systems, however crystal structure data shows the bond distance to be 2.00 Å.<sup>16</sup> The variation in disulfide bond distance may be attributed to the use of a gas phase computer modelling system.

#### 4.4 References

- 1) Automated Gradient Operators Manual 660, Waters, 34 Maple Street, Millford, Massachusetts, 01757 (1983)
- 2) F. W. H. Kruger and W. J. McGill, J. Appl. Polym. Sci., 42, 2669 (1991)
- 3) R. O. Babbit, Ed., The Vanderbilt Rubber Handbook, R.T Vanderbilt Co., Norwalk (1978)
- 4) J van Alphen, in Rubber Chemicals, C.M. van Turnhoput, Ed., Reidel, Dordrecht, Holland (1973)
- 5) C. W. Bedford and L. B Sebrell, Ind. Eng. Chem., 14, 25 (1922)

- 6) B. A. Dogadkin and V. A. Shershnev, *Rubb. Chem. Technol.*, 33, 401 (1960)
- 7) D. Craig, *Rubb. Chem. Technol.*, 29, 994 (1956)
- 8) G. A. Blokh, *Organic Accelerators in the Vulcanisation of Rubber*, Israel Program for Scientific Translations Ltd. (1968)
- 9) F. W. H. Kruger and W. J. McGill, *J. Appl. Polym. Sci.*, 42, 2643 (1991)
- 10) M. Geysler and W. J. McGill, *J. Appl. Polym. Sci.*, 55, 215 (1995)
- 11) R. S. Kapur, J. L. Koenig, J. R. Shelton, *Rubb. Chem. Technol.*, 47, 991 (1974)
- 12) C. P. Reyneke-Barnard, M. H. S. Gradwell and W. J. McGill, *J. Appl. Polym. Sci.*, 77, 2718 (2000)
- 13) H. J. Möckel, *J. Chromatogr.* 317, 589 (1984)
- 14) N. H. Snow, *J. Chem. Ed.*, 73, 592 (1996)
- 15) A. Y. Coran, *Rubber Chem. Technol.*, 37, 689 (1964)
- 16) Y. Wang, J. H. Liao and C. -H. Ueng, *Acta Cryst.*, c42, 1420 (1986)
- 17) I. L. Karle, J. A. Estlin and K. Britts, *Acta Cryst.*, 22, 273 (1967)
- 18) HyperChem, 3rd manual (1994)
- 19) R. C. Weast, Ed., *CRC Handbook of Chemistry and Physics*, 51<sup>st</sup> Ed., The Chemical Rubber Co. Publishers, Cleveland (1970)
- 20) *Lange's Handbook of Chemistry*, 15<sup>th</sup> ed, Edited by J.A. Dean, McGraw-Hill, New York (1999)

# 5 Tetraethylthiuram disulfide

## rate study

---

5.1	Purification of tetraethylthiuram disulfide (TETD) .....	105
5.2	Reaction rate analysis .....	105
5.2.1	Method of RP-HPLC analysis for the isothermal curative interactions and model compound study .....	105
5.2.2	Dynamic study of TETD and sulfur by thermal analysis.....	106
5.2.3	Curative interactions .....	107
5.2.4	Model compound reactions and rate analysis .....	108
5.2.5	Rate analysis of cis-1,4-polyisoprene, tetraethylthiuram disulfide....	110
5.3	Computer modelling.....	113
5.4	References .....	115

## 5.1. Purification of tetraethylthiuram disulfide (TETD)

The compound was not purified as it was obtained as an analytical grade chemical bought from Fluka (98%). The melting point was determined to be in the range 70.7°C ( $T_{\text{onset}}$ ) - 75.0°C ( $T_{\text{max}}$ ). IR ( $\text{CHCl}_3$ ) 2982.0, 2936.3, 2360.8, 1492.4, 1422.6, 1383.2, 1354.3, 1272.0, 1220.0, 1201.9, 1147.0, 1006.0, 970.1, 915.5.  $^1\text{H-NMR}$  ( $\text{CDCl}_3$ ) 4.04 (10H, m,  $2\text{CH}_3\text{CH}_2$ ).  $^{13}\text{C-NMR}$  ( $\text{CDCl}_3$ ) 193.11, 52.44, 48.00, 13.89, 11.85.

## 5.2. Reaction rate analysis

### 5.2.1 Method of RP-HPLC analysis for the isothermal curative interactions and model compound study

The reaction products for the isothermal curative study were separated via an isocratic system employing a mobile phase of 90:10 (vol:vol), methanol:water, using a C-18 reverse phase column described in the experimental section. The UV/Vis detector was set at a wavelength of 260 nm. The compounds of interest were separate into well-defined peaks, with the TETD and sulfur having retention times of 3.9 and 25.0 minutes respectively. The model compound reaction products required a gradient elution system to separate the peaks of interest. The gradient programme is listed in the table below.

Table 5.1: Gradient elution profile<sup>1</sup> employed for the separation of the compound reaction products

Time (/min)	Flow rate (/mL min <sup>-1</sup> )	% MeOH	% H <sub>2</sub> O	Elution Profile <sup>1</sup>
	1	75	25	*
15	1	100	0	6

In the gradient elution system the TETD and sulfur peaks were observed at retention times of 9.4 and 32.8 minutes respectively.

## 5.2.2 Dynamic study of TETD and sulfur by thermal analysis

The DSC curve in Figure 5.1, showed that the TETD melts at around 74.9°C ( $T_{max}$ ), with the onset at 70.5°C. This is in agreement with literature values (69 - 71°C<sup>2</sup>). The TETD melt is not exclusively a fusion process, since TETD reacts in the melt to form various products. When TETD was heated by Grooff<sup>3</sup> at 150°C, it was found that the TETD predominated but trace amounts of tetraethylthiuram monosulfide (TETM) and tetraethylthiuram polysulfide (TETP) were also detected. TETD and TETP's were only found to decompose at 170°C to yield tetraethylthiourea (TETU), CS<sub>2</sub> and sulfur.

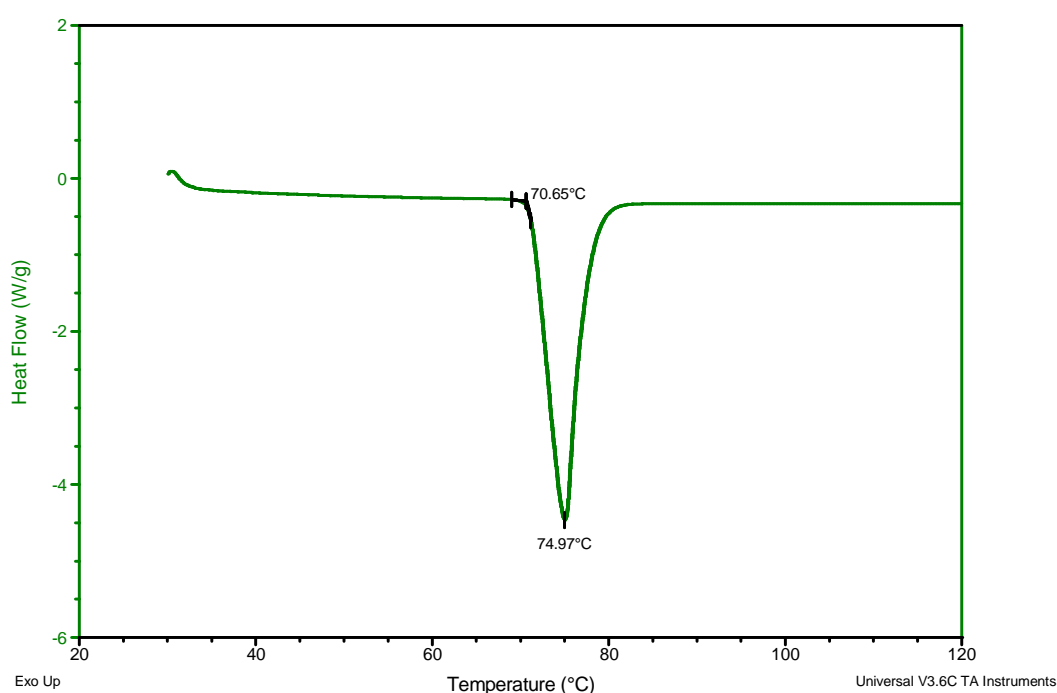
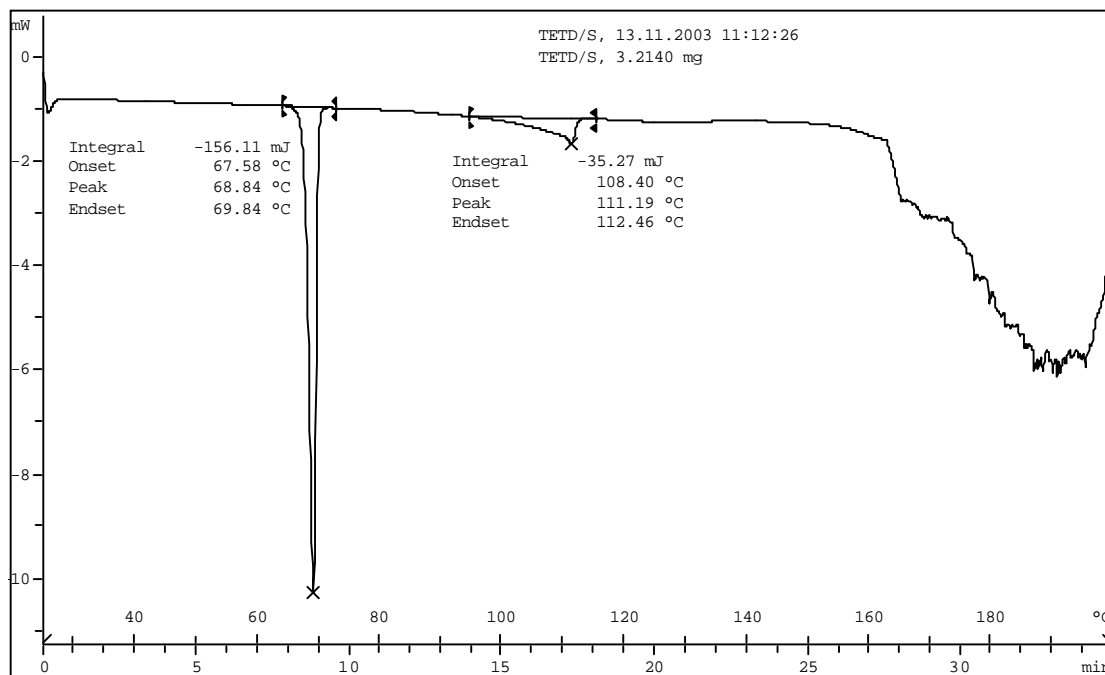


Figure 5.1: DSC thermogram depicting the tetraethylthiuram disulfide melt

When TETD and sulfur were heated together (see Figure 5.2), it was found that the two substances maintained their individual melts. The TETD melt onset was seen at 67.6°C, while the peak maximum occurred at 68.8°C. A broad endotherm was seen to occur from 108.4°C to 112.5°C which may incorporate both sulfur transitions. S<sub>α</sub>-S<sub>β</sub> and S<sub>β</sub>-S<sub>λ</sub> transition occurring at 107.0°C<sup>4</sup> and 113°C<sup>4</sup> respectively. Although no significant change in the temperature of the sulfur transitions was observed, the change in peak shape is likely the result of the presence of molten TETD.



**Figure 5.2:** DSC thermogram depicting the heat of tetraethylthiuram disulfide with sulfur

A broad endotherm associated with degradative processes accompanied by gas evolution is seen to commence from approximately 160°C.

### 5.2.3 Curative interactions

It can be seen in Figure 5.3 that TETD is highly reactive in the presence of sulfur, producing a large number of polysulfidic species. One would thus expect, based on the commonly accepted thiuram disulfide vulcanisation mechanism, that TETD would be a good accelerator. This is known to be true, and was also confirmed in these experiments.



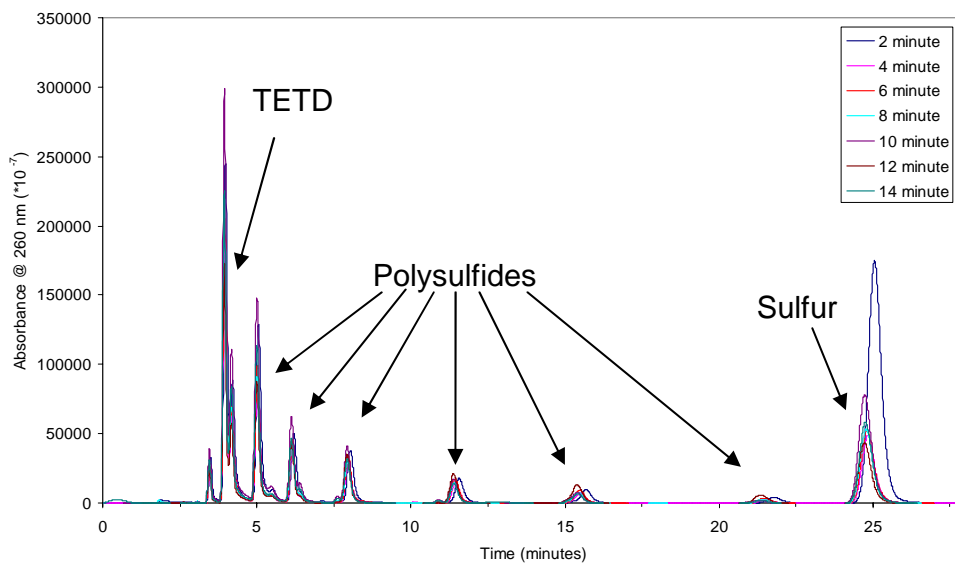


Figure 5.3: Tetraethylthiuram disulfide/S<sub>8</sub> (1:1 molar ratio) isothermal interactions

#### 5.2.4 Model compound reactions and rate analysis

Compared to the isothermal curative interaction analyses there were slightly fewer reaction products produced in the model compound study, as may be seen in Figure 5.4. Nevertheless significant quantities of polysulfides were still observed.

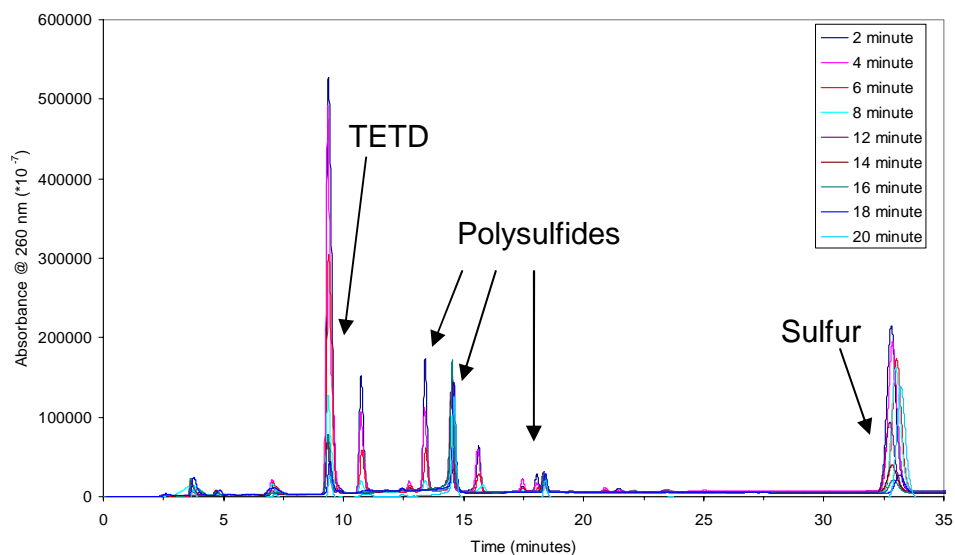
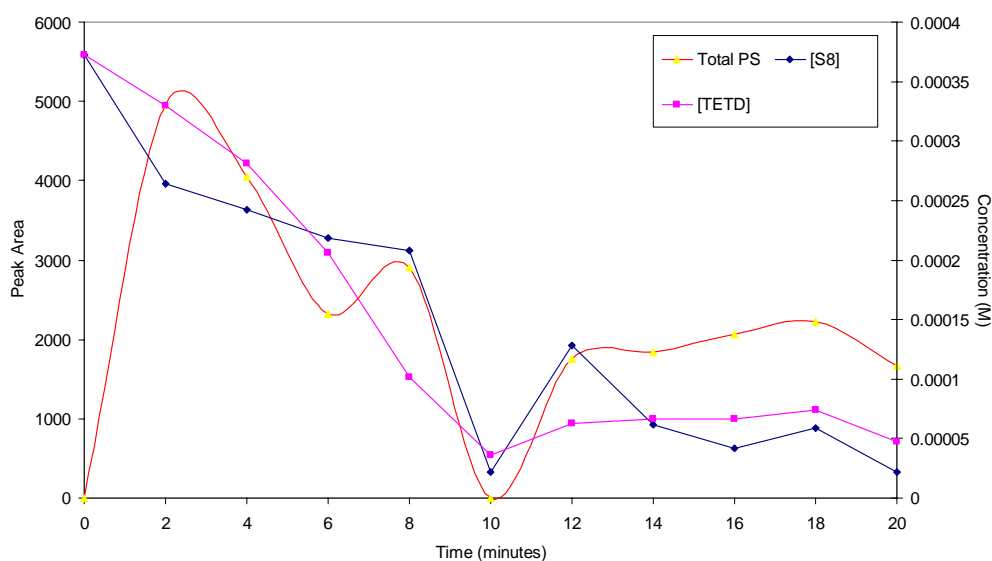


Figure 5.4: Chromatogram depicting the model compound interactions of tetraethylthiuram disulfide with sulfur and squalene

Figure 5.5 depicts a rapid decrease in accelerator concentration over the first 12 minutes, but the final TETD concentration still remains greater than that of the sulfur. In systems which exhibit the rapid depletion of one component relative to the other, characteristic S shaped torque versus time rheometer curves are observed. This results from one component being limiting. It should be noted though that as thiuram disulfide accelerators may crosslink olefin networks in the absence of sulfur, crosslinking does not stop when all the sulfur has reacted.



**Figure 5.5:** Reaction profile depicting the consumption of tetraethylthiuram disulfide and sulfur and the relative amounts of polysulfides at different time intervals

Polysulfide abundance peaks after 2 minutes, being actively formed and removed via interactions with the accelerator and sulfur; and the reaction of polysulfides with the olefin. It can be seen from Table 5.2, that the slope of the tangent and the initial slope methods gave the most accurate determination of the relative rates whereas the rates constants determined by the first order approximation were less accurate, especially where the tetraethylthiuram disulfide data was considered.

Table 5.2: Rate data for the tetraethylthiuram disulfide model compound reactions

Data used	Rate and statistical data						
	Tangent slope (/mol L <sup>-1</sup> min <sup>-1</sup> )	Initial slope (/mol L <sup>-1</sup> min <sup>-1</sup> )	R <sup>2</sup>	N <sup>*</sup>	First order (/s <sup>-1</sup> )	R <sup>2</sup>	N <sup>*</sup>
Sulfur	5.30 x 10 <sup>-5</sup>	2.04 x 10 <sup>-5</sup>	0.893	6	1.60 x 10 <sup>-3</sup>	0.934	6
Tetraethylthiuram disulfide	4.10 x 10 <sup>-5</sup>	3.00 x 10 <sup>-5</sup>	0.954	6	2.78 x 10 <sup>-3</sup>	0.961	5

\* N denotes the number of points used to construct the plot

### 5.2.5 Rate analysis of cis-1,4-polyisoprene, tetraethylthiuram disulfide and sulfur cured system

Figure 5.6, depicts a conventional torque verses time rheometer trace, with the sample being completely cured within 10 minutes. The maximum slope of the rate acceleratory region was determined to be 32 (relative torque/time in minutes).

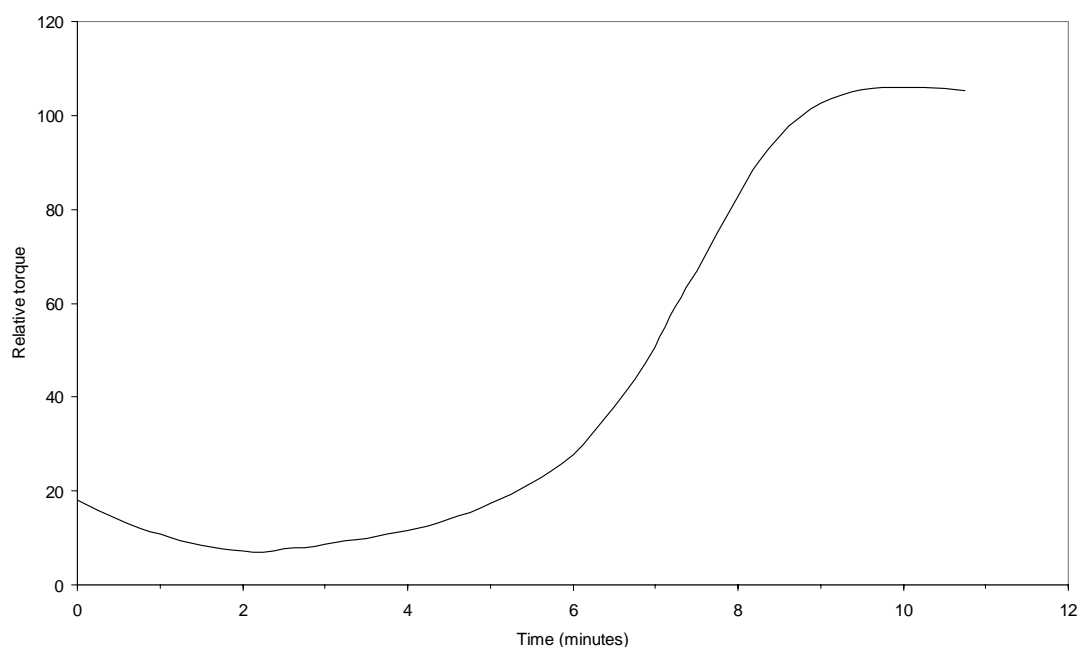
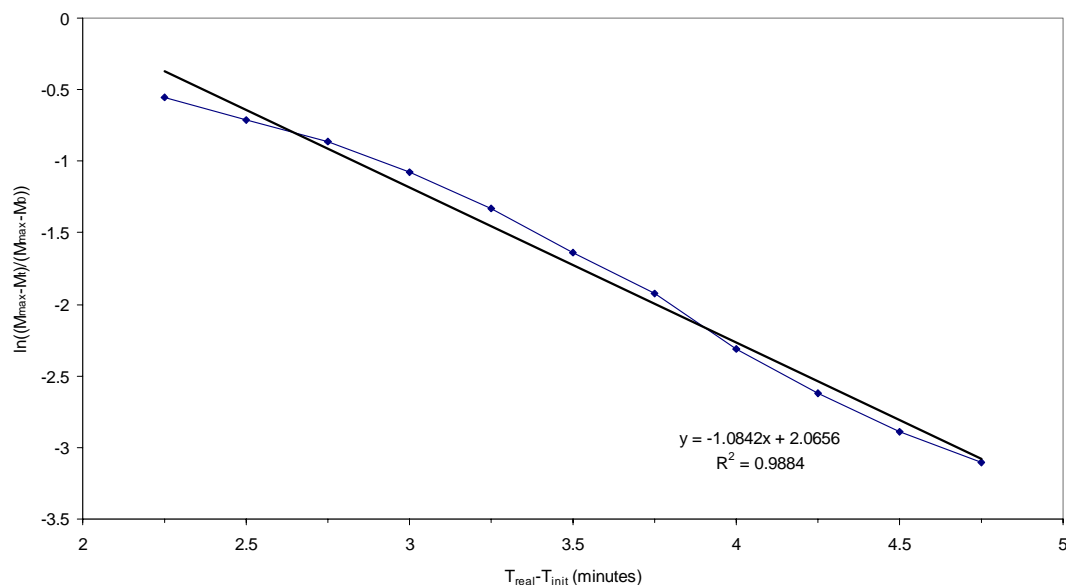


Figure 5.6: The rheometer curve depicting the cure of the tetraethylthiuram disulfide/S<sub>8</sub>/IR system

A relatively large number of points were available in the linear accelerator region for the determination of the rate constant assuming first order kinetics. The rate constant as determined in Figure 5.7 was found to be 1.084 ( $R^2 = 0.988$ ).



**Figure 5.7:** Determination of the first order rate constant form rheometer data derived from the cure of tetraethylthiuram disulfide/S<sub>8</sub>/IR system

The maximum slope for the curing of cis-1,4-polyisoprene by means of tetraethylthiuram disulfide and sulphur as determined from the rheometric curve in Figure 5.6 as well as the Coran<sup>5</sup> ( $k_2$ ) and first order crosslinking rate constants may be seen in the Table below.

**Table 5.3:** Summary of the rate data obtained for the vulcanisation of cis-1,4-polyisoprene by tetraethylthiuram disulfide in the presence of sulfur

<b>Rate and statistical data</b>			
<i>First order crosslinking</i> (/min <sup>-1</sup> )	$R^2$	<i>Maximum slope</i> (/relative torque.min <sup>-1</sup> )	<i>Coran's<sup>5</sup> rate constant</i> (/min <sup>-1</sup> )
1.0840	0.988	32	0.9870

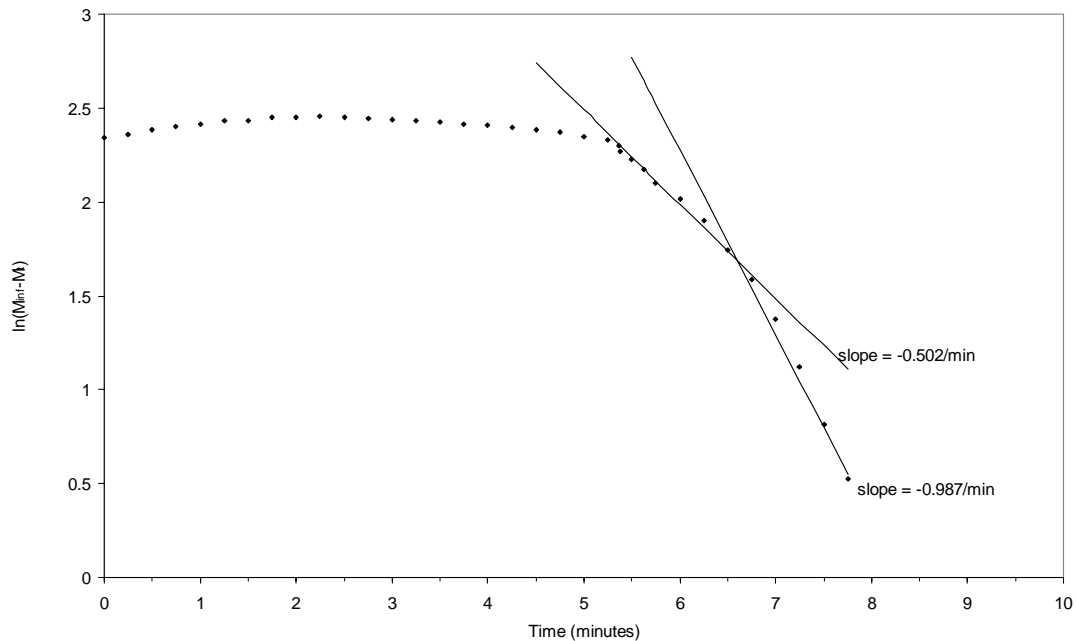


**Figure 5.8:** Determination of the Coran rate constant ( $k_2$ ) constant from the rheometer data derived from the cure of tetraethylthiuram disulfide/S<sub>8</sub>/IR system

It is interesting to note that the determination of the Coran<sup>5</sup> rate constant revealed the presence of two linear regions as seen in Figure 5.8. There is an initial slow region governed by a Coran rate constant of 0.502 minute<sup>-1</sup> and the faster dominant process governed by the rate constant of 0.987 minute<sup>-1</sup>. This is indicative of two crosslinking reaction mechanisms operating during vulcanisation. The first slow reaction is most likely the disproportionation of two thiuram polysulfide pendent groups on neighbouring rubber chains to form a crosslink and tetraethylthiuram monosulfide (TETM) or a tetraethylthiuram polysulfide (TMTP).<sup>5,6,7</sup> This is considered to be a slow crosslinking reaction that should obey a second order rate law, but has been approached in a simplified manner as a pseudo first order reaction in an investigation pertaining to tetramethylthiuram disulfide. The faster process is considered to be the reaction of thiuram polysulfide pendent groups with polythiol pendent groups on neighbouring chains to produce crosslinks and dithiocarbamic acid.<sup>8</sup> It is, however, more likely that the fast reaction process consist of a combination of two fast crosslinking reactions: the first consisting of reactions between thiuram polysulfide pendent groups with polythiol pendent groups to produce crosslinks and dithiocarbamic acid as mentioned previously; while the second would be the reaction of dimethylammonium pendent groups (formed from the interaction of amine

produced by the decomposition of dithiocarbamic acid with a polythiol pendent group) with thiuram polysulfide pendent groups to produce crosslinks an tetraethylthiourea.<sup>9</sup>

### 5.3. Computer modelling

As can be seen from Figure 5.9, tetraethylthiuram disulfide is not a planar molecule. A large number of initial input structures had to be drawn to obtain the appropriate optimised geometry. The structure below depicts the typical thiuram disulfide structure with the dihedral angle found to be 93° about the disulfide linkage.<sup>10,11</sup> This contrasts sharply with the trans configuration observed for TMTD (see Chapter 4).

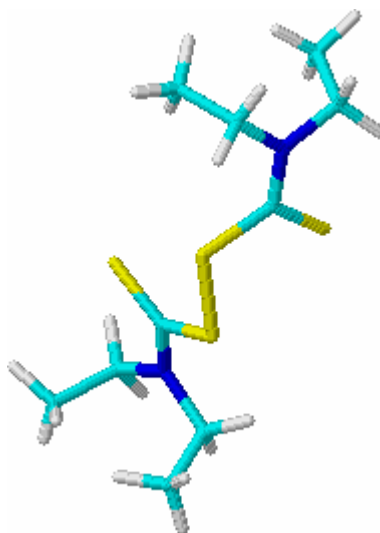
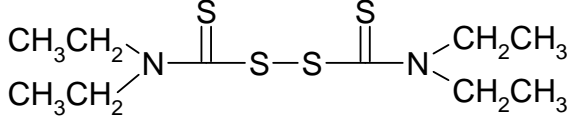



Figure 5.9: Geometry optimised structure for tetraethylthiuram disulfide

As expected the bond distance and charges for the symmetrically placed atoms were different, but the difference is small (see Table 5.4). The energy of the geometry optimised structure is arbitrary as it is dependent on the number of atoms in the molecule. The energy of the geometry optimised structure is related to the difference in energy between the atoms in the molecule and the atoms in their free state (the single atoms). The gradient is of more importance, with a low value indicating that a potential energy minimum has been found, as was the case here. It should be noted that the Taft parameter obtained is for a single ethyl group and during calculations they will be treated as additive parameters.

Table 5.4: Computer modelled parameters for tetraethylthiuram disulfide

Tetraethylthiuram disulfide Energy = 60.802 kJ/mol Gradient = 0.00932						
Bond distance Å	N-C	C-S	S-S	S-C	C-N	
	1.365	1.813	2.022	1.813	1.369	
Charge (Mulliken)						
		0.014			-0.211	
	-0.269	-0.201	0.004	0.065	0.018	-0.301

Taft constant =  $-0.10^{12}$

When one examines computer modelling data it is important to understand the relevance and validity of data. Figure 5.9 and the data in Table 5.3 indicate that the electronic environment that each atom finds itself in is slightly different. This may be seen in the  $^1\text{H-NMR}$  spectrum where complex proton couplings produce multiplettes. These coupled groups are, however, interpreted as single units exhibiting only half the number of protons expected. This makes proton assignments easier even though we know the integration takes into account twice as many protons as a result of molecular symmetry. These subtle changes in chemical environments produce large proton multiplettes which imply complex proton couplings. However, in the  $^{13}\text{C-NMR}$  these complex systems allow for carbons that might be considered to be hidden as result of symmetry where peak intensity is doubled accounting for two carbons, now become two separate peaks with half the original peak intensity. This explains why five different  $^{13}\text{C}$  assignments were made, where different electronic environments as a result of molecular geometry out-weigh the molecular symmetry about the nitrogen atom. Once again these five peaks are twice the intensity as a result of symmetry about the disulfide linkage. The low abundance of  $^{13}\text{C}$  makes these discrete observations possible.

It should be noted from Table 5.4 that all bonds correspond closely to previously determined single bond distance with the C-N bond expressing partial double bond character.<sup>13</sup> Once again the disulfide linkage is longer than one would expect for a

typical thiuram disulfide with crystal structure data depicting the bond distance to be of the order of 2.00 Å.<sup>11</sup> This may be attributed to the modelled data being derived for a gas phase consideration.<sup>14</sup> The relative atomic charges are substantially different to the previously considered tetramethylthiuram disulfide, with the sulfur atoms in the disulfide linkage possessing greatly reduced positive charges.

#### 5.4. References

- 1) Automated Gradient Operators Manual 660, Waters, 34 Maple Street, Millford, Massachusetts, 01757 (1983)
- 2) F. W. H. Kruger and W. J. McGill, *J. Appl. Polym. Sci.*, 44, 581 (1992)
- 3) D. Groof, "A Comparative Study of the Tetramethylthiuram and Tetraethylthiuram Disulfide Accelerated Sulfur Vulcanisation of Cis-1,4-polyisoprene", MSc Dissertation, University of Port Elizabeth, South Africa (1997)
- 4) F. W. H. Kruger and W. J. McGill, *J. Appl. Polym. Sci.*, 42, 2643 (1991)
- 5) A. Y. Coran, *Rubber Chem. Technol.*, 37, 689 (1964)
- 6) F. W. H. Kruger and W. J. McGill, *J. Appl. Polym. Sci.*, 45, 563 (1992)
- 7) A. Y. Coran, *Rubber Chem. Technol.*, 38, 1 (1965)
- 8) M. Geysler and W. J. McGill, *J. Appl. Polym. Sci.*, 60, 439 (1996)
- 9) F. W. H. Kruger and W. J. McGill, *J. Appl. Polym. Sci.*, 42, 2669 (1991)
- 10) Y. Wang, J. H. Liao and C. -H. Ueng, *Acta Cryst.*, c42, 1420 (1986)
- 11) I. L. Karle, J. A. Estlin and K. Britts, *Acta Cryst.*, 22, 273 (1967)
- 12) Lange's Handbook of Chemistry, 15<sup>th</sup> ed, Edited by J.A. Dean, McGraw-Hill, New York (1999)
- 13) R. C. Weast, Ed., *CRC Handbook of Chemistry and Physics*, 51<sup>st</sup> Ed., The Chemical Rubber Co. Publishers, Cleveland (1970)
- 14) HyperChem, 3ed manual (1994)



# 6 N,N'-dicyclopentamethylenethiuram disulfide rate study

---

6.1	Purification of N,N'-dicyclopentamethylenethiuram disulfide (CPTD) .....	117
6.2	Reaction rate analysis .....	117
6.2.1	RP-HLPC analysis for the isothermal curative interactions and the model compound study .....	117
6.2.2	Dynamic study of the curative interactions via thermal analysis .....	118
6.2.3	Curative interactions .....	121
6.2.4	Model compound reactions .....	122
6.2.5	Rate analysis of cis-1,4-polyisoprene, N,N'-dicyclopentamethylenethiuram disulfide and sulfur cured system .....	124
6.3	Computer modelling .....	126
6.4	References .....	128

## 6.1 Purification of N,N'-dicyclopentamethylenethiuram disulfide (CPTD)

The N,N'-dipentamethylenethiuram disulfide purchased for this study was of industrial grade and manufactured by Robinson Brothers. Therefore it was necessary to purify the compound. Purification was performed via recrystallisation using the miscible solvent method. The compound was dissolved in a minimum amount of toluene and then recrystallised by the addition of petroleum ether 60-80°C. The mother liquid was then placed on ice for half an hour to ensure complete crystallisation. The mixture was then filtered using Whatman 42 filter paper and the compound dried in a vacuum desiccator containing P<sub>2</sub>O<sub>5</sub>. The purity of the compound was confirmed via RP-HPLC, NMR, thin layer chromatography (dichloromethane/toluene 1:1) and DSC analysis. The melting point was determined to be 114.5°C (T<sub>onset</sub>) with the peak maximum occurring at 131.0°C (T<sub>max</sub>). IR (CHCl<sub>3</sub> cm<sup>-1</sup>) 2980.4, 2946.8, 2860.4, 1479.3, 1433.0, 1352.5, 1279.4, 1244.1, 1225.3, 1134.5, 1109.0, 1007.6, 962.3, 893.7. <sup>1</sup>H-NMR (CDCl<sub>3</sub>) 4.25 (4H, m, 2CH<sub>2</sub>), 1.78 (6H, m, 3CH<sub>2</sub>). <sup>13</sup>C-NMR (CDCl<sub>3</sub>) 193.05, 56.13, 52.97, 26.90, 25.98, 24.63, 24.48.

## 6.2 Reaction rate analysis

### 6.2.1 RP-HPLC analysis for the isothermal curative interactions and the model compound study

Both the isothermal and model compound reaction products were separated via a gradient elution programme<sup>1</sup>, as seen in Table 6.1. The detector was set a wavelength of 260 nm. The column employed was a C-18 reverse phase column as described in the experimental section.

Table 6.1: Gradient elution profile employed for the separation of both the isothermal and model compound reaction products

Time (min)	Flow rate (/mL min <sup>-1</sup> )	% MeOH	% H <sub>2</sub> O	Elution Profile <sup>1</sup>
	1	80	20	-
15	1	100	0	10

CPTD and sulfur were resolved into well defined separate peaks for analysis. The retention times for CPTD and sulfur were 7.1 and 22.6 minutes respectively.

## 6.2.2 Dynamic study of the curative interactions via thermal analysis

The dynamic studies to monitor the curative interactions were all run at a 5°C/min heating rate under an inert nitrogen atmosphere. N,N'-dicyclopentamethylenethiuram disulfide and sulfur were analysed in a 1:1 molar ratio via DSC and TGA. The thermogram in Figure 6.1 depicts the N,N'-dicyclopentamethylenethiuram disulfide melt, which is observed at 131.0°C ( $T_{max}$ ). The melt is broad with the onset of melt occurring at approximately 115°C.

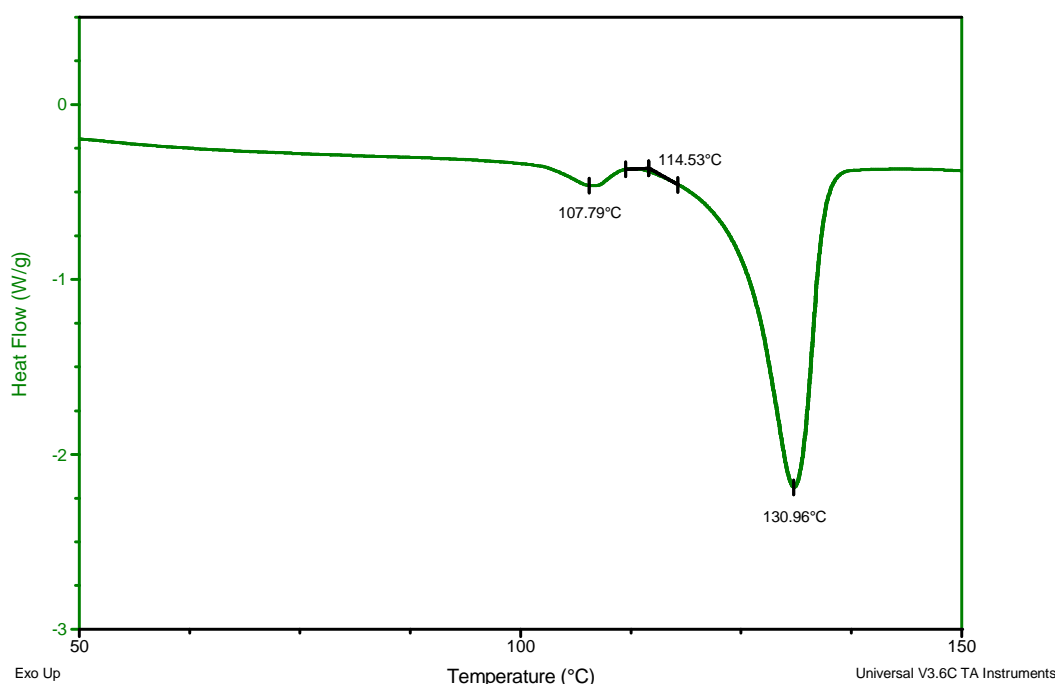


**Figure 6.1:** DSC thermogram depicting the N,N'-dicyclopentamethylenethiuram disulfide melt

The compound has been reported to melt at 132°C.<sup>2</sup> The broad temperature range at which the compound was seen to melt may be as a result of molecular changes occurring in the melt. It has previously been reported that certain disulfides may undergo changes to species of different sulfur rank. MBTS for example undergoes a significant amount of conversion to 2-bisbenzothiazole-2,2'-monosulfide (MBTM) when heated at its melt<sup>3</sup>. Most accelerator melts are not just fusion processes but rather a system of elimination reactions producing a spectrum of more stable molecules. The broad temperature range at which the compound was seen to melt may also be attributed to the presence of a large number of imperfect crystals that

may result from the varied conformations that the piperidine moiety may exhibit. Computer modelling showed these groups to be in the chair conformation, but during crystallisation they would gain enough energy through solvation to contort to the chair as well as twist conformations with a limiting energy barrier of 45 kJ/mol which is seen in similar structures<sup>4</sup>. A small peak at 107°C is attributed to the evaporation of residual toluene (b.p. = 110.6°C).<sup>5</sup> It is, however, more likely that the broadness of the melt is due to freezing point depression as a result of the trace amounts of toluene. Even at the higher temperatures not all the toluene would have evaporated. This would be due to the occlusion of the toluene in the crystal lattice causing a fair amount of imperfect crystals, thus broadening the melt further. Before experiments were run on the compound, it was placed in a vacuum dessicator for a further 48 hours to remove any remaining solvent.

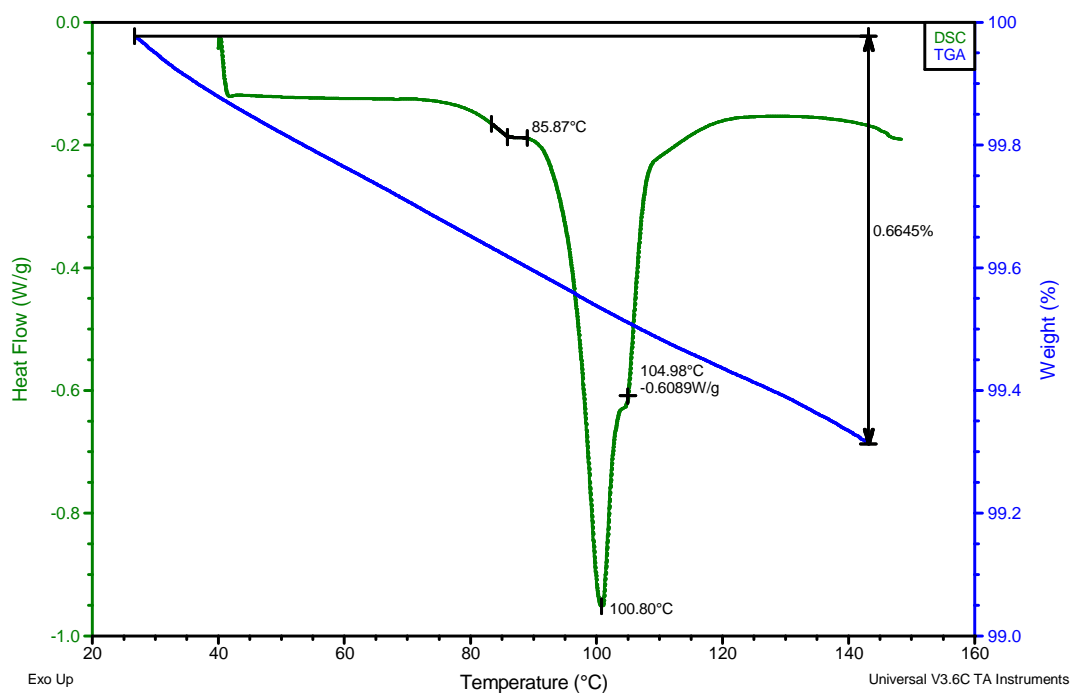


**Figure 6.2: DSC and TGA Thermograms depicting the heat of N,N'-dicyclopentamethylenethiuram disulfide with sulphur**

The master batch (1:1 molar ratio) of N,N'-dicyclopentamethylenethiuram disulfide/S<sub>8</sub> when examined dynamically via DSC yielded interesting results. The N,N'-dicyclopentamethylenethiuram disulfide melt was no longer observed (see Figure 6.2) The formation of alternative products on mixing was considered, and RP-HPLC analysis of the unreacted master batch gave two well defined peaks corresponding to the accelerator and sulfur thus disproving this possibility. The only

reasonable explanation that may be attributed to this would be the solubilisation of N,N'-dicyclopentamethylenethiuram disulfide in the sulfur melt.

Once both components have entered the molten state either via solubilisation or by means of melting, they may react to form various accelerator polysulfides, thiols, decomposition products and different cyclic sulfur compounds. Thus the transitions seen from 85°C to 120°C may be attributed to sulfur transitions, the mutual solubilisation of sulfur and N,N'-dicyclopentamethylenethiuram disulfide<sup>2</sup>, and their reaction. The small peak at 86°C is associated with the formation of N,N'-dicyclopentamethylenethiuram hexasulfide.<sup>2</sup>

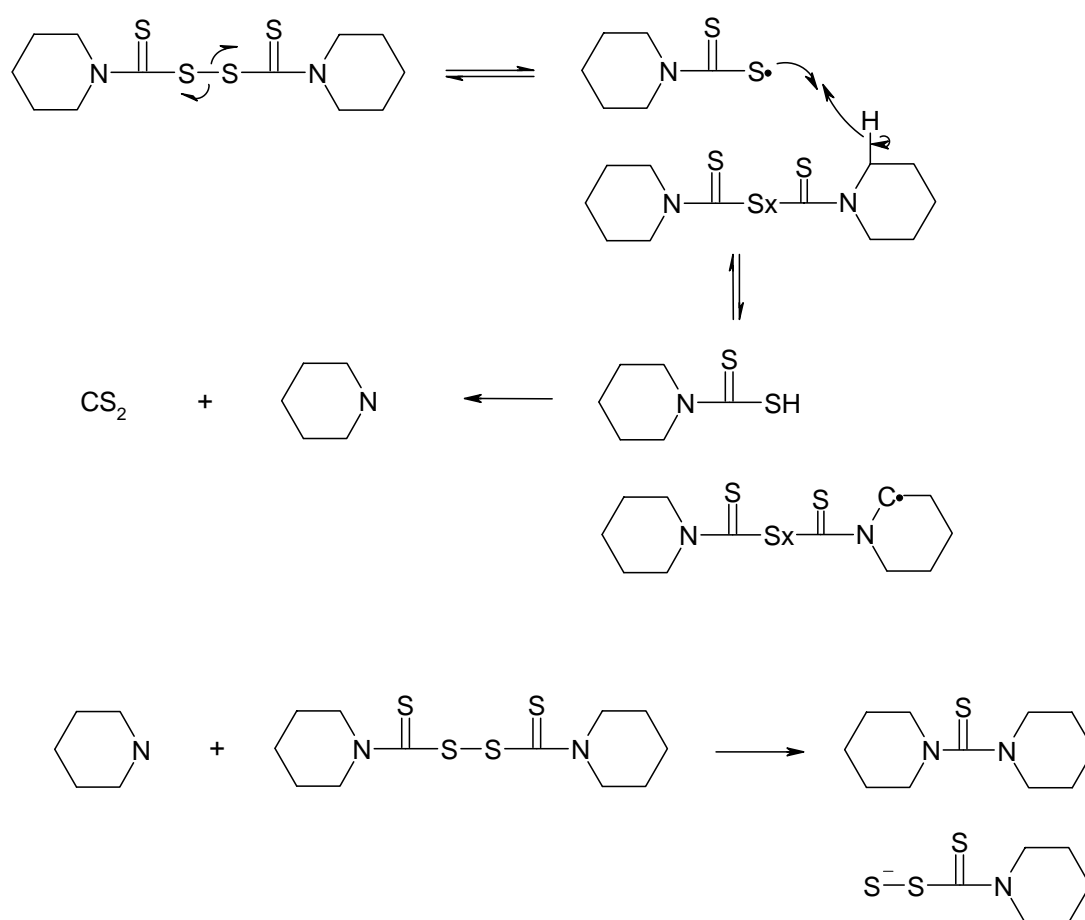


**Figure 6.3:** The proposed mechanism for the production of CPTU and amine from CPTD<sup>2,7</sup>

The beginning of the endotherm at 150°C observed in Figure 6.2 can be attributed to N,N'-dicyclopentamethylenethiuram monosulfide decomposition. It readily decomposes to N,N'-dicyclopentamethylene thiourea (CPTU) and CS<sub>2</sub>. This is seen

in the accelerated formation CPTU above 150°C as compared to TMTD.<sup>6</sup> The mass loss of less than 1% may be attributed to the loss of amine and CS<sub>2</sub>, which readily form upon the radical decomposition of CPTD as seen in Figure 6.3.

The formation of cyclopentamethylene dithiocarbamic acid (Hpmtc) occurs more readily in CPTD than in TMTD since methylene radical formation is much more favourable than that of the methyl radical. The resultant Hpmtc decomposes to the amine, which later acts on the CPTD to produce CPTU. Both amine and CPTU are volatile and may be lost by evaporation.<sup>6</sup>

### 6.2.3 Curative interactions

There are large number of interactions that occur between CPTD and S<sub>8</sub> (see Figure 6.4). It can be seen that when CPTD is heated in the presence of sulfur, polysulfides of different sulfur rank are formed as well as the decomposition products seen earlier.

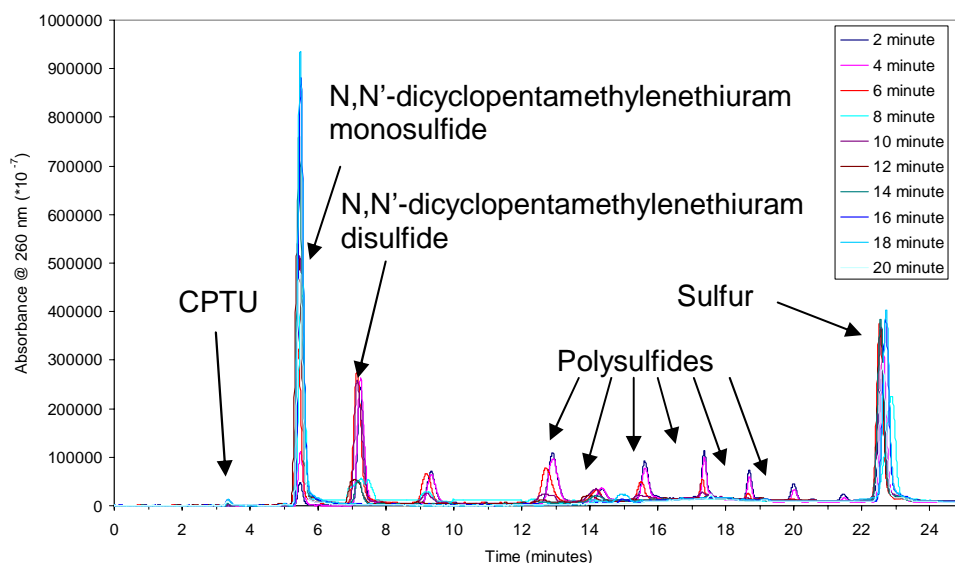


**Figure 6.4:** CPTD/S<sub>8</sub> (1:1 molar ratio) isothermal interactions

Polysulfide formation is fast, with a large number of polysulfides being formed in the first two minutes of reaction. Also noticeable is a very large peak ( $t_R = \pm 5.5$  minutes). This is most likely N,N'-dicyclopentamethylenethiuram monosulfide (CPTM) which is readily formed in CPTD systems but as the peak was not identified one would also have to consider the possibility of the peak being due to the formation of sulphonamide.

## 6.2.4 Model compound reactions

It has been observed that the N,N'-dicyclopentamethylenethiuram disulfide is a fast vulcanisation accelerator.

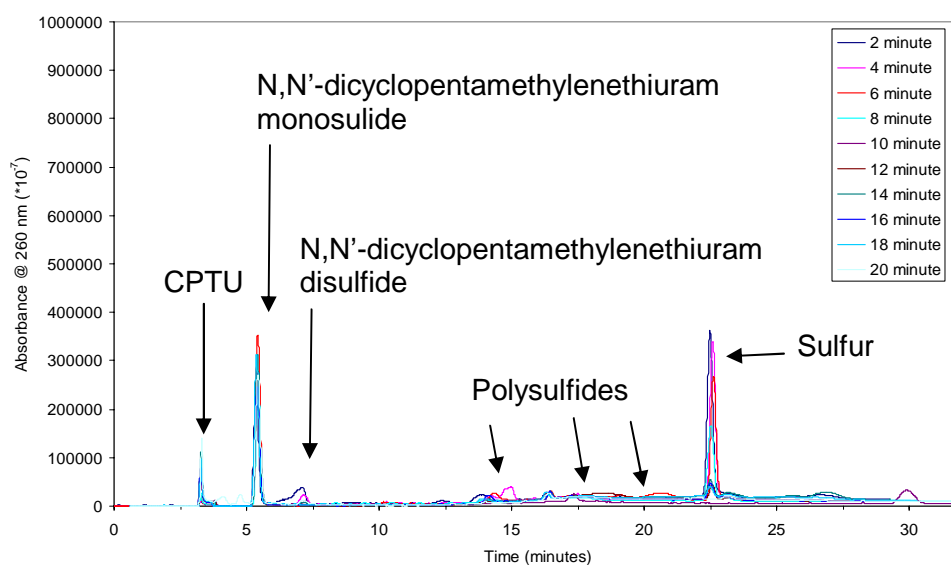


**Figure 6.5:** Chromatogram depicting the model compound interactions of N,N'-dicyclopentamethylenethiuram disulfide with sulfur and squalene

The rate of crosslinking is so fast that polysulfides are barely visible in the chromatogram above (Figure 6.5). The chromatograms in Figure 6.5 were smoothed for aesthetic purposes due to the presence of poor baselines. The reason for the baselines being poor relative to Figure 6.4 was probably due to column degeneration. After 4 minutes all the accelerator has reacted to produce active sulfurating agent, increasing the rate at which sulfur is depleted until at about 12 minutes sulfur depletion stops. One may interpret the system as now being an unaccelerated system as all the accelerator has been used.

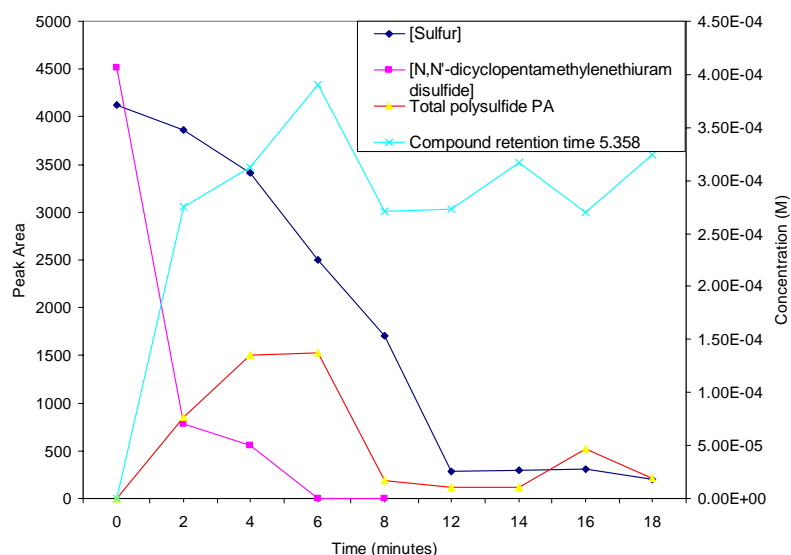


**Figure 6.6:** Reaction profile depicting the consumption of N,N'-dicyclopentamethylenethiuram disulfide and sulfur and the relative amounts of polysulfides at different time intervals

It can be seen in Figure 6.6 that the total polysulfide peak area throughout the experimental range is low implying that pendent group formation is fast. After 10 minutes vulcanisation is complete.<sup>8,9,10</sup>

**Table 6.2:** Rate data for the N,N'-dicyclopentamethylenethiuram disulfide model compound reactions

Data used	Rate and statistical data						
	Tangent slope (/mol L <sup>-1</sup> min <sup>-1</sup> )	Initial slope (/mol L <sup>-1</sup> min <sup>-1</sup> )	R <sup>2</sup>	N <sup>*</sup>	First Order (/s <sup>-1</sup> )	R <sup>2</sup>	N <sup>*</sup>
Sulfur	2.70 x 10 <sup>-5</sup>	2.88 x 10 <sup>-5</sup>	0.978	6	0.0034	0.991	7
N,N'-dicyclopentamethylenethiuram disulfide	1.70 x 10 <sup>-4</sup>	8.91 x 10 <sup>-5</sup>	0.744	4			

\* N denotes the number of points used in the determination of the plot

The high rate of sulfur loss after all the accelerator is consumed tends to suggest a high degree of instability in the Hpmtc formed, thus allowing for the formation of a large amount of free amine which is able to facilitate S<sub>8</sub> ring opening. Because of the



very rapid consumption of CPTD the first order plot for CPTD consumption is meaningless and no statistically significant results could be obtained (see Table 6.2).

### 6.2.5 Rate analysis of cis-1,4-polyisoprene, N,N'-dicyclopentamethylenethiuram disulfide and sulfur cured system

As can be seen from the rheometer trace in Figure 6.7, the N,N'-dicyclopentamethylenethiuram disulfide has a relatively long induction period, especially when we consider the fact that a large number of polysulfides have already formed in the second minute of the reaction. These polysulfides then react with the rubber chain to produce pendent groups. These then combine to form crosslinks as seen in the linear region when the torque increases. It should be noted that the rate constant determined for the model compound reactions and those of the rubber vulcanised sample will generally not be comparable since two different aspects of the vulcanisation process are being examined.

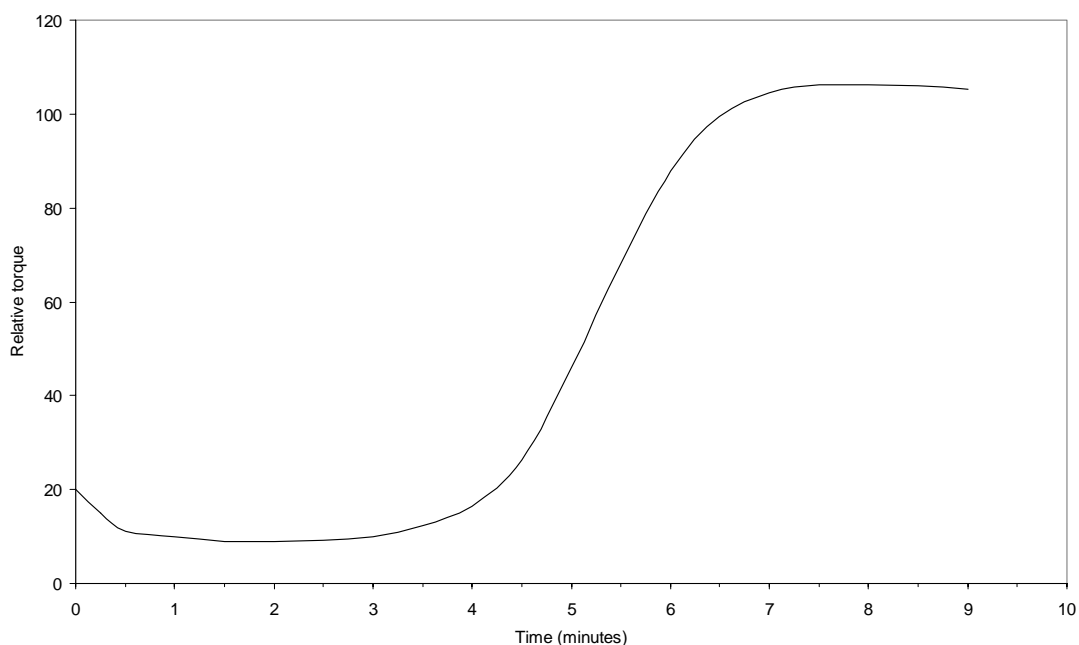
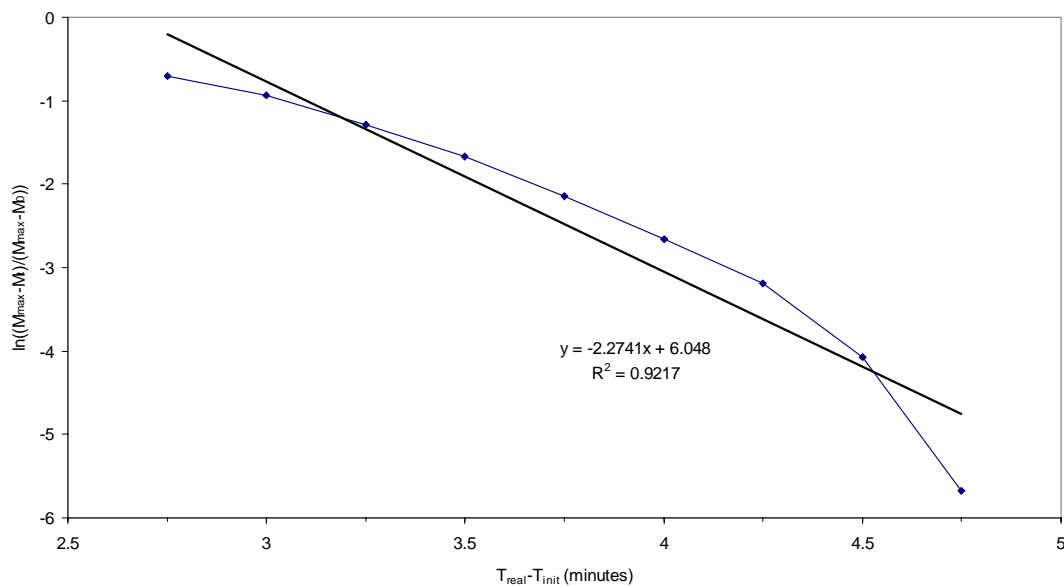


Figure 6.7: The rheometer curve depicting the cure of the N,N'-dicyclopentamethylenethiuram disulfide/S<sub>8</sub>/IR system

In the model compound study the rate at which accelerator is consumed by a large number of reactions is examined, while in the rubber system the rate at which crosslinks are formed is investigated.



**Figure 6.8:** Determination of the first order rate constant from rheometer data derived from the cure of N,N'-dicyclopentamethylenethiuram disulfide/S<sub>8</sub>/IR system

The rate in the linear region was then examined as per method discussed in the Introduction. The time at which the linear region was assumed to start was varied to obtain the best fit. The first order rate constant for the crosslinking reaction was determined to be 2.274 ( $R^2 = 0.922$ ), as seen in Figure 6.8 while the maximum slope as determined from Figure 6.7 was found to be 41.9 (relative torque/time in minutes).

**Table 6.3:** Summary of the rate data obtained for the vulcanisation of cis-1,4-polyisoprene by N,N'-dicyclopentamethylenethiuram disulfide in the presence of sulfur

<b>Rate and statistical data</b>			
<i>First order crosslinking (/min<sup>-1</sup>)</i>	<i>R<sup>2</sup></i>	<i>Maximum slope (/relative torque.min<sup>-1</sup>)</i>	<i>Coran's<sup>11</sup> rate constant (/min<sup>-1</sup>)</i>
2.2740	0.922	41.9	2.0480

The various rate data that were derived from the vulcanisation of cis-1,4-polyisoprene by means of N,N'-dicyclopentamethylenethiuram disulfide in the presence of sulfur are summarised in Table 6.3.

It should be noted that the Coran<sup>11</sup> ( $k_2$ ) rate constant determination presented two linear regions as was seen in Chapter 5 for the vulcanisation of cis-1,4-polyisoprene by means of tetraethylthiuram disulfide in the presence of sulphur. The latter slope is presented in table 6.3, thus the rate constant is representative of the maximum rate of change. This is likely as result of two different vulcanisation mechanisms expressing dominance at various degrees of cure governed by the intermediates that abound as time progresses. As discussed in Chapter 5 the initial slow linear region may correspond to the disproportionation of two thiuram terminated polysulfidic pendent groups on neighbouring polymer chains to produce a crosslink and a thiuram monosulfide or a thiuram polysulfide derivative.<sup>12,13,14</sup> While the second region consists of the fast dominant crosslinking reactions involving either the reaction of thiuram polysulfide pendent groups with polythiol pendent groups or the reaction of ammonium (derivative) terminated polysulfide pendent groups with polythiol pendent groups on neighbouring chain to produce crosslinks etc.<sup>15</sup> One has to just keep in mind though that the rate constant determined by Coran<sup>11</sup> is not related to the rate of crosslinking, but rather to the rate at which pendent groups the precursors to crosslink formation are activated. This is one of the chief concepts his theory relies upon, with his use of instruments such as the Agfa Vulkameter and Monsanto Oscillating Disk Rheometer the inference is made that the rate of crosslinking in the region where his rate constant is operational ( $k_2$ )<sup>11</sup> is not rate limiting. This is interesting since the first linear region as mentioned previously, is considered to be a rate limiting crosslinking reaction governed by the disproportionation of thiuram terminated pendent groups,<sup>12,13,14</sup> thus the torque vs. time curves produced by the Agfa Vulkameter and Monsanto Oscillating Disk Rheometer in this region are directly related to the rate of crosslink formation. The first order rate constant for crosslink formation (the first parameter in Table 6.3) does bare a certain relevance to the actual rate of crosslink formation as it considers the whole rate acceleratory region.

### 6.3 Computer modelling

In the geometry optimised structure, the piperidine rings conform to the expected chair conformations (see Figure 6.9). The dihedral angle about the disulfide linkage is approximately 90° conforming to what is seen in tetramethyl and tetraethylthiuram disulfide as well the crystal data for N,N'-dicyclopentamethylene thiuram disulfide.<sup>16,17,18</sup> The molecular complexity and the ease at which the structure converts between the chair, boat and twist conformations makes <sup>13</sup>C NMR spectral interpretations difficult. It is noted that two asymmetric duplets were detected,

explaining why seven and not five carbons were reported. Simplified  $^{13}\text{C}$  spectra may be obtained by increasing the temperature at which the  $^{13}\text{C}$  data collections were determined. This would resolve the spectra into five peaks as a result of the maintenance of a “constant” chemical environment for the analysis.

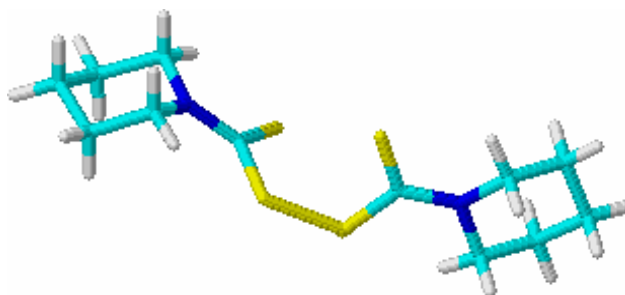


Figure 6.9: Geometry optimised structure for N,N'-dicyclopentamethylenethiuram disulfide

Even though the NMR analysis proved difficult, Table 6.4 reveals that the molecular parameters for the symmetric structure are reproducible in the mirrored regions, with both the corresponding bond distances and charges (Mulliken symbols) being equal. The Taft constant was not found in the literature and was therefore estimated from data obtained by Morita<sup>19</sup> by means of a linear extrapolation.

The calculated bond lengths are all of the expected magnitude and in good agreement with the crystal structure data.<sup>5,18</sup> The C-N bond once again present a partial double bond character.<sup>5</sup> If the trend observed for the crystal structure data is correct, one may expect the disulfide bond distance to be smaller than the calculated values with expected bond distance being closer to 2.00 Å for TMTD and TETD,<sup>16,17</sup> with the actual bond distance for the S-S bond in N,N'-dicyclopentamethylenethiuram disulfide from crystal structure data being 1.995 Å. The calculated atomic charges are smaller than previously encountered.<sup>18</sup> This may be as a result of the aliphatic side groups increased ability to alleviate charge variations by donating electron density.

Table 6.4: Computer modelled parameters for N,N'-dicyclopentamethylenethiuram disulfide

<p style="text-align: center;"><b>N,N'-</b> <b>dicyclopentamethylenethiuram</b> <b>disulfide</b> <b>Energy = 70.028 kJ/mol</b> <b>Gradient = 0.00983</b></p>					
<b>Bond distance</b> Å	<b>N-C</b>	<b>C-S</b>	<b>S-S</b>	<b>S-C</b>	<b>C-N</b>
	1.350	1.810	2.024	1.810	1.350
<b>Charge (Mulliken)</b>					
		-0.072			-0.072
	-0.353	0.042	-0.043	-0.0430	0.042

Taft constant estimated to be  $-0.152^{19}$

## 6.4 References

- 1) Automated Gradient Operators Manual 660, Waters, 34 Maple Street, Millford, Massachusetts, 01757 (1983)
- 2) C. P. Reyneke-Barnard, M. H. S. Gradwell and W. J. McGill, J. Appl. Polym. Sci., 77, 2718 (2000)
- 3) B. Morgan, Benzothiazole accelerated sulfur vulcanisation of 2,3-dimethyl-2-butene, PhD Thesis, University of Port Elizabeth, South Africa (1998)
- 4) J. McMurry, Organic Chemistry, 4<sup>th</sup> Ed, Brooks/Cole Publishing Company, New York (1996)
- 5) R. C. Weast, Ed., CRC Handbook of Chemistry and Physics, 51<sup>st</sup> Ed., The Chemical Rubber Co. Publishers, Cleveland (1970)
- 6) C. P. Reyneke-Barnard, M. H. S. Gradwell and W. J. McGill, J. Appl. Polym. Sci., 78, 1112 (2000)
- 7) C. P. Reyneke-Barnard, M. H. S. Gradwell and W. J. McGill, J. Appl. Polym. Sci., 77, 2732 (2000)
- 8) B. A. Dogadkin and V. A. Shershnev, Rubb. Chem. Technol., 33, 401 (1960)
- 9) B. A. Dogadkin and V. A. Shershnev, Chem. Abstr., 52, 10626c (1958)
- 10) B. A. Dogadkin, V. A. Shershnev and A. V. Dobromyslova, Chem. Abstr, 55, 5006c (1961)
- 11) A. Y. Coran, Rubber Chem. Technol., 37, 689 (1964)

- 12) F. W. H. Kruger and W. J. McGill, *J. Appl. Polym. Sci.*, 45, 563 (1992)
- 13) A. Y. Coran, *Rubber Chem. Technol.*, 38, 1 (1965)
- 14) M. Geysler and W. J. McGill, *J. Appl. Polym. Sci.*, 60, 439 (1996)
- 15) F. W. H. Kruger and W. J. McGill, *J. Appl. Polym. Sci.*, 42, 2669 (1991)
- 16) Y. Wang, J. H. Liao and C. H. Ueng, *Acta Cryst.*, c42, 1420 (1986)
- 17) I. L. Karle, J. A. Estlin and K. Britts, *Acta Cryst.*, 22, 273 (1967)
- 18) M. F. Dix, A. D. Rae, *Cryst. Struct. Commun.*, 2, 159 (1973)
- 19) E. Morita, *Rubb. Chem. Technol.*, 57, 746 (1984)

# 7 N,N'-Bis( $\sigma$ -methoxyphenyl)thiuram disulfide rate study

---

7.1	Synthesis and purification of N,N'-bis( $\sigma$ -methoxyphenyl)thiuram disulfide ..	131
7.2	Reaction rate analysis .....	132
7.2.1	RP-HPLC analysis of the isothermal curative interactions and model compound study.....	132
7.2.2	Dynamic study of N,N'-bis( $\sigma$ -methoxyphenyl)thiuram disulfide sulfur interactions via thermal analysis. ....	132
7.2.3	Curative interactions .....	133
7.2.4	Model compound reactions .....	134
7.2.5	Reaction of cis-1,4-polyisoprene, N,N'-bis( $\sigma$ -methoxyphenyl)thiuram disulfide and sulfur .....	136
7.3	Computer modelling.....	138
7.4	References .....	140

## 7.1 Synthesis and purification of N,N'-bis( $\sigma$ -methoxyphenyl)thiuram disulfide

Distilled water (70 mL) was placed into a 250 mL double necked round bottomed flask. The reaction vessel was kept at approximately 5°C throughout the synthesis while the reaction mixture was stirred continuously to prevent local excesses. NaOH (0.4278 mol, 17.1132 g) was added to the solution followed by  $\sigma$ -anisidine (0.09000 mol, 11.0837 g), which was redistilled under vacuum to yield a slightly yellow clear liquid (b.p. 224°C). CS<sub>2</sub> (0.08996 mol, 35.44 mL) was then added drop wise over an hour. The reaction mixture went from a light transparent homogenous mixture to a milky white liquid. After the addition of all the CS<sub>2</sub> the reaction mixture was stirred for a further hour with a steady N<sub>2</sub> purge to remove any unreacted CS<sub>2</sub>. K<sub>3</sub>Fe(CN)<sub>6</sub> (0.08996 mol, 90.04 mL of a 0.9991 M solution) was then added to the reaction mixture over a two hour period, the reaction mixture then went yellow with a white precipitate.

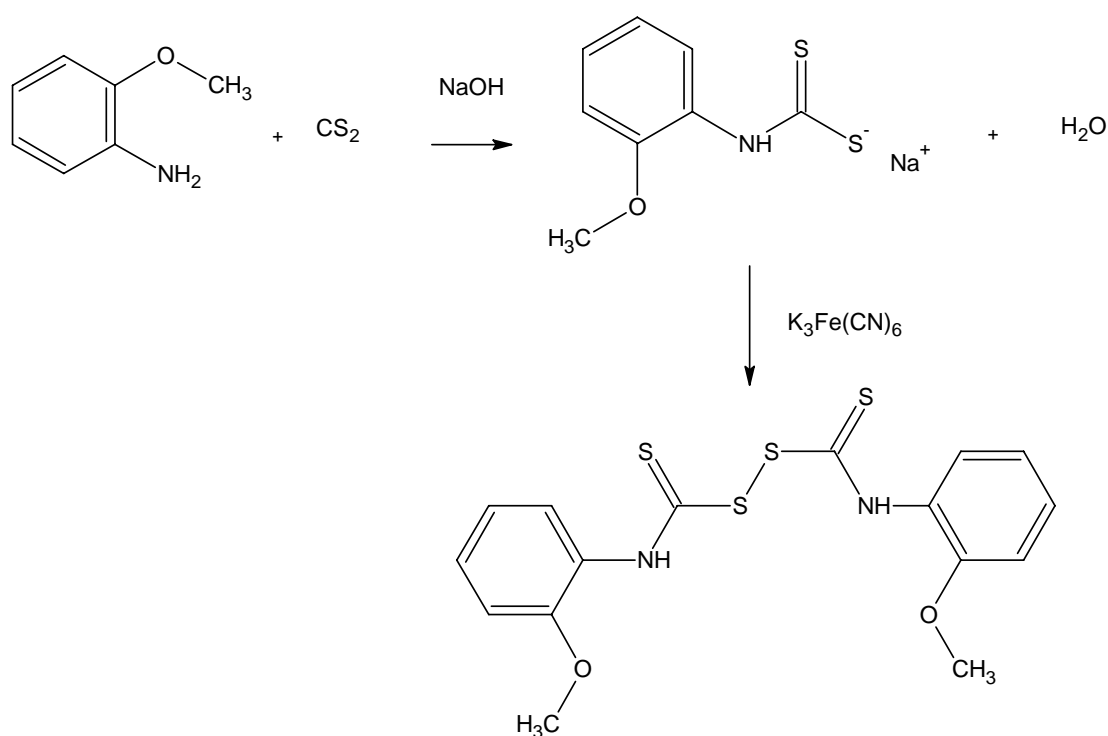


Figure 7.1: Synthetic scheme for the synthesis of N,N'-bis( $\sigma$ -methoxyphenyl)thiuram disulfide

Purification was achieved initially by simple frontal analysis to remove all the inorganic material. Firstly the compound was filtered and then rinsed in the filter paper with cold water. A 30 cm silica gel column was prepared in a 90:10 (volume



ratio), dichloromethane:diethyl ether. The crude compound was then dissolved in dichloromethane and applied to the column. The 90:10 dichloromethane:diethyl ether was used as the mobile phase, requiring 800 mL to elute all the compound from the column. The eluent that remained was a transparent yellow colour. This solution was then evaporated off to leave an orange/yellow compound. This compound was then recrystallised by means of the miscible solvent method. A minimum amount of dichloromethane was added to the compound to dissolve it and crystallization was achieved by the addition of petroleum ether 60-80°C. This was performed five times. Purity was established via RP-HPLC, DSC, TLC (90:10 dichloromethane:diethyl ether) and NMR. NMR did, however, show the presence of solvent peaks. The yield was determined to be 35.12% (6.2655 g), while the melting point was found to be in the range of 131.0°C ( $T_{\text{onset}}$ ) with the peak maximum occurring at 133.1°C ( $T_{\text{max}}$ ). IR ( $\text{CHCl}_3$   $\text{cm}^{-1}$ ) 3023.0, 2968.9, 2840.6, 2341.3, 1602.9, 1543.5, 1507.6, 1463.1, 1436.2, 1368.9, 1257.1, 1240.0, 1184.3, 1113.8, 1047.3, 1029.1, 784.8.  $^1\text{H-NMR}$  ( $\text{CDCl}_3$ ) 8.12 (1H, s, NH), 8.03 (1H, d, J 7.47, ArH), 7.26 (1H, m, ArH), 7.02 (2H, m, ArH), 3.84 (3H, m,  $\text{CH}_3$ ).  $^{13}\text{C-NMR}$  ( $\text{CDCl}_3$ ) 178.55, 151.68, 127.02, 126.89, 124.34, 121.10, 111.53, 56.15.

## **7.2 Reaction rate analysis**

### **7.2.1 RP-HPLC analysis of the isothermal curative interactions and model compound study**

Both the isothermal and model compound reaction products were separated by RP-HPLC with an isocratic elution system employing a 100% methanol mobile phase. The detector was set at a wavelength of 260 nm. The column employed was a C-18 reverse phase column as described in the experimental section. The N,N'-bis( $\sigma$ -methoxyphenyl)thiuram disulfide and sulfur were found to have retention times of 2.75 and 10.43 minutes respectively.

### **7.2.2 Dynamic study of N,N'-bis( $\sigma$ -methoxyphenyl)thiuram disulfide sulfur interactions via thermal analysis**

N,N'-bis( $\sigma$ -methoxyphenyl)thiuram disulfide was determined to melt above 131.0°C ( $T_{\text{onset}}$ ) with the peak maximum occurring at 133.1°C ( $T_{\text{max}}$ ). As can be seen in the dynamic study in Figure 7.2, all the thermal processes seem to be displaced from

expected temperatures. Two transitions are seen between 100°C and 120°C having peak maximums at 112.7°C and 117.6°C. The  $S_{\alpha}$ - $S_{\beta}$  sulfur transition which is known to occur at 107.0°C<sup>1</sup> appears to have been lost or shifted to the first transition having a peak maximum of 112.7°C. The  $S_{\beta}$ - $S_{\lambda}$  transition that is known to occur at 113°C<sup>1</sup> may now be seen at 117.6°C. The N,N'-bis( $\sigma$ -methoxyphenyl)thiuram disulfide melt remains unchanged and is seen to occur at 133°C ( $T_{max}$ ).

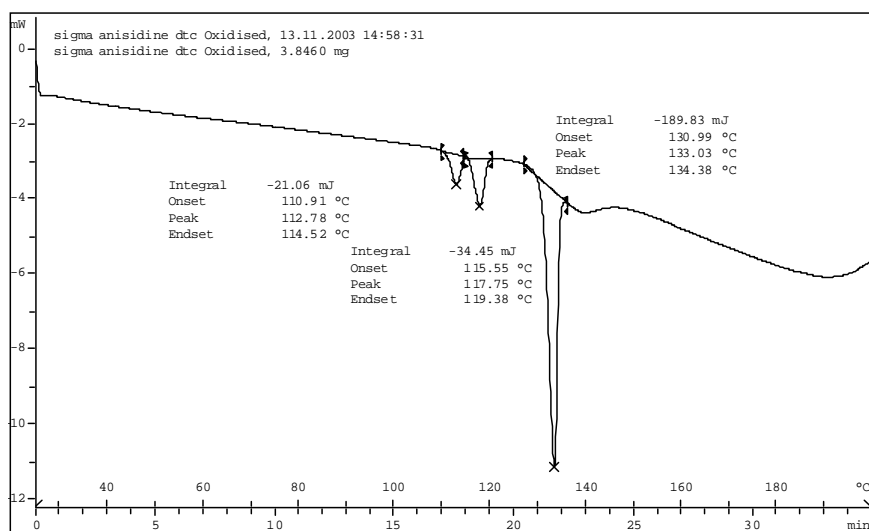


**Figure 7.2:** DSC thermogram depicting the heat of N,N'-bis( $\sigma$ -methoxyphenyl)thiuram disulfide with sulfur

### 7.2.3 Curative interactions

The number of interaction products observed in the isothermal curative interaction study was minimal. This would possibly indicate a poor accelerator (see Figure 7.3). It should be noted that all the aromatic derivatives that were produced displayed a similar low reactivity in the isothermal curative interaction study. Similar behaviour was observed with N,N'-diphenylthiuram disulfide.

It is not certain whether the product produced was primarily produced as a result of thermal instability of the accelerator or an actual interaction of the accelerator with sulfur.

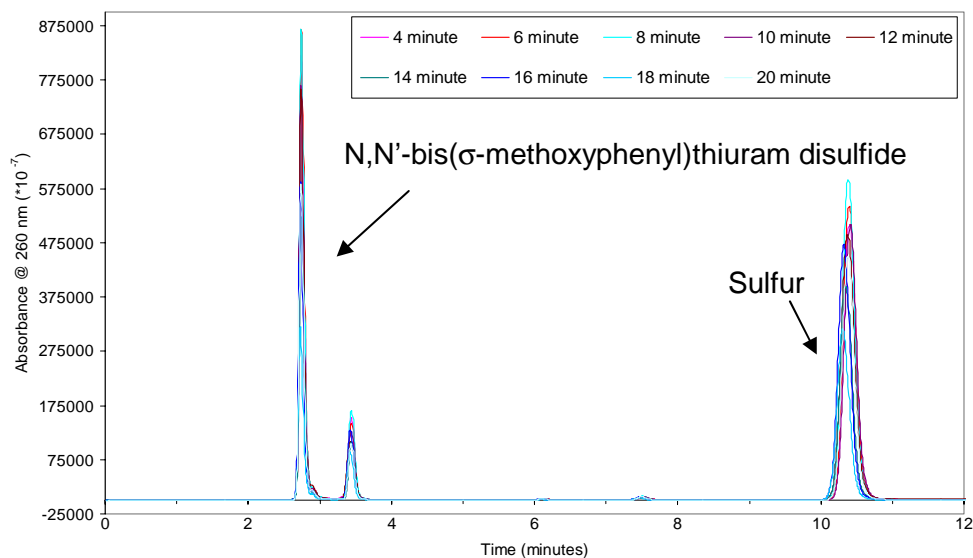


Figure 7.3: N,N'-bis(σ-methoxyphenyl)thiuram disulfide /S<sub>8</sub> (1:1 molar ratio) isothermal interactions

#### 7.2.4 Model compound reactions

The number of interaction products observed during the model compound study were minimal, similar to the isothermal curative study (cf. Figures 7.3 and 7.4).

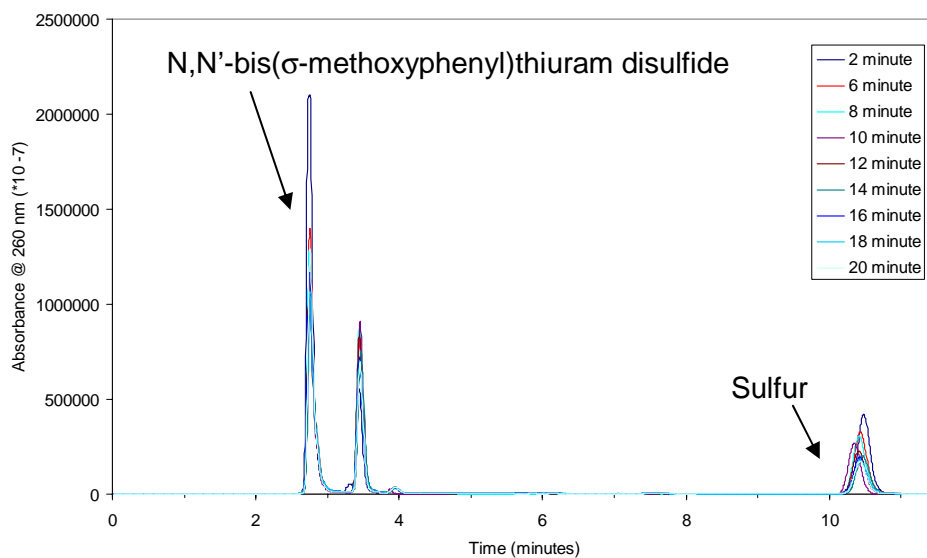
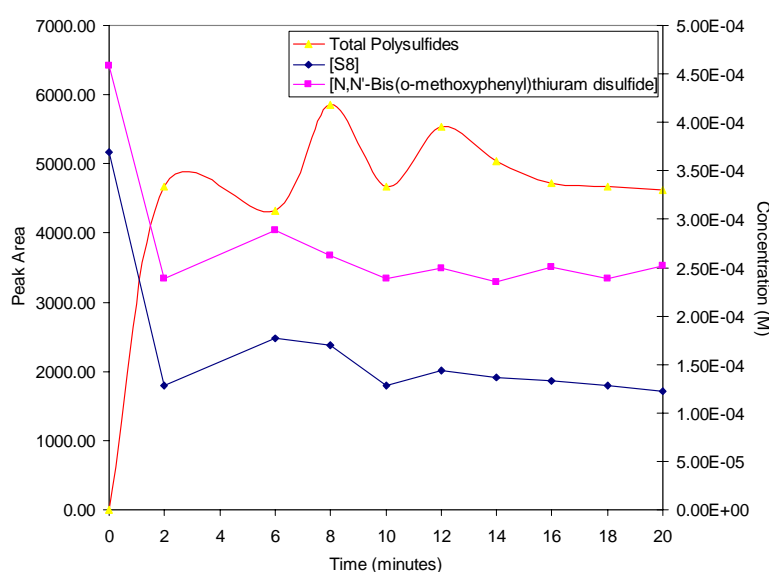


Figure 7.4: Chromatogram depicting the model compound interactions of N,N'-bis(σ-methoxyphenyl)thiuram disulfide with sulfur and squalene

This was quite unusual as it was noted in the N,N'-diphenylthiuram disulfide study that even though the number of interaction products produced in the isothermal study were few, the number of reaction products produced in the model compound study were substantially more. This might indicate the reduced activity of the accelerator as a crosslinking agent in general, or it may indicate a certain incompatibility of the accelerator in the squalene system

It should be noted as seen in Figure 7.5, that there is a rapid consumption of accelerator and sulfur during the first two minutes, thereafter an equilibrium concentration value is reached.



**Figure 7.5: Reaction profile for the consumption of N,N'-bis( $\sigma$ -methoxyphenyl)thiuram disulfide and sulfur**

It should be noted that throughout the reaction time investigated the polysulfide concentration is relatively constant (except during the first 2 minutes). This would imply that even though the accelerator reacts with sulfur to produce active accelerator polysulfides, their reactivity toward the squalene chain is low. This would then explain the relatively unchanged accelerator and sulfur concentrations at higher reaction times especially when equilibrium processes are operational.

In this reaction study the initial slopes method proved to be less accurate in determining the relative rate as compared to the other compounds investigated. This was primarily as a result of experimental error and the few data points available. Even though fewer points were used to determine the initial slope the values that were

determined were similar to the slopes of the tangents in the initial regions. One should, however, be cautious when considering the value of the slope of the tangent as it may be prone to exaggerate small variations especially where tangents are chosen indiscriminately.

Table 7.1: Rate data for the N,N'-bis( $\sigma$ -methoxyphenyl)thiuram disulfide model compound reactions

Data used	Rate and statistical data						
	Tangent slope (/mol L <sup>-1</sup> min <sup>-1</sup> )	Initial slope (/mol L <sup>-1</sup> min <sup>-1</sup> )	R <sup>2</sup>	N*	First Order (/s <sup>-1</sup> )	R <sup>2</sup>	N*
Sulfur	3.20 x 10 <sup>-5</sup>	2.49 x 10 <sup>-5</sup>	0.242	4	4.39 x 10 <sup>-4</sup>	0.977	7
N,N'-bis( $\sigma$ -methoxyphenyl)-thiuram disulfide	9.10 x 10 <sup>-5</sup>	2.45 x 10 <sup>-5</sup>	0.986	3	6.71 x 10 <sup>-4</sup>	0.999	3

\* N denotes the number of points used in the determination of the plot

Both the slope of the tangent and the initial slope and the first order consideration of the sulfur data gave much more reliable results in terms of the method and number of data points employed respectively for the rate determination, while the N,N'-bis( $\sigma$ -methoxyphenyl)thiuram disulfide allowed the use of fewer points, due to non-linearity, thus reducing the reliability of the results (see Table 7.3).

### 7.2.5 Reaction of cis-1,4-polyisoprene, N,N'-bis( $\sigma$ -methoxyphenyl)thiuram disulfide and sulfur

As in all the other aromatic thiurams considered, the cure seems to be a marching cure with little or no induction period. The rate of cure is slow, reaching a maximum torque values after 45 minutes, after which time there was a reduction in torque indicating some reversion (see Figure 7.6). The maximum slope as determined from Figure 7.6 was 0.314 (relative torque/time in minutes)

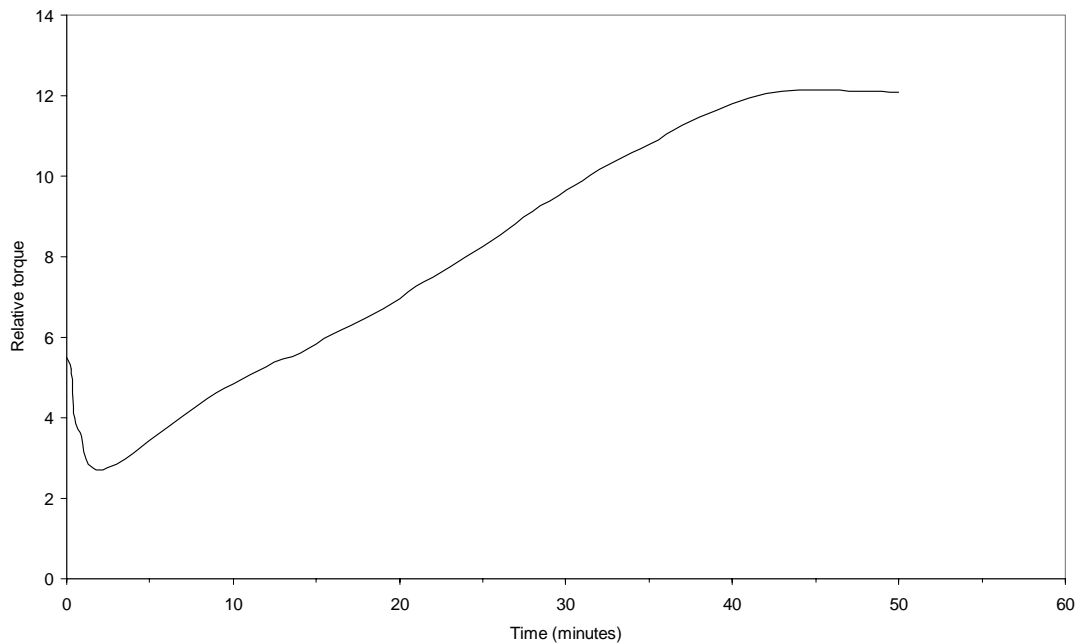


**Figure 7.6:** Rheometer curve depicting the cure of the N,N'-bis( $\sigma$ -methoxyphenyl)thiuram disulfide/S<sub>8</sub>/IR system

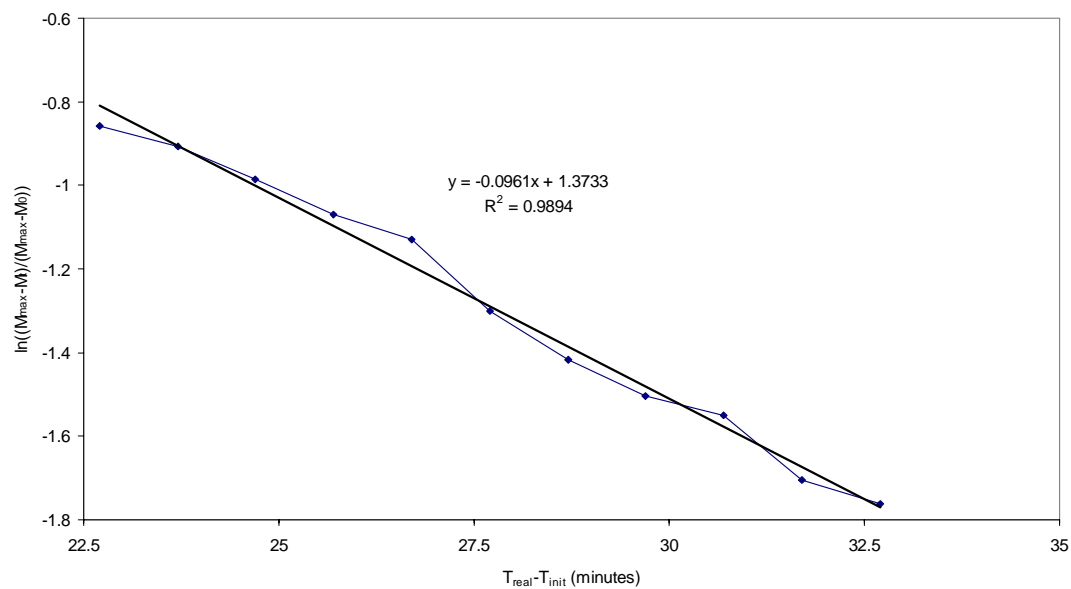


**Figure 7.7:** Determination of the first order rate constant from rheometer data derived from the cure of N,N'-bis( $\sigma$ -methoxyphenyl)thiuram disulfide/S<sub>8</sub>/IR system

The first order rate constant was determined to be 0.0961 ( $R^2 = 0.989$ ), as seen in Figure 7.7. Once again the marching cure allowed a large number of points to be used for the rate constant determination, increasing the accuracy of the

determination. Table 7.2 presents a summary of the rate data available for the vulcanisation of cis-1,4-polyisoprene by means of N,N'-bis( $\sigma$ -methoxyphenyl)thiuram disulfide in the presence of sulphur.

Table 7.2: Summary of the rate data obtained for the vulcanisation of cis-1,4-polyisoprene by N,N'-bis( $\sigma$ -methoxyphenyl)thiuram disulfide in the presence of sulfur

<b>Rate and statistical data</b>			
<i>First order crosslinking (/min<sup>-1</sup>)</i>	<i>R<sup>2</sup></i>	<i>Maximum slope (/relative torque.min<sup>-1</sup>)</i>	<i>Coran's<sup>2</sup> rate constant (/min<sup>-1</sup>)</i>
0.0961	0.989	0.314	0.0148

### 7.3 Computer modelling

Computer modelling algorithms are path dependent, i.e. the final optimised structure is dependent on the initial inputs. A large number of initial structures were drawn before settling on the final structure obtained in Figure 7.8. Some doubt existed over the accuracy of this minimum structure because of the positioning of the thione and methoxy groups.

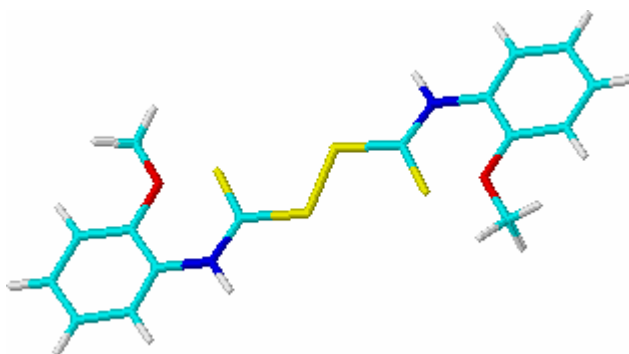


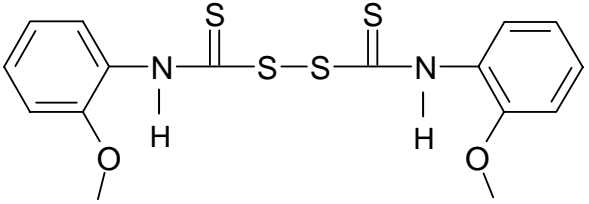
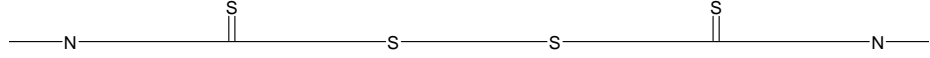
Figure 7.8: Geometry optimised structure for N,N'-bis( $\sigma$ -methoxyphenyl)thiuram disulfide

Figure 7.8, however, is the most accurate representation of the structure. Attempts to obtain a structure with the methoxy group opposite to the thione group proved impossible. This may have been as a result of unfavourable hydrogen bonding between the methoxy oxygen and the amine hydrogen atoms. For hydrogen bonding<sup>3</sup> to occur the hydrogen donor distance must be less than 3.2Å and the angle made by

covalent bonds to the donor and acceptor atoms must be less than 120°. This condition may have been fulfilled causing unfavourable strain within the molecule.

Once again variation within the calculated bond distances and charges are observed. This results from different chemical environments being experienced by each atom. This is seen in the complex proton couplings with multiplettes being observed and more specifically in the <sup>13</sup>C spectra which accounts for all the aromatic carbons in half the molecule. No symmetry was observed across the aromatic ring as was the case with N,N'-diphenylthiuram disulfide. Thus eight carbon peaks were observed which is half the total, with the spectral lines being twice as intense as a result of molecular symmetry about the disulfide linkage. The crystallised compound is needle/plate like as expected from the rigid aromatic structure. The molecule doesn't exhibit the conventional dihedral angle of approximately 90° seen for tetramethylthiuram disulfide<sup>4</sup>, tetraethylthiuram disulfide<sup>5</sup> and N,N'-dicyclopentamethylenethiuram disulfide preferring the trans configuration. This may result from steric effects and hydrogen bonding and could also be a vestige of the gas phase computer modelling calculations.<sup>3</sup>

**Table 7.3:** Computer modelled parameters for N,N'-Bis(σ-methoxyphenyl)thiuram disulfide

<b>N,N'-bis(σ-methoxyphenyl)thiuram disulfide</b> <b>Energy = 116.452 kCal/mol</b> <b>Gradient = 0.0483</b>					
<b>Bond distance</b> <b>Å</b>	<b>N-C</b>	<b>C-S</b>	<b>S-S</b>	<b>S-C</b>	<b>C-N</b>
	1.402	1.754	2.041	1.755	1.401
<b>Charge (Mulliken)</b>					
	-0.147	-0.349	-0.023	-0.049	-0.123
	0.274		0.258		

Taft constant = 0.33<sup>6,7</sup> (calculated)



It is noted that from Table 7.3 that all the atomic bond distances are of single bond character including the C-N bond distance which in previously examined molecules exhibited partial double bond ( $1.352\text{\AA}$ )<sup>8</sup> character which is in agreement with the crystal data.<sup>4,5,6</sup> Once again the disulfide bond distance is longer than the previously observed  $1.9\text{\AA}$ <sup>3,4</sup> for TMTD and TETD, this may be attributed to an anomaly introduced as a result of the gas phase calculations and more specifically to Hyperchem's reduced ability to model thiuram disulfide molecular structures.<sup>3</sup> It appears as though an electronegative atom in the substituent may promote the lengthening of the disulfide linkage by means of the removal of electron density and thus the weakening of the disulfide bond. This is seen in N,N'-dimorpholinethiuram disulfide,<sup>9</sup> assuming that inductive effects may act over long distance as hypothesised by Pauling,<sup>10</sup> the oxygen atom in this molecule has increased the S-S bond distance to  $2.01\text{\AA}$  as compared to that of  $1.65\text{\AA}$  seen in N,N'-dicyclopentamethylenethiuram disulfide<sup>6</sup>. As N,N'-dimorpholinethiuram disulfide and N,N'-dicyclopentamethylenethiuram disulfide are essentially similar differing only by the replacement of a carbon atom in the four position by an oxygen atom in the piperidine heterocycle, one may assume that either the change in bond distance is due to a long range inductive effect or hydrogen bonding involving the nitrogen atoms in the crystal structure.

#### 7.4 References

- 1) F. W. H. Kruger and W. J. McGill, *J. Appl. Polym. Sci.*, 42, 2643 (1991)
- 2) A. Y. Coran, *Rubber Chem. Technol.*, 37, 689 (1964)
- 3) HyperChem, 3ed manual (1994)
- 4) Y. Wang, J. H. Liao and C. -H. Ueng, *Acta Cryst.*, c42, 1420 (1986)
- 5) I. L. Karle, J. A. Estlin and K. Britts, *Acta Cryst.*, 22, 273 (1967)
- 6) Lange's Handbook of Chemistry, 15<sup>th</sup> ed, Edited by J.A. Dean, McGraw-Hill, New York (1999)
- 7) E. Morita, *Rubb. Chem. Technol.*, 57, 746 (1984)
- 8) R. C. Weast, Ed., *CRC Handbook of Chemistry and Physics*, 51<sup>st</sup> Ed., The Chemical Rubber Co. Publishers, Cleveland (1970)
- 9) G. C. Rout, M. Seshasayee, G. Aravamudan, *Cryst. Struct. Commun.*, 2, 1389 (1982)
- 10) Wheland and Pauling, *J. Am. Chem. Soc.*, 57, 2086 (1935)

# 8 N,N'-Bis(4-sec-butylphenyl)thiuram disulfide rate study

---

8.1	Synthesis and purification of N,N'-bis(4-sec-butylphenyl)thiuram disulfide .....	142
8.2	Reaction rate analysis .....	143
8.2.1	RP-HPLC analysis for the isothermal curative interactions and model compound study.....	143
8.2.2	Dynamic study of N,N'-bis(4-sec-butylphenyl)thiuram disulfide/sulfur .....	143
8.2.3	Curative interactions .....	144
8.2.4	Model compound reactions .....	145
8.2.5	Analysis of cis-1,4-polyisoprene, N,N'-bis(4-sec-butylphenyl)thiuram disulfide and sulfur cured system .....	148
8.3	Computer modelling.....	150
8.4	References .....	151

## 8.1 Synthesis and purification of N,N'-bis(4-sec-butylphenyl)thiuram disulfide

Distilled water (70 mL) was placed into a 250 mL double necked round bottomed flask. The reaction vessel was kept at approximately 5°C throughout the synthesis, while the reaction mixture was stirred continuously to prevent local excesses. NaOH (0.18039 mol, 7.2154 g) was added to the solution followed by 4-sec-butylaniline (0.0893 mol, 13.3306 g), which was redistilled under vacuum to yield a transparent light yellow liquid (b.p. 245°C). CS<sub>2</sub> (0.07075 mol, 4.27 mL) was then added drop wise over a period of an hour. The reaction mixture went from a light yellow homogenous mixture to a thicker yellow/orange liquid. After the addition of all the CS<sub>2</sub> the reaction mixture was stirred for a further hour with a steady N<sub>2</sub> purge to remove any unreacted CS<sub>2</sub>. K<sub>3</sub>Fe(CN)<sub>6</sub> (0.0892 mol, 89.143 mL of a 0.999 M solution) was then added to the reaction mixture over a two hour period, the reaction mixture then went orange as a result of Fe<sup>3+</sup> with the presence of finely divided white and black particulates. The white precipitate being the thiuram product while the later was ascribed to the formation of finely divided metallic Fe.

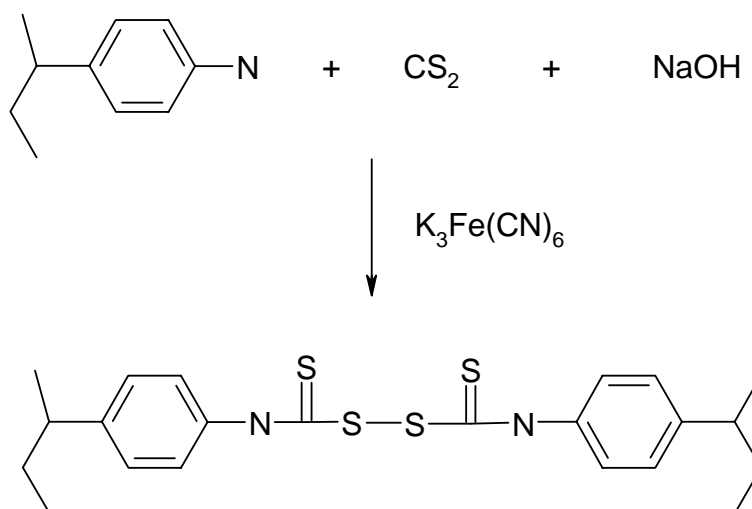


Figure 8.1: Synthetic scheme for the synthesis of N,N'-bis(4-sec-butylphenyl)thiuram disulfide

Purification was achieved initially by simple frontal analysis to remove all the inorganic material. A 30 cm silica gel column was prepared in a 90:10 (volume ratio) dichloromethane:diethyl ether. The crude compound was then dissolved in the same solution (200 mL) and applied to the column. The 90:10 dichloromethane:diethyl ether was used as the mobile phase, requiring 300 mL to elute all the compound from

the column. The eluent that remained was a transparent orange colour. This solution was then evaporated off to leave an orange compound. This compound was then recrystallised by means of the miscible solvent method. A minimum amount of dichloromethane was added to the compound to dissolve it and crystallisation was achieved by the addition of petroleum ether 60-80°C. This was performed five times. Purity was established via RP-HPLC, DSC, TLC (90:10/dichloromethane:diethyl ether) and NMR. NMR did however show the presence of solvent peaks. The reaction yield was determined to be 31.94% (5.0700 g), while the melting point was found to be 116.7°C ( $T_{\text{onset}}$ ) with a peak maximum occurring at 120.1°C ( $T_{\text{max}}$ ). IR ( $\text{CHCl}_3$   $\text{cm}^{-1}$ ) 3407.4, 3366.2, 2964.9, 2931.5, 2874.8, 1586.8, 1523.7, 1472.3, 1355.7, 1261.0, 1199.9, 1017.8, 928.5.  $^1\text{H-NMR}$  ( $\text{CDCl}_3$ ) 7.93 (1H, s, NH), 7.30 (2H, m, Ar), 7.28 (2H, m, Ar), 2.62 (1H, m, CH), 1.57 (2H, m,  $\text{CH}_2$ ), 1.24 (3H, m,  $\text{CH}_3$ ), 0.8 (3H, m,  $\text{CH}_3$ ).  $^{13}\text{C-NMR}$  ( $\text{CDCl}_3$ ) 180.33, 147.33, 135.09, 128.56, 125.99, 125.73, 41.79, 41.67, 31.46, 22.07, 12.50.

## **8.2 Reaction rate analysis**

### **8.2.1 RP-HPLC analysis for the isothermal curative interactions and model compound study**

Both model compound and isothermal reaction products were effectively separated via RP-HPLC analysis employing a 90:10, methanol:water mobile phase. The UV detector was set at a wavelength of 260 nm to maintain uniformity throughout all the analyses. The N,N'-bis(4-sec-butylphenyl)thiuram disulfide was detected as a well defined separate peak having a retention time of 6.1 minutes, while the sulfur appeared at 25.0 minutes.

### **8.2.2 Dynamic study of N,N'-bis(4-sec-butylphenyl)thiuram disulfide/sulfur interactions via thermal analysis**

The melting point of N,N'-bis(4-sec-butylphenyl)thiuram disulfide was determined to be 116.7°C ( $T_{\text{onset}}$ ) with the peak maximum occurring at 120.1°C ( $T_{\text{max}}$ ). It is difficult to see from the DSC thermogram in Figure 8.2 whether there is any interaction between the sulfur and the accelerator since the melts of the pure accelerator and sulfur are so close together. Hence little change in temperatures on mutual solubilisation can

be expected. The peak observed at 112.9°C corresponds closely to the  $S_{\beta}$ - $S_{\lambda}$  transition that is known to occur at 113°C<sup>1</sup>.

The mass loss of just under 8% may be as a result of compound instability, or possibly the remains of residual solvent. The latter would seem unlikely though since the compound was placed in vacuum desiccator for extended periods of time. It is unusual though that the first sulfur transition at 107°C is lost, while the second remains. It was, however, noted in this study that the first transition is considerably weaker than the second, even though in the majority of cases considered the second sulfur transition peak is lost in the accelerator melt, especially when mutual solubilisation of accelerator in sulfur is operational.

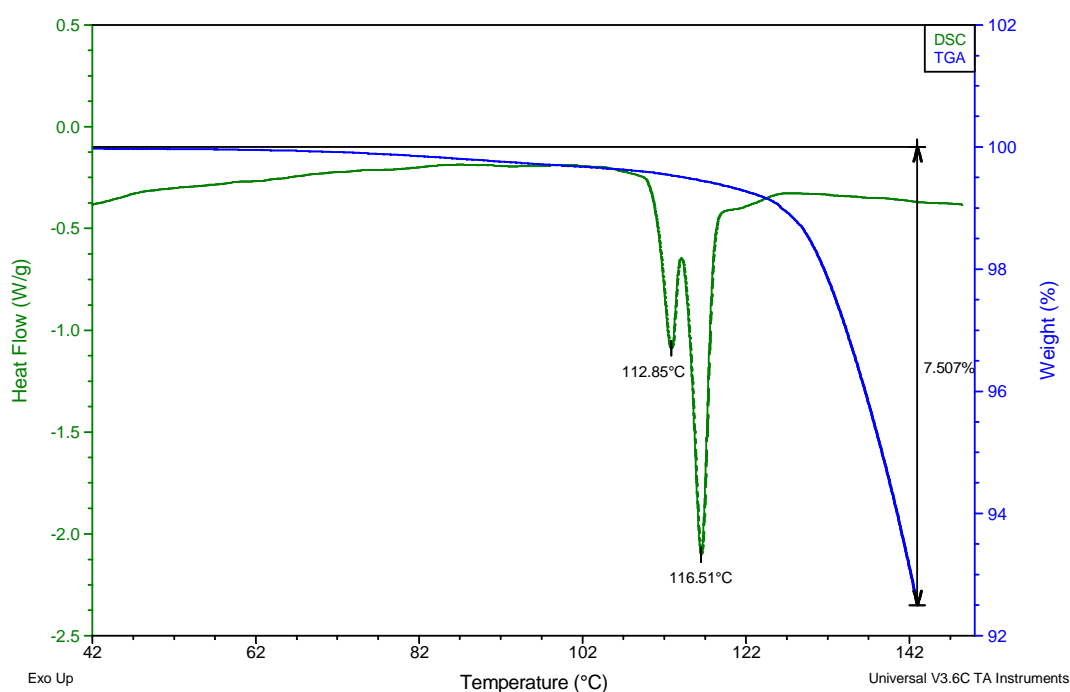


**Figure 8.2:** Thermogram depicting the heat of N,N'-bis(4-sec-butylphenyl)thiuram disulfide with sulfur

### 8.2.3 Curative interactions

Figure 8.3 depicts the interactions that occur between the accelerator and sulfur. It is seen that a minimal number of reaction products are produced when the reaction mixture is heated.

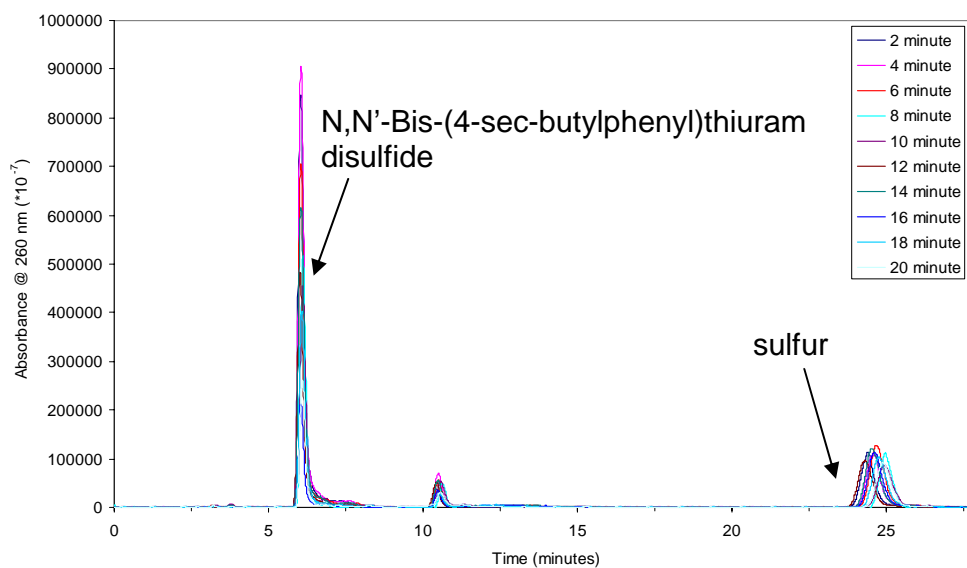


**Figure 8.3:** N,N'-bis(4-sec-butylphenyl)thiuram disulfide/S<sub>8</sub> (1:1 molar ratio) isotherm interactions

This may be an indication of a poor accelerator. If the vulcanisation rate, however, is not diminished the vulcanisation process would be driven by a mechanism that is independent of the normal conventional requirement of polysulfides as the active sulfurating agents. It was observed, however, that this accelerator has a subdued action, presenting a marching cure as seen in Figure 8.7.

#### 8.2.4 Model compound reactions

In vulcanisation it is generally considered that for a reaction to take place in a curative interaction, the sample needs to be heated above its melting point (or at least above the melting point of sulfur). This is a generalisation with respect to this system since it is well known that many reactions are able to take place in the solid state, for example Schiff base reactions in the formation of imines.<sup>2,3</sup>

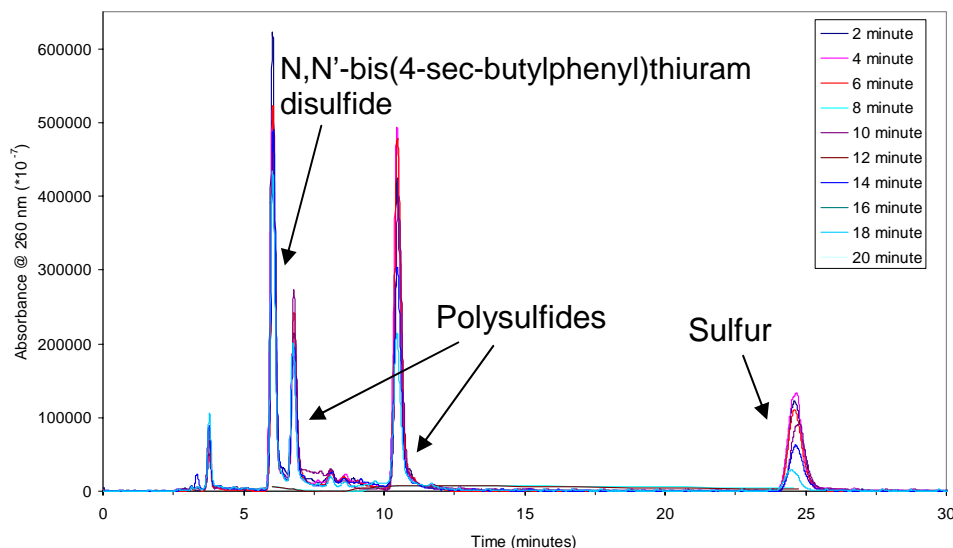


**Figure 8.4:** Chromatogram depicting the model compound interactions of N,N'-bis(4-sec-butylphenyl)thiuram disulfide with sulfur and squalene

There are a relatively large number of reaction products in the model compound study as opposed to the isothermal curative interaction analysis. These products are exclusively derived from accelerator and sulfur fragments left after reaction of the ternary mixture.

It can be seen in Figure.8.5 that the sulfur concentration decreases at a similar rate to that of the polysulfides during the course of the reaction. The rate at which the accelerator is consumed is slow, even though the initial change is large. The figure seems to imply that a large number of polysulfides are present and thus a large consumption of accelerator occurs, especially if one only considers the integration of the peak area. It should be noted though that the peak areas are low and it is assumed, as generally is in these cases, that the polysulfides have a similar molar extinction coefficient as the accelerator from which they are derived, this would correlate to a maximum total polysulfide concentration of 2.5 mg/25 mL. This is substantially lower than that observed in TMTD.

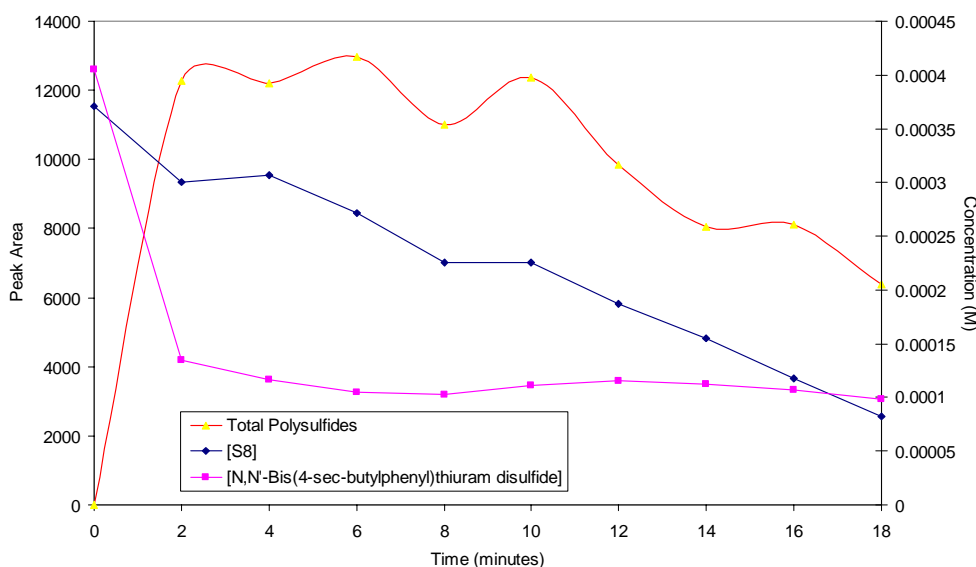


**Figure 8.5:** Reaction profile depicting the consumption of N,N'-bis(4-sec-butylphenyl)thiuram disulfide and sulfur and the relative amounts of polysulfides at different time intervals

The consumption of reactants observed in Figure 8.5 compares well with the N,N'-diphenylthiuram disulfide model compound reaction system. Similar oscillations in sulfur concentration are being observed over time intervals for both systems.

**Table 8.1:** Rate data for the N,N'-bis(4-sec-butylphenyl)thiuram disulfide model compound reactions

Data used	Rate and statistical data						
	Tangent slope (/mol L <sup>-1</sup> min <sup>-1</sup> )	Initial slope (/mol L <sup>-1</sup> min <sup>-1</sup> )	R <sup>2</sup>	N <sup>*</sup>	First order (/s <sup>-1</sup> )	R <sup>2</sup>	N <sup>*</sup>
Sulfur	1.60x10 <sup>-5</sup>	1.60x10 <sup>-5</sup>	0.973	9	1.34x10 <sup>-3</sup>	0.912	9
N,N'-bis(4-sec-butylphenyl)thiuram disulfide	1.30x10 <sup>-4</sup>	7.20x10 <sup>-5</sup>	0.795	3	1.05x10 <sup>-3</sup>	0.999	3

\* N denotes the number of points used in the plot

The rate of change in concentration and the rate constants were determined by means of the slope of the tangent and initial slopes method and taking into consideration first and second order plots respectively (see Table 8.1). The sulfur data proved again most effective in determining the rate constant, while the



accelerator data made use of too few points. Interestingly though, the data corresponded well with the second order approximation (see Figure 8.6).

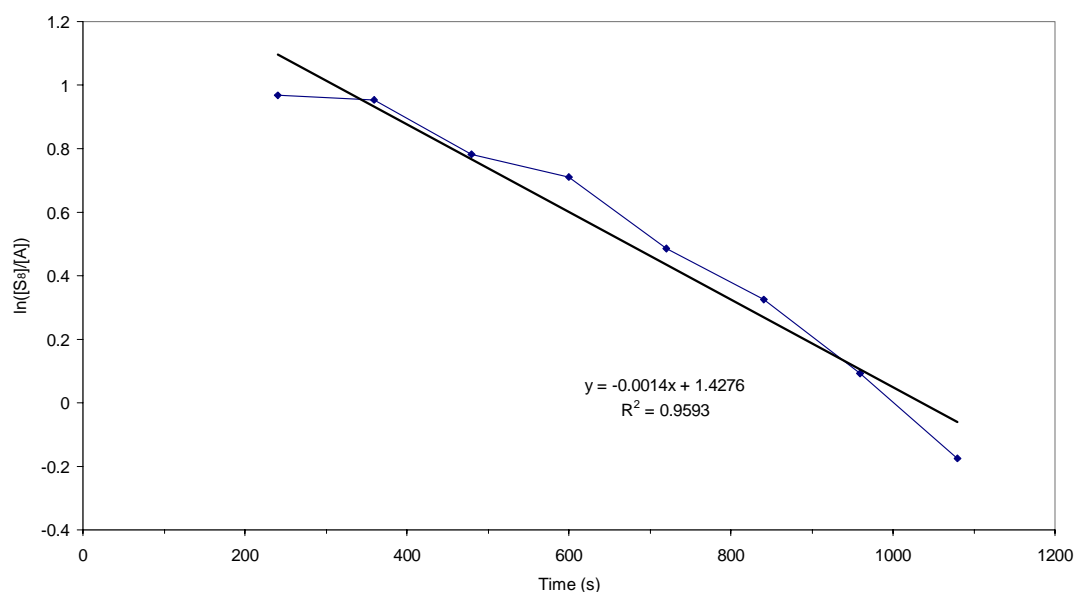
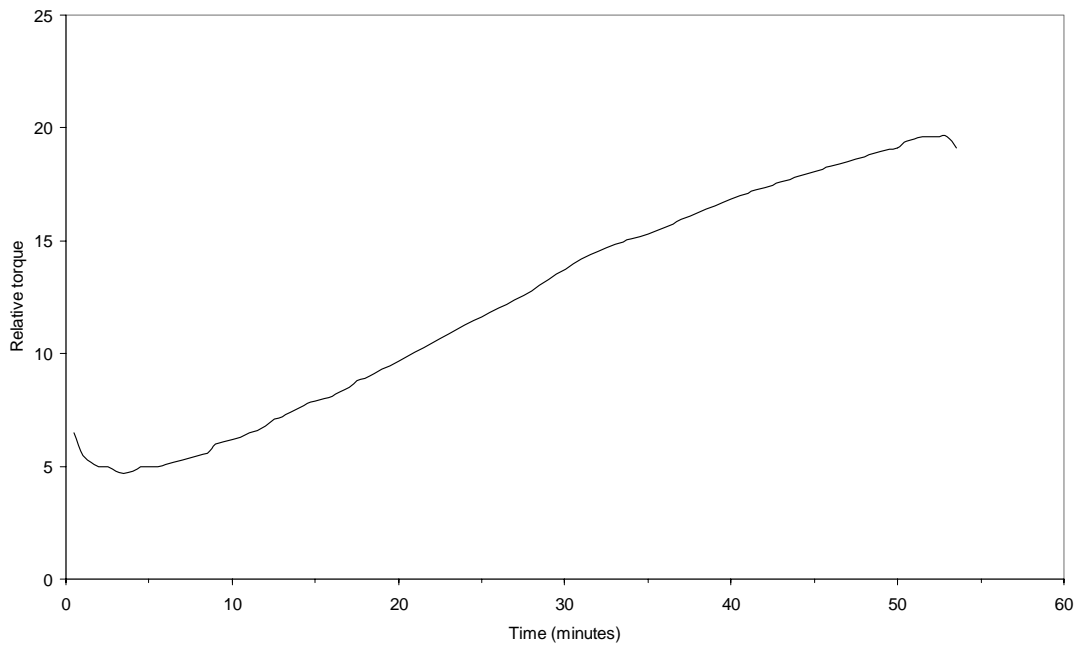


**Figure 8.6:** Determination of the second order rate constant in relation to N,N'-bis(4-sec-butylphenyl)thiuram disulfide sulfur concentration data

The fact that the second order consideration gives a better fit for the data obtained is a good indication that a different mechanism is operational from what has been observed in systems such as TMTD and TETD. Both sets of rate data as seen in Table 8.1, correspond closely to each other, even though the accelerator data used to determine the initial slope does not allow for a close linear fit.

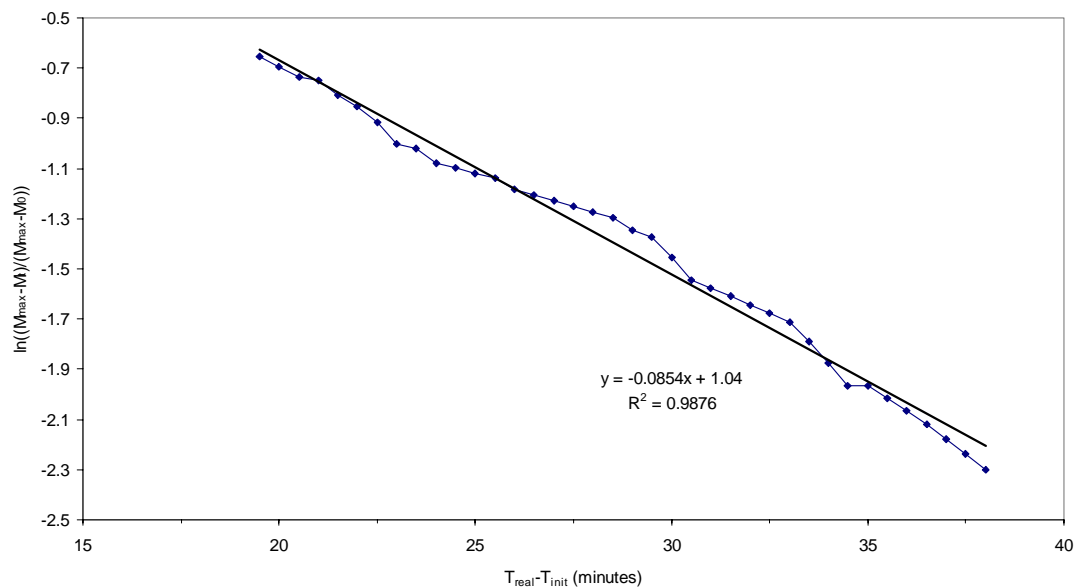
### **8.2.5 Analysis of cis-1,4-polyisoprene, N,N'-bis(4-sec-butylphenyl)thiuram disulfide and sulfur cured system**

Figure 8.7 shows the rheometer plot produced for this cure system. This figure shows the best of a number of experimental runs and was thus used for the rate determination. The rate of cure is extremely slow, with small incremental changes in torque over large periods of time. The maximum slope for this cure system was determined to be 0.5 (relative torque/time in minutes) which is slightly greater than the 0.284 (relative torque/time in minutes) observed for the unaccelerated sulfur vulcanisation system.



**Figure 8.7:** The rheometer curve depicting the cure of the N,N'-bis(4-secbutylphenyl)thiuram disulfide/S<sub>8</sub>/IR system

The low rate of acceleration did, however, allow for a large number of data points to be plotted increasing the accuracy of the rate constant determination as compared to the TMTD, TETD, CPTD and the N,N'-dimorpholinethiuram disulfide systems.



**Figure 8.8:** Determination of the first order rate constant from rheometer data derived from the cure of N,N'-bis(4-sec-butylphenyl)thiuram disulfide/S<sub>8</sub>/IR system

From about 10 minutes the curve effectively increases linearly until at 30 minutes an inflection point is observed. The rate constant from Figure 8.8 was determined to be 0.0854 ( $R^2 = 0.988$ ), this is greater than the 0.0301 rate constant of unaccelerated sulfur vulcanisation. Thus a measure of acceleration was observed in the N,N'-bis(4-sec-butylphenyl)thiuram disulfide/S<sub>8</sub>/IR system, even though it was to a small extent as compared to TMTD, TETD, CPTD and the morpholine analogue. Table 8.2 presents a summary of the rate data obtained for vulcanisation of cis-1,4-polyisoprene by means of N,N'-bis(4-sec-butylphenyl)thiuram disulfide in the presence of sulfur.

Table 8.2: Summary of the rate data obtained for the vulcanisation of cis-1,4-polyisoprene by N,N'-bis(4-sec-butylthiuram)thiuram disulfide in the presence of sulfur

Rate and statistical data			
First order crosslinking (/min <sup>-1</sup> )	R <sup>2</sup>	Maximum slope (/relative torque.min <sup>-1</sup> )	Coran's <sup>4</sup> rate constant (/min <sup>-1</sup> )
0.0850	0.988	0.5	0.0190

### 8.3 Computer modelling

Figure 8.9 depicts the geometry optimised structure for N,N'-bis(4-sec-butylphenyl)thiuram disulfide. The molecule is almost planar with the molecule being slightly skewed about the disulfide linkage, with the one thione sulfur entering the plane of the page while the other points outward. The calculated dihedral angle is almost 180° different from the 93° dihedral angle seen in both tetramethyl and tetraethylthiuram disulfide.<sup>5,6</sup> The same trend in positioning is followed by the aromatic rings with their para substituents found at opposite sides of the plane produced by the flat aromatic rings.

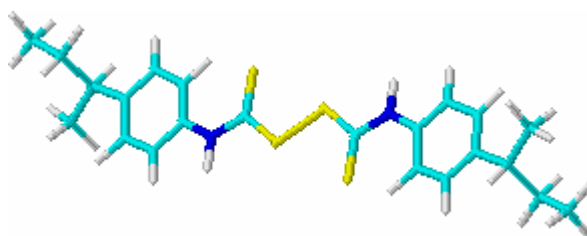
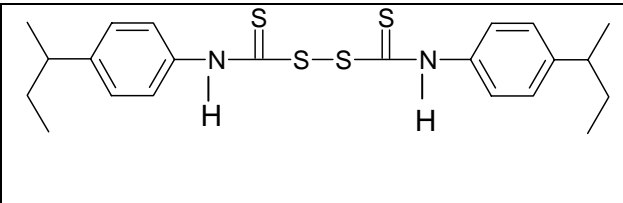
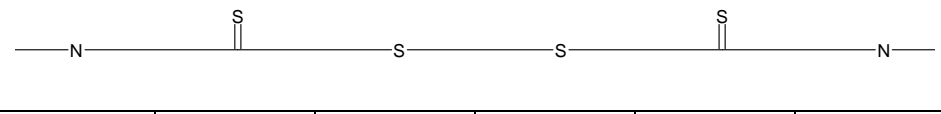


Figure 8.9: Geometry optimised structure for N,N'-bis(4-sec-butylphenyl)thiuram disulfide

The gradient obtained for this structure was not as low as obtained for the previous structures even though the programme was set to follow the maximum number of iterations. The bond distances and charges as seen in Table 8.3 are of the correct order with variations being observed across the symmetry axis. It is noted that the disulfide bond distance corresponds to a single bond of the order of 2.04 Å.<sup>7</sup>

These variations are so slight that major changes in the <sup>13</sup>C spectrum are not seen, while the total number of aromatic carbons in half the molecule are detected as a result of slightly differences in chemical environment across the aromatic moieties.

**Table 8.3:** Computer modelled parameters for N,N'-bis(4-sec-butylphenyl)thiuram disulfide

<b>N,N'-Bis(4-sec-butylphenyl)thiuram disulfide</b> <b>Energy = 107.160 kJ/mol</b> <b>Gradient = 0.0116</b>						
<b>Bond distance</b> <b>Å</b>	<b>N-C</b>	<b>C-S</b>	<b>S-S</b>	<b>S-C</b>	<b>C-N</b>	
		1.346	1.811	2.024	1.811	1.346
<b>Charge</b> <b>(Mulliken)</b>						
		-0.317			-0.341	
	-0.128	0.257	-0.020	-0.096	0.258	-0.119

Taft constant = 0.41<sup>8,9</sup> (calculated)

#### 8.4 References

- 1) F. W. H. Kruger and W. J. McGill, J. Appl. Polym. Sci., 42, 2643 (1991)
- 2) T. A. Geissman, Principals of Organic Chemistry, 2<sup>nd</sup> Ed, Linus Pauling ed, W.H. Freeman and Company, London (1962)
- 3) G. P. Ellis, Modern Textbook of Organic Chemistry, Butterworths, London (1966)
- 4) A. Y. Coran, Rubber Chem. Technol., 37, 689 (1964)
- 5) Y. Wang, J. H. Liao and C. H. Ueng, Acta Cryst., c42, 1420 (1986)
- 6) I. L. Karle, J. A. Estlin and K. Britts, Acta Cryst., 22, 273 (1967)

- 7) R. C. Weast, Ed., CRC Handbook of Chemistry and Physics, 51<sup>st</sup> Ed., The Chemical Rubber Co. Publishers, Cleveland (1970)
- 8) Lange's Handbook of Chemistry, 15<sup>th</sup> ed, Edited by J.A. Dean, McGraw-Hill, New York (1999)
- 9) E. Morita, Rubb. Chem. Technol., 57, 746 (1984)

## 9 N,N'-dimorpholinethiuram disulfide rate study

---

9.1	Synthesis and purification of N,N'-dimorpholinethiuram disulfide .....	154
9.2	Reaction rate analysis .....	155
9.2.1	RP-HPLC analysis for the isothermal curative interactions and model compound study.....	155
9.2.2	N,N'-dimorpholinethiuram disulfide melt determination.....	156
9.2.3	Curative interactions .....	157
9.2.4	Model compound reactions and rate analysis .....	158
9.2.5	Rate analysis of cis-1,4-polyisoprene, N,N'-dimorpholinethiuram disulfide and sulfur cured system .....	162
9.3	Computer modelling.....	164
9.4	References .....	165

## 9.1 Synthesis and purification of N,N'-dimorpholinethiuram disulfide

Distilled water (70 mL) was placed into a 250 mL double necked round bottomed flask. The reaction vessel was kept at approximately 5°C throughout the synthesis, while the reaction mixture was stirred continuously to prevent local excesses. NaOH (0.1820 mol, 7.3192 g) was added to the solution followed by morpholine (0.1234 mol, 10.7410 g), which was redistilled under vacuum to yield a transparent light yellow liquid (b.p. 125°C–131°C). CS<sub>2</sub> (0.1234 mol, 7.5 mL) was then added dropwise over a period of an hour. The reaction mixture went from a light yellow homogenous mixture to a thicker yellow/creamy liquid. After the addition of all the CS<sub>2</sub> the reaction mixture was stirred for a further hour with a steady N<sub>2</sub> purge to remove any unreacted CS<sub>2</sub>. K<sub>3</sub>Fe(CN)<sub>6</sub> (0.1234 mol, 123.26 mL of a 1.0010 M aqueous solution) was then added to the reaction mixture over a two hour period, the reaction mixture then went light green with finally divided white and brown particulates. The white particles were determined to be the thiuram product while the brown precipitate was ascribed to the formation of an insoluble Fe<sup>2+</sup> compound that had formed an agglomerate with part of the thiuram product formed.

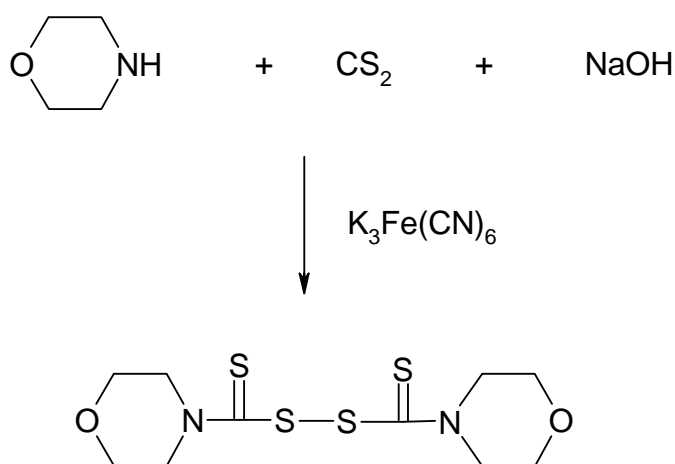


Figure 9.1: Synthetic scheme for the synthesis of N,N'-dimorpholinethiuram disulfide

Purification was achieved initially by simple frontal analysis to remove all the inorganic material. A 30 cm silica gel column was prepared in a 80:20 (volume ratio) dichloromethane:diethyl ether. The crude compound was then dissolved in the same solution (100 mL) and applied to the column. The 80:20 dichloromethane:diethyl ether was used as the mobile phase, requiring 300 mL to elute all the compound from

the column. The eluent that was obtained was a transparent yellow colour. This solution was then evaporated off to leave a yellow/white compound. This compound was recrystallised by means of a miscible solvent method. A minimum amount of toluene was added to the compound to dissolve it and crystallisation was achieved by the addition of petroleum ether 60-80°C. This was performed five times. Purity was established via RP-HPLC, DSC, TLC (80:20 dichloromethane:diethyl ether) and NMR. NMR did however show the presence of solvent peaks. The reaction yield was determined to be 18.67% (3.7379 g) and the melting point was found to be 148.8°C ( $T_{\text{onset}}$ ) with a peak maximum occurring at 150.9°C. IR ( $\text{CHCl}_3$   $\text{cm}^{-1}$ ) 3011.8, 2360.9, 1539.5, 1471.8, 1425.4, 1267.7, 1180.4, 1113.3, 1027.9, 980.9, 808.0.  $^1\text{H-NMR}$  ( $\text{CDCl}_3$ ) 4.31 (4H, m,  $2\text{CH}_2$ ), 3.86 (4H, m,  $2\text{CH}_2$ ).  $^{13}\text{C-NMR}$  ( $\text{CDCl}_3$ ) 194.33, 66.81, 66.64, 66.56, 53.28.

## 9.2 Reaction rate analysis

### 9.2.1 RP-HPLC analysis for the isothermal curative interactions and model compound study

Gradient elution had to be performed to achieve the separation of the isothermal curative interaction products, making use of a reverse phase C-18 column and a detector setting of 260 nm as seen in the Experimental section and previous discussions.

The gradient elution profile employed for the separation of the isothermal interaction products can be found in Table 9.1. The N,N'-dimorpholinethiuram disulfide and sulfur were separated into well defined peaks having retention times of 4.1 and 21.1 minutes respectively.

Table 9.1: Gradient elution profile<sup>1</sup> employed for the separation of the isothermal reaction products

Time (min)	Flow rate (/mL min <sup>-1</sup> )	% MeOH	% H <sub>2</sub> O	Elution Profile <sup>1</sup>
0	1	75	25	0
10	1	90	10	9
15	1	100	0	6



The model compound reactions were separated by means of an isocratic system where 100% MeOH was the mobile phase, the N,N'-dimorpholinethiuram disulfide and sulfur appeared as well separated peaks at 2.9 and 10.3 minutes respectively.

### 9.2.2 N,N'-dimorpholinethiuram disulfide melt determination

N,N'-dimorpholinethiuram disulfide exhibits a clean sharp melt at 150.1°C ( $T_{max}$ ) with the onset occurring at 148.8°C (see Figure 9.2)

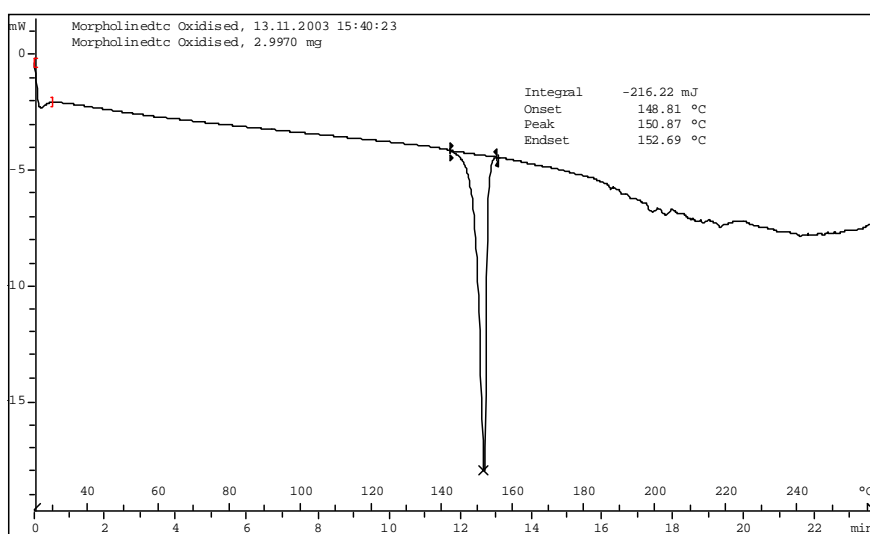
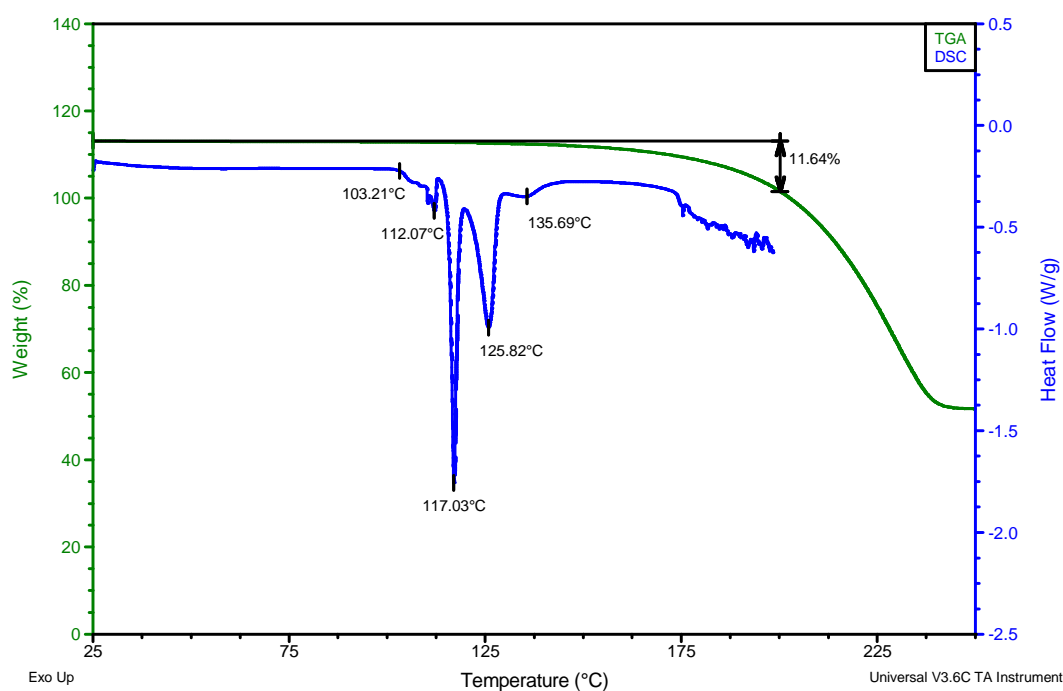


Figure 9.2: DSC thermogram depicting the N,N'-dimorpholinethiuram disulfide melt

Figure 9.3 depicts an extensive interaction between the sulfur and N,N'-dimorpholinethiuram disulfide in the dynamic investigation. This is further reinforced by Figure 9.4 which shows an extensive interaction between sulfur and the accelerator during the isothermal curative interaction investigation. Figure 9.3 clearly depicts the coalescence of the sulfur transitions into one single broad peak. The onset and peak maximum temperatures correspond to the temperatures at which the  $S_{\alpha}$ - $S_{\beta}$  and  $S_{\beta}$ - $S_{\lambda}$  sulfur transitions are known to occur namely at 107.0°C<sup>2</sup> and 113°C<sup>2</sup> respectively. The melting point of the N,N'-dimorpholinethiuram disulfide is no-longer apparent. There appears to be a measure of mutual solubilisation operational, if one interprets the sulfur transitions to have remained relatively unchanged, the melting point of N,N'-dimorpholinethiuram disulfide appears to have been depressed to the broad endotherm observed at 135.7°C corresponding to the depressed melt of the unreacted N,N'-dimorpholinethiuram disulfide. No broad endotherm that would be indicative of the decomposition of N,N'-dimorpholinethiuram disulfide to thiourea or a monosulfide is seen.

The thermogram in Figure 9.3 does tend to indicate that once the first sulfur transition has been reached sufficient energy is available to the system to enable reactions between sulfur and the accelerator. The production of the thiuram monosulfide and higher polysulfides may be possible and could explain the presence of the peak maxima observed at 117.0°C and 125.8°C. Some decomposition to thiourea and amine is expected though as depicted by the minor mass loss of approximately 12 % at 200°C observed in Figure 9.3.



**Figure 9.3:** Thermogram depicting the heat of N,N'-dimorpholinethiuram disulfide with sulfur

### 9.2.3 Curative interactions

There are a large number of interactions that occur between the accelerator N,N'-dimorpholinethiuram disulfide and the sulfur resulting in a large number of polysulfides and other products being formed. One may expect that with such a large number of products being formed as seen in Figure 9.4, that this accelerator would be quite effective at increasing the rate of vulcanisation through the presence of polysulfides, the active sulfurating agent, as well as the result of the formation of amine from decomposition pathways.

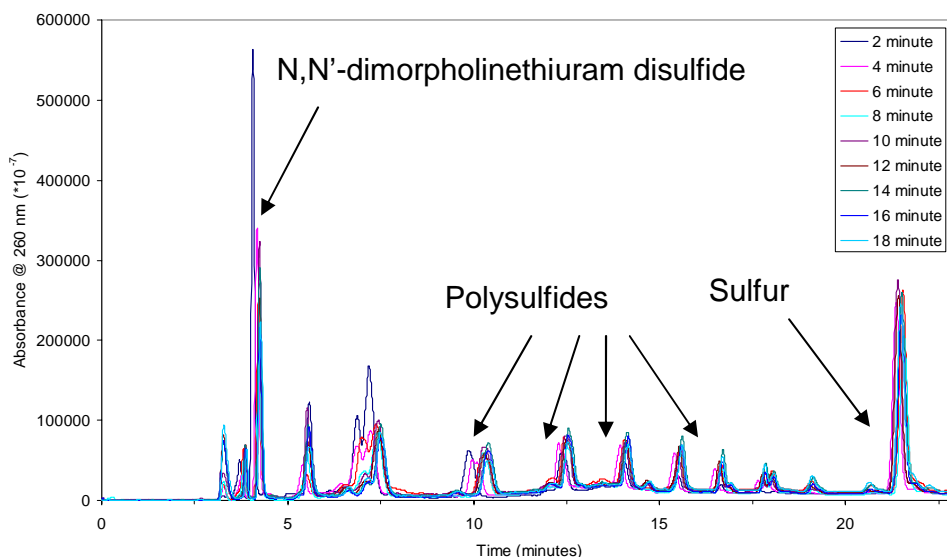


**Figure 9.4:** N,N'-dimorpholinethiuram disulfide/S<sub>8</sub> (1:1 molar ratio) isotherm interactions

As a result of the gradient elution profile it proved difficult to determine which peaks were as a result of polysulfides. Ordinarily for isocratic systems there is a linear relation between the logarithm of the retention time and sulfur rank.<sup>3,4</sup> It is, however, not possible to perform this method for gradient systems. Thus the arrows in Figure 9.4 point at peaks surmised to be polysulfides.

#### 9.2.4 Model compound reactions and rate analysis

As in most of the cases examined, the presence of an olefin drastically reduces the number of polysulfides that are observed in the system since the reaction of the polysulfidic accelerator species with the aliphatic chain doesn't seem to be a limiting process.

As can be seen from Figure 9.5, the number of polysulfidic species existing between the accelerator and sulfur peaks has been substantially reduced, especially when one considers that as many as 12 different polysulfidic species could potentially form.

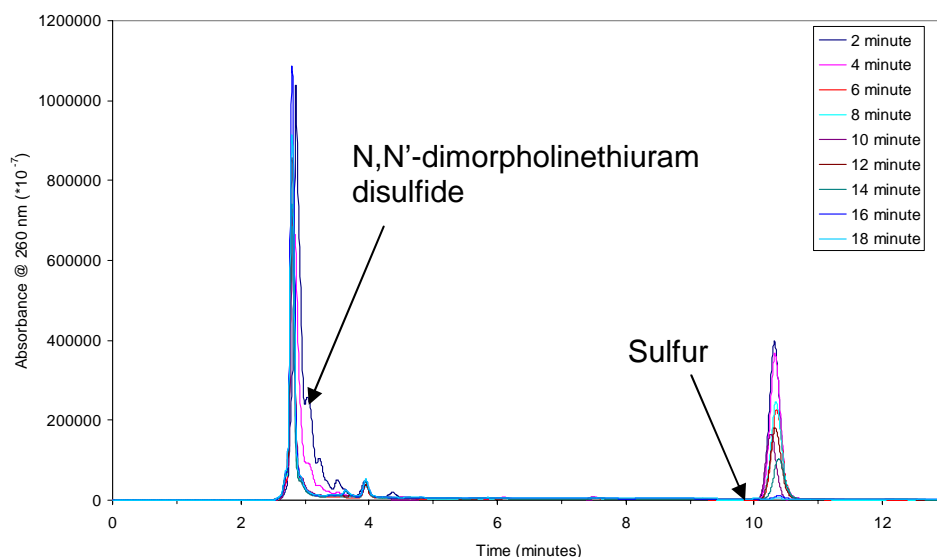
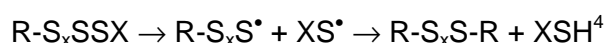


**Figure 9.5:** Chromatogram depicting the model compound interactions of N,N'-dimorpholinethiuram disulfide with sulfur and squalene

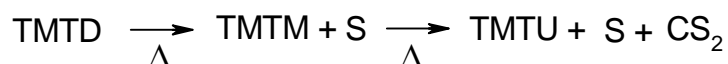
One may question the level of separation achieved for this system as the N,N'-dimorpholinethiuram disulfide peak appears to have a shoulder. This presented an interesting case since the more complex gradient elution system applied in the isocratic study as well as numerous other mobile phases proved to provide a similarly dissatisfactory accelerator peak for this system. This may be due to a concentration effect, more specifically a concentration dependent tautomerism. As the reaction progresses the sulfur concentration decreases slowly with the accelerator concentration reaching a minimum at 6 minutes after which the concentration gradually increases again. The increase in N,N'-dimorpholinethiuram disulfide concentration may result from the reaction of accelerator fragments such as thiuram persulfenyl and thiuram sulfenyl radicals formed as a result of the disproportionation of thiuram terminated pendent groups during crosslink formation.<sup>5</sup> These radicals could interact with one another to form accelerator polysulfides which would ultimately form polysulfidic crosslinks, N,N'-dimorpholinethiuram disulfide and N,N'-dimorpholinethiuram polysulfides.

RH

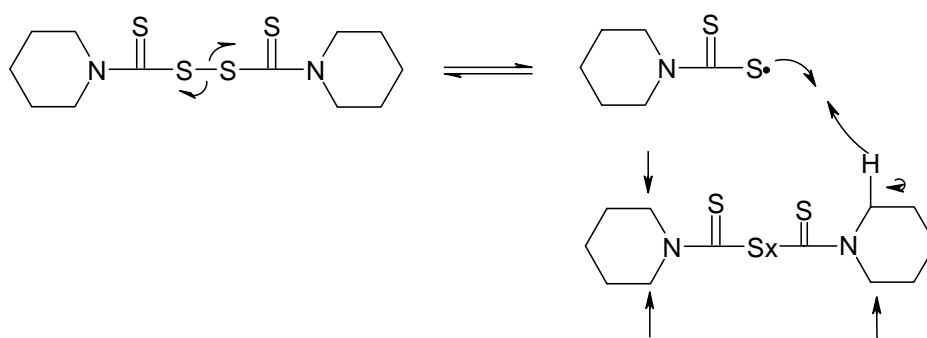


where RH = rubber chain and XSH = morpholinedithiocarbamic acid (XSH)

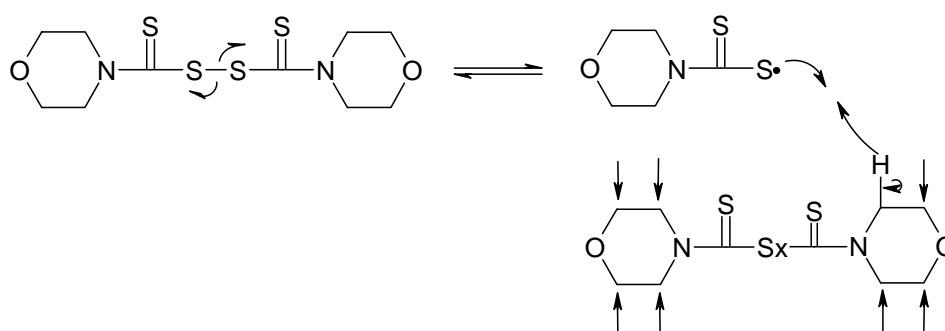
The decomposition step which is favoured by so many other accelerators may be a less dominant process. When TMTD is heated to its melt many decomposition products are formed, such as TMTM, TMTP's and TMTU, with later occurring at much higher temperatures than that of the melt.<sup>6,7,8,9</sup>



N,N'-dicyclopentamethylenethiuram disulfide is much more reactive in its melt than TMTD, producing N,N'-dicyclopentamethylenethiuram monosulfide. This is ascribed to the relative ease with which methylene radicals may be formed as compared to methyl radicals.<sup>10</sup>



Reactive sites available for hydrogen abstraction in N,N'-dicyclopentamethylene thiuram disulfide



Reactive sites available for hydrogen abstraction in N,N'-dimorpholinethiuram disulfide

Figure 9.6: A comparison between the reactive sites available for hydrogen abstraction in N,N'-dicyclopentamethylenethiuram disulfide<sup>10,11</sup> and N,N'-dimorpholinethiuram disulfide

One may expect N,N'-dimorpholinethiuram disulfide to undergo similar processes to a greater extent since more positions are available for the radical abstraction of hydrogen. In N,N'-dicyclopentamethylenethiuram<sup>10,11</sup> disulfide four positions adjacent to the nitrogen atoms are available, whereas in N,N'-dimorpholinethiuram disulfide has eight reactive sites. The reactive sites are adjacent the heteroatoms because the electronegativity of the heteroatoms polarize and therefore weaken the H-C bonds. Once radical formation has occurred the heteroatoms possess lone pairs of electrons that may participate in resonance stabilization. The intermediates showed in Figure 9.6 lead to dithiocarbamic acid formation and ultimately thiourea.

It can also be seen in Figure 9.7 that at longer reaction times the number of polysulfides has increased slightly. The reason for this is unknown.

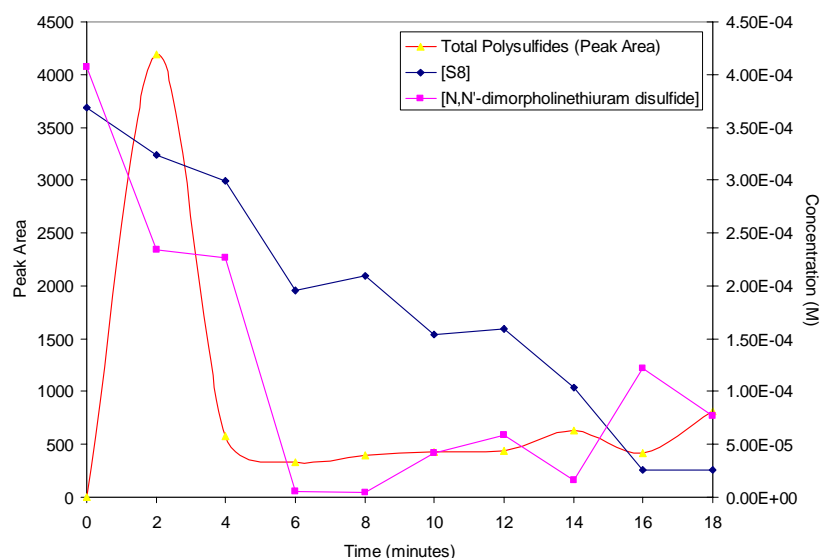


**Figure 9.7:** Reaction profile depicting the consumption of N,N'-dimorpholinethiuram disulfide and sulfur and the relative amounts of polysulfides at different time intervals

Once again the initial slope method seemed to be the more feasible method to determine the rate constant, especially using the sulfur data which decreases steadily, but not dramatically as to reduce the number of points that may be used for the determination. The sulfur data gave more reliable data for the determinations whereas the accelerator gave a maximum of four data points per plot. The rate constants obtained from the plots are displayed in Table 9.2.

Table 9.2: Rate data for the N,N'-dimorpholinethiuram disulfide model compound reactions

Data used	Rate and statistical data						
	Tangent slope (/mol L <sup>-1</sup> min <sup>-1</sup> )	Initial slope (/mol L <sup>-1</sup> min <sup>-1</sup> )	R <sup>2</sup>	N*	First order (/s <sup>-1</sup> )	R <sup>2</sup>	N*
Sulfur	1.60x10 <sup>-5</sup>	1.91x10 <sup>-5</sup>	0.962	10	1.57x10 <sup>-3</sup>	0.921	7
N,N'-dimorpholinethiuram disulfide	1.30x10 <sup>-4</sup>	6.70x10 <sup>-5</sup>	0.905	4	1.11x10 <sup>-2</sup>	0.818	4

\* N denotes the number of points used in the plot

It should be noted that the second order plot was an extremely poor approximation for this system with there being no linear relation within the obtained data. The rate constant determined via the various methods are quite comparable, except for the N,N'-dimorpholinethiuram disulfide rate constant determined by the initial slope method which is out one order of magnitude. Once again this may be ascribed to the fact that only four data points were used to determine this value as the rate at which the accelerator was consumed was too fast. This prevented an accurate rate constant determination.

### 9.2.5 Rate analysis of cis-1,4-polyisoprene, N,N'-dimorpholinethiuram disulfide and sulfur cured system

N,N'-dimorpholinethiuram disulfide is a good accelerator as can be seen from the rheometer trace in Figure 9.8. The system behaves similar to what one may expect in the general vulcanisation scheme with a very slight scorch delay being observed compared to TMTD and TETD.

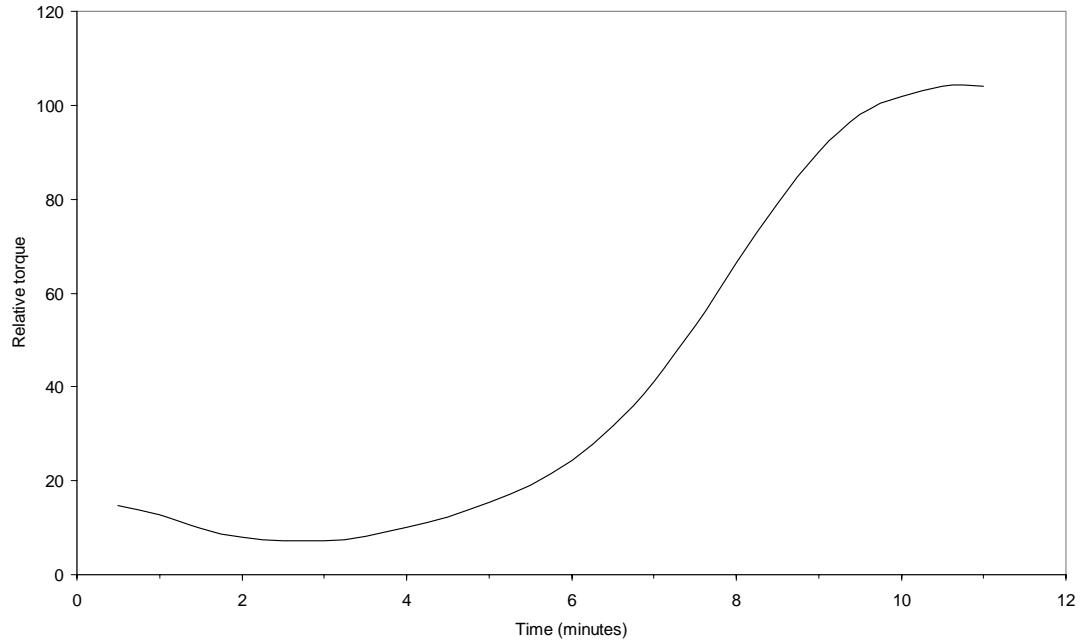


**Figure 9.8:** The rheometer curve depicting the cure of the N,N'-dimorpholinethiuram disulfide/S<sub>8</sub>/IR system

This again has the advantage of allowing more points to be used to determine the rate constant since the linear acceleratory region has a longer duration.

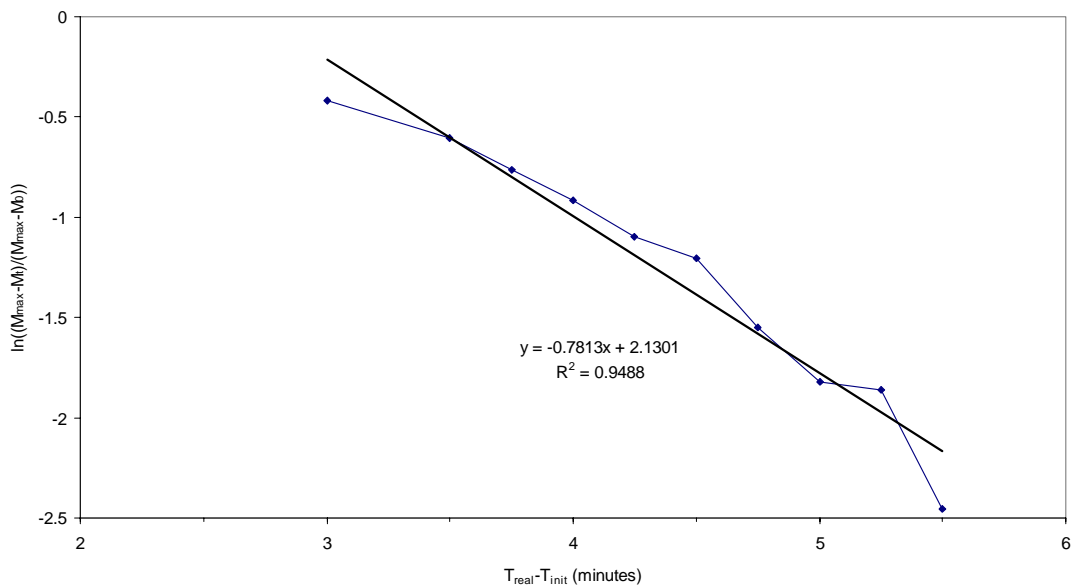


**Figure 9.9:** Determination of the first order rate constant from rheometer data derived from the cure of N,N'-dimorpholinethiuram disulfide/S<sub>8</sub>/IR system



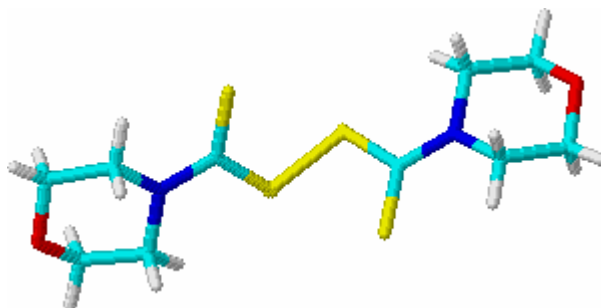
The rate constant determined from the first order plot in Figure 9.9 was found to be 0.7813 ( $R^2 = 0.949$ ), while the maximum slope as determined from Figure 9.8 was found to be 26.3 (relative torque/time in minutes). Table 9.3 represents a summary of the rate data obtained for the crosslinking of cis-1,4-polyisoprene by means of N,N'-dimorpholinethiuram disulfide in the presence of sulphur.

**Table 9.3:** Summary of the rate data obtained for the vulcanisation of cis-1,4-polyisoprene by N,N'-dimorpholinethiuram disulfide in the presence of sulfur

<b>Rate and statistical data</b>			
<i>First order crosslinking (/min<sup>-1</sup>)</i>	<i>R<sup>2</sup></i>	<i>Maximum slope (/relative torque.min<sup>-1</sup>)</i>	<i>Coran's<sup>12</sup> rate constant (/min<sup>-1</sup>)</i>
0.7813	0.949	26.3	1.4170

### 9.3 Computer modelling

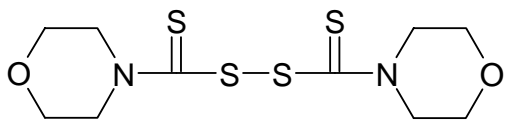

N,N'-dimorpholinethiuram disulfide takes on a chair/twist conformation, with the structure morpholine groups placed at opposite ends of the molecule almost perpendicular to one another. The disulfide dihedral angle conforms closely to the previously observed 93° as seen in tetramethyl (TMTD)<sup>13</sup> and tetraethylthiuram disulfide (TETD)<sup>14</sup> as well as to the crystal data obtained for this structure which depicts a dihedral angle of 99.0°.<sup>15</sup> This seems to be the most feasible structure as seen by the very low gradient obtained indicative of a local minimum.



**Figure 9.10:** Geometry optimised structure for N,N'-dimorpholinethiuram disulfide

The variation in structural parameters across the main axis of symmetry as seen in Table 9.4, is greater when compared to the other molecules investigated. Even though one may interpret the morpholine structures to contain equivalent carbon atoms, <sup>13</sup>C-NMR analysis reveals five distinct peaks which account for all the carbon atoms in half the molecule. Thus no equivalent chemical environments are observed in the morpholine moiety.

Table 9.4: Computer modelled parameters for N,N'-dimorpholinethiuram disulfide

N,N'-dimorpholinethiuram disulfide Energy = 63.876 kJ/mol Gradient = 0.00563						
Bond distance Å	N-C	C-S	S-S	S-C	C-N	
	1.416	1.812	2.160	1.813	1.418	
Charge (Mulliken)						
		-0.290			-0.327	
	-0.147	0.268	-0.017	-0.083	0.260	-0.132

Taft and Hammett constants are not available

No Taft or Hammett parameters are available for the morpholine substituent. The parameters may be calculated with the aid of the software ACD/Chemsketch which contains QSAR software which may be used to calculate such parameters. This software was, however, not available.

It is noted that all the bond distances exhibited in Table 9.4 are of single bond character and correspond well with the values observed in the crystal structure data obtained for this molecule.<sup>15</sup> The disulfide bond distance is longer than the expected 2.04 Å<sup>16</sup> for conventional disulfide bonds with the observed disulfide bond distance from the crystal structure was determined to be 2.01 Å.<sup>15</sup>

#### 9.4 References

- 1) Automated Gradient Operators Manual 660, Waters, 34 Maple Street, Millford, Massachusetts, 01757 (1983)
- 2) F. W. H. Kruger and W.J. McGill, J. Appl. Polym. Sci., 42, 2643 (1991)
- 3) H. J. Möckel, J. Chromatogr. 317, 589 (1984)
- 4) N. H. Snow, J. Chem. Ed., 73, 592 (1996)
- 5) F. W. H. Kruger and W. J. McGill, J. Appl. Polym. Sci., 45, 563 (1992)

- 6) C. W. Bedford and L.B Sebrell, *Ind. Eng. Chem.*, 14, 25 (1922)
- 7) B. A. Dogadkin and V. A Shershnev, *Rubber Chem. Technol.*, 33, 401 (1960)
- 8) D. Craig, *Rubber Chem. Technol.*, 29, 994 (1956)
- 9) G. A. Blokh, *Organic Accelerators in the Vulcanisation of Rubber*, Israel Program for Scientific Translations Ltd. (1968)
- 10) C. P. Reyneke-Barnard, M. H. S. Gradwell and W. J. McGill, *J. Appl. Polym. Sci.*, 77, 2718 (2000)
- 11) C. P. Reyneke-Barnard, M. H. S. Gradwell and W. J. McGill, *J. Appl. Polym. Sci.*, 77, 2732 (2000)
- 12) A. Y. Coran, *Rubber Chem. Technol.*, 37, 689 (1964)
- 13) Y. Wang, J. H. Liao and C. -H. Ueng, *Acta Cryst.*, c42, 1420 (1986)
- 14) I. L. Karle, J. A. Estlin and K. Britts, *Acta Cryst.*, 22, 273 (1967)
- 15) G. C. Rout, M. Seshasayee, G. Aravamudan, *Cryst. Struct. Commun.*, 2, 1389 (1982)
- 16) R. C. Weast, Ed., *CRC Handbook of Chemistry and Physics*, 51<sup>st</sup> Ed., The Chemical Rubber Co. Publishers, Cleveland (1970)

# 10 Discussion

---

10.1	Introduction.....	168
10.2	General trends.....	168
10.3	Determining the validity of experimental rate data.....	178
10.3.1	The validity of the rates derived from the initial slopes method in relation to chemical processes .....	178
10.3.2	Observations made with the aid of $^{13}\text{C}$ NMR data and computer modelling in relation to reaction rate.....	181
10.3.3	The validity of first order rate data in relation to chemical processes.....	183
10.4	Comparison of the first order rate constants presented by the various accelerators in relation to the rate observed in rubber vulcanisation .....	184
10.5	Comparison of sulfur rate constant with the rate constants derived from the rheometric analysis.....	186
10.5.1	Squalene as model compound.....	187
10.6	Linear free energy relationships.....	188
10.6.1	Obtaining valid Taft substitution constants for complex molecular systems.....	188
10.6.2	Data assemblies that were considered in the linear free energy investigation.....	189
10.6.3	The linear free energy relationships that were investigated.....	190
10.7	References .....	193

## 10.1 Introduction

Before one examines the free energy relationships that may exist between the various accelerators, it is important to take note and discuss the trends that have already been discovered. This allows for a general comparison and more specifically a comparison within the various groups of accelerators used. The preliminary comparison focuses on individual and groups of accelerators and the trends observed while the later part will focus on linear free energy relations with regards to substituents electronic effects. The discussion will also focus on the validity of the results observed within and across different methodologies in an attempt to ascertain which set of data might more accurately represent trends and be more generally applicable across the groups of accelerators examined.

The rate constant data will also be interpreted and assigned to possible chemical processes that may be operational as well as what specific rate data represent with relevance to limitations within the different methods employed.

## 10.2 General trends

General trends may readily be observed when examining the rheometrical data obtained for the seven accelerators. It is seen that as a group the aromatic thiuram accelerators increase the rate of vulcanisation only slightly when compared to sulfur (see Table 10.1 and Figure 10.1). Please note that the two graphs in Figure 10.1 have different scales. It can also be seen that of the aromatic thiuram disulfides, N,N'-diphenylthiuram disulfide is the best at enhancing the rate of vulcanisation.

Table 10.1: Rate constant for the vulcanisation of IR/Accelerator/sulfur systems  
(1:1 molar ratios)

<b>Accelerator name</b>	<b>First order crosslinking rate constant (/min<sup>-1</sup>)</b>	<b>Max slope</b>	<b>Coran rate constant</b>	<b><math>\tau_5</math> (/min)</b>	<b><math>\tau_{95}</math> (/min)</b>	<b>Cure index*</b>
Sulfur alone	0.0301	0.284	0.222	11.8	32.3	48.7
N,N'-Bis-(4-sec-butylphenyl)thiuram disulfide	0.0854	0.500	0.019	1.3	23.8	44.4
N,N'-diphenylthiuram disulfide	0.2370	0.863	0.023	1.3	38.8	26.8
N,N'-Bis( $\sigma$ -methoxyphenyl)thiuram disulfide	0.0961	0.314	0.015	1.5	22.0	48.8
N,N'-dimorpholinethiuram disulfide	0.7810	26.3	1.417	3.3	9.5	166.7
Tetramethylthiuram disulfide	2.5890	55.8	2.464	2.9	5.4	390.2
Tetraethylthiuram disulfide	1.0840	32.0	0.987	4.1	8.8	213.3
N,N'-dicyclopentamethylene-thiuram disulfide	2.2740	41.9	2.048	3.0	6.3	307.7

\*Cure index<sup>1</sup> = 1000/( $\tau_{95}$ - $\tau_5$ ) 1000 divided by the difference between the time (min) to reach 95% and 5% of the total torque

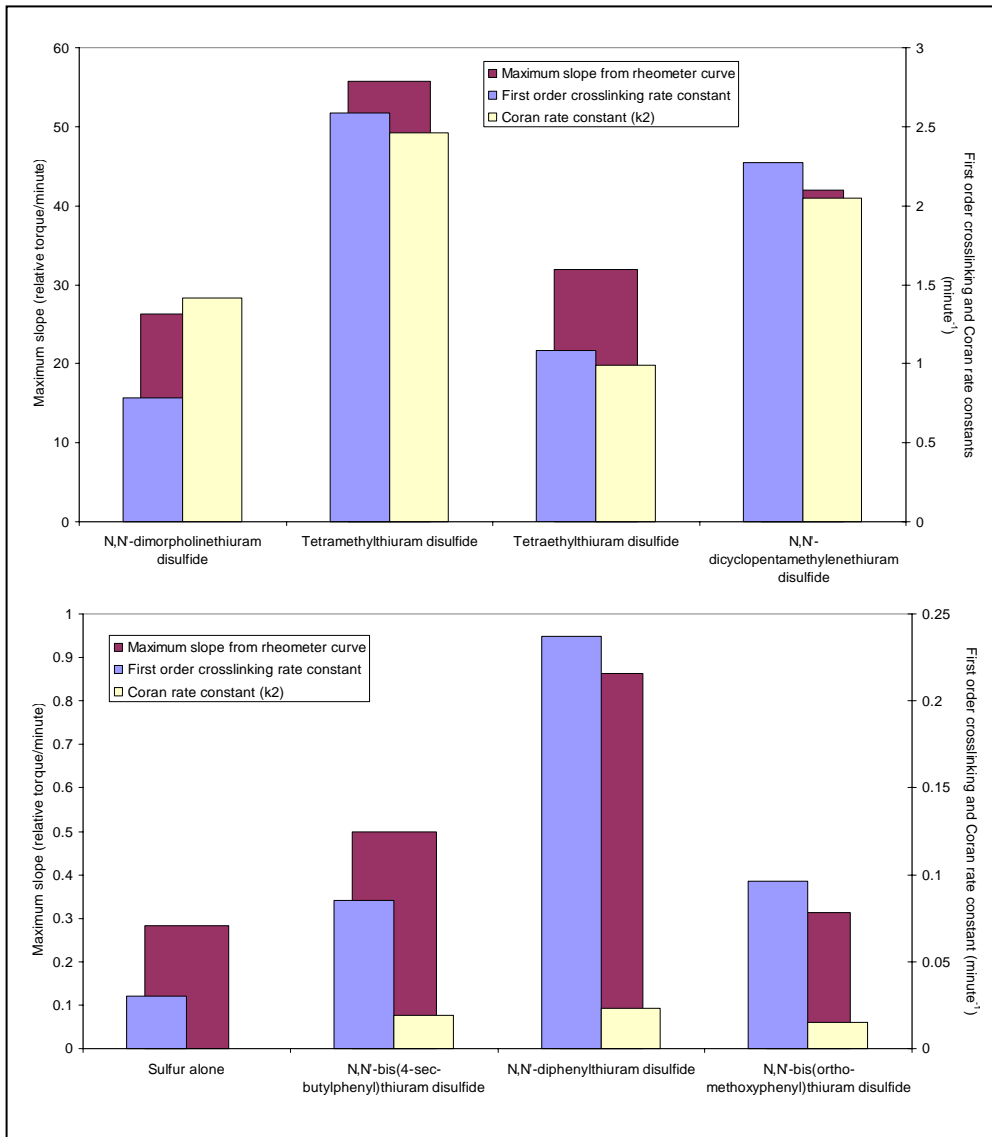


**Figure 10.1:** Comparison of rate constants in accelerator/sulfur/IR cured system in a 1:1 molar ratio curative loading

The aromatic thiuram accelerators present marching cures similar to that which is observed in sulfur and amine facilitated cure systems. As noted earlier thiuram vulcanisation is not a discrete system, but a complex one where species formed in situ may also act as vulcanisation aids, increasing the rate of vulcanisation. This is true for both dithiocarbamic acids and amines which are liberated during subsequent reactions in the proposed thiuram vulcanisation mechanism.

It should, however, be noted that the rate at which amines accelerate sulfur vulcanisation is far inferior to both that of dithiocarbamic acids and thiurams. Amine vulcanisation is considered to be a facilitated process as apposed to an accelerated system, since the amine in amine/sulfur cured rubber systems

facilitates S<sub>8</sub> ring opening which promotes crosslink formation (see Figure 10.2).<sup>2</sup> The nitrogen of the thiuram disulfide itself may also facilitate S<sub>8</sub> ring opening.

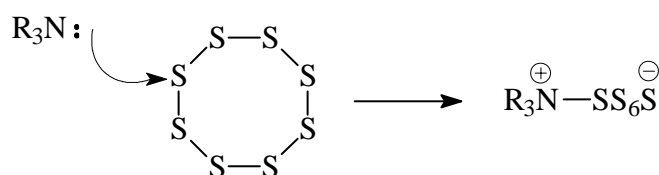
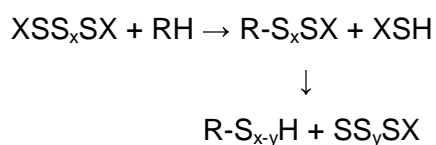


Figure 10.2: Amine facilitated ring opening of S<sub>8</sub> sulfur<sup>2</sup>

Three distinct reaction processes may limit the rate at which vulcanisation occurs. The homolytic or heterolytic cleavage of the disulfide linkage to produce reactive precursors could limit the process. Coleman et al.<sup>2</sup> have postulated a radical mechanism for this process but as substituent effects become more dominant variations in the mechanism may be expected.

Secondly pendent group formation may be a limiting process. Here accelerator polysulfides, the active sulfurating agents react with the hydrocarbon backbone either by a radical mechanism as per Coleman et al.<sup>3</sup> or by the more widely accepted concerted reaction mechanism of Geyser and McGill.<sup>4</sup> This involves the discrete cleavage of S-S bonds with the formation of a new C-S bond by means of a hydrogen abstraction reaction with the hydrocarbon chain.



The third limiting process is considered to be one of the many crosslinking reactions. Here two pendent groups react to form a crosslink by means of a disproportionation reaction.<sup>5,6,7</sup> This reaction is, however, only limiting during the initial stages of vulcanisation and does not exercise an appreciable dominance during the later stages of vulcanisation with the reaction being minor and insignificant. Substituent effects would affect the rate of the reaction and the mechanism due to changes in the electronic environment about the reactive sites of the accelerators. In this study rate changes were investigated but the mechanistic for each accelerator system considered were not investigated. The mechanism for each system would, however, follow that of the conventional thiuram disulfide mechanism but as the electronic



character of the active sites change different path ways within the mechanism may exhibit greater dominance.

It is, however noted that the calculated bond distances across all the accelerators employed for this study were similar. Only N,N'-dimorpholinethiuram disulfide presented a substantially different calculated disulfide bond length, being greater than that which was observed for the other thiuram adducts (see Figure 10.3). This may be as result of the single bond character which predominates throughout the molecule, whereas most of the other thiuram disulfide accelerators investigated have C-N bonds that have a partial double bond character.

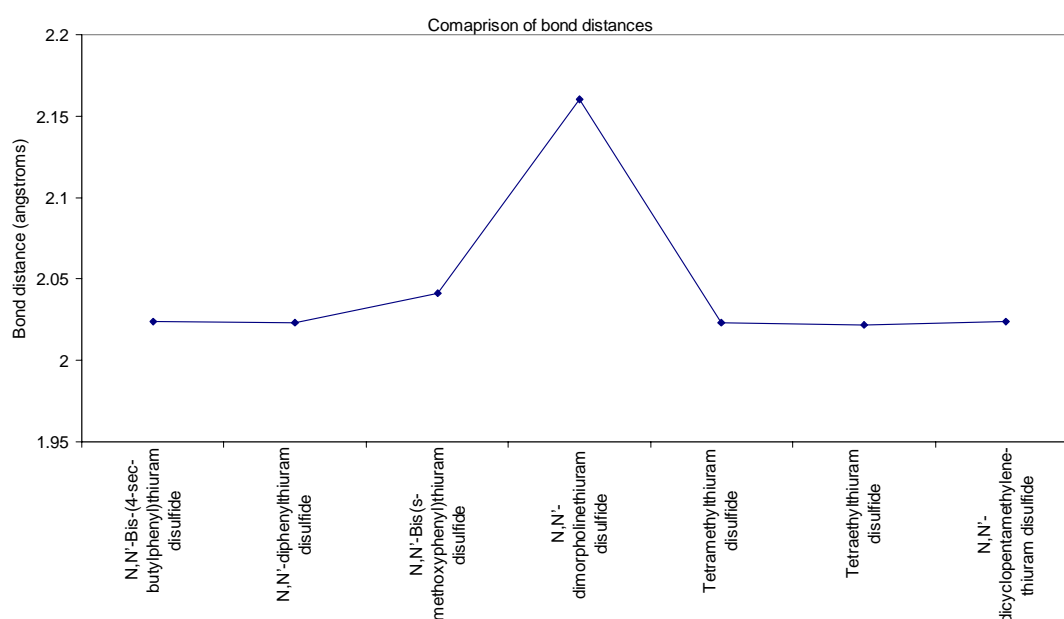


**Figure 10.3:** Comparison of the calculated disulfide bond distances for thiuram accelerators used in this study

It is generally noted that active accelerator polysulfides may readily be observed during isothermal investigations of thiuram accelerator in the presence of sulfur. It was, however, shown that the number of interaction products observed for the aromatic thiuram adducts were less than for the other thiuram accelerators investigated.

The large number of accelerator polysulfides present in the cyclic and linear aliphatic thiuram adducts may explain why they are able to increase the rate of vulcanisation to such a great extent (see Figure 10.4). The model compound study for the morpholine thiuram disulfide derivative showed less accelerator polysulfides, this

may have been erroneous due to the poor chromatographic separation that was obtained.

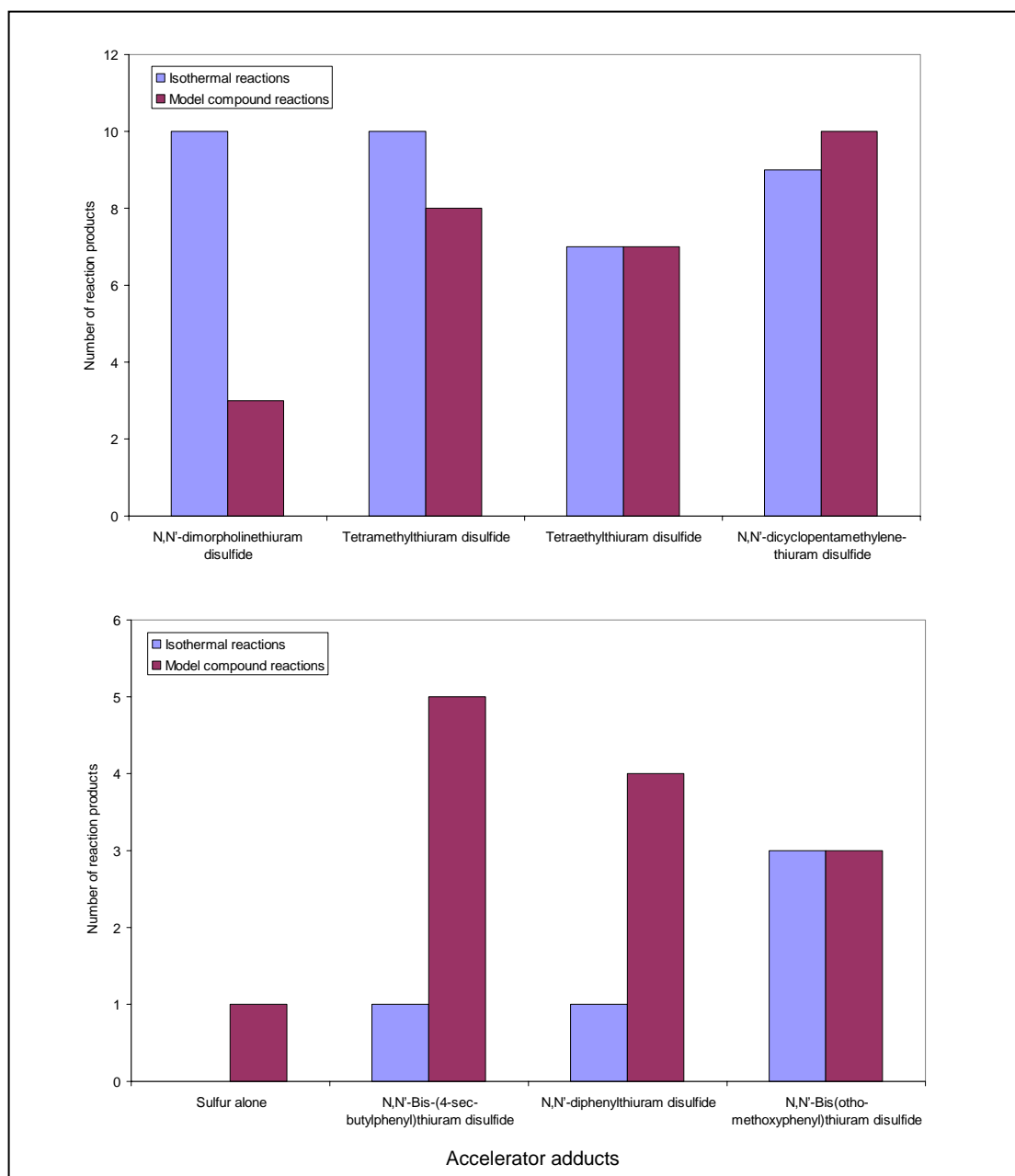


**Figure 10.4:** Number of reaction products observed in both the isothermal and model compound study (sulfur is noted included as it is reactant)

Figure 10.5 depicts a possible relationship between  $^{13}\text{C}$  chemical shifts and the rate of vulcanisation. Higher  $^{13}\text{C}$  shifts are associated with accelerators which have a greater acceleratory effect (positive trend), while generally as the charge on the thione carbon becomes more negative vulcanisation rates increase (negative trend). The change in  $^{13}\text{C}$  chemical shifts may be indicative of different reaction mechanisms

operating through each of the series. It may, however, be a coincidence to the fact that each of the nitrogen atoms in the aromatic derivatives are bonded to a hydrogen. This alone may drive the difference in mechanism.

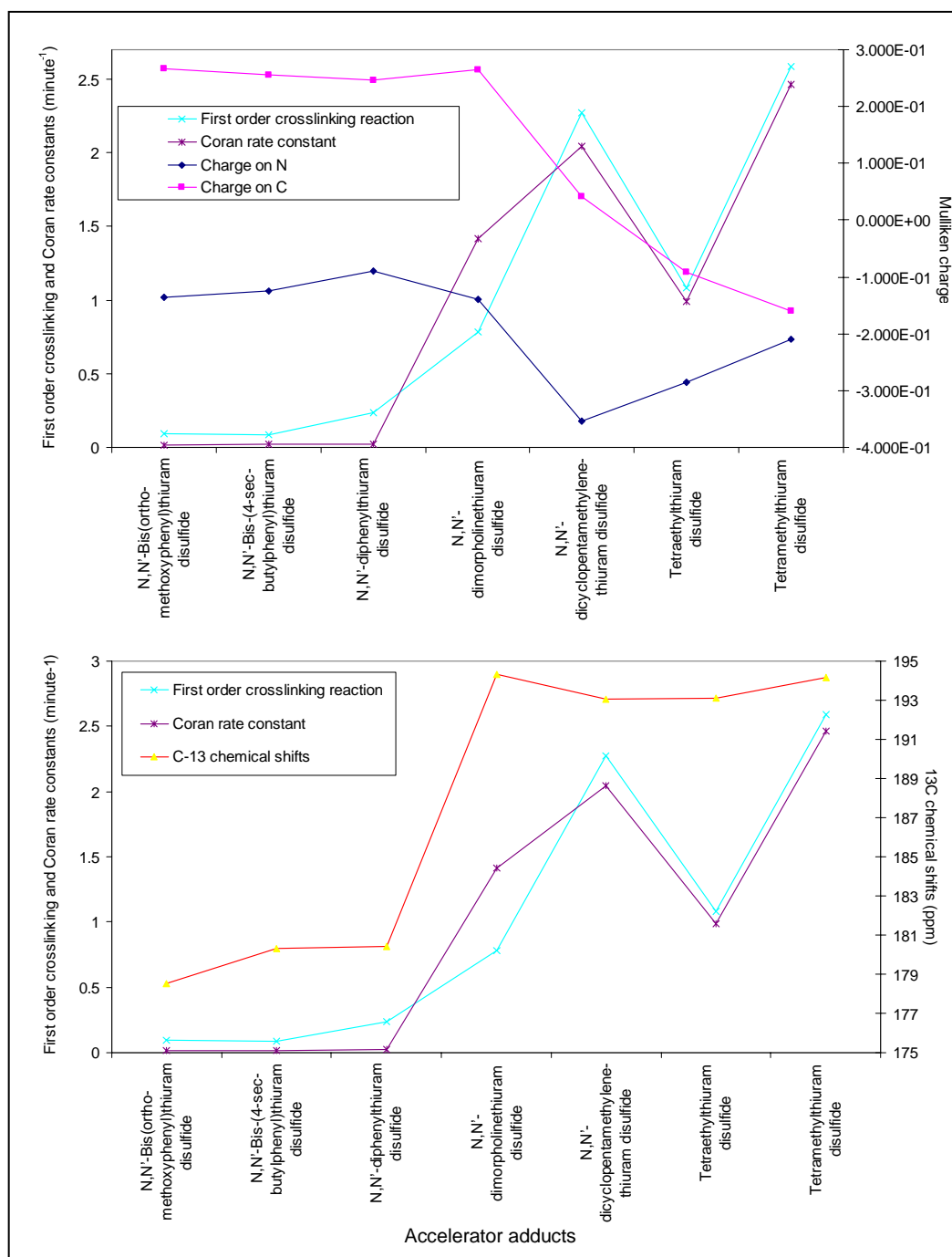


Figure 10.5: Comparison of molecular properties versus the rate of cure as seen in the rubber system

If one sketches resonance structures for the various aromatic accelerators, one is readily able to conclude that any effect that substituents would have on the homolytic

cleavage of the disulfide linkage, would have to be by means of inductive effects. Resonance would only be important in stabilising the amine decomposition products. Steric effects shouldn't be a controlling effect, since the reaction centres are not in close proximity to the substituents.

There is marked increase in the rate at which N,N'-dimorpholinethiuram disulfide accelerates sulfur vulcanisation as compared to the aromatic thiuram adducts. There is no trend observed in the cyclic aliphatics since N,N'-dicyclopentamethylenethiuram disulfide is a far superior accelerator than the morpholine analogue. This may be as result of the electronegative oxygen atom impeding the acceleratory process by electronic effects, or rather promoting the decomposition reaction thus removing accelerator from the system. This idea may be supported by long disulfide bond distance seen in Figure 10.3, even though these values are not truly representative as seen by the much smaller disulfide bond distances that were observed from the crystal structure analysis of both TMTD and TETD ( $\pm 2.0 \text{ \AA}$ ).<sup>8,9</sup>

N,N'-dimorpholinethiuram disulfide has a longer induction period (see Table 10.1) as compared to most of the accelerators. This may be as a result of a greater energy required to produce active sulfurating agent. This, however, seems spurious in view of how many products are produced during the isothermal curative interactions. This may be a melt effect since the morpholine adduct has the second highest melting point at approximately 148°C, reducing the morpholine adducts ability to enter the more reactive molten state. It should be noted that TETD does not follow this general trend, since it has a low melting temperature of approximately 70°C and still exhibits a long induction time. Low melting points are of greater importance when the accelerators are in the presence of sulfur, since this would promote polysulfide formation.

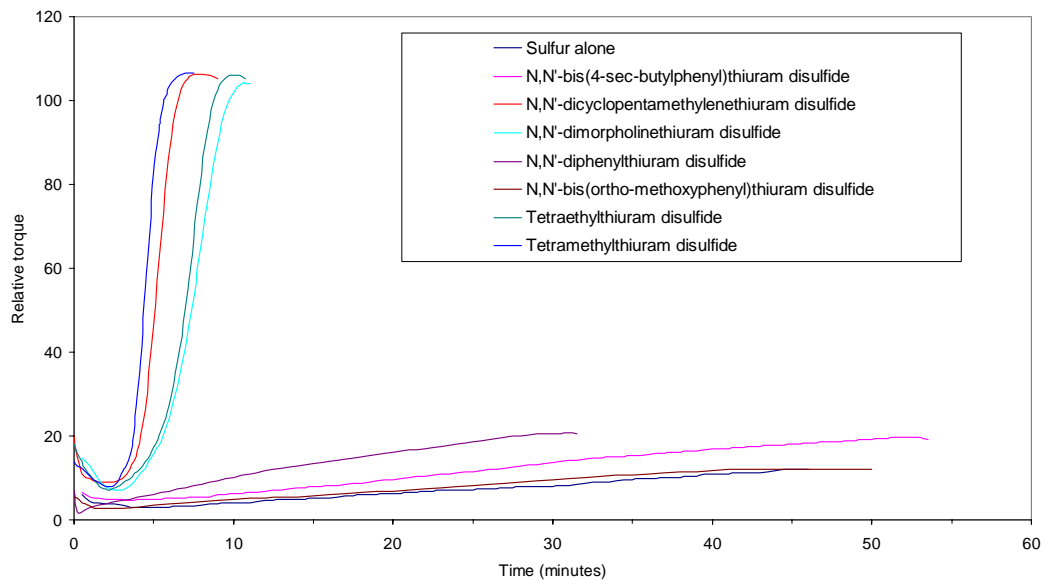
It is suspected from previous discussions in chapters 9 and 6 that in N,N'-dimorpholinethiuram disulfide vulcanisation, the active accelerator may actually be morpholinedithiocarbamic acid. This might explain the longer induction time and the lower relative torque values, as the crosslinking agent is depleted faster. This may be as a result of the greater number of hydrogen abstraction reactions that may occur, relative to N,N'-dicyclopentamethylenethiuram disulfide.

It was inadvertently discovered that morpholine is relatively more stable than the other amines precursors. It was redistilled once during this investigation and was reused over a considerable time period with no alteration in purity, whereas aniline for example, was found to be very labile even when stored in a dark bottle under an inert atmosphere at reduced temperatures.

TMTD and TETD are better accelerators than both the aromatics and N,N'-dimorpholinethiuram disulfide. N,N'-dicyclopentamethylenethiuram disulfide, however, was the most effective accelerator of those that were investigated. Of the two linear aliphatics, TETD was found to be the most effective accelerator. No reason is given in the literature for this behaviour. One may feel tempted to say that of the two adducts, the ethyl group, being more positively inductive, may favour homolytic cleavage product formation. When one examines the disulfide bond distances though, one sees a decrease in bond length for the ethyl adduct. It is noted that this trend is also found in the crystal structure data where TMTD has a longer bond length (1.997 Å) than TETD (1.996 Å).<sup>8,9</sup> This may imply stronger bonding and therefore a reduced ability for TETD to produce homolytic cleavage products. The reason for the increased rate must lie more in other complex limiting reaction processes in the vulcanisation mechanism.

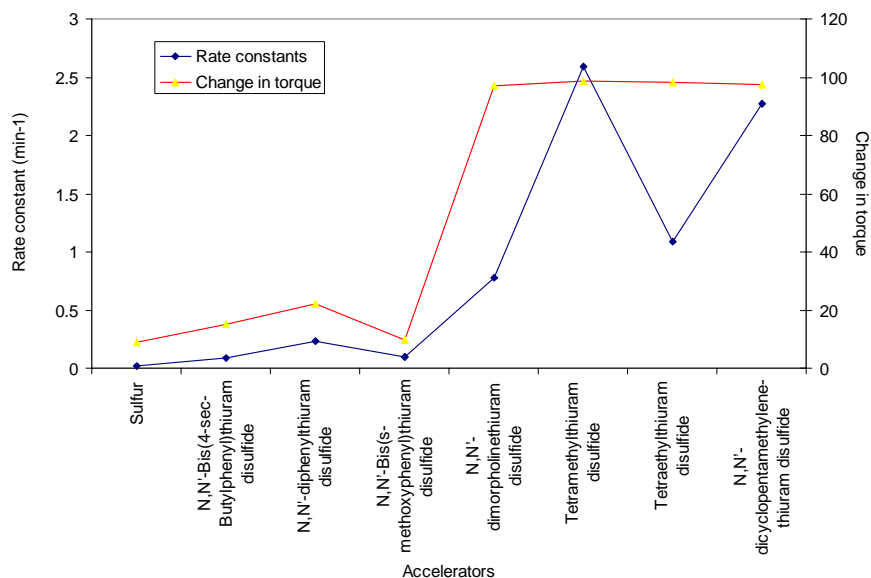
Even though the reactions and the mechanism by which the change in reactivity is effected, is not clearly defined and their influence ascribed, the observations seen in the rate data and maximum torque allow for an adequate description of accelerator effectiveness. It should be noted that this method of rate analysis is directly related to the changes in physical properties of the rubber. As time progresses and the number of crosslinks increases, the modulus increases and the torque required to maintain the oscillatory motions increases.

Figure 10.6 shows that the final relative torque for the four fast accelerators, TMTD, TETD, CPTD and N,N'-dimorpholinethiuram disulfide are similar. All display the characteristic S-shaped cure of industrial vulcanisation. The aromatic accelerators as noted earlier display marching cure systems, their final relative torques vary to a greater extent than do the previously mentioned accelerators since vulcanisation may not be complete at the end of the various experiments. This lack of agreement between the maximum torque and the rate data may be due to varying degrees of reversion between the various accelerators examined.



**Figure 10.6:** Comparison of the torque time curves obtained for the various accelerators investigated

It is noted that from Figure 10.7, that sulfur has slightly slow rate of cure as compared to the aromatics has a higher change in torque. Even though the aromatics increase the rate of vulcanisation, the change in torque experienced are less than that for sulfur alone.



**Figure 10.7:** Comparison of rubber first order cure rate constants and the ultimate change in torque obtained for the accelerators investigated

The reason for this is not readily apparent since one may expect an increased plasticization effect as a result of the accelerator melt which would also tend to give a

large ultimate change in torque. This is, however, not seen and may tend to indicate a negligible lubrication effect as a result of the accelerator melt.

It is noted from Table 10.1, that the cure index data gives a conflicting idea as to the order of the increased rate of acceleration in the aromatic thiuram adducts. As seen previously cure indices are not meaningful measures for marching cures. It is noted that the rate determination by the first order approximation as shown in the experimental offers greater accuracy due to the use of a greater number of data points.

### **10.3 Determining the validity of experimental rate data**

#### **10.3.1 The validity of the rates derived from the initial slopes method in relation to chemical processes**

When examining reaction rates it is important to understand that it is difficult obtain truly representative data when examining a complex reaction system with generalised data. If one examines a simple reaction such as an esterification, the reaction rate may be examined with ease. The influence of solvent, temperature, reagent concentration and type of catalysis may be analysed. This may be considered to be a discrete and well defined system.

Vulcanisation consists of a complex cascade of reactions. In vulcanisation, however, each succeeding or synchronous reaction is dependent on preceding reactions for products, with the slowest reaction governing the overall rate and equilibrium positions of dependent reactions in series. When performing the rate analysis, the disappearance of starting material, being the accelerator and sulfur, were monitored over time. As mentioned earlier in chapter one, thiuram vulcanisation is a complex assortment of different reactions, and when applying simplified approximations as a means to determine the rate we may experience problems. Firstly applying different rate laws to a system in an attempt to obtain rate constants is only valid if all systems which are to be examined obey the same rate law. It was noted that all the systems obeyed the first order approximation to a certain extent, while certain accelerators such as the aromatic adducts gave a closer correlation to a second order rate method. This together with the fact that the aromatic adducts didn't exhibit a large number of isothermal reaction products (see Figure 10.4) would indicate a substantially different vulcanisation mechanism as compared to TMTD and TETD.

It should be noted that the different methods of analysis, that is initial slope versus the more stringent rate laws, examine different regions in the reaction systems progression. Generally speaking the initial slopes method focuses more specifically on the first six to eight minutes of reaction when considering the change in accelerator concentration.

**Table 10.2: Model compound relative rate constants from initial slopes method for both accelerator and sulfur data**

Accelerator	Rate data from accelerator concentration			Rate data from sulfur concentration		
	Initial slope (/mol L <sup>-1</sup> min <sup>-1</sup> )	R <sup>2</sup>	N	Initial slope (/mol L <sup>-1</sup> min <sup>-1</sup> )	R <sup>2</sup>	N
N,N'-diphenylthiuram disulfide	3.83x10 <sup>-5</sup>	0.904	4	1.39x10 <sup>-5</sup>	0.965	8
N,N'-bis(σ-methoxyphenyl)thiuram disulfide	2.45x10 <sup>-5</sup>	0.848	3	2.49x10 <sup>-5</sup>	0.767	4
N,N'-Bis(4-sec-butylphenyl)thiuram disulfide	7.20x10 <sup>-5</sup>	0.795	3	1.60x10 <sup>-5</sup>	0.978	10
N,N'-dicyclopentamethylenethiuram disulfide	8.91x10 <sup>-5</sup>	0.744	4	2.88x10 <sup>-5</sup>	0.940	6
N,N'-dimorpholinethiuram disulfide	6.70x10 <sup>-5</sup>	0.905	4	1.91x10 <sup>-5</sup>	0.962	10
Tetramethylthiuram disulfide	6.46x10 <sup>-5</sup>	0.901	4	2.56x10 <sup>-5</sup>	0.951	6
Tetraethylthiuram disulfide	3.00x10 <sup>-5</sup>	0.988	6	2.04x10 <sup>-5</sup>	0.955	6

The change in sulfur concentration over time allows for the lengthening of this initial region due to the greater adherence to linearity. Table.10.2 shows the initial slope relative rate data derived from both the accelerator and sulfur data. It is seen that the sulfur rate data has a narrower range relative to the accelerator data (1.39x10<sup>-5</sup> to 2.88x10<sup>-5</sup> for the sulfur data relative to 2.45x10<sup>-5</sup> to 8.91x10<sup>-5</sup> for the accelerator data). There is no considerable variation in rate with many of the accelerators exhibiting the same relative rate. This is best illustrated in the figure below.



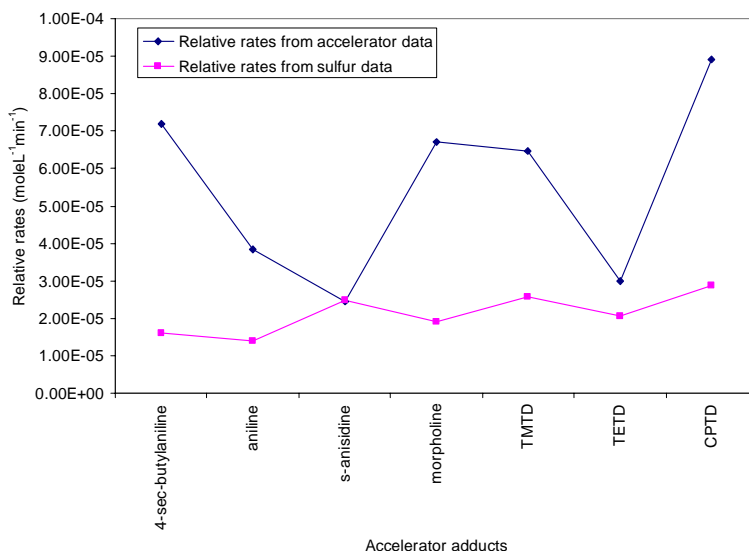


**Figure 10.8:** Comparison of the relative rates determined by the initial slopes method for both the accelerator and sulfur data

The similarity in reaction rates for accelerator consumption indicates a similarity of chemical processes in the early region of the vulcanisation process. The time region considered in the initial slope method corresponds closely to the scorch times seen in rubber systems with linearity in the initial slopes method being reduced at and beyond the scorch times. The data tells us that the rate at which the thiuram disulfides undergo homolytic cleavage and the subsequent accelerator polysulfide formation is not rate limiting. This results from the fact that similar steep slopes are seen for all the accelerators considered and since this region corresponds to the scorch time, we may attribute the process to that of accelerator polysulfide formation, pendent group formation as well as accelerator decomposition.<sup>12,13</sup> The various thiuram adducts have only slight differences in the relative rates at which these changes are undergone. It was noted that the aromatic compounds have a reduced tendency to produce polysulfidic species as seen in the curative interaction study (see Figure 10.4). The number of reaction products produced in the model compound study were considerably more in certain of the aromatic thiuram adducts when compared to the isothermal curative reactions.

Generally accelerators with lower melting points and slightly larger disulfide bond distance produced a larger number of polysulfidic species. The reduced ability of the aromatic thiuram adducts to produce polysulfidic species is overcome during the solubilisation of accelerator in model compound thus reducing the activation energy required to produce polysulfides (see Figure 10.4).

One may conclude from the above results that steric effects do not limit polysulfide formation but rather the stability of the polysulfidic species formed is the limiting factor governed by the electronic influence of substituents. It may also be assumed that there is an increased activation energy in the aromatic thiuram adducts for the production of polysulfides in the presence of sulfur.

### 10.3.2 Observations made with the aid of $^{13}\text{C}$ NMR data and computer modelling in relation to reaction rate

An important observation that was made in terms of substituent effects was that electron withdrawing groups on the aromatic ring reduced the nitrogen atoms ability to deshield the thione carbon (see Figure 10.9).

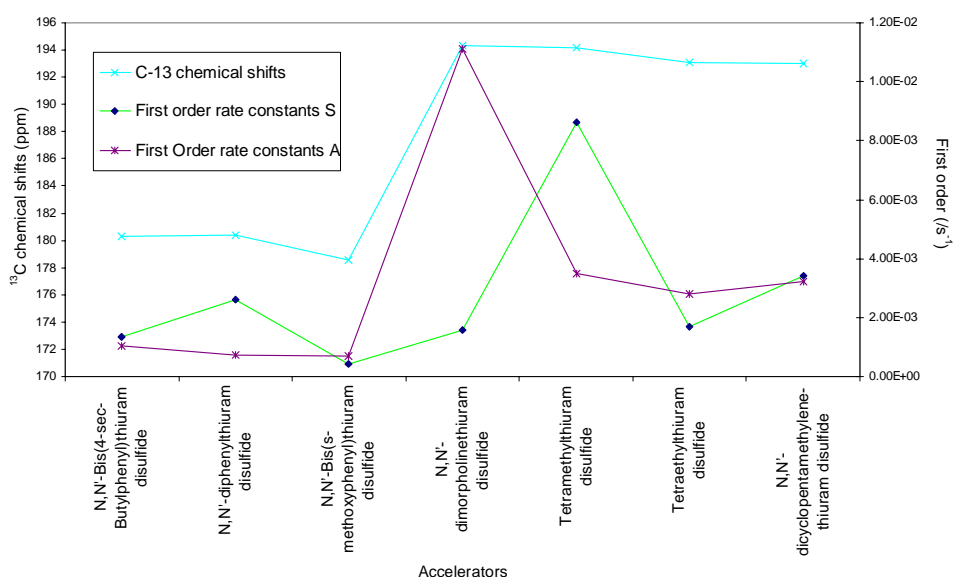


**Figure 10.9:** Comparison of the reaction rates observed in relation to the  $^{13}\text{C}$  chemical shift values for the thione carbon atom

All the accelerators that increased the rate of vulcanisation had substantially deshielded carbon atoms. The accelerators which have a fast rate of crosslinking are associated with  $^{13}\text{C}$  chemical shifts for the thione carbon of greater than 190 ppm, with 193 ppm being observed as a limiting value. It is also noted from the figure that when electro-negative groups are bonded to the nitrogen atom, it has a reduced ability to deshield the thione carbon atom.

This may give some insight into certain chemical aspects of vulcanisation. It is noted that the electronic effects influence accelerator polysulfide formation, but the rate is not severely effected in the initial stages.

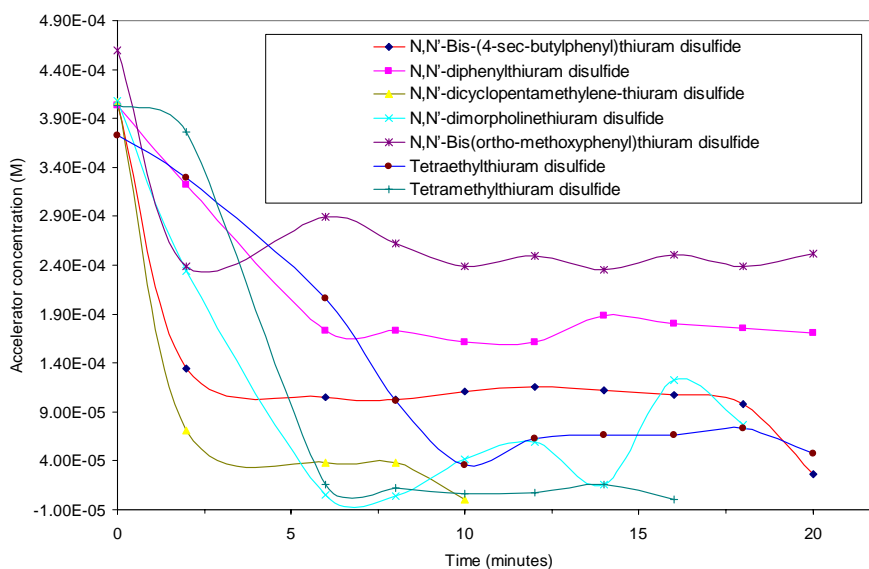


**Figure 10.10: Comparison of accelerator consumption in the model compound study**

The initial rates were very similar, but it appears as though the reactivity of pendent groups may be substantially impeded. As may be seen from Figure 10.10, there is a large amount of residual accelerator left in the poorer accelerators. This may be as a result of an unfavourable reaction mass action, between the accelerator polysulfide and the pendent groups. When this equilibrium position is reached accelerator consumption is slow and negligible with a slow rate of crosslinking releasing small amounts of accelerator or amine decomposition products. The latter is less likely though since it would imply the consumption of accelerator over time. This would also increase the rate at which vulcanisation is increased since the dithiocarbamic acid is an intermediate in the amine decomposition pathway. The dithiocarbamic acid may have a reduced activity. It is suspected that the aromatic thiuram adducts are less reactive as a result of the greater instability of the thiuram sulfenyl radicals, this is seen in the relatively high electron densities that are found on the thione carbon atoms, as seen in Figure 10.5.

This would have the tendency to destabilise both negative charges and radicals. After the accelerator sulfur pendent group system has reached an equilibrium condition the rate at which crosslinking occurs is slow and is primarily driven by sulfur

consumption (via insertion in the accelerator polysulfides). Accelerators with high rates of vulcanization tend to have higher rates of sulfur consumption.

### 10.3.3 The validity of first order rate data in relation to chemical processes

The rate laws examine a different aspect of the rate or more specifically a different chemical process contributes to the rate constants observed. The reason for this being that data which adhere to this rate law occur after the second minute of reaction, and the interval over which linearity is maintained is generally shorter.

**Table 10.3:** First order rate constants derived from the model compound study for both the accelerator as well as the sulfur data

Accelerator	Rate data from accelerator concentration			Rate data from sulfur concentration		
	First order (/s <sup>-1</sup> )	R <sup>2</sup>	N	First order (/s <sup>-1</sup> )	R <sup>2</sup>	N
N,N'-diphenylthiuram disulfide	7.46×10 <sup>-4</sup>	0.807	4	2.62×10 <sup>-3</sup>	0.932	4
N,N'-bis(σ-methoxyphenyl)thiuram disulfide	6.71×10 <sup>-4</sup>	0.999	3	4.39×10 <sup>-4</sup>	0.931	7
N,N'-Bis(4-sec-Butylphenyl)thiuram disulfide	1.05×10 <sup>-3</sup>	0.890	4	1.34×10 <sup>-3</sup>	0.912	9
N,N'-dicyclopentamethylenethiuram disulfide	3.40×10 <sup>-3</sup>	1	2	3.23×10 <sup>-3</sup>	0.921	7
N,N'-dimorpholinethiuram disulfide	1.11×10 <sup>-2</sup>	0.908	4	1.57×10 <sup>-3</sup>	0.921	7
Tetramethylthiuram disulfide	3.47×10 <sup>-3</sup>	0.897	5	8.62×10 <sup>-3</sup>	0.981	6
Tetraethylthiuram disulfide	2.78×10 <sup>-3</sup>	0.950	5	1.60×10 <sup>-3</sup>	0.910	6

The first order data obtained may actually be representative of this process, and the region employed occurs well after the induction period where active polysulfides and pendent groups may be formed. Since the preceding steps of this vulcanisation process may not be considered limiting, rate constant obtained from the first order approximation should approximate that which is seen in the disproportionation of crosslinks.

It is important to note that even though both first order rate constants, that is those obtained from the accelerator and sulfur data, may be representative experimentally, uncertainties limit the accuracy of the data obtained. One of the problems encountered was the rapid consumption of accelerator, especially N,N'-dicyclopentamethylenethiuram disulfide. This prevented an accurate rate constant being determined as seen in Figure 10.10 and Table 10.3; only 2 points were used for the determination.

It is important to note that combining the two sets of data to obtain the best values from each set could not be considered. In further discussions use is made of the first order rate constants that were derived from the sulfur data because they are derived from more data points.

#### 10.4 Comparison of the first order rate constants presented by the various accelerators in relation to the rate observed in rubber vulcanisation

When looking at the rate constant data derived from the first order approximation it is important to investigate any similarities that may exist between the two sets of first order data derived from the model compound study.

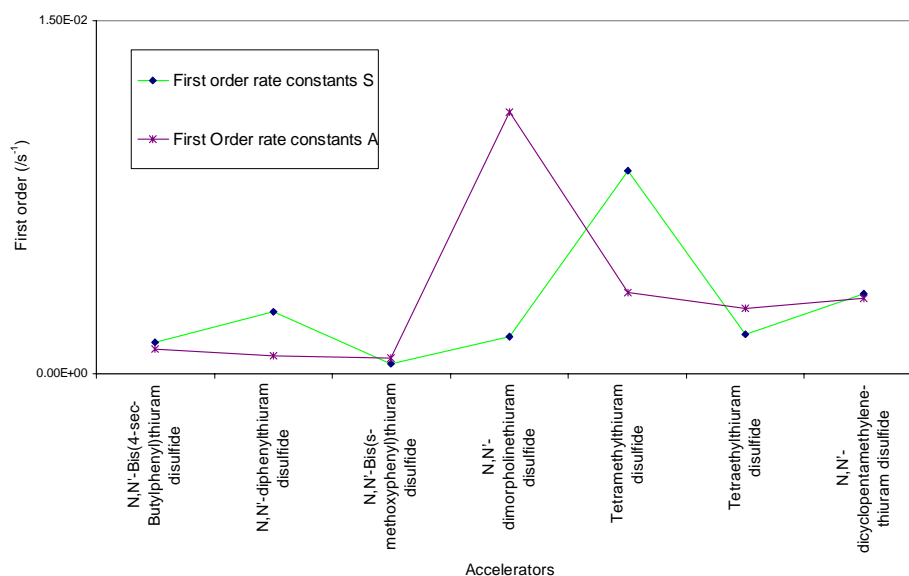


Figure 10.11: Comparison of the first order rate data derived from the model compound study for both the sulfur and accelerator data

There is a good correlation between the two types of data for the aromatic thiuram adducts although the accuracy in the determination of the rate constant with regard to the accelerator data is low (see Table 10.3 and Figure 10.11). Even though direct relationships between the data did not exist some relationships were shown on the basis of simple kinetic models for example that of Coran.<sup>6,7</sup>

The accelerator data has a tendency to give larger rate constants than one would expect especially in comparison to the rate data derived from the rubber studies. The morpholine adduct is shown to have a greater rate of accelerator consumption than TETD thus one may wish to infer a higher rate of crosslinking but this is not seen, similarly for TMTD and TETD. This may be as a result of the accelerator being labile, it has been already shown that both N,N'-dimorpholinethiuram disulfide and N,N'-dicyclopentamethylene-thiuram disulfide have far more complex reaction pathways which don't necessarily result in crosslinking. The radicals that are formed could easily undergo radical addition to the squalene backbone preventing their participation in crosslinking. Certain accelerators like TMTD may have a greater tendency to decompose. It is well known that the TMTD melt endotherm is not exclusively attributable to fission processes but includes a decomposition component. The sulfur data as said earlier would be more reliable, but it too does not give us a true idea of the relative rate of acceleration. It is seen that the rate constant obtained for N,N'-dimorpholinethiuram disulfide is less than that seen for N,N'-diphenylthiuram disulfide and similar to that of N,N'-bis(4-sec-butylphenyl)thiuram disulfide.

It is known that the morpholine adduct increases the rate of vulcanisation to far greater extent than do the aromatic adducts. It should be noted that because of the complexity of the vulcanisation process the relation between accelerator and sulfur consumption is not stoichiometric. N,N'-dimorpholinethiuram disulfide has a low first order rate constant with regards to sulfur, but the crosslinking reacting in rubber is fast. This may be simply explained by the fact that thiuram disulfide accelerators may act as autonomous crosslinking agents.

The rate constants derived from the accelerator data TMTD and TETD data display a rapid consumption of accelerator, with the TMTD displaying a greater rate. This is not what is seen in the rubber analysis with the TETD having the greater rate of vulcanisation. This may be attributable to increased decomposition in the TMTD as compared to the TETD system. There is some agreement between the accelerator and sulfur derived first order rate constants in this system. It is noted that the TMTD

system, which has the faster rate of accelerator consumption, also has the greater rate constant for sulfur consumption. Finally as mentioned previously the accelerator data obtained for the determination of the N,N'-dicyclopentamethylenethiuram disulfide rate constant was not accurate as a result of the rapid rate of accelerator consumption, limiting the number of points available for the rate determination. It was, however, shown that for rate constant for this accelerator from the sulfur data showed the largest rate of sulfur consumption, which agrees with what is observed in the rheometrical analysis.

### **10.5 Comparison of sulfur rate constant with the rate constants derived from the rheometric analysis**

When examining the agreement between the rate constants derived from the model compound study and the rheometric data, it is important to take stock of the differences in each analysis and most importantly what is being observed in each process. As has been previously discussed, the model compound study allows one to determine the rate constants from directly measuring the amount of curatives consumed over time. This technique is limited in that the rate constant cannot discretely be ascribed to single chemical process due to the interdependence of various reactions and also the prevalence of competing decomposition reactions as in the case of TMTD,<sup>14,15,16,17</sup> etc. Thus the rate is a generalised representative of a complex system, which may not truly be assigned to one particular chemical process.

In the rheometric analysis one is able to define the rate as being attributed to the rate at which crosslinking occurs. The measurement made is directly related to changes in the physical properties which arise as the number of chemical crosslinks increase. When comparing the two methods of rate analysis, it is clear that only the sulfur data corresponds closely to the rate determined by physical measurements (see Figure 10.12). This correspondence is greater for data of accelerators which have a greater ability to increase the rate of vulcanisation. This may be true in the case of N,N'-dicyclopentamethylenethiuram disulfide which has the highest rate of cure. When we examine the accelerator N,N'-dimorpholinethiuram disulfide for example, it has a moderate acceleration effect and presents the largest ultimate change in torque. This may be ascribed to the accelerator's reduced lability.

The variation in the first order rate constants as derived from the accelerator data may be attributed to decomposition and other secondary factors. These factors

prevent the observation of a linear or some easily defined relation between the consumption of sulfur and accelerator. As mentioned earlier there is no stoichiometric relation due to the polysulfidic nature of the species produce and the large variations that may be observed in the number of sulfur atoms that may occur in the species produced.

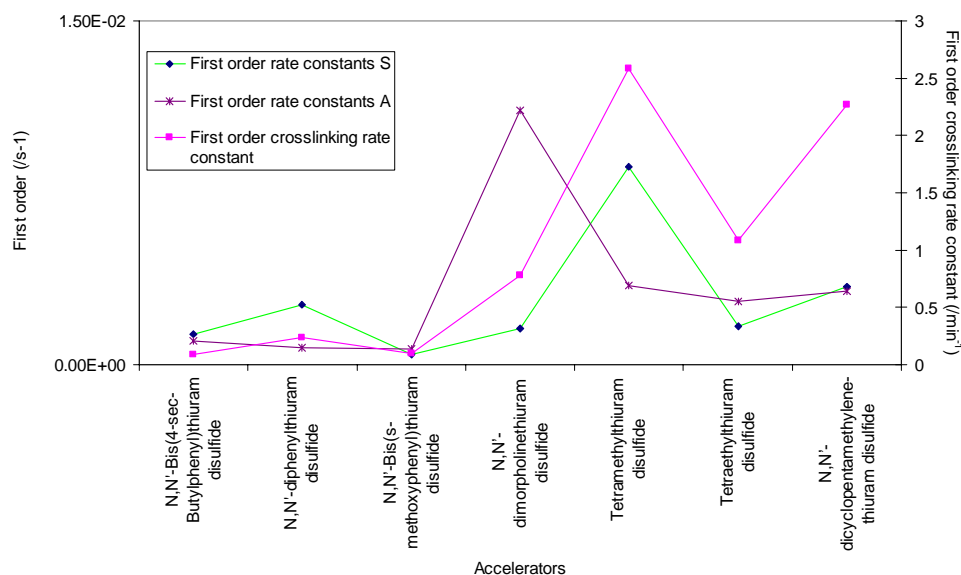


Figure 10.12: Comparison of rate constants determined from the model compound study and rheometric data

It is interesting to note that the change in physical properties has a close agreement to the depletion of sulfur, this seen in Figure 10.12.

### 10.5.1 Squalene as model compound

It should be noted that experimental precautions need to be taken when working with squalene. It was discovered during these analyses that the compound has a tendency to scorch producing charred residues that were insoluble even in the amended 100 mL of THF. The amount of charring was reduced by increasing the vigour at which the samples were agitated and ensuring that the reagents were thoroughly mixed allowing no time for the curatives to settle. If we take the rate at which sulfur is consumed in the model compound reactions to be representative and in good agreement with the rate at which crosslinking occurs, we may say that squalene appears to be an effective model for cis-1,4-polyisoprene.



Caution should be expressed though since the rate of sulfur consumption in relation to the rate obtained from rheometric data are very loosely related in light of the complexity of the vulcanisation mechanism. It should be noted that the mere fact that the model compound is in the liquid phase could alter the reactions of the model compound and reducing the data's relevance to a real rubber system.

## 10.6 Linear free energy relationships

### 10.6.1 Obtaining valid Taft substitution constants for complex molecular systems

Many combinations of data were assessed in order to obtain or rather investigate possible relationships that may exist among the consort of available experimental data and established chemical data available for the molecules that were investigated. This would colligate the discoveries that were made in a final assessment to relate observed chemical behaviour to substituent effects. It is important to note that the Taft substituent constant for a group is the sum of the individual Taft constants for the molecular fragments involved (please see Chapter 2 for the derivation).

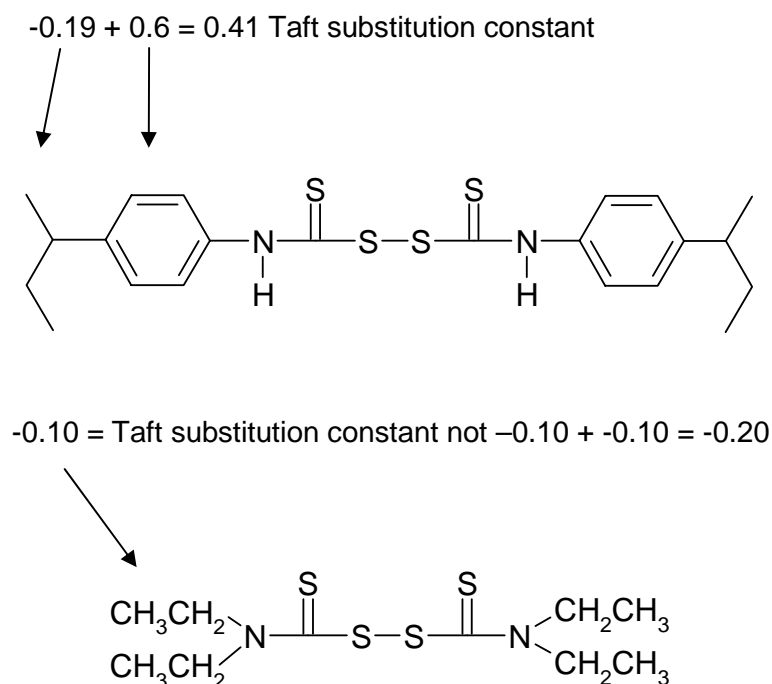


Figure 10.13: Example of the calculation employed when determining Taft substitution constants

Taft constants were calculated as per the method detailed in the experimental section of this thesis. Methyl and hydrogen groups are designated a substitution constant of zero. The Taft substitution constant calculated for N,N'-bis(4-sec-butylphenyl)thiuram disulfide and tetraethylthiuram disulfide is shown in the figure above. No reasonable free energy relationship could be derived when adjacent molecular structure substitution constants were added to derive a new apparent substitution constant. Thus the analysis was restricted to substitution constants derived from the addition of the various constants of structures that occur in series i.e. molecular subunits that are bonded to one another as seen in Figure 10.17.

### **10.6.2 Data assemblies that were considered in the linear free energy investigation**

Various combinations of data were assessed to investigate possible trends. It was discovered that no linear free energy relationships could be established with data containing scorch times, molecular masses, disulfide bond lengths, or  $^{13}\text{C}$  chemical shifts; the reason being that for many of these operators principals which exclude the data are discernable. Scorch times were not applicable since the aromatic thiuram adducts presented marching cures with no appreciable scorch time being observed. Molecular mass and melting points showed no relation to any operator. It was thought that a linear free energy relationship may have existed between molecular mass and the melting point as well as between the melting point and the rate of acceleration. Relying on the generalised principal that increase molecular mass is generally accompanied by an increase in melting point, this however, only would truly be applicable to a homologous series of compounds like lauric, palmitic and stearic acid in which there is an increase in the number of carbons in the aliphatic chain of the waxes. The compounds analysed in this study don't vary discretely like the above mentioned series, but vary in both functionality and stereochemistry. This is noted in the previous chapters where plate/needle like crystals were generally obtained as the final purified products in the case of the aromatics thiuram adducts, ascribed to the rigidity of the aromatic rings. Similarly reduced melting points generally promote reactivity as mentioned previously. Another generalisation that is made is that scorch time increases with increased decomposition temperature. Other possible linear free energy relationships were investigated, but no relationships were observed.<sup>1,18,19,20,21,22,23,24,25,26</sup>

Reasonable relationships could only be attained using the first order rate data derived from the rheometric data of the polyisoprene/sulfur/accelerator systems with no relation being evident even from the more reliable sulfur rate data as derived for the model compound study. The only reasonable explanation that may be given for the data presenting incongruities relative to the rheometric data, is that the sulfur data would take into consideration many overlapping reactions which involve sulfur and don't necessarily involve reaction with accelerator thus not relying on substitution electronic effects for any form of governance. The sulfur data could thus only be used as an approximate representation of the rates that may be observed in the reactions involving accelerator but the correlation is poor in these accelerator systems. The sulfur data is thus not truly representative of the rate-limiting step as is found in the case of the rheometrical data.

A relationship between reactivity and the  $^{13}\text{C}$  chemical shifts for the thione carbon was observed but it is not a linear relationship and therefore no figure has been added to depict this linear free energy relationship. It is noted that accelerators which have groups with strongly deshielded thione carbon atoms have high rates of vulcanisation. It is seen that above a certain threshold no further deshielding of the thione carbon increases the rate of vulcanisation (see Figure 10.5).

### **10.6.3 The linear free energy relationships that were investigated**

It was seen that in the polyisoprene/sulfur/accelerator system that an increased rate of vulcanisation was experienced when the substitution constant became smaller. Much more efficient vulcanisation rates were exhibited with substituents which presented negative substitution constants (see Figure 10.14).

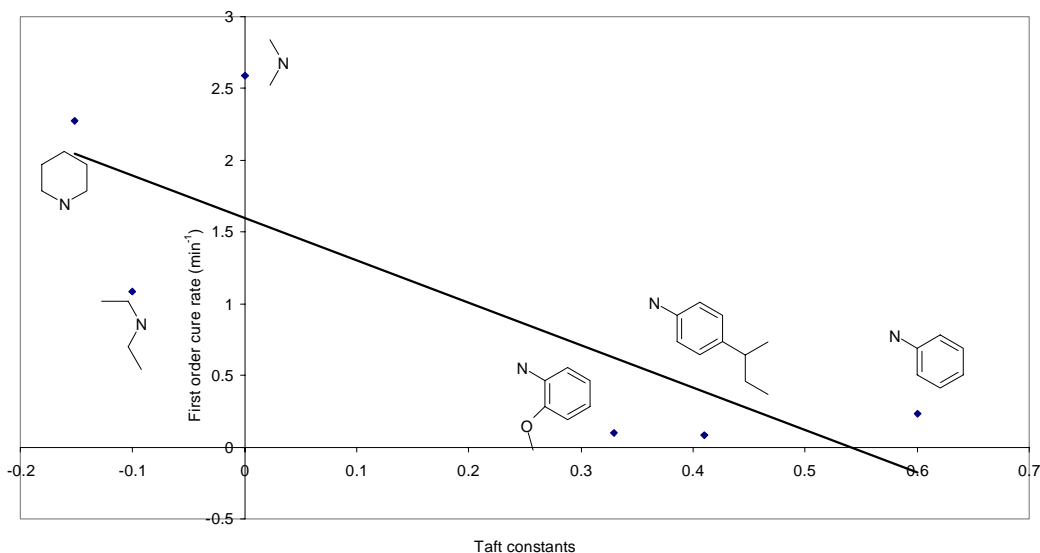


**Figure 10.14:** The linear free energy relationship between cure rate in the rubber system and substituents effects

The negative values of the substitution constants are associated with groups which are electron donating. It thus appears as though electron donating groups on the thiuram nitrogen increases the rate at which vulcanisation is accelerated.

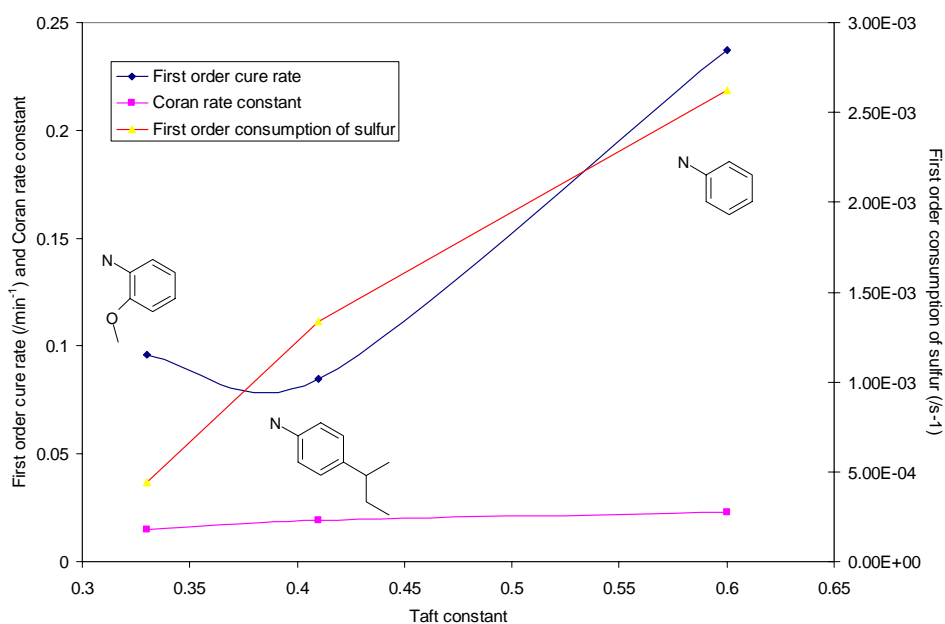


**Figure 10.15:** The relationships that exist between the first order cure rate, Coran constant and first order consumption of sulfur in relation to the Taft constants for the aromatic thiuram disulfide derivatives

The negative slope, that is the negative reaction constant  $\rho$ , implies that electron-donating groups promote the reaction. N,N'-diphenylthiuram disulfide TMTD are the only accelerator that don't obey this generalised statement. It should be noted that the line in Figure 10.14 doesn't infer a linear trend, but simply that there is an increase in rate associated with low Taft constants. Such a relationship may be linear in the case of a homologous series of aliphatic compounds.

A somewhat different picture may be observed for the aromatic thiuram disulfide derivatives when the N,N'-diphenylthiuram disulfide compound is included in our investigation. Figure 10.15 infers that the aromatic thiuram disulfide accelerators with more positive Taft constants increase the rate of reaction as seen through the Coran, first order cure and first order consumption of sulfur rate constants. Thus one sees that electron withdrawing groups in the case of the aromatic substituents promote the vulcanisation reaction.

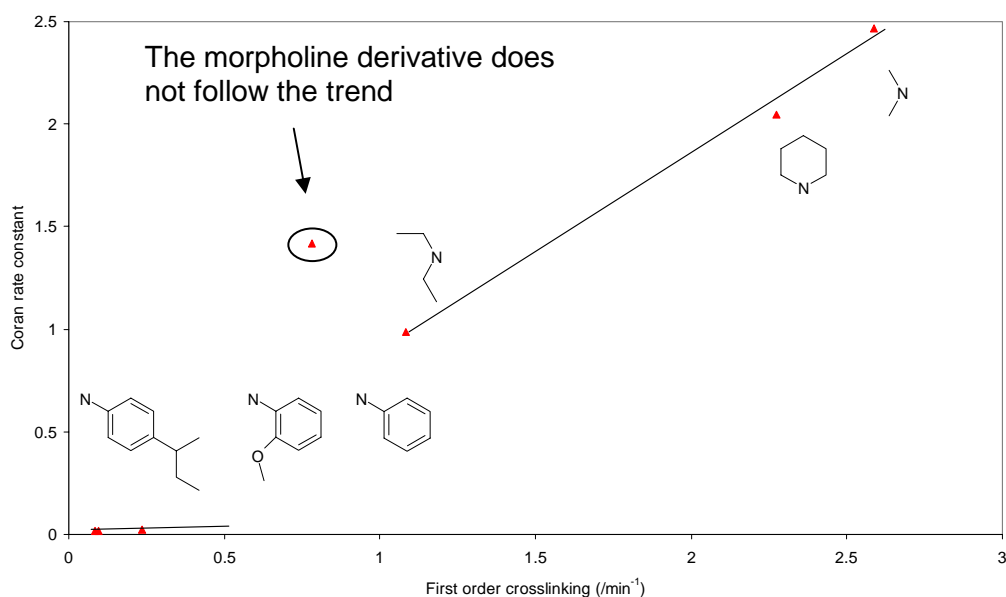


**Figure 10.16: The relationship between the Coran and first order crosslinking rate constant**

This may infer the operation of a different vulcanisation mechanism. This is further reinforced by what is seen in Figure 10.16. Figure 10.16 exhibits different slopes for the aliphatic and aromatic thiuram disulfide derivatives in a plot of the Coran rate constant vs. the first order crosslinking rate constant.

As seen previously the aromatic derivatives presented marching cures, while the other accelerator systems showed the characteristic S-shaped indicative of inductive, acceleratory and depletive processes that occur in a dynamic system in which starting materials are not replenished.

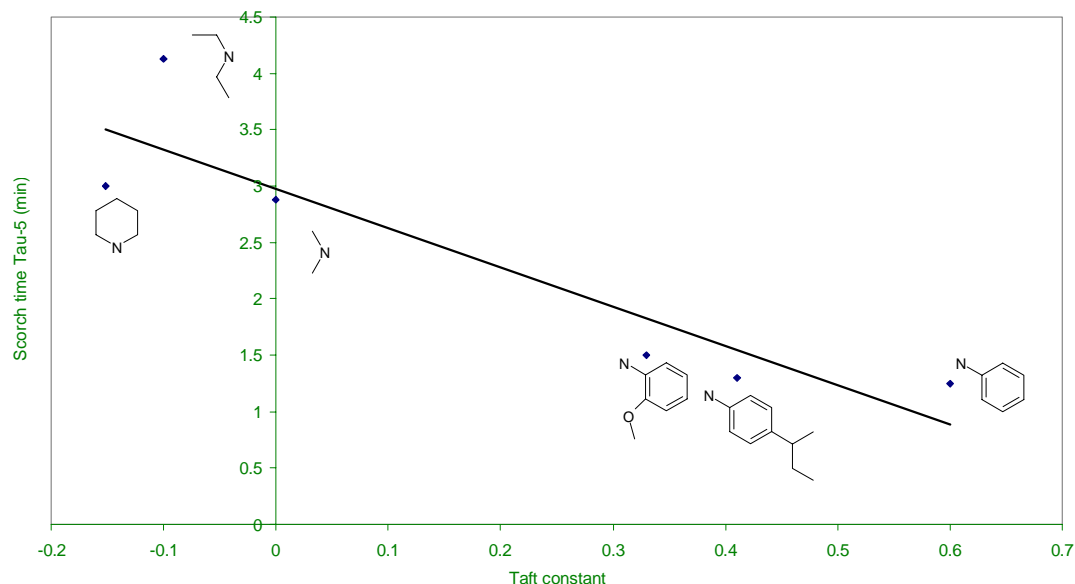


**Figure 10.17:** Linear free energy relationship that exists between scorch time and Taft substitution constants

It can be seen in Figure 10.17 that as the substitution constant decreases and becomes more negative scorch time generally increases. TETD is very different though having a much greater increase in scorch time than what is seen relative to the other accelerators examined. Scorch time generally increases with an increase in decomposition temperature. TETD is seen to melt at approximately 75°C. The melt endotherm is not exclusively attributed to a fission process but is accompanied by partial decomposition. Thus one may expect a substantially reduced scorch time, this is however, not seen.<sup>11,18,19,20,21,22,23,24,25,26</sup>

## 10.7 References

- 1) A.B. Sullivan, L.H. Davis and O.W. Maender, *Rubber Chem. Technol.*, 56, 1061 (1983)
- 2) H. Krebs, *Rubb. Chem. and Technol.*, 30, 962, (1957)
- 3) M.M. Coleman, J.R. Koenig and J.L. Koenig, *Rubb. Chem. Technol.*, 46, 957 (1973)

- 4) M. Geysler and W.J. McGill, *J. Appl. Polym. Sci.*, 60, 439 (1996)
- 5) F.W.H. Kruger and W.J. McGill, *J. Appl. Polym. Sci.*, 45, 563 (1992)
- 6) A.Y. Coran, *Rubb. Chem. Technol.*, 37, 689 (1964)
- 7) A.Y. Coran, *Rubb. Chem. Technol.*, 38, 1 (1965)
- 8) Y. Wang, J. H. Liao and C. –H. Ueng, *Acta Cryst.*, c42, 1420 (1986)
- 9) I.L. Karle, J.A. Estlin and K. Britts, *Acta Cryst.*, 22, 273 (1967)
- 10) C.P. Reyneke-Barnard, M.H.S. Gradwell, W.J. McGill, *J. Appl. Polym. Sci.*, 78, 1099 (2000)
- 11) C.P. Reyneke-Barnard, M.H.S. Gradwell, W.J. McGill, *J. Appl. Polym. Sci.*, 78, 1112 (2000)
- 12) M. Porter, *The Chemistry of Sulfides*, Ed. A.V. Tobolsky, Interscience Publishers, New York, 165 (1968)
- 13) F.W.H. Kruger and W.J. McGill, *J. Polym. Sci.*, 42, 2669 (1991)
- 14) C.W. Bedford and L.B. Sebrell, *Ind. Eng. Chem.*, 14, 25 (1922)
- 15) B.A. Dogadkin and V.A. Shershnev, *Rubber Chem. Technol.*, 33, 401 (1960)
- 16) D. Craig, *Rubber Chem. Technol.*, 29, 994 (1956)
- 17) G.A. Blokh, *Organic Accelerators in the Vulcanisation of Rubber*, Israel Program for Scientific Translations Ltd., 1968
- 18) Wheland and Pauling, *J. Am. Chem. Soc.*, 57, 2086 (1935)
- 19) Miller, B, *Advanced Organic Chemistry Reaction Mechanisms*, Prentice Hall, New Jersey, p122 (1998)
- 20) N.B. Chapman and J. Shorter Ed., *Correlation Analysis in Chemistry*, Plenum Press, New York, 87 (1978)
- 21) C.D. Johnson, *The Hammett Equation*, Cambridge University Press, Cambridge, (1973)
- 22) L.P. Hammett, *J. Am. Chem. Soc.*, 59, 96. (1937)
- 23) Y. Ogata, A. Kawasaki and N. Okumura, *J. Org Chem.*, 29, 1985, (1964)
- 24) Y. Okamoto, T. Inukai and H.C. Brown, *J. Am. Chem. Soc.*, 80, 4972 (1958)
- 25) E. Morita and A.B. Sullivan, *Rubber Chem. Technol.*, 54, 1132 (1981)
- 26) E. Morita, *Rubber Chem. Technol.*, 55, 352 (1982)

# 11 Conclusions

---

11.1. Conclusion.....	196
11.2. Further work.....	197



### 11.1. Conclusion

The project was successful in that many of the objectives that were set out at the onset were fulfilled during this study. The addition reaction of amine to  $\text{CS}_2$  in basic medium and subsequent oxidation with  $\text{K}_3\text{Fe}(\text{CN})_6$  all in a 1;1 molar ratio, proved to be a feasible method for the production of thiurams. The yields achieved, however, were low. This may be overcome by either optimising the reaction conditions to improve the efficacy of  $\text{K}_3\text{Fe}(\text{CN})_6$  as an oxidant, or by means of the use of alternate reaction pathways that don't rely on the dithiocarbamate as a precursor.

The rate determination of thiuram disulfide/sulfur model compound was a success, with data primarily following first order kinetics. It was shown that the first order sulfur rate data presented a closer agreement to the cis-1,4-polyisoprene system, even though no linear free energy relationship could be found to link the two systems. The accelerator and sulfur initial slope rate data proved that the homolytic cleavage of thiuram disulfide and subsequent accelerator polysulfide formation, were not limiting steps.

Squalene may be considered a suitable model compound for cis-1,4-polyisoprene, although charring and solution effects should be considered when it is to be used in a study. The lack of agreement between the data derived from the model compound and polyisoprene study does not shed doubt as to the validity of squalene as a suitable model for polyisoprene, but rather results from the collection of different types data in each of the two systems. This may be ascribed to autonomous crosslinking, decomposition and accelerator release in the case of the accelerator data; the non-stoichiometric consumption of sulfur in polysulfide formation, crosslinking and network maturation reactions in the case of sulfur data; the direct relationship between changes in torque and crosslink density and the lack of such a close tie between crosslink increase and the consumption of both accelerator and sulfur.

Generally the groups of accelerators examined, linear, cyclic and aromatic thiuram disulfide adducts, produced vastly varied rate data. The aromatic thiuram disulfide adducts only had a slight acceleratory effect on the rate of vulcanisation as compared to the unaccelerated sulfur system. The morpholine adduct had a moderately larger rate of acceleration followed by tetramethyl and tetrethylthiuram disulfide, with N'N-dicyclopentamethylenethiuram disulfide having the fastest rate of acceleration.

The reduced ability of the aromatics to accelerate the rate vulcanisation may lie in the aromatic adducts reduced ability to produce polysulfides.

Certain of the rate data was found to be relatable to Taft substitution constants and physical properties derived from computer modelling, NMR and rheological data. Generally it was found that aliphatic thiuram disulfide accelerators with small to negative Taft substitution constants had an increased ability to accelerate the rate of rubber vulcanisation, while the opposite trend was observed for the aromatic thiuram disulfides where a positive Taft constant was seen to promote the reaction. This may infer the operation of different vulcanisation mechanisms in the aliphatic and aromatic thiuram disulfide derivatives. The opposite may also be true though but too little data exists to verify this. This data ties up with similar electronic data, notably  $^{13}\text{C}$  NMR data. Even though a linear relationship could not be found between the rate of cure in the rubber system and thione carbon chemical shifts as result of a limiting value, it was discovered that accelerators with deshielded thione carbon atoms caused an increased rate of vulcanisation with optimum  $^{13}\text{C}$  chemical shifts values occurring between 190-193 ppm.

Even though the aromatics presented marching cures, scorch times - relying on the  $\tau_5$  times, were found to be related very loosely to Taft substitution constants. Generally as the electron donating ability of the substituents increases, that is the Taft substitution constant becomes smaller to negative, we find an increase in vulcanisation scorch times. Tetraethylthiuram disulfide was, however, found not to obey this generalisation.

Thus  $^{13}\text{C}$  NMR, computer modelling and Taft substitution constant may be used as a qualitative guide to approximate thiuram disulfide reactivity. This would make the preliminary choice of accelerators easier after which experimental data should be sort to conclusively prove that particular curative systems crosslinking efficiency, taking into consideration end product requirements.

## 11.2. Further work

More thiuram disulfide accelerators should be examined to increase the validity of this study. Accelerators should be chosen in an attempt to illuminate resonance contributions, which serve to confuse matters. Alternately a study which takes into consideration both electronic and resonance substitution constants should be

entered into. Effort should be made to quantify model compound crosslink products in an attempt to obtain feasible relationships between model compound systems and rubber systems.

# Appendix A

## N,N'-diphenylthiuram disulfide

---

### List of figures

Figure A.4: $^1\text{H}$ -NMR spectrum for N,N'-diphenylthiuram disulfide.....	200
Figure A.5: $^{13}\text{C}$ -NMR spectrum for N,N'-diphenylthiuram disulfide.....	201
Figure A.6: IR spectrum for N,N'-diphenylthiuram disulfide.....	202
Figure A.7: Determination of relative rate using the initial slope method in relation to the sulfur concentration data.....	203
Figure A.8: Determination of relative rate using the initial slope method in relation to the N,N'-diphenylthiuram disulfide concentration data...	203
Figure A.9: Determination of the first order rate constant in relation to sulfur concentration data.....	204
Figure A.10: Determination of the first order rate constant in relation to N,N'-diphenylthiuram disulfide concentration data.....	204

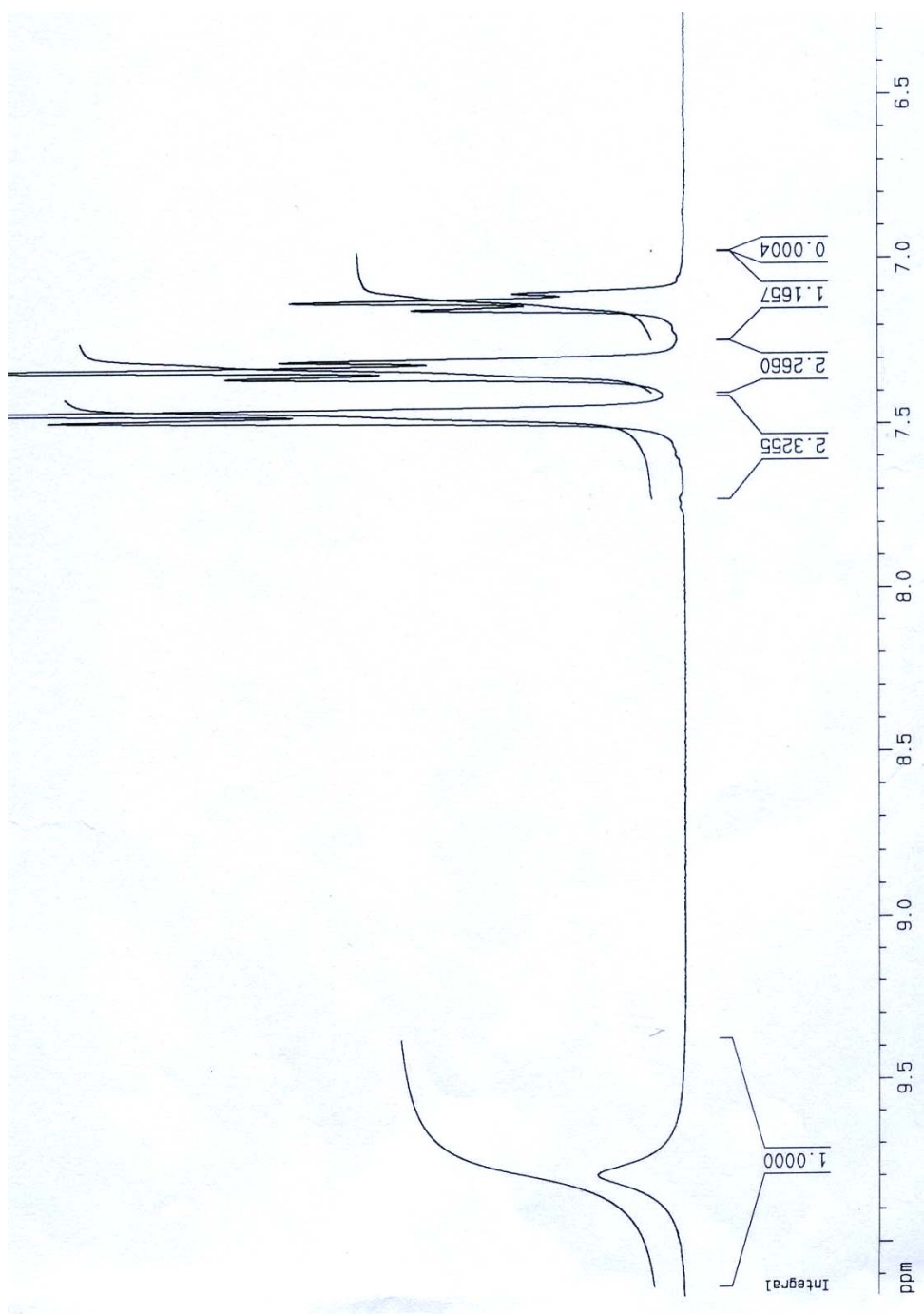


Figure A.1: <sup>1</sup>H-NMR spectrum for N,N'-diphenylthiuram disulfide

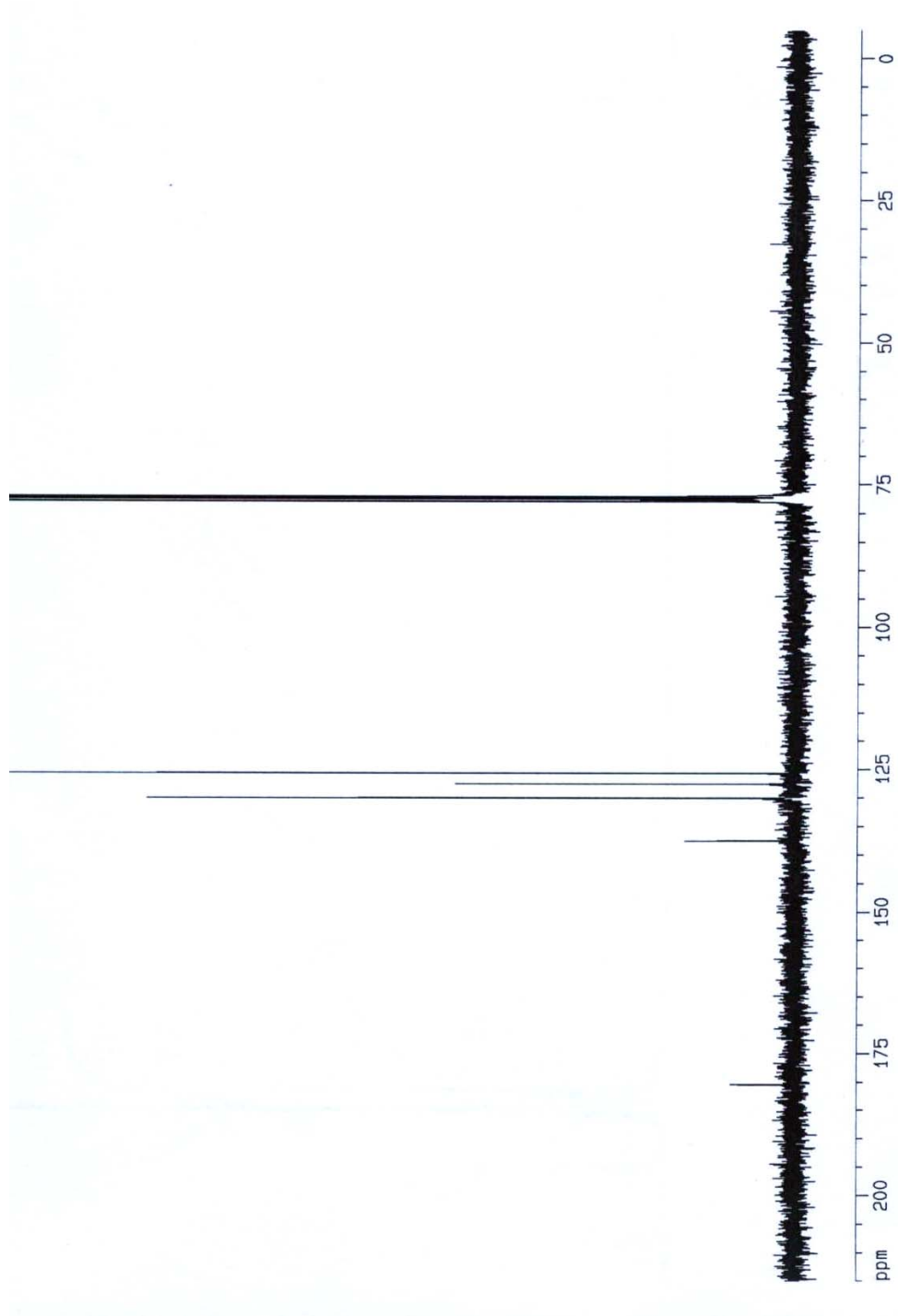


Figure A.2:  $^{13}\text{C}$ -NMR spectrum for  $\text{N,N}'$ -diphenylthiuram disulfide

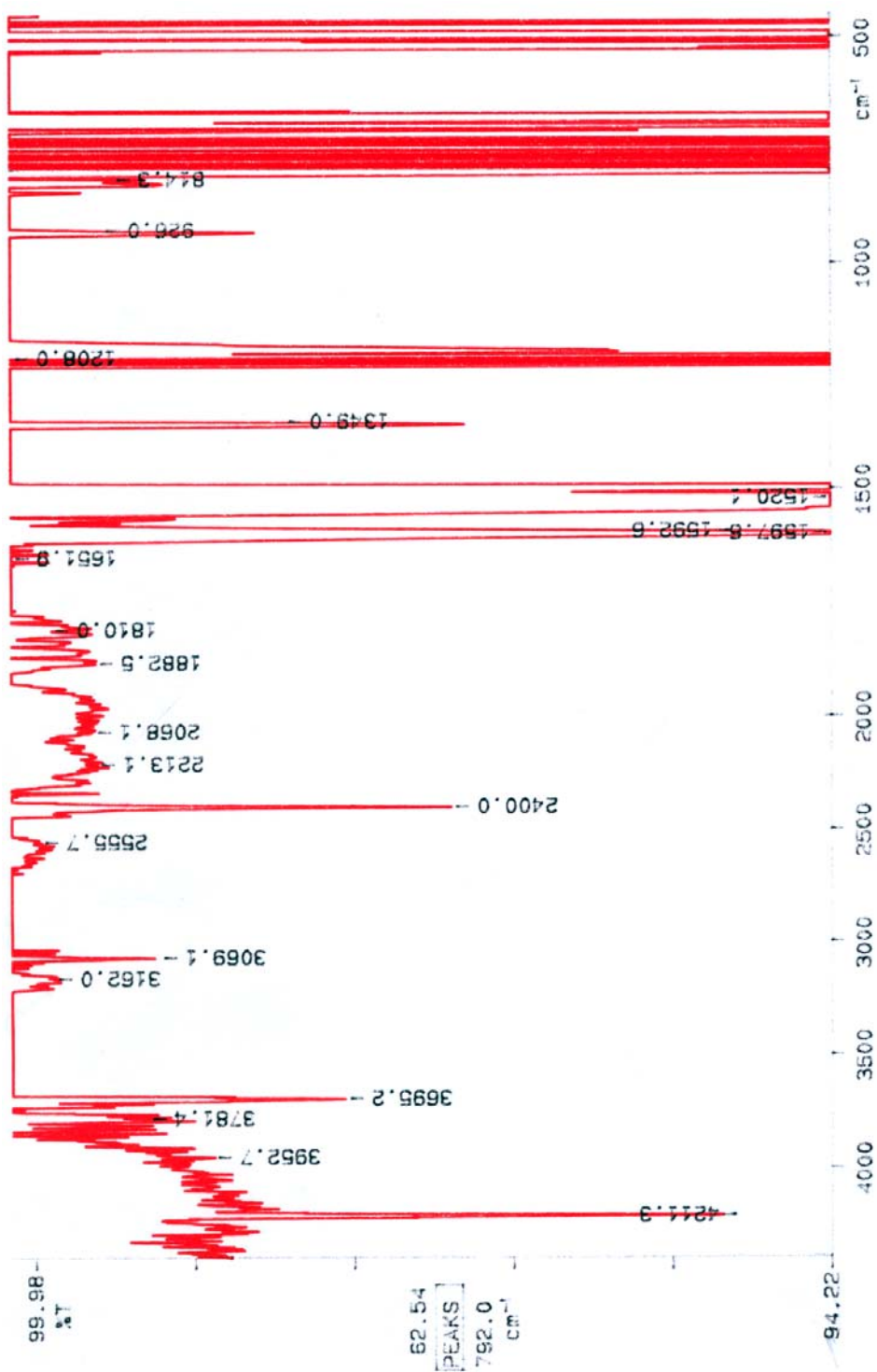
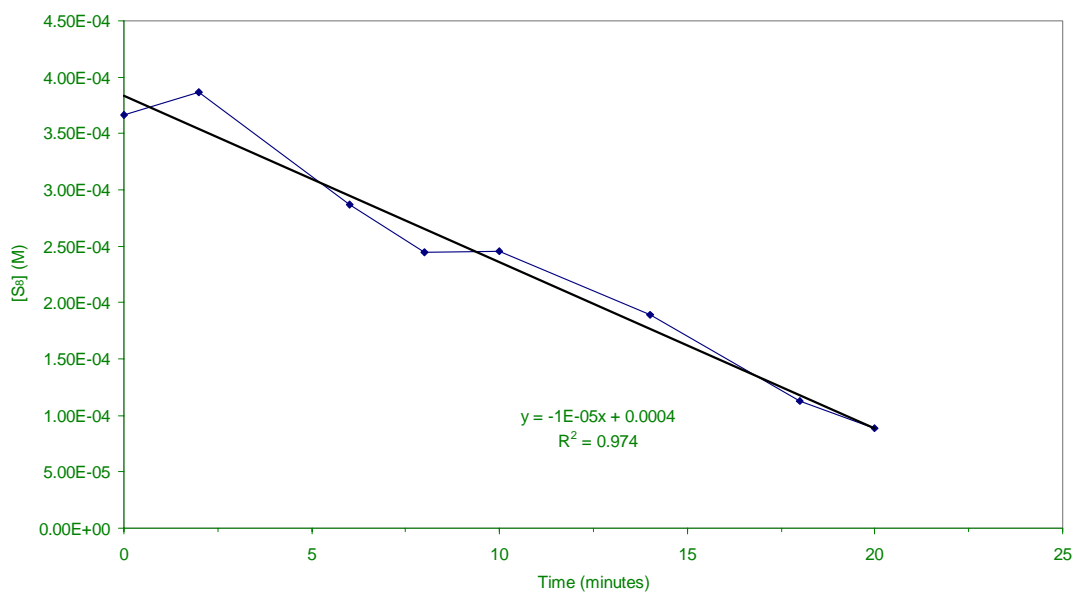
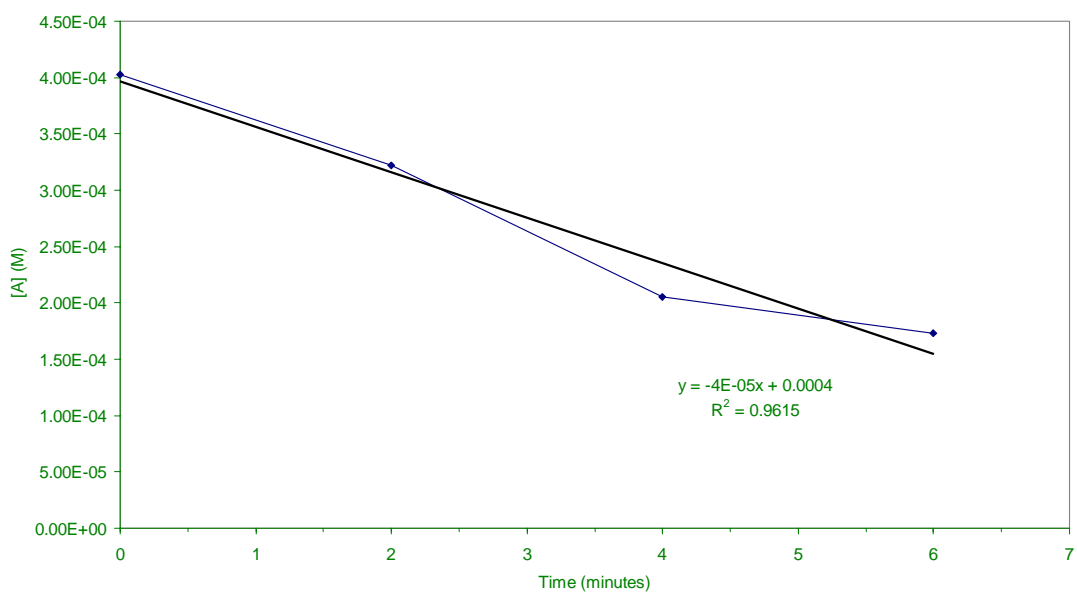


Figure A.3: IR spectrum for N,N'-diphenylthiuram disulfide



**Figure A.4:** Determination of relative rate using the initial slope method in relation to the sulfur concentration data



**Figure A.5:** Determination of relative rate using the initial slope method in relation to the N,N'-diphenylthiuram disulfide concentration data (the letter A in the above graph represents the accelerator)



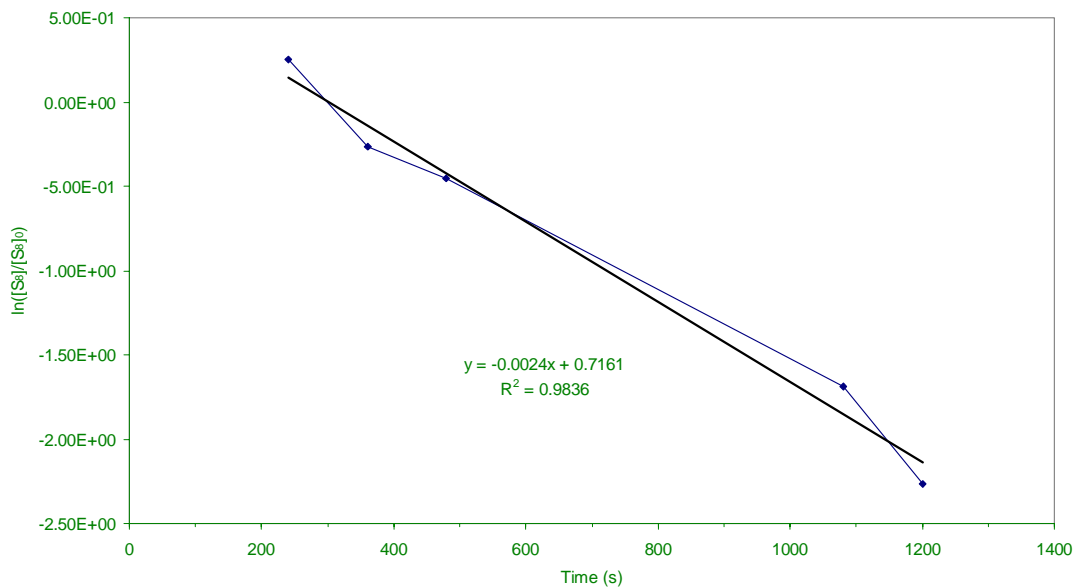


**Figure A.6:** Determination of the first order rate constant in relation to sulfur concentration data

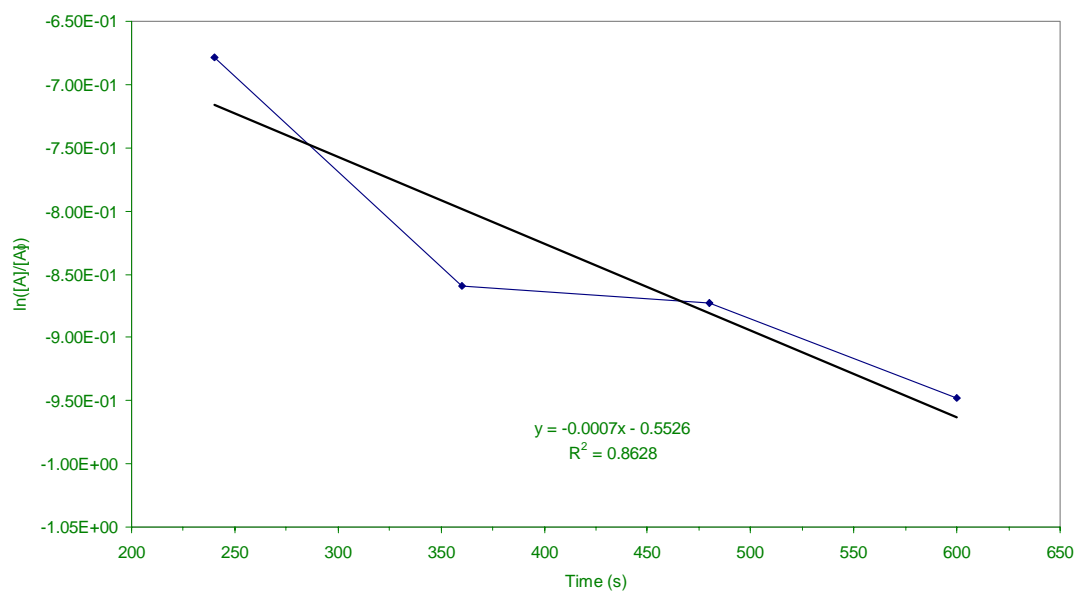


**Figure A.7:** Determination of the first order rate constant in relation to N,N'-diphenylthiuram disulfide concentration data (the letter A in the above graph represents the accelerator data)

# Appendix B

## Tetramethylthiuram disulfide

---

### List of figures

Figure B.1: $^1\text{H}$ -NMR spectrum for Tetramethylthiuram disulfide.....	206
Figure B.2: $^{13}\text{C}$ -NMR spectrum for Tetramethylthiuram disulfide.....	207
Figure B.3: IR spectrum for Tetramethylthiuram disulfide.....	208
Figure B.4: Determination of relative rate using the initial slope method in the tetramethylthiuram disulfide model compound reactions in relation to the sulfur concentration data.....	209
Figure B.5: Determination of relative rate using the initial slope method in relation to the tetramethylthiuram disulfide concentration data.....	209
Figure B.6: Determination of the first order rate constant for the tetramethylthiuram disulfide model compound reactions in relation to sulfur concentration data.....	210
Figure B.7: Determination of the first order rate constant in relation to the tetramethylthiuram disulfide concentration data.....	210
Figure B.8: Determination of the Coran rate constant ( $k_2$ ) constant from the rheometer data derived from the cure of tetramethylthiuram disulfide/ $S_8$ /IR system.....	211

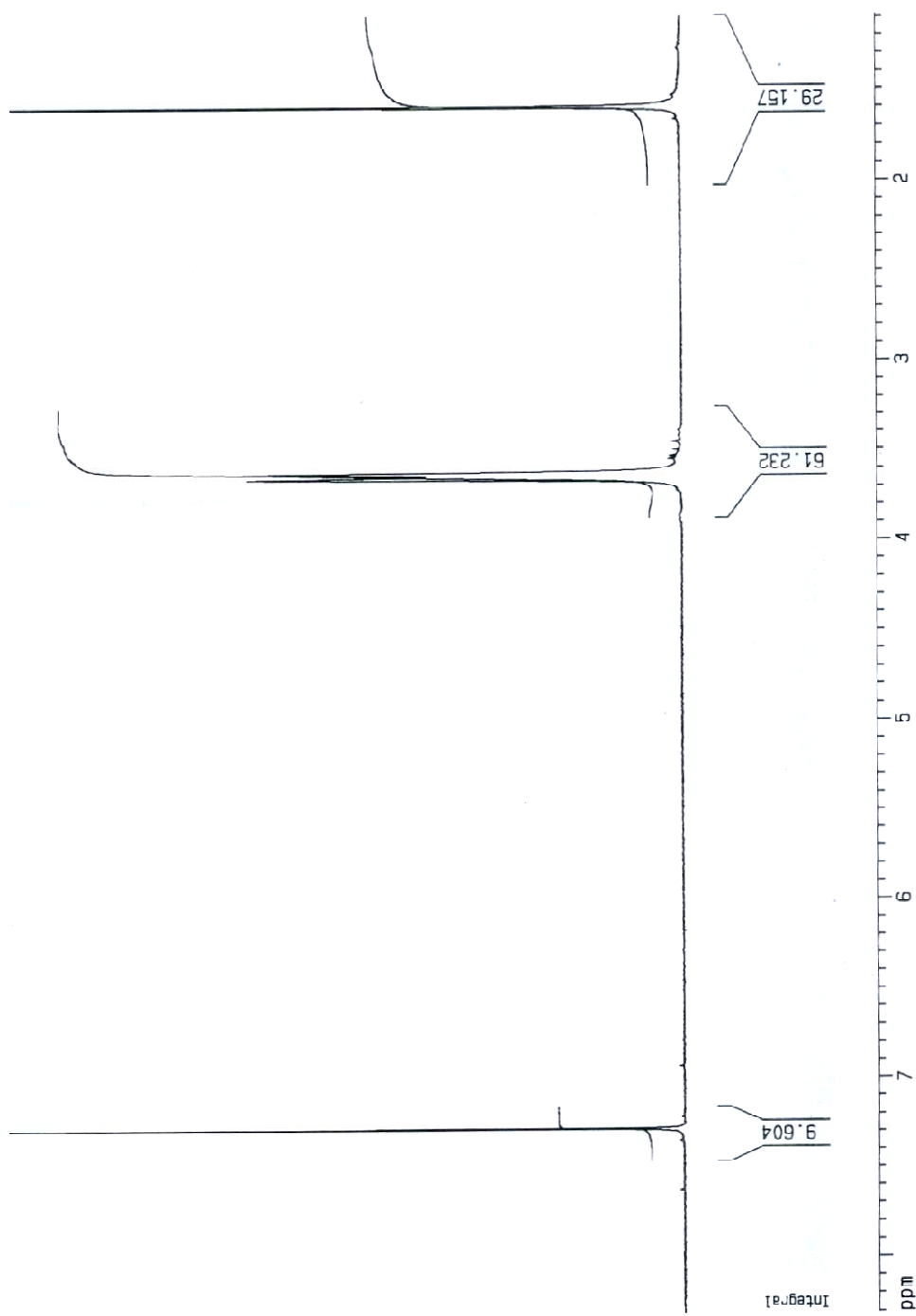


Figure B.1: <sup>1</sup>H-NMR spectrum for Tetramethylthiuram disulfide

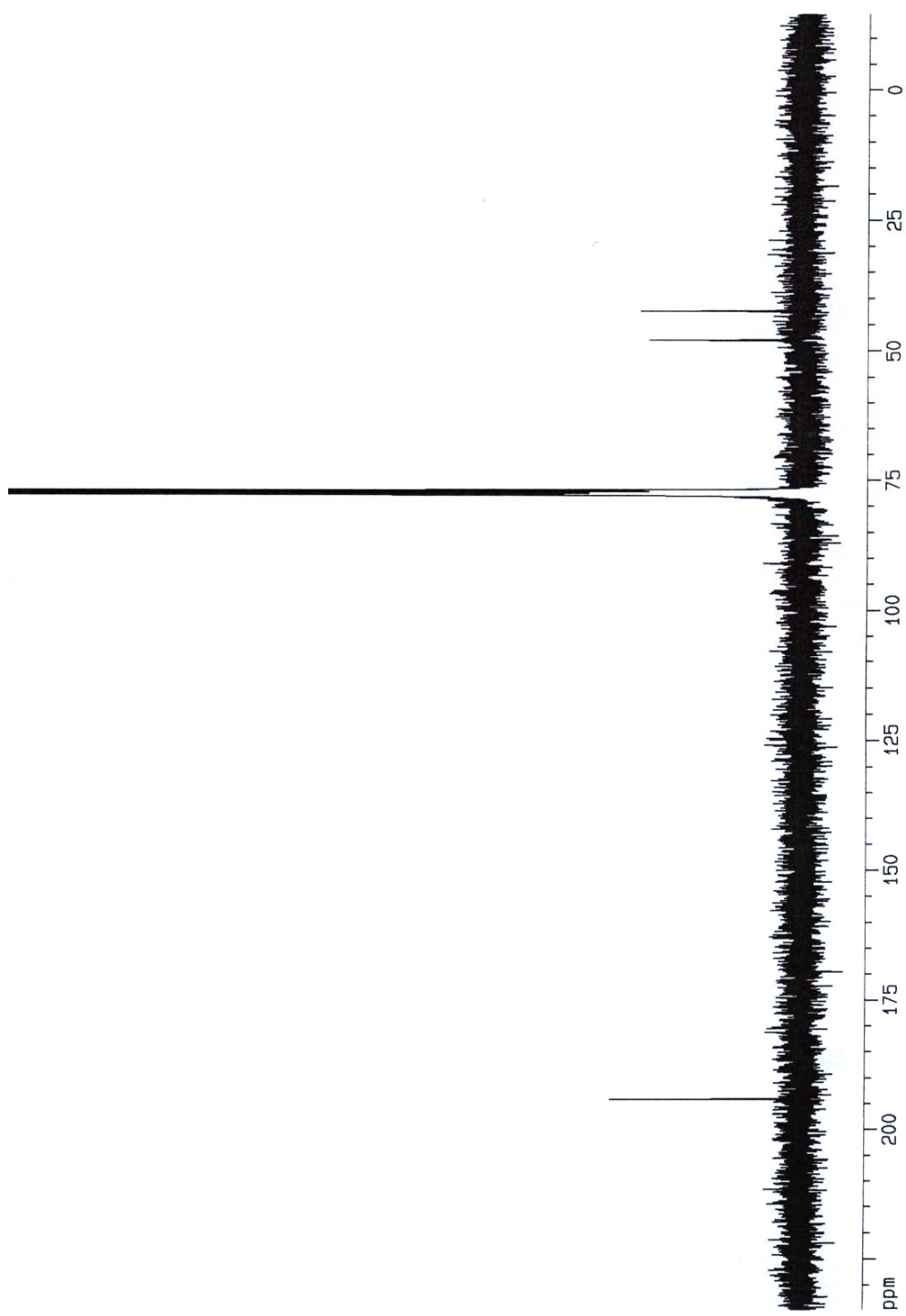


Figure B.2:  $^{13}\text{C}$ -NMR spectrum for Tetramethylthiuram disulfide

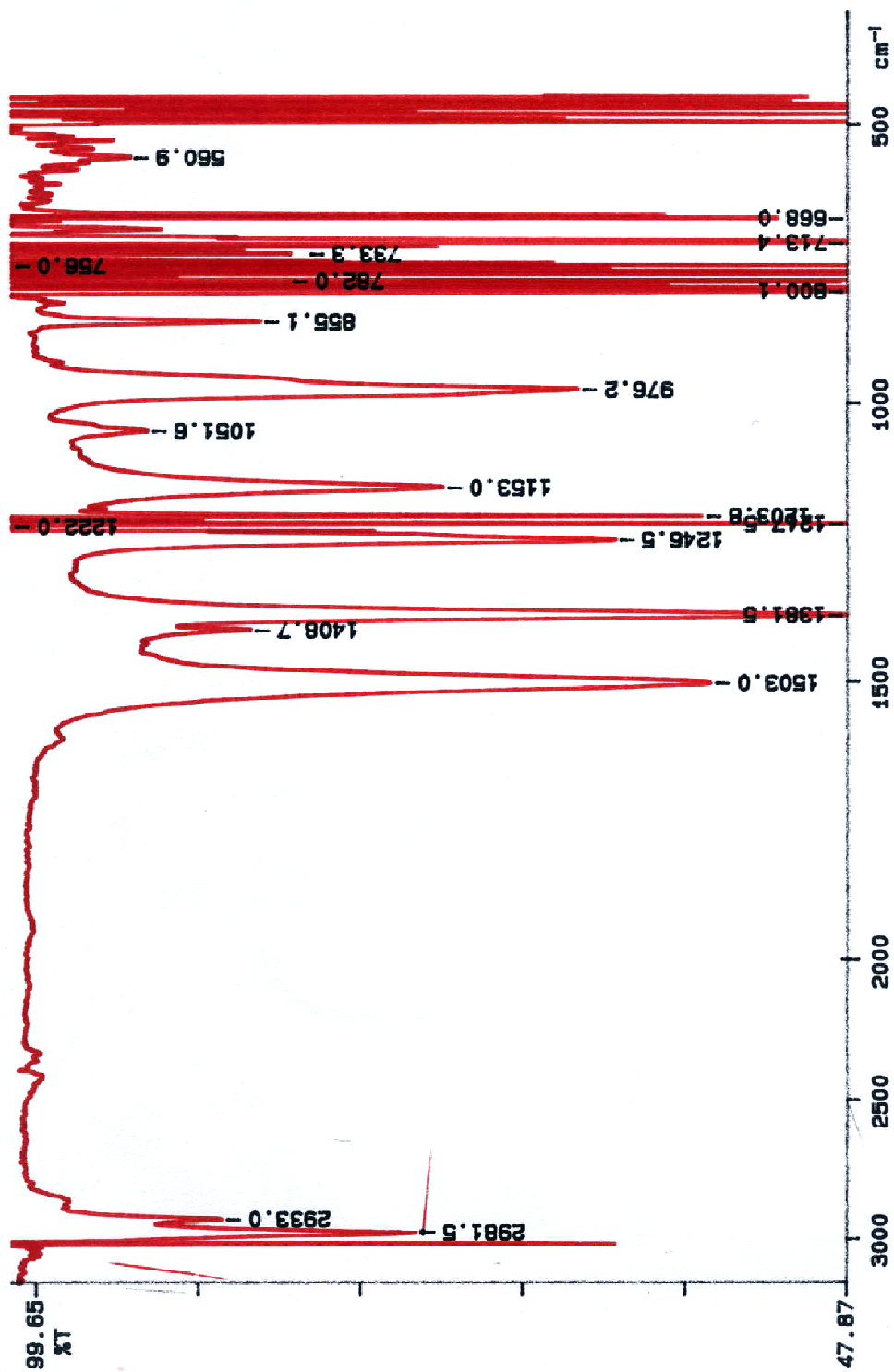
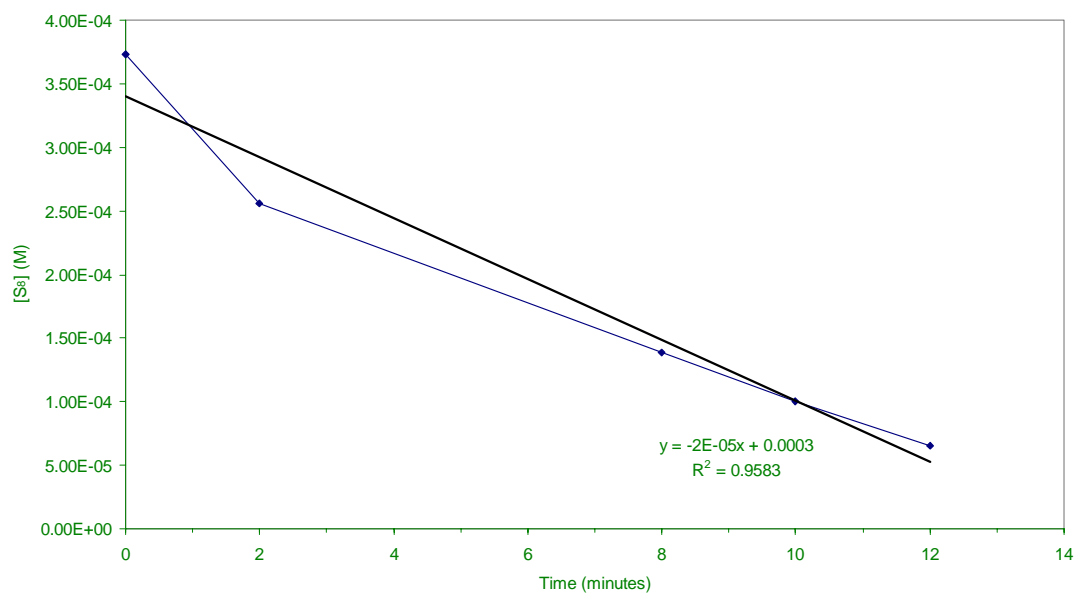
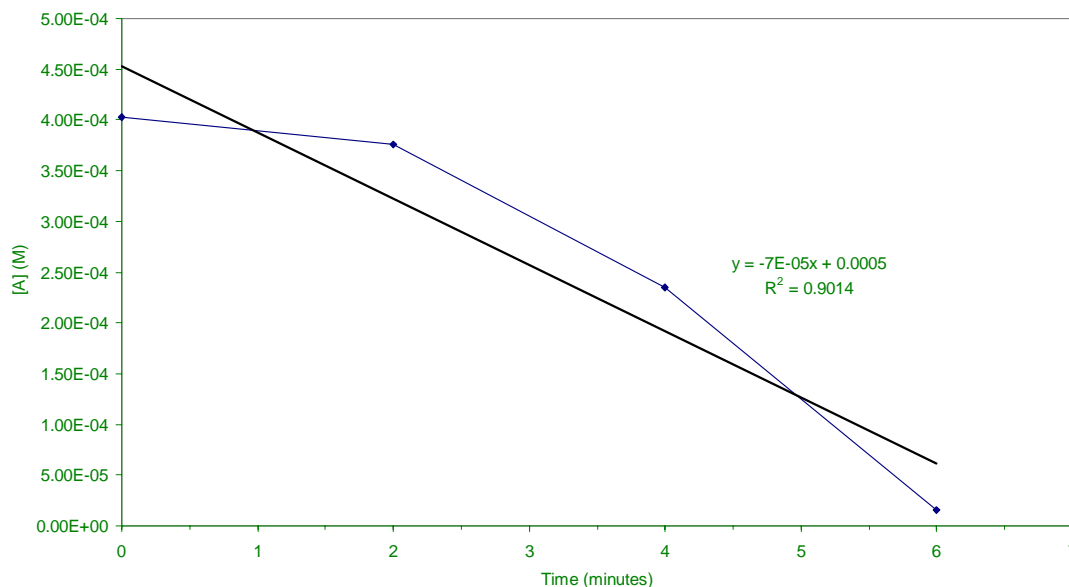


Figure B.3: IR spectrum for Tetramethylthiuram disulfide



**Figure B.4:** Determination of relative rate using the initial slope method in the tetramethylthiuram disulfide model compound reactions in relation to the sulfur concentration data



**Figure B.5:** Determination of relative rate using the initial slope method in relation to the tetramethylthiuram disulfide concentration data (the accelerator is represented by the letter A in the graph)

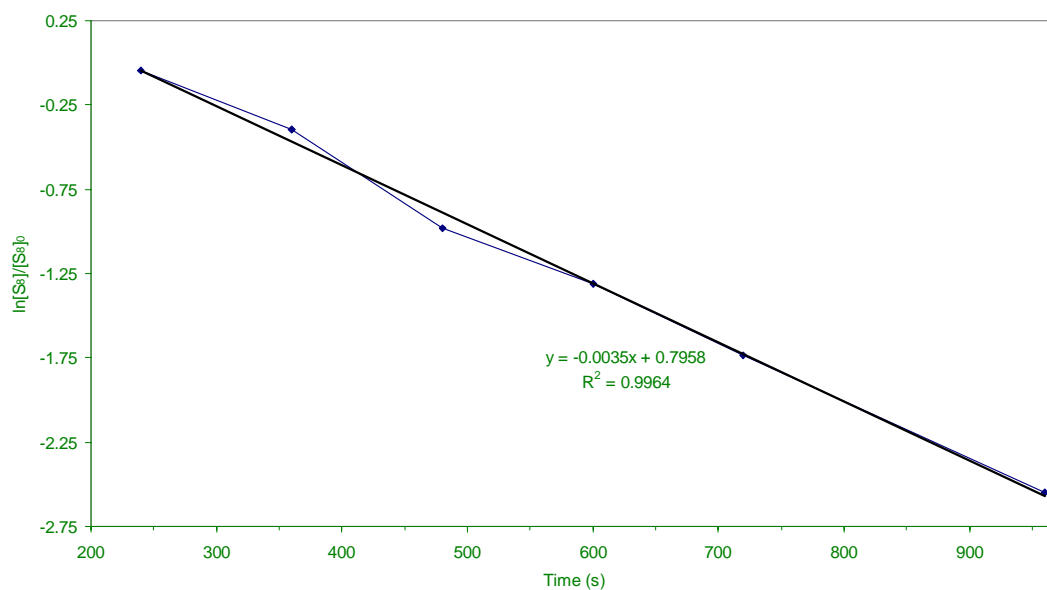


**Figure B.6:** Determination of the first order rate constant for the tetramethylthiuram disulfide model compound reactions in relation to sulfur concentration data

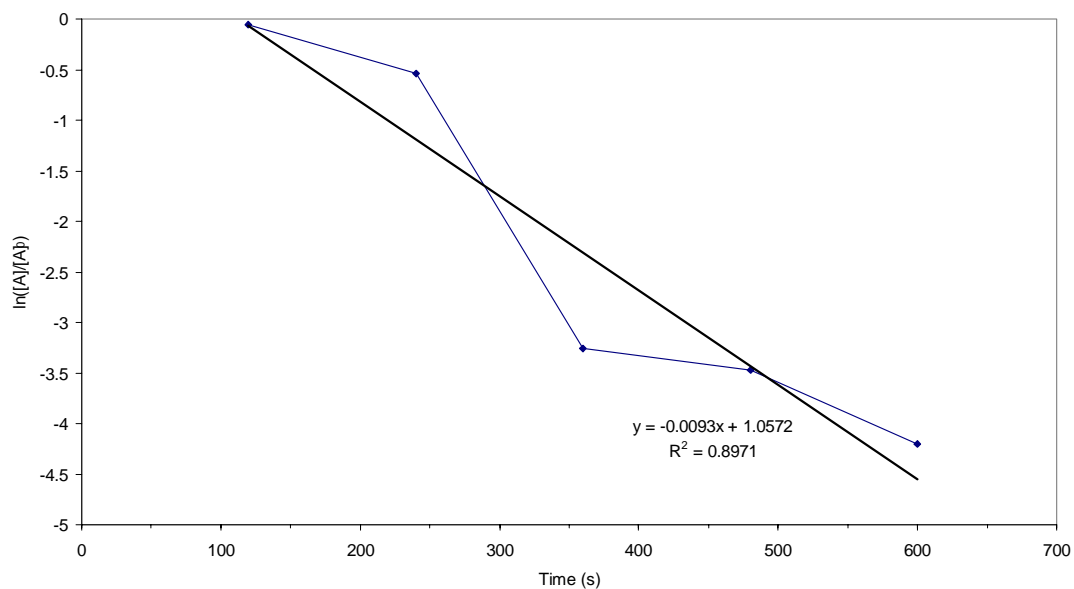


**Figure B.7:** Determination of the first order rate constant in relation to the tetramethylthiuram disulfide concentration data (the accelerator is represented by the letter A in the graph)

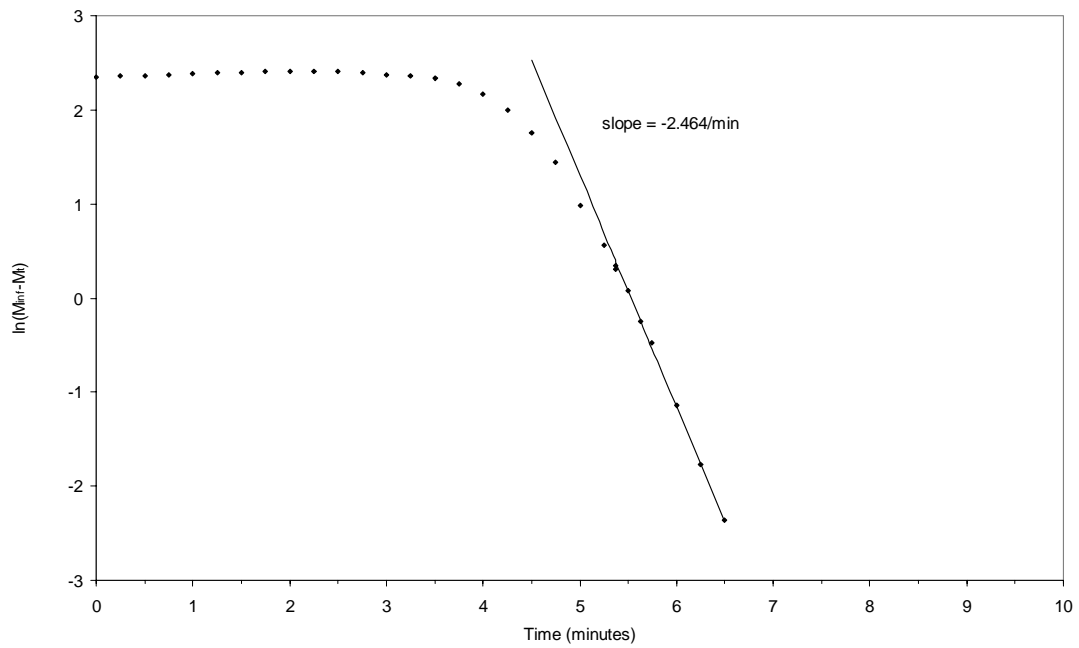


**Figure B.8:** Determination of the Coran rate constant ( $k_2$ ) constant from the rheometer data derived from the cure of tetramethylthiuram disulfide/ $S_8$ /IR system



# Appendix C

## Tetraethylthiuram disulfide

---

### List of figures

Figure C.1: $^1\text{H}$ -NMR spectrum for Tetraethylthiuram disulfide.....	213
Figure C.2: $^{13}\text{C}$ -NMR spectrum for Tetraethylthiuram disulfide.....	214
Figure C.3: IR spectrum for Tetraethylthiuram disulfide.....	215
Figure C.4: Determination of relative rate using the initial slope method in the tetraethylthiuram disulfide model compound reactions in relation to the sulfur concentration data.....	216
Figure C.5: Determination of relative rate using the initial slope method in relation to the tetraethylthiuram disulfide concentration data.....	216
Figure C.6: Determination of the first order rate constant for the tetraethylthiuram disulfide model compound reactions in relation to sulfur concentration data.....	217
Figure C.7: Determination of the first order rate constant in relation to the tetraethylthiuram disulfide concentration data.....	217

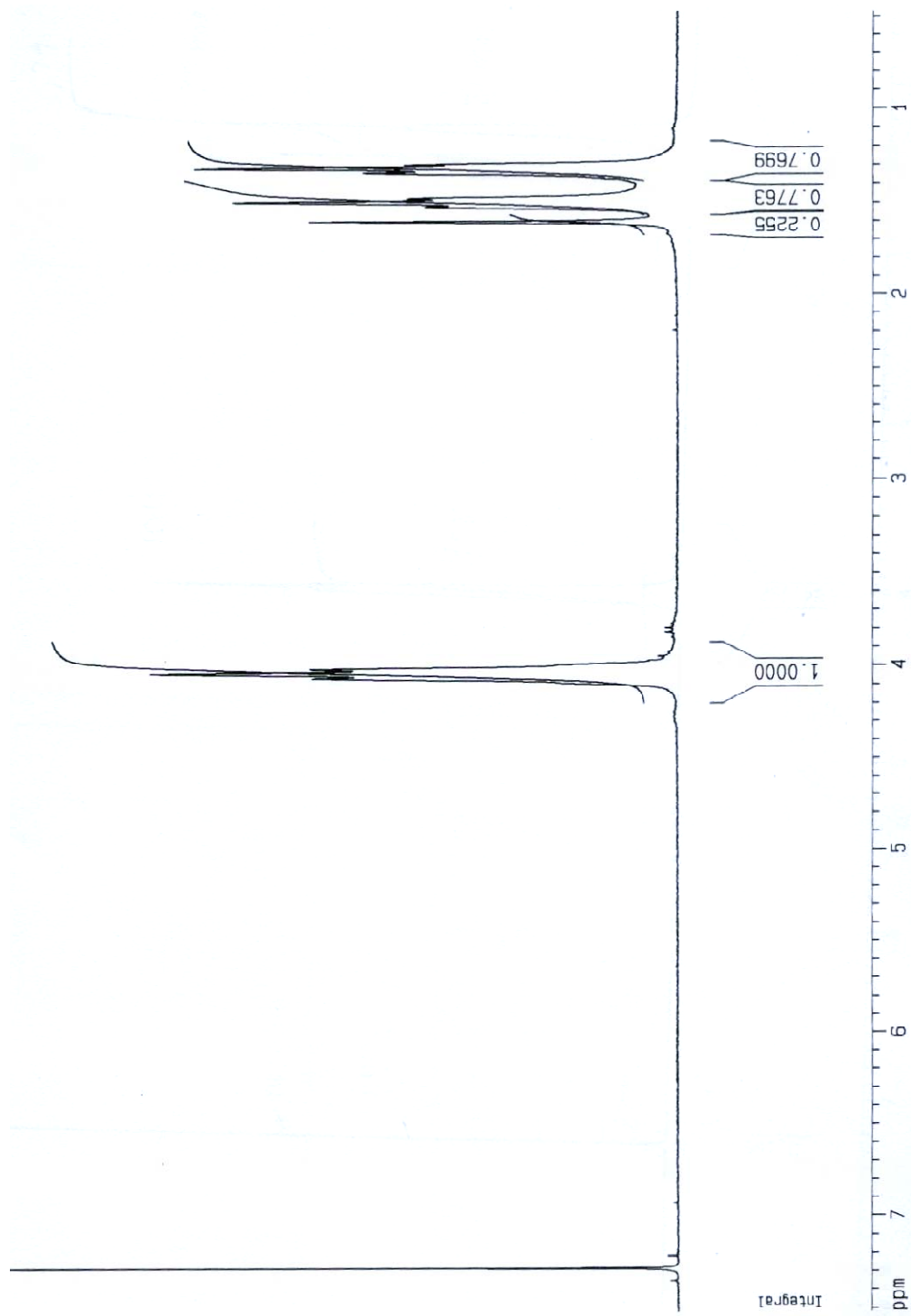


Figure C.1: <sup>1</sup>H-NMR spectrum for Tetraethylthiuram disulfide

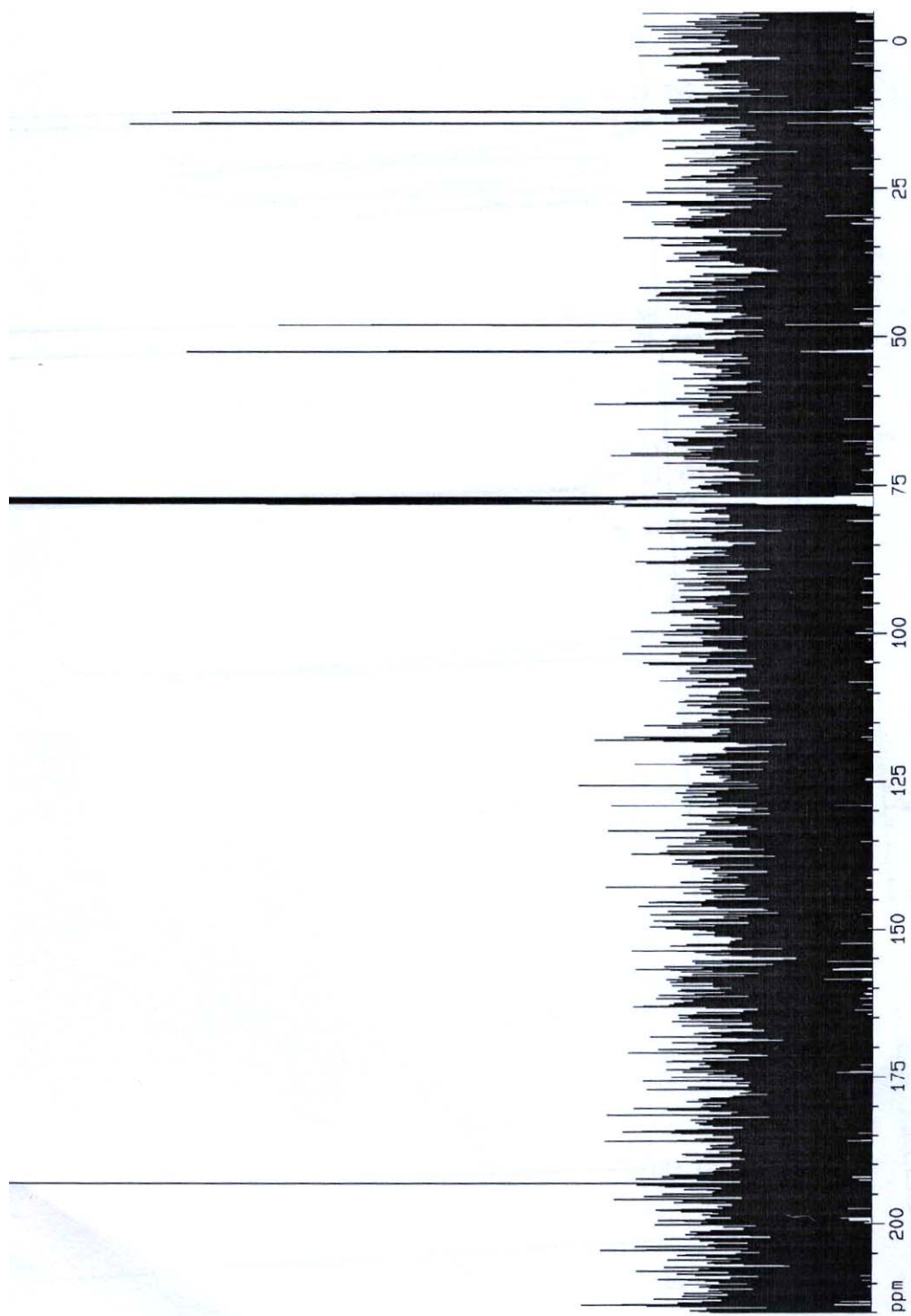


Figure C.2:  $^{13}\text{C}$ -NMR spectrum for Tetraethylthiuram disulfide

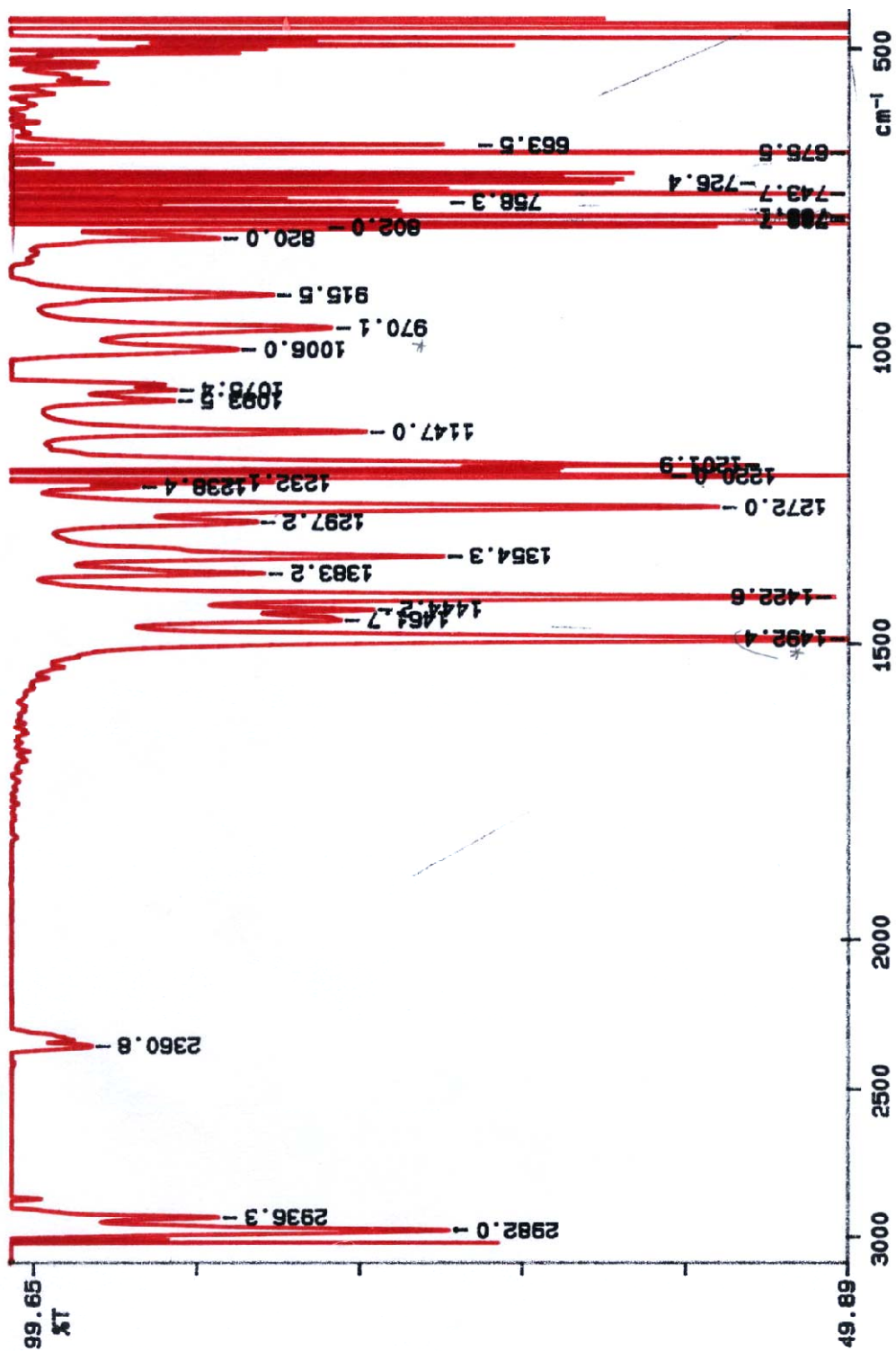
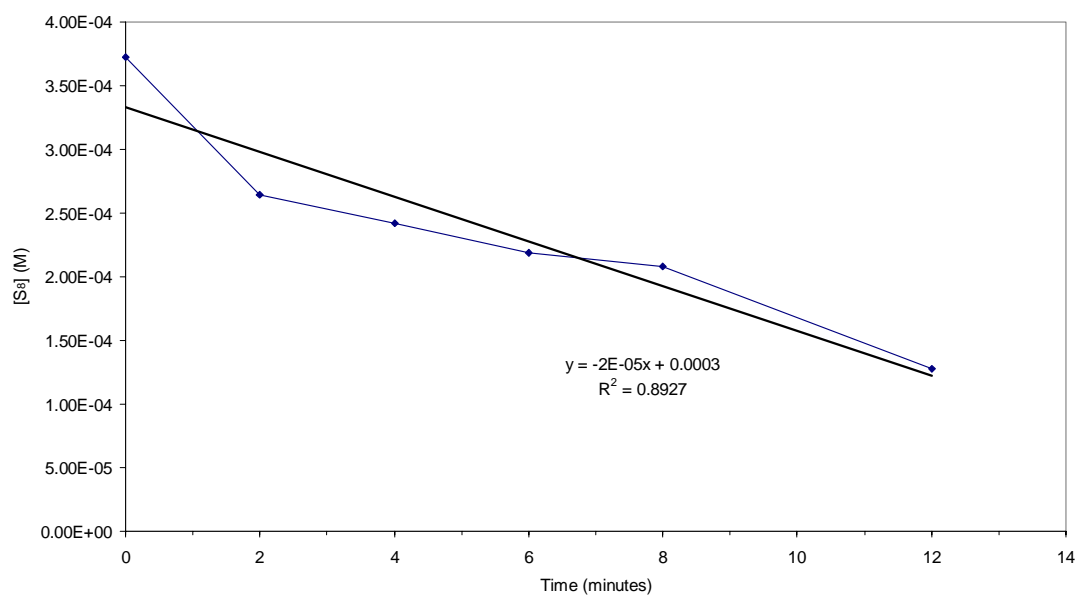
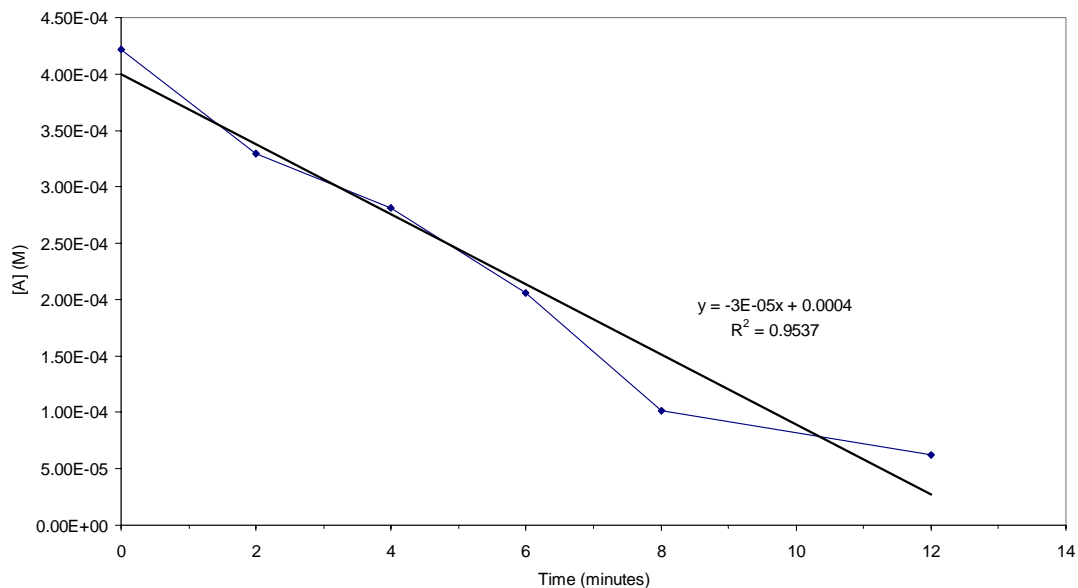


Figure C.3: IR spectrum for Tetraethylthiuram disulfide



**Figure C.4:** Determination of relative rate using the initial slope method in the tetraethylthiuram disulfide model compound reactions in relation to the sulfur concentration data



**Figure C.5:** Determination of relative rate using the initial slopes method in relation to the tetraethylthiuram disulfide concentration data (the accelerator is represented by the letter A in the graph)

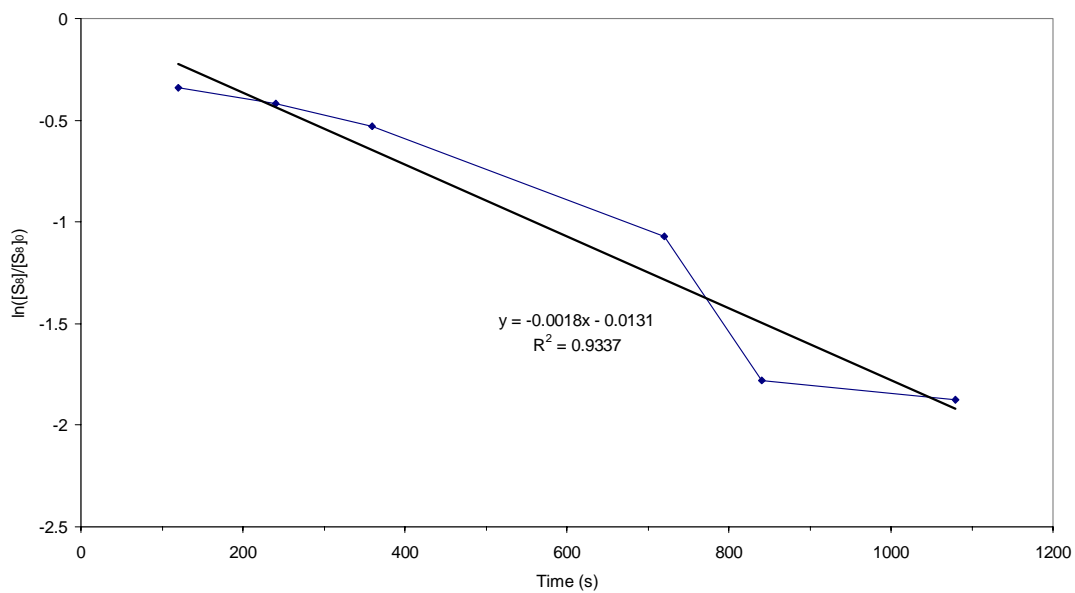


**Figure C.6:** Determination of the first order rate constant for the tetraethylthiuram disulfide model compound reactions in relation to sulfur concentration data

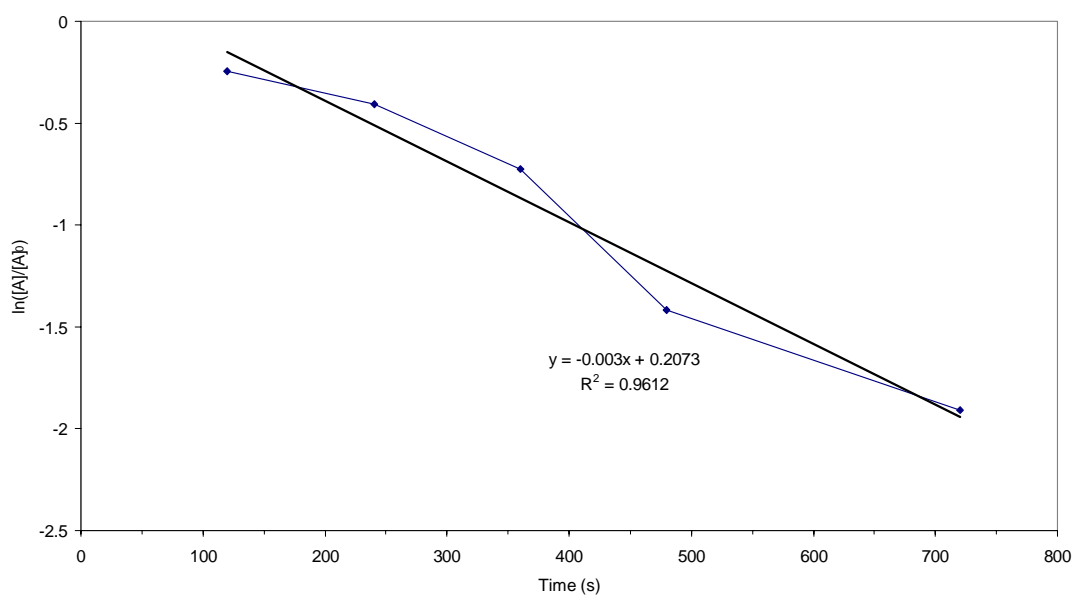


**Figure C.7:** Determination of the first order rate constant in relation to the tetraethylthiuram disulfide concentration data (the accelerator is represented by the letter A in the graph)

# Appendix D

## N,N'-dicyclopentamethylenethiuram disulfide

---

### List of figures

Figure D.1: <sup>1</sup> H-NMR spectrum for N,N'-dicyclopentamethylenethiuram disulfide.....	219
Figure D.2: <sup>13</sup> C-NMR spectrum for N,N'-dicyclopentamethylenethiuram disulfide.....	220
Figure D.3: IR spectrum for N,N'-dicyclopentamethylenethiuram disulfide.....	221
Figure D.4: Determination of relative rate using the initial slope method in the N,N'-dicyclopentamethylenethiuram disulfide model compound reactions in relation to the sulfur concentration data.....	222
Figure D.5: Determination of relative rate using the initial slope method in relation to the N,N'-dicyclopentamethylenethiuram disulfide concentration data.....	222
Figure D.6: Determination of the first order rate constant for the N,N'-dicyclopentamethylenethiuram disulfide model compound reactions in relation to sulfur concentration data.....	223
Figure D.7: Determination of the first order rate constant in relation to N,N'-dicyclopentamethylenethiuram disulfide concentration data.....	223
Figure D.8: Determination of the Coran rate constant ( $k_2$ ) constant from the rheometer data derived from the cure of N,N'-dicyclopentamethylenethiuram disulfide/S <sub>8</sub> /IR system.....	224

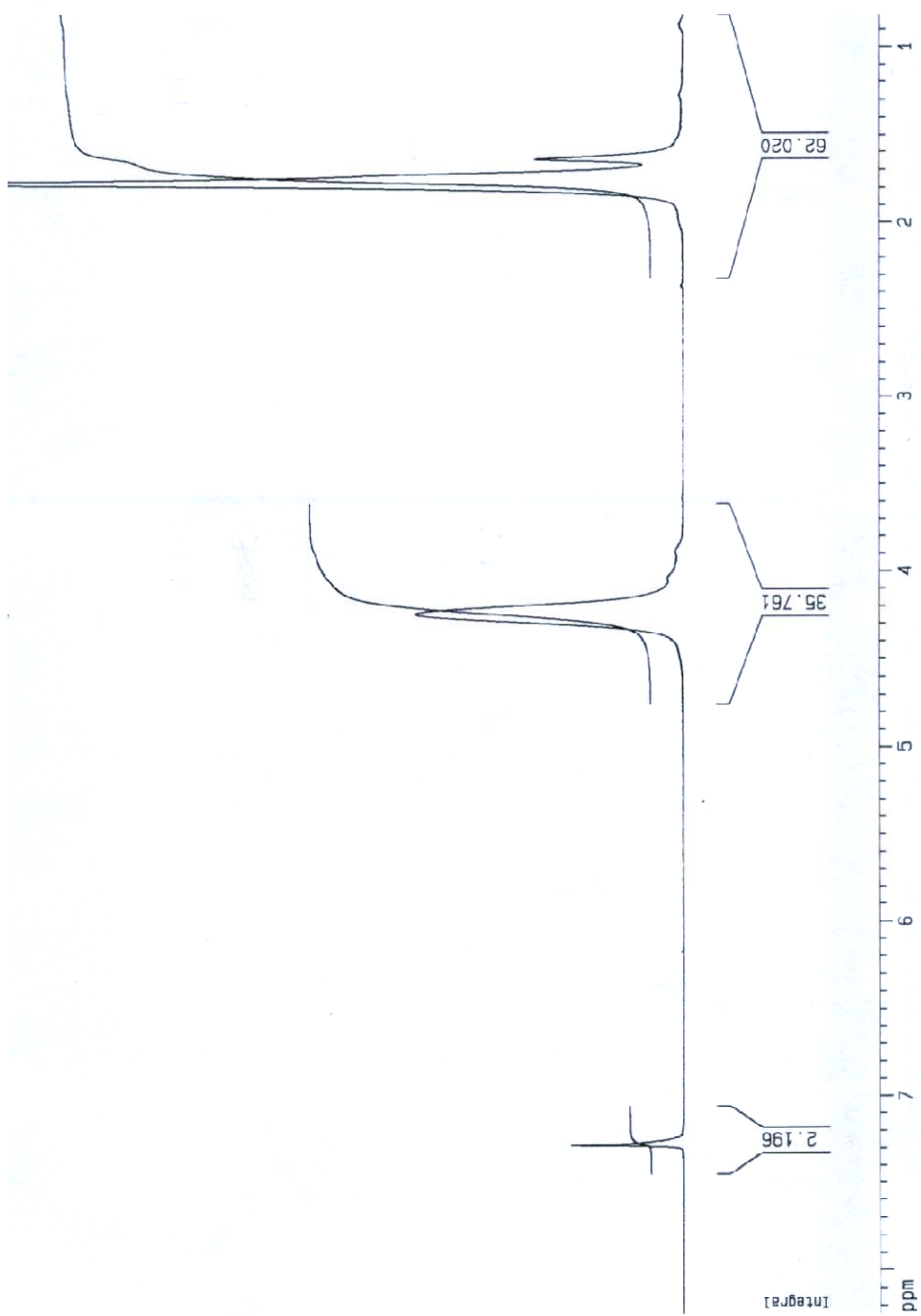


Figure D.1: 1H-NMR spectrum for N,N'-dicyclopentamethylenethiuram disulfide



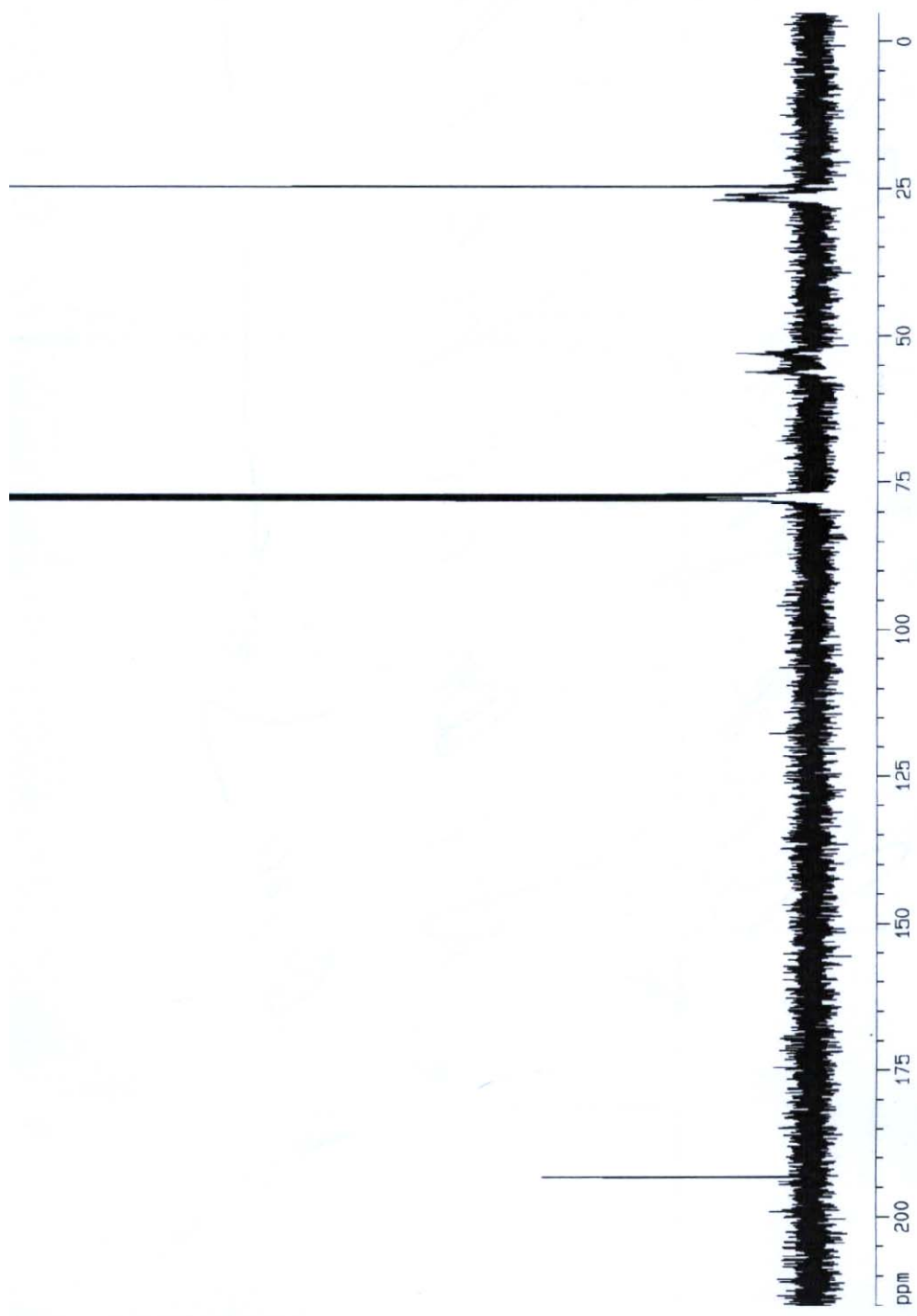


Figure D.2:  $^{13}\text{C}$ -NMR spectrum for N,N'-dicyclopentamethylenethiuram disulfide

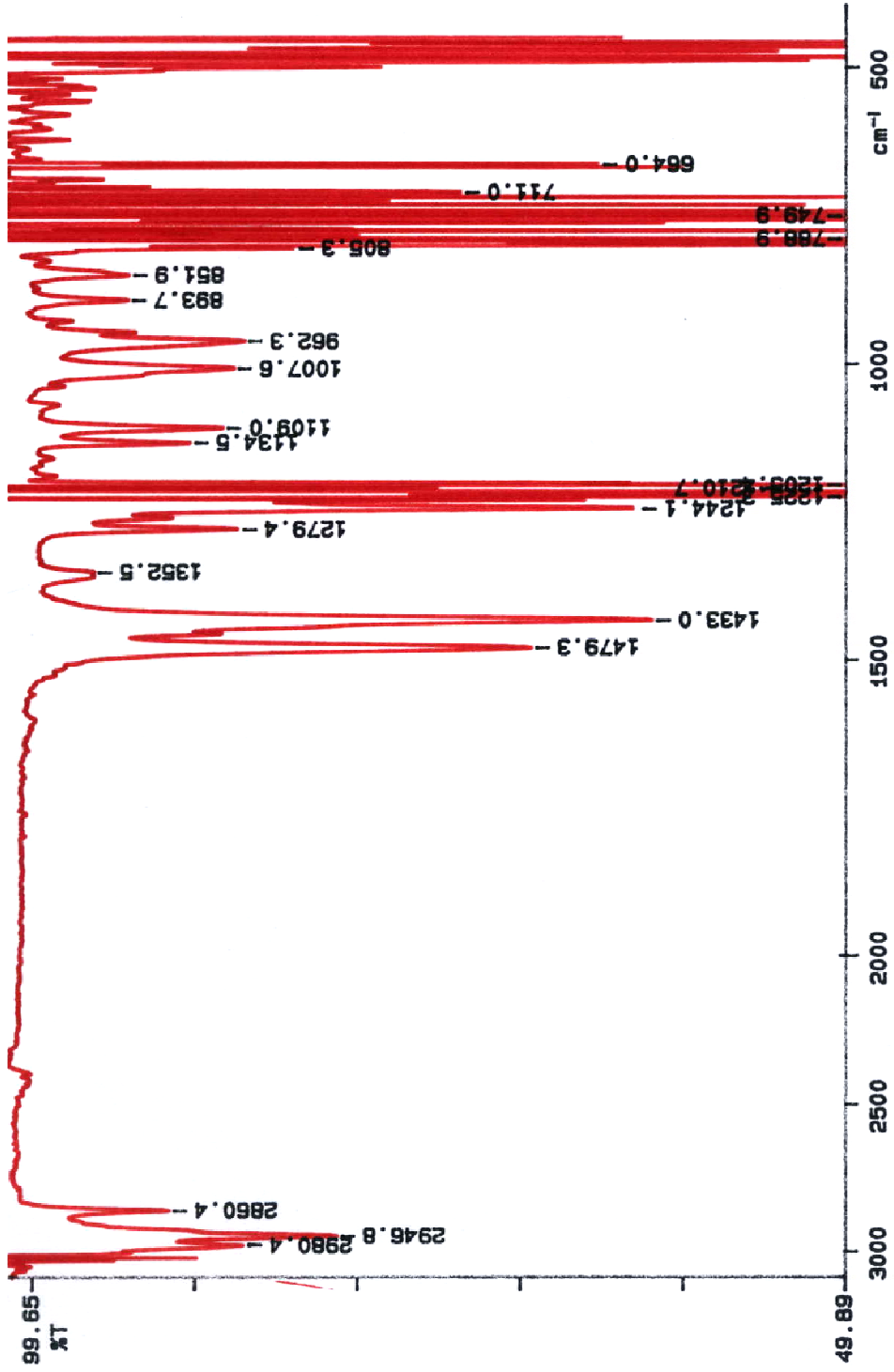
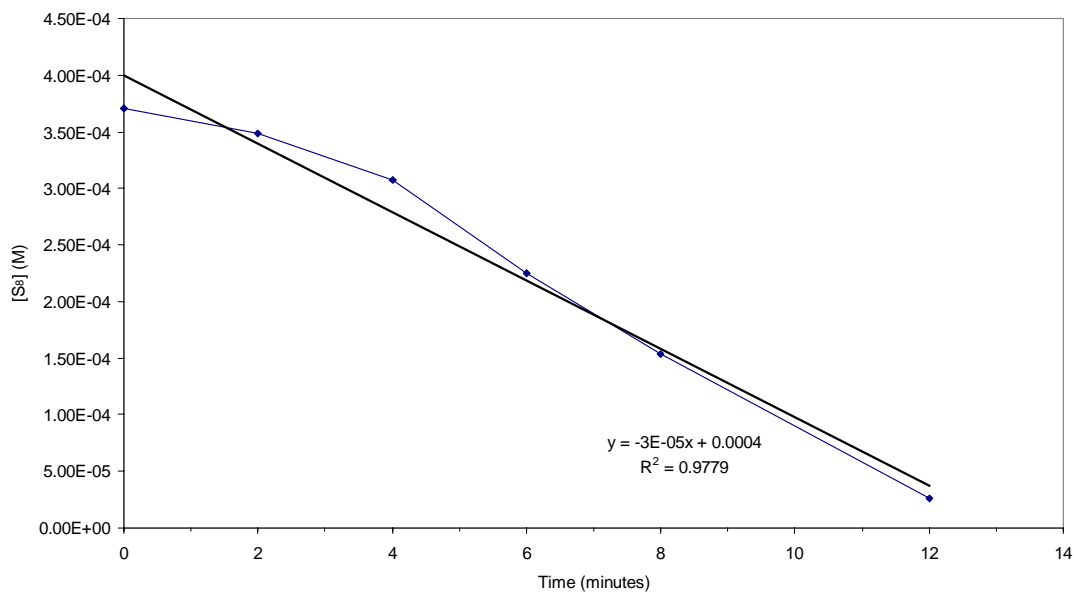
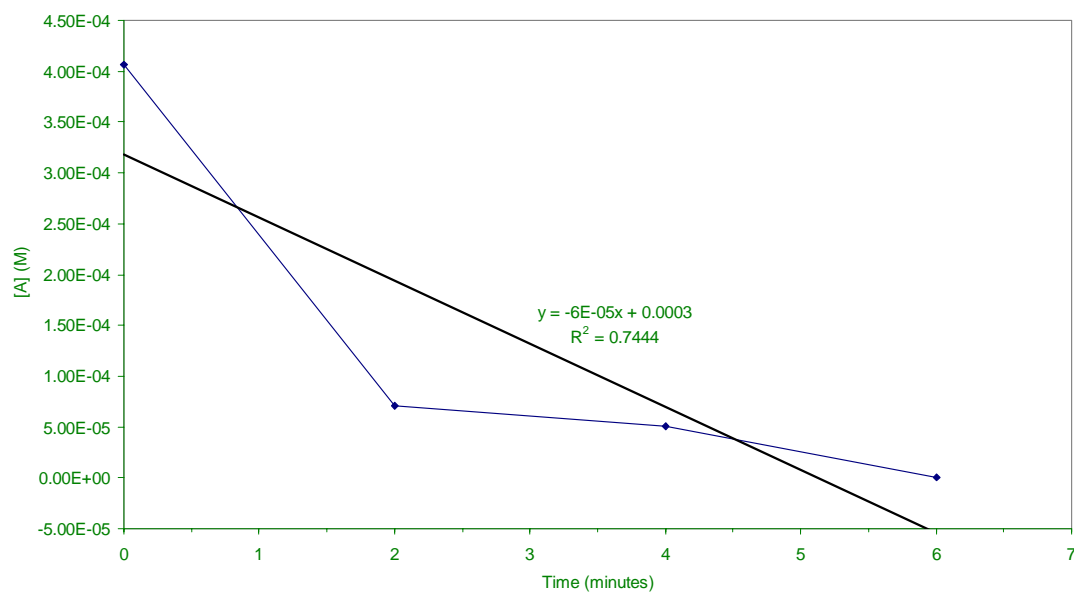


Figure D.3: IR spectrum for N,N'-dicyclopentamethylenethiuram disulfide



**Figure D.4:** Determination of relative rate using the initial slope method in the N,N'-dicyclopentamethylenethiuram disulfide model compound reactions in relation to the sulfur concentration data



**Figure D.5:** Determination of relative rate using the initial slope method in relation to the N,N'-dicyclopentamethylenethiuram disulfide concentration data

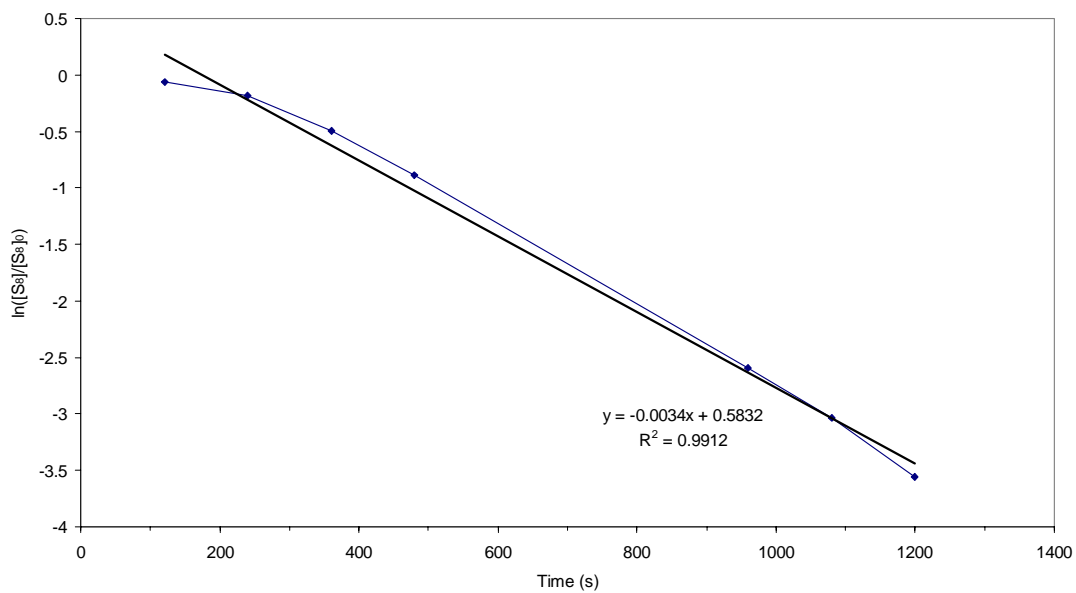


**Figure D.6:** Determination of the first order rate constant for the N,N'-dicyclopentamethylenethiuram disulfide model compound reactions in relation to sulfur concentration data

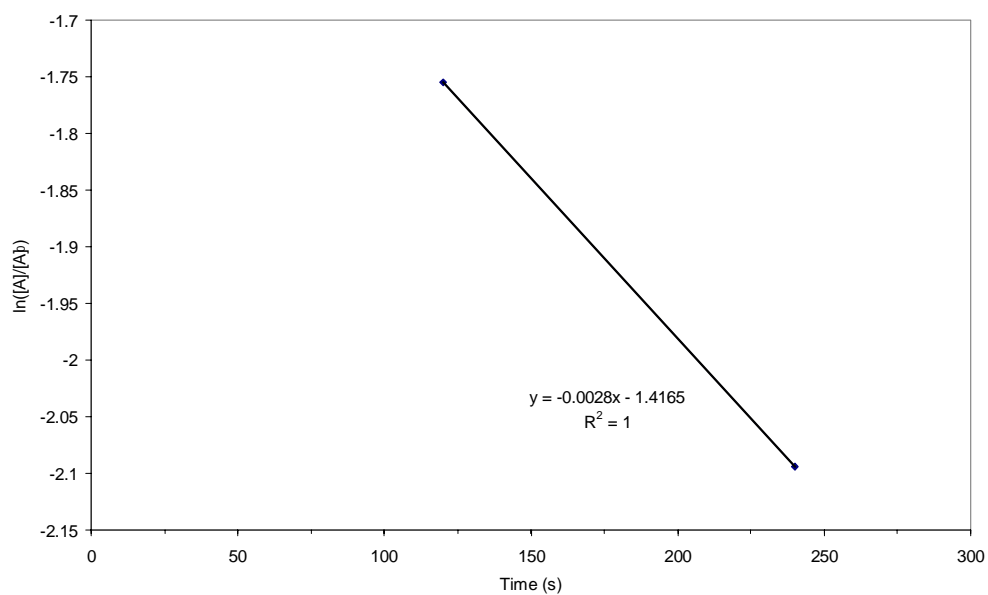


**Figure D.7:** Determination of the first order rate constant in relation to N,N'-dicyclopentamethylenethiuram disulfide concentration data (the accelerator is represented by the letter A in the graph)

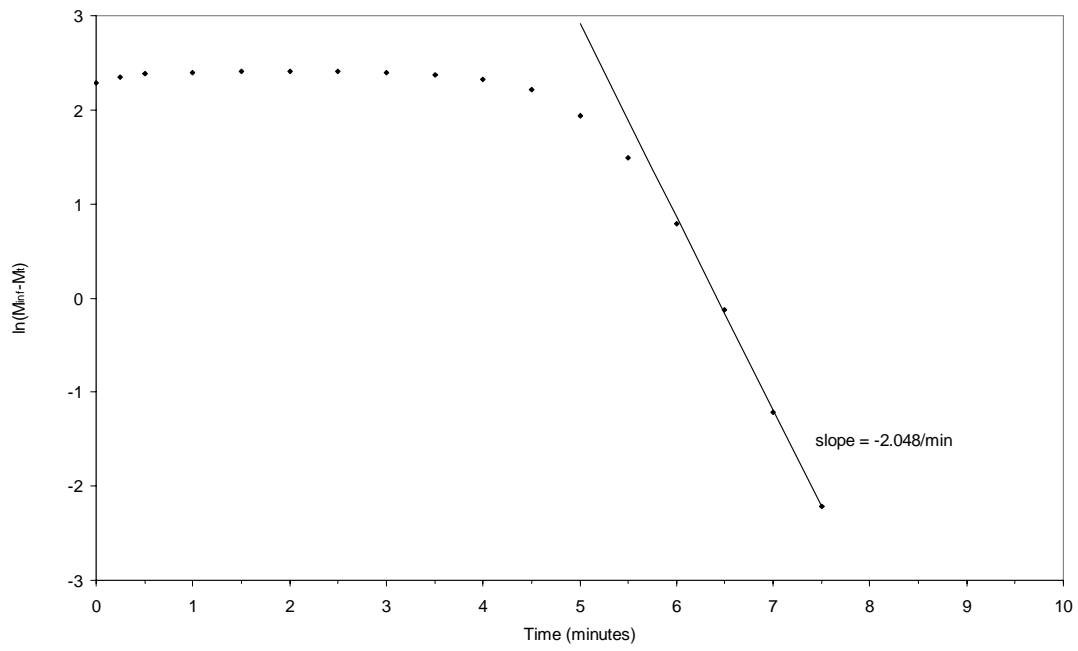


**Figure D.8:** Determination of the Coran rate constant ( $k_2$ ) constant from the rheometer data derived from the cure of N,N'-dicyclopentamethylenethiuram disulfide/ $S_8$ /IR system

# Appendix E

## N,N'-Bis( $\sigma$ -methoxyphenyl)thiuram disulfide

---

### List of figures

Figure E.1: $^1\text{H}$ -NMR spectrum for N,N'-Bis( $\sigma$ -methoxyphenyl)thiuram disulfide.....	226
Figure E.2: $^{13}\text{C}$ -NMR spectrum for N,N'-Bis( $\sigma$ -methoxyphenyl)thiuram disulfide.....	227
Figure E.3: IR spectrum for N,N'-Bis( $\sigma$ -methoxyphenyl)thiuram disulfide.....	228
Figure E.4: Determination of relative rate using the initial slope method in relation to the sulfur concentration data.....	229
Figure E.5: Determination of relative rate using the initial slope method in relation to the N,N'-bis( $\sigma$ -methoxyphenyl)thiuram disulfide concentration data.....	229
Figure E.6: Determination of the first order rate constant for the N,N'-bis( $\sigma$ -methoxyphenyl)thiuram disulfide model compound reactions in relation to sulfur concentration data.....	230
Figure E.7: Determination of the first order rate constant in relation to N,N'-bis( $\sigma$ -methoxyphenyl)thiuram disulfide concentration data.....	230
Figure E.8: Determination of the Coran rate constant ( $k_2$ ) constant from the rheometer data derived from the cure of N,N'-Bis( $\sigma$ -methoxyphenyl)thiuram disulfide/ $\text{S}_8$ /IR system.....	231

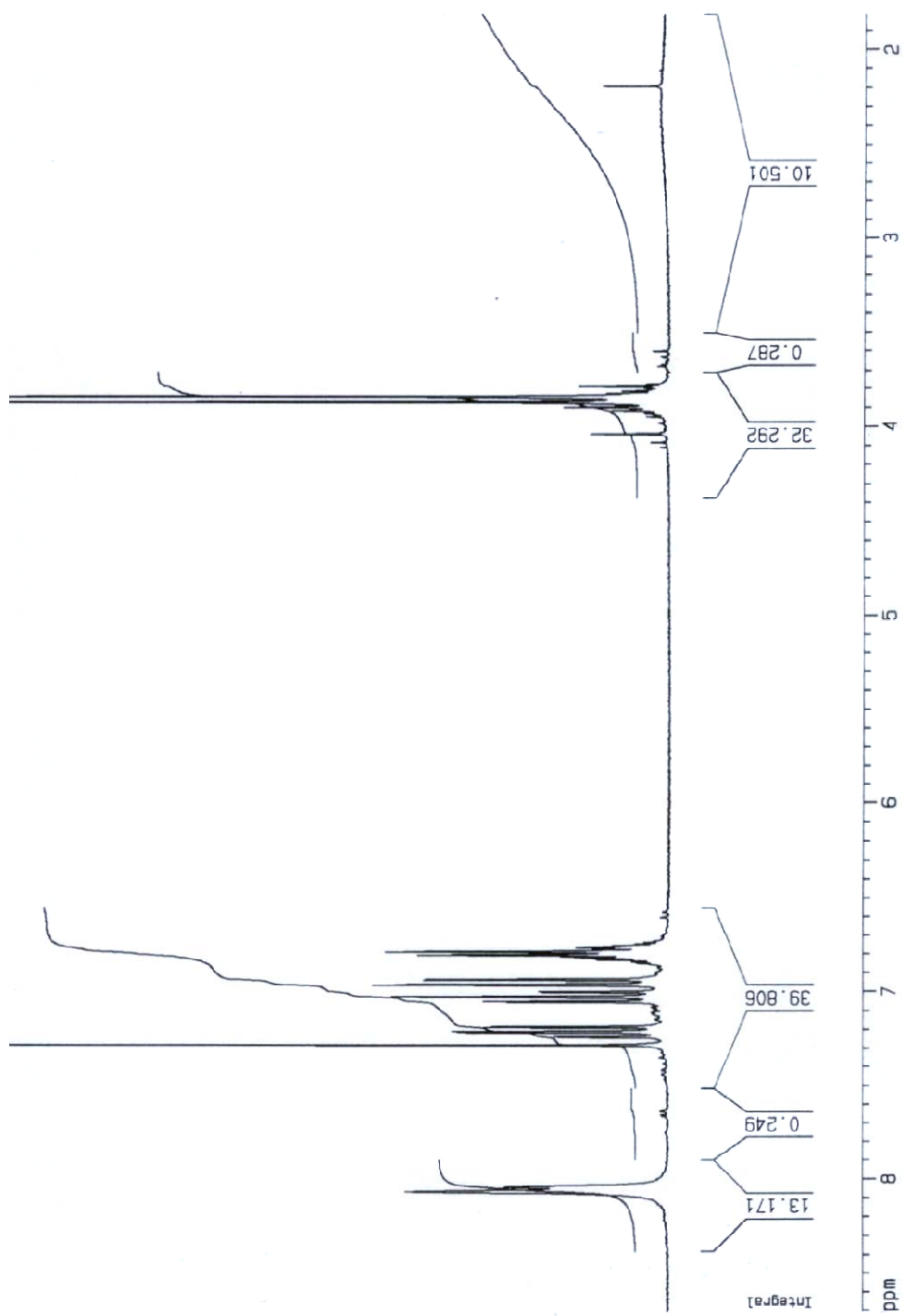


Figure E.1: 1H-NMR spectrum for N,N'-Bis(σ-methoxyphenyl)thiuram disulfide

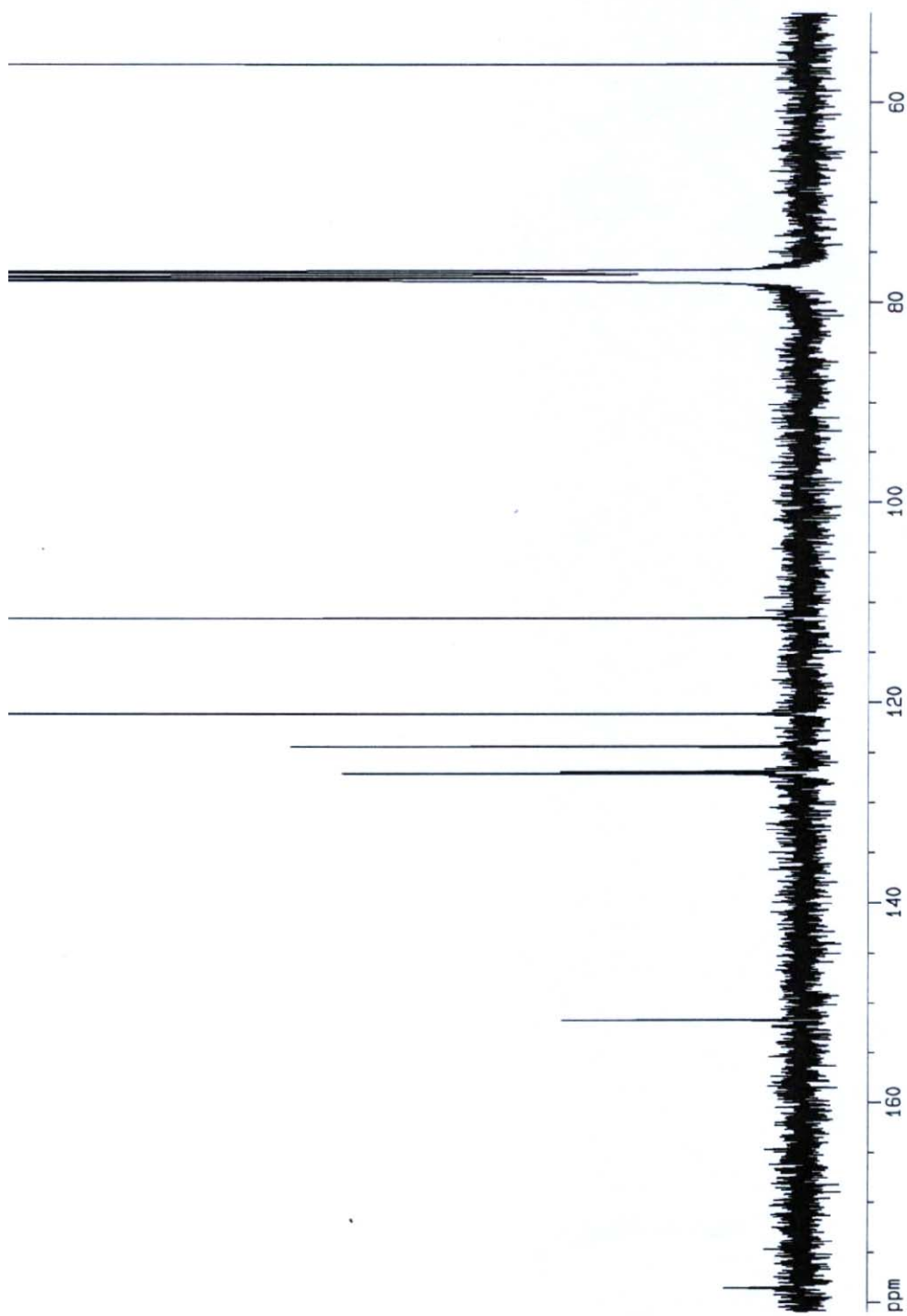


Figure E.2:  $^{13}\text{C}$ -NMR spectrum for  $\text{N,N}'\text{-Bis}(\sigma\text{-methoxyphenyl})\text{thiuram disulfide}$



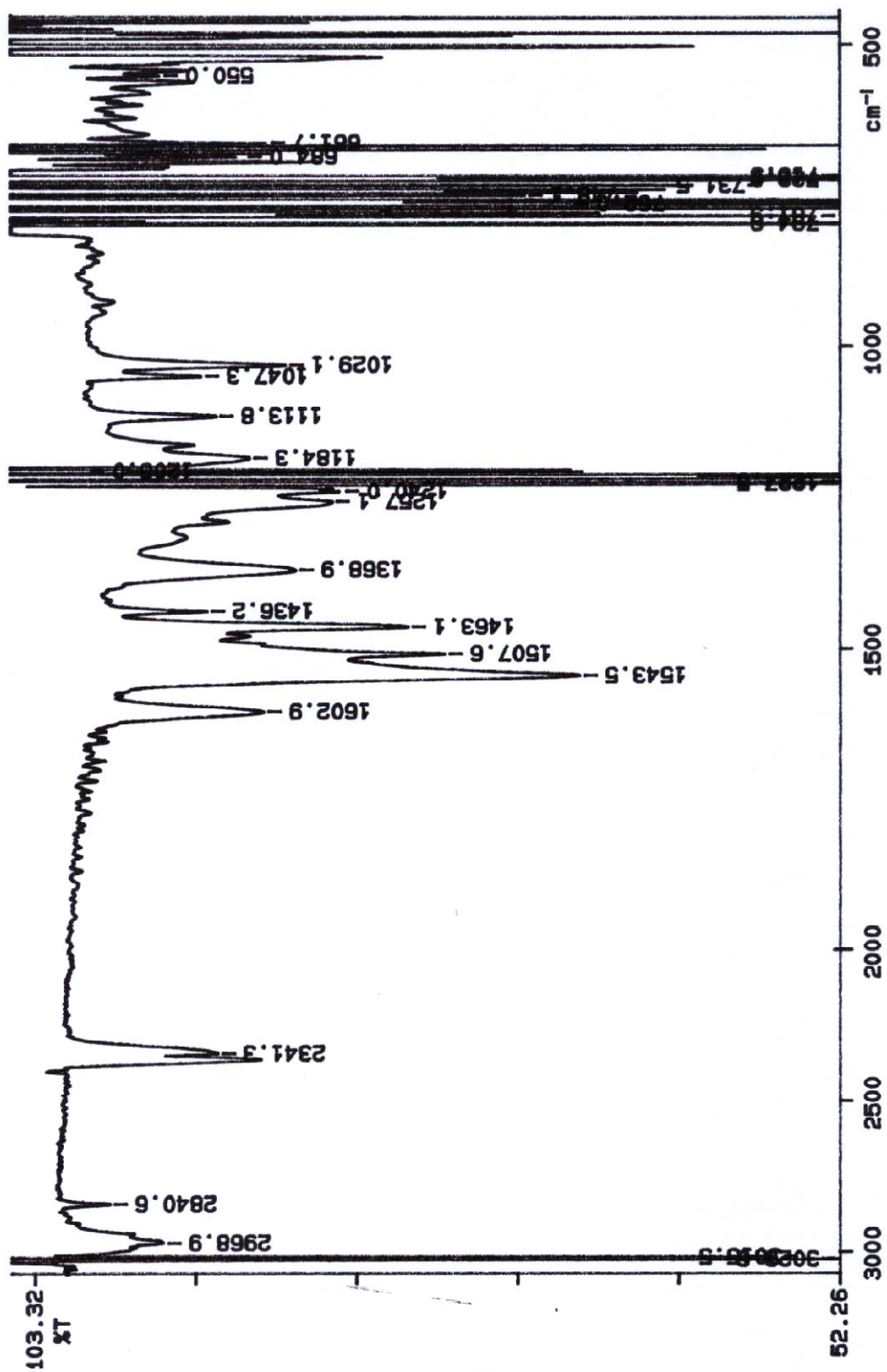
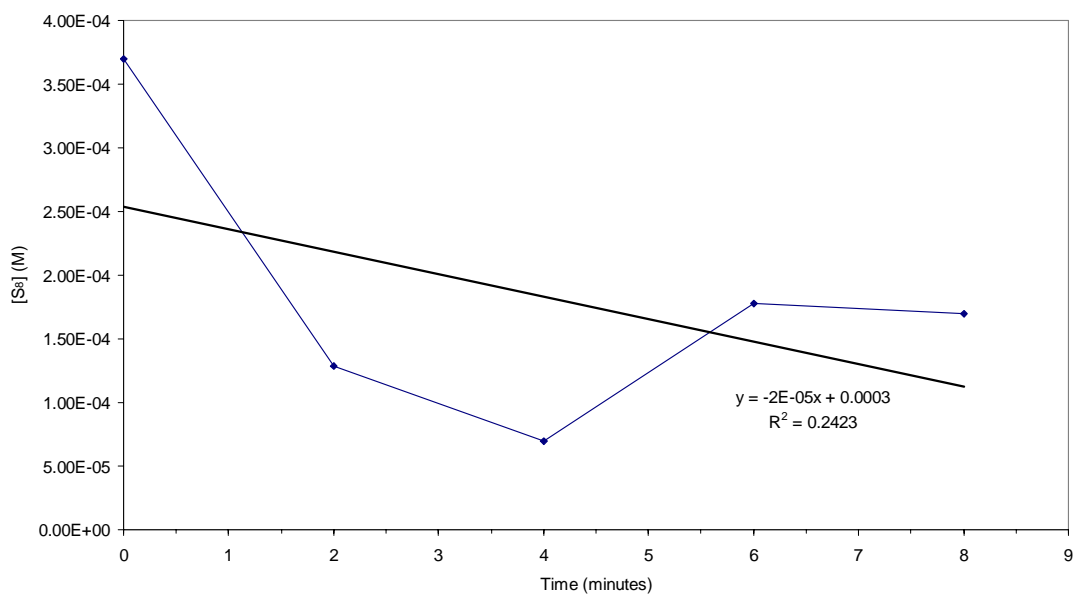
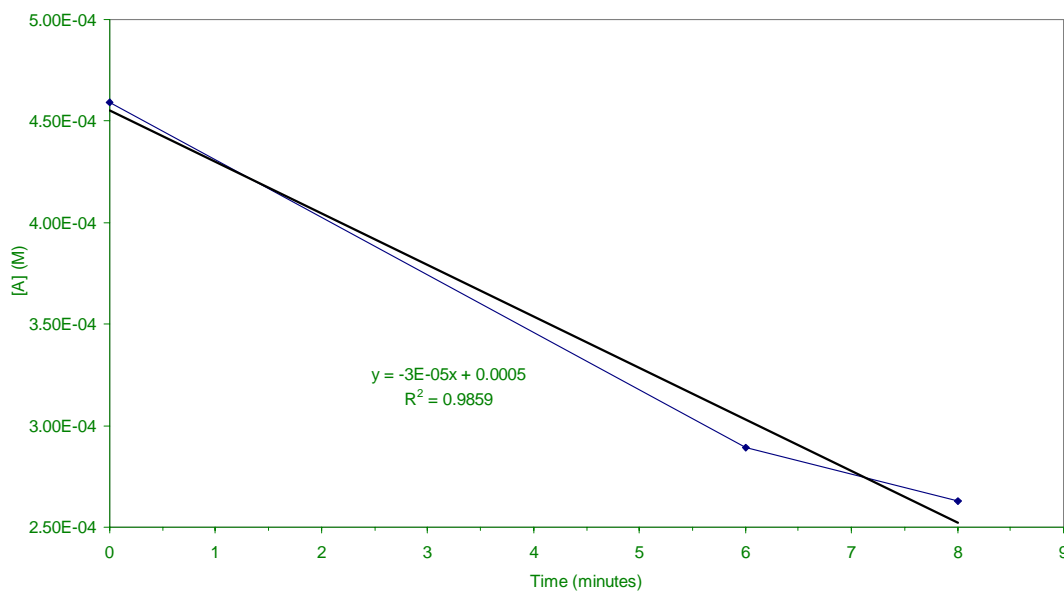


Figure E.3: IR spectrum for N,N'-Bis( $\sigma$ -methoxyphenyl)thiuram disulfide



**Figure E 4:** Determination of relative rate using the initial slope method in relation to the sulfur concentration data



**Figure E 5:** Determination of relative rate using the initial slope method in relation to the N,N'-bis( $\sigma$ -methoxyphenyl)thiuram disulfide concentration data (the letter A represents the accelerator in the above figure)

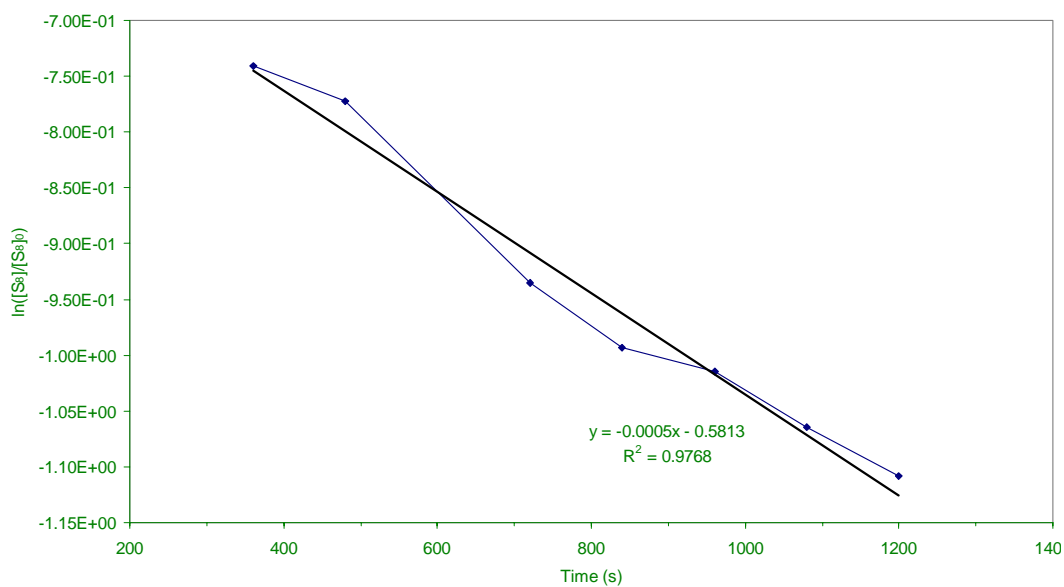


**Figure E 6:** Determination of the first order rate constant for the  $N,N'$ -bis( $\sigma$ -methoxyphenyl)thiuram disulfide model compound reactions in relation to sulfur concentration data

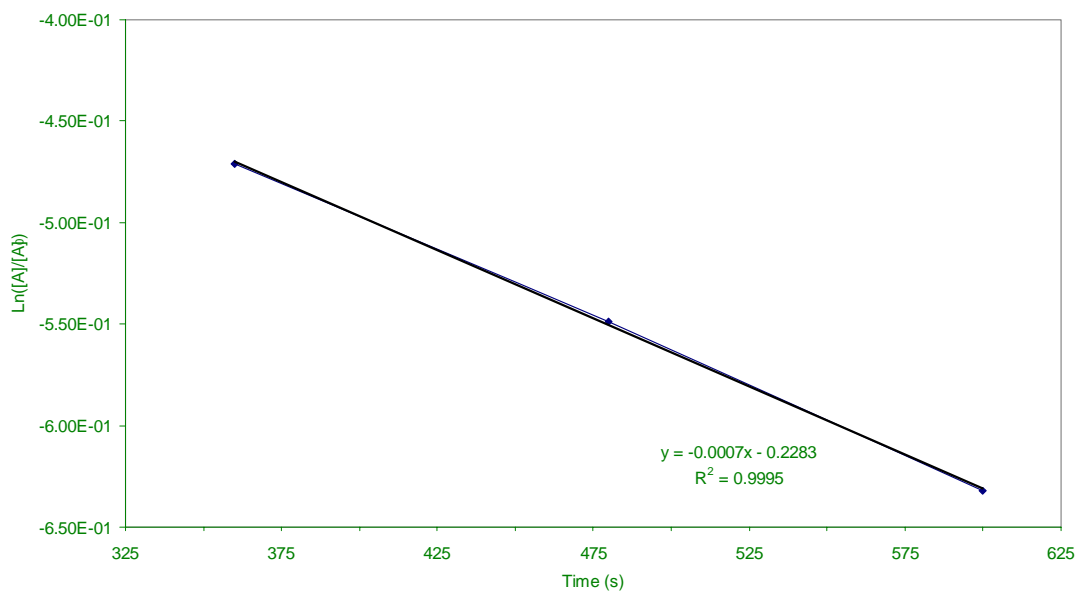


**Figure E 7:** Determination of the first order rate constant in relation to  $N,N'$ -bis( $\sigma$ -methoxyphenyl)thiuram disulfide concentration data (the letter A represents the accelerator in the above figure)

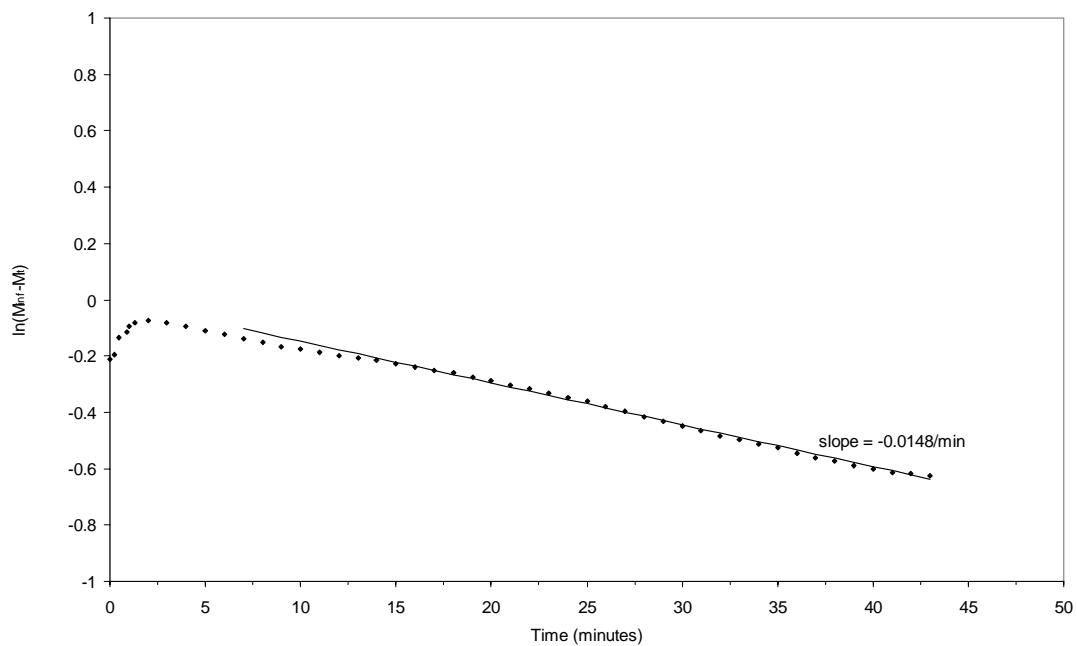


Figure E 8: Determination of the Coran rate constant ( $k_2$ ) constant from the rheometer data derived from the cure of  $N,N'$ -Bis( $\sigma$ -methoxyphenyl)thiuram disulfide/ $S_8$ /IR system

# Appendix F

## N,N'-Bis(4-sec-butylphenyl)thiuram disulfide

---

### List of figures

Figure F 1: $^1\text{H}$ -NMR for N,N'-Bis(4-sec-butylphenyl)thiuram disulfide in $\text{CDCl}_3$ .....	233
Figure F 2: $^{13}\text{C}$ -NMR for N,N'-Bis(4-sec-butylphenyl)thiuram disulfide in $\text{CDCl}_3$ .....	234
Figure F 3: IR spectrum for N,N'-Bis(4-sec-butylphenyl)thiuram disulfide in $\text{CHCl}_3$ .....	235
Figure F 4: Determination of relative rate using the initial slope method in the N,N'-Bis(4-sec-Butylphenyl)thiuram disulfide model compound reactions in relation to the sulfur concentration data.....	236
Figure F 5: Determination of relative rate using the initial slope method in relation to the N,N'-Bis(4-sec-Butylphenyl)thiuram disulfide concentration data.....	236
Figure F 6: Determination of the first order rate constant for the N,N'-Bis(4-sec-Butylphenyl)thiuram disulfide model compound reactions in relation to sulfur concentration data.....	237
Figure F 7: Determination of the first order rate constant in relation to N,N'-Bis(4-sec-Butylphenyl)thiuram disulfide concentration data.....	237
Figure F.8: Determination of the Coran rate constant ( $k_2$ ) constant from the rheometer data derived from the cure of N,N'-Bis(4-sec-butylphenyl)thiuram disulfide/ $\text{S}_8$ /IR system.....	238

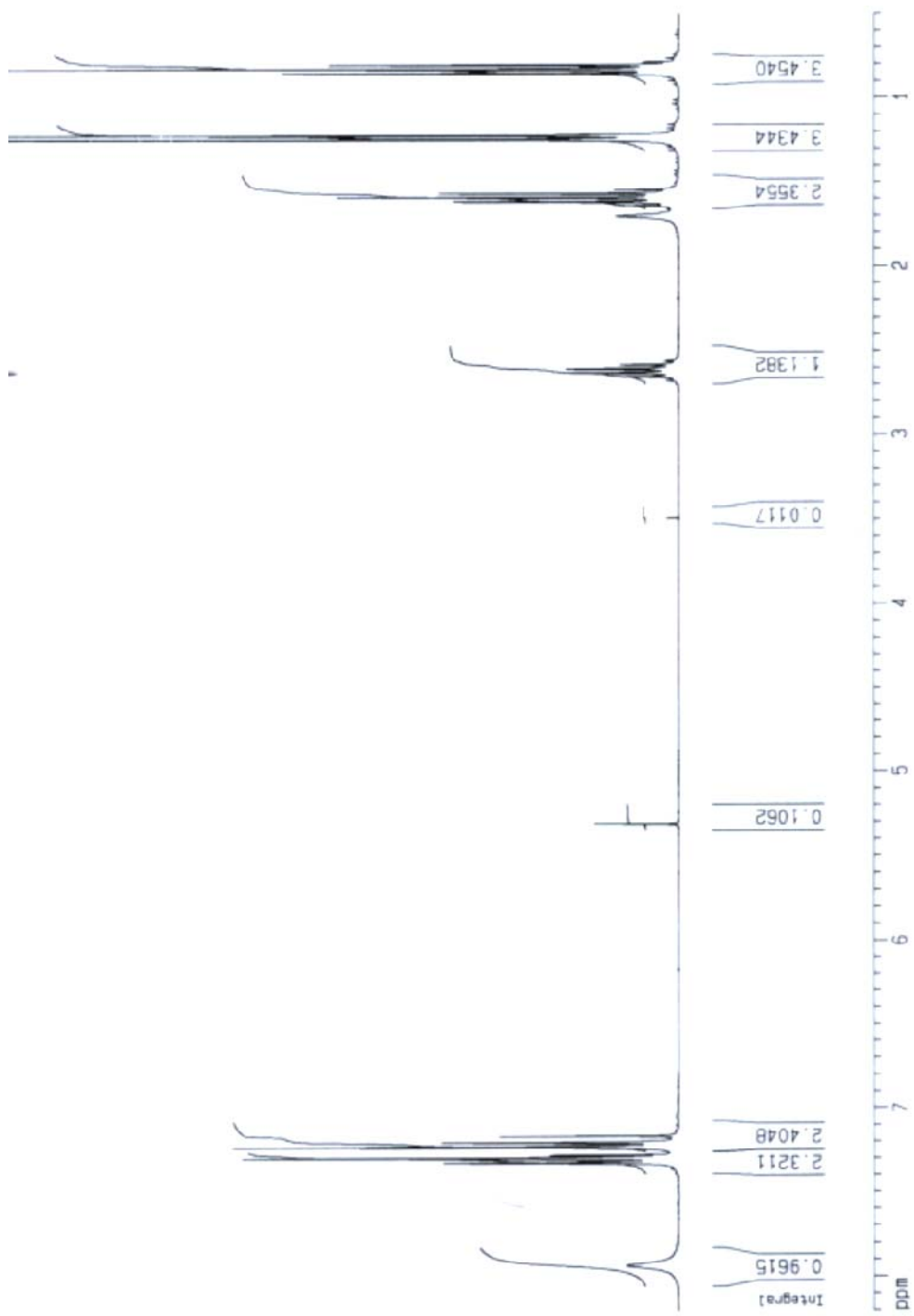


Figure F. 1: <sup>1</sup>H-NMR for N,N'-Bis(4-sec-butylphenyl)thiuram disulfide in CDCl<sub>3</sub>

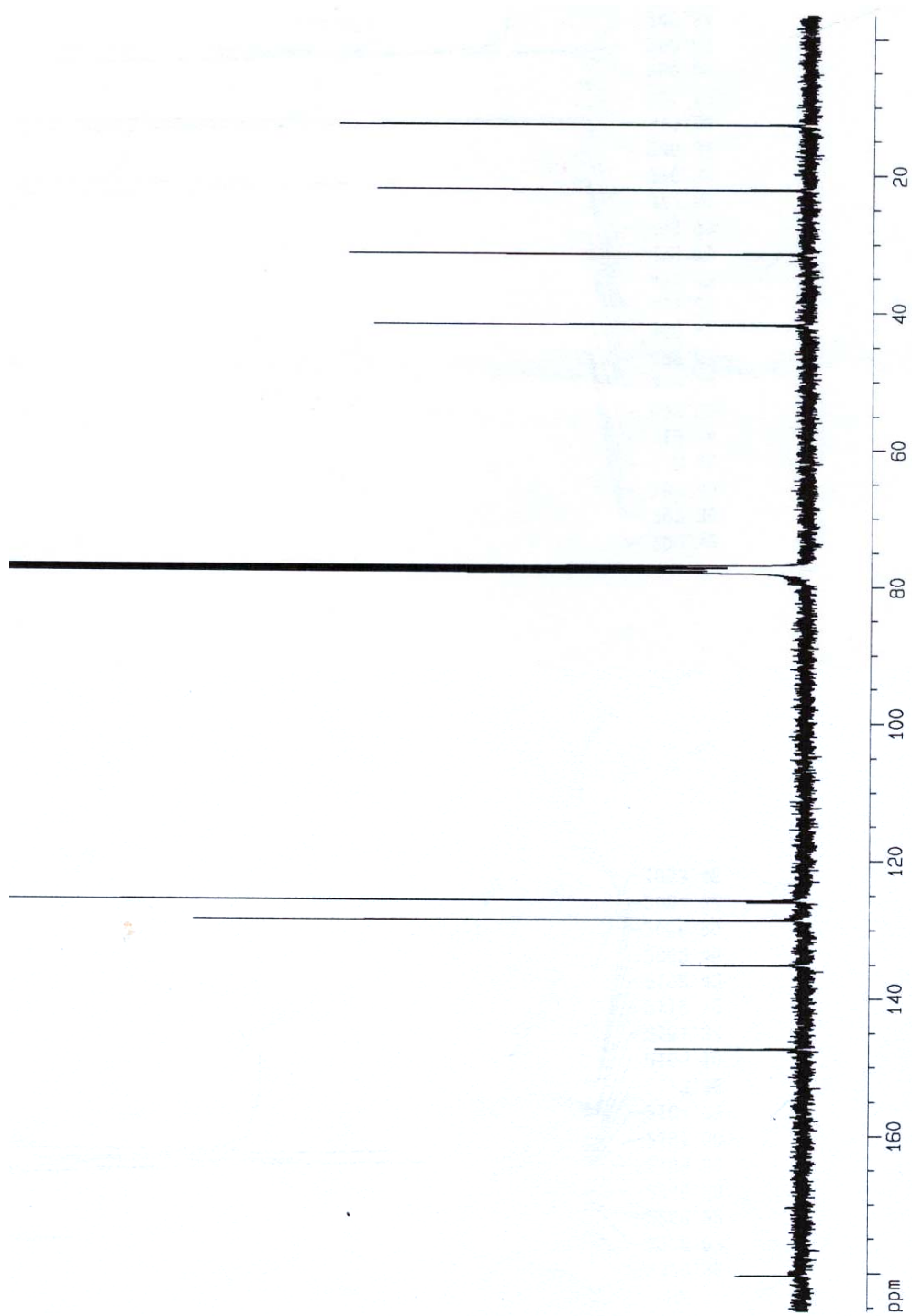


Figure F 2:  $^{13}\text{C}$ -NMR for  $\text{N,N}'\text{-Bis}(4\text{-sec-butylphenyl})\text{thiuram disulfide}$  in  $\text{CDCl}_3$

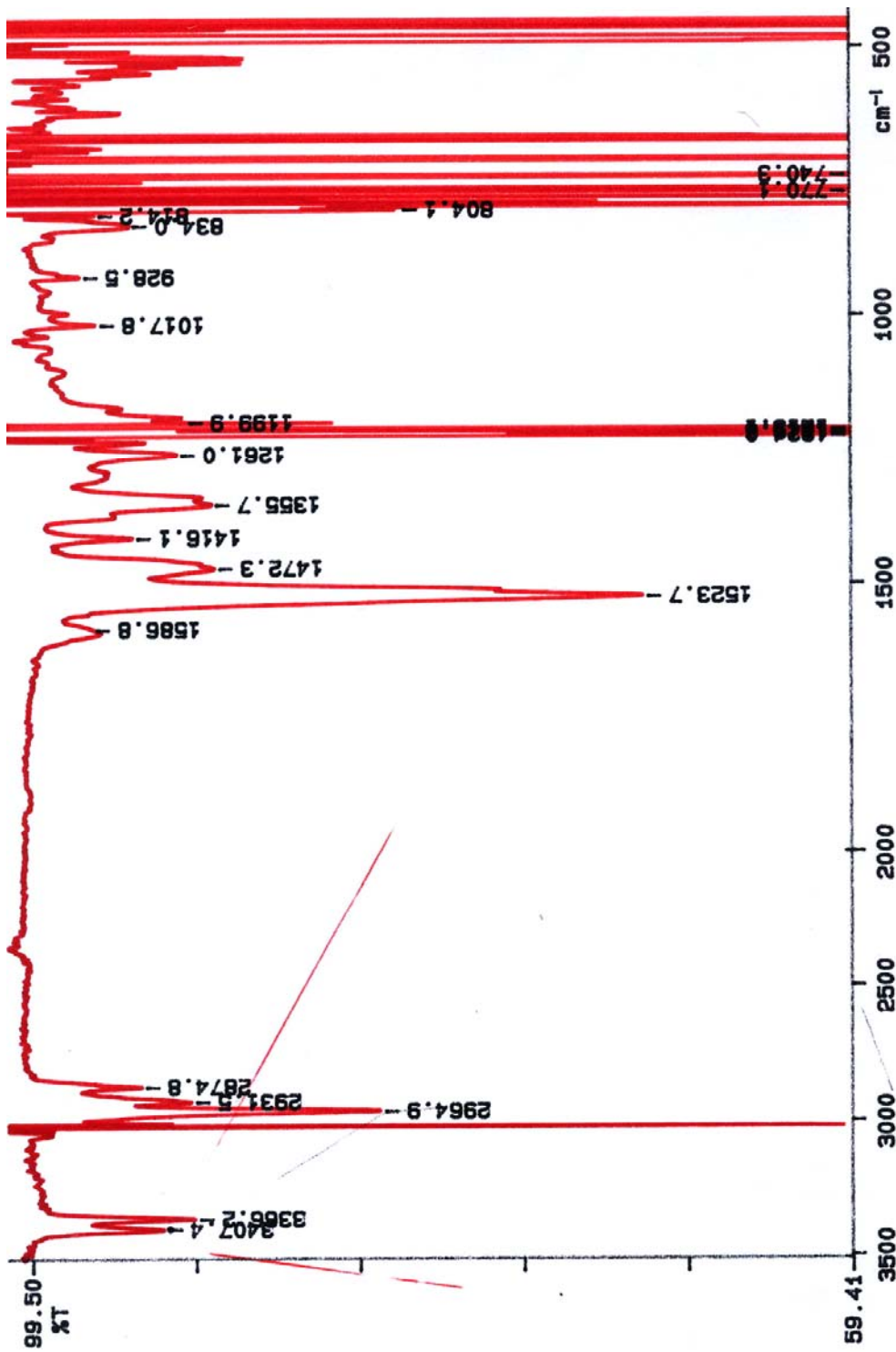


Figure F. 3: IR spectrum for N,N'-Bis(4-sec-butylphenyl)thiuram disulfide in CHCl<sub>3</sub>



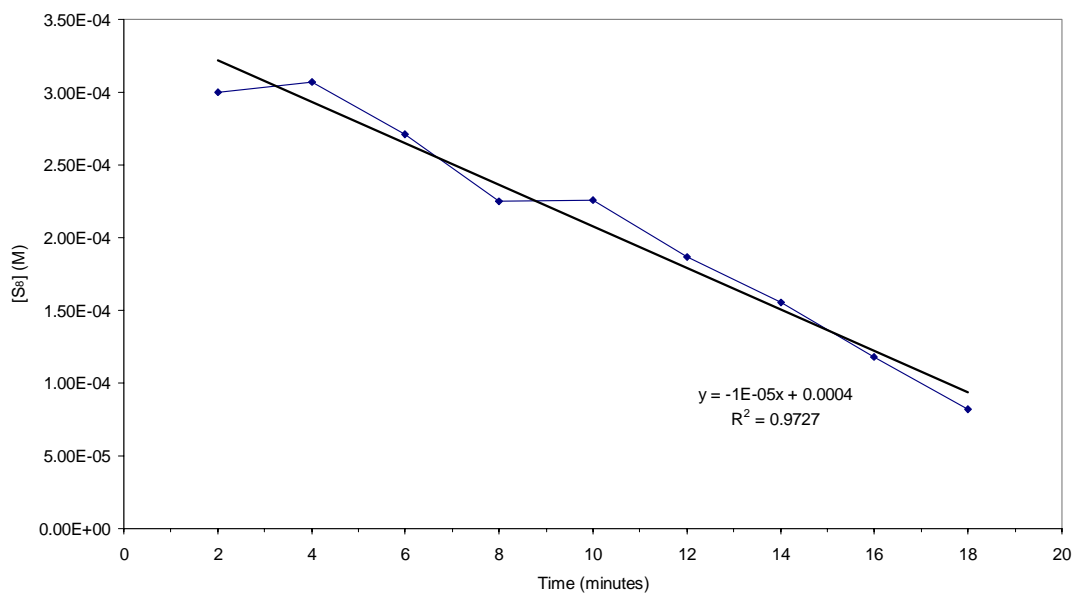


Figure F 4: Determination of relative rate using the initial slope method in the N,N'-Bis(4-sec-Butylphenyl)thiuram disulfide model compound reactions in relation to the sulfur concentration data

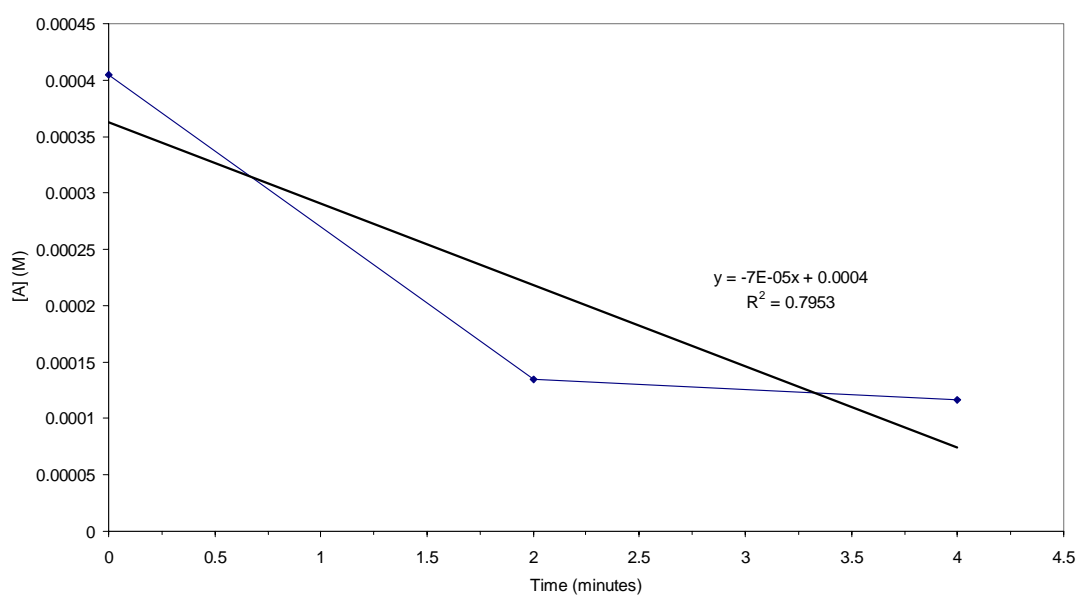
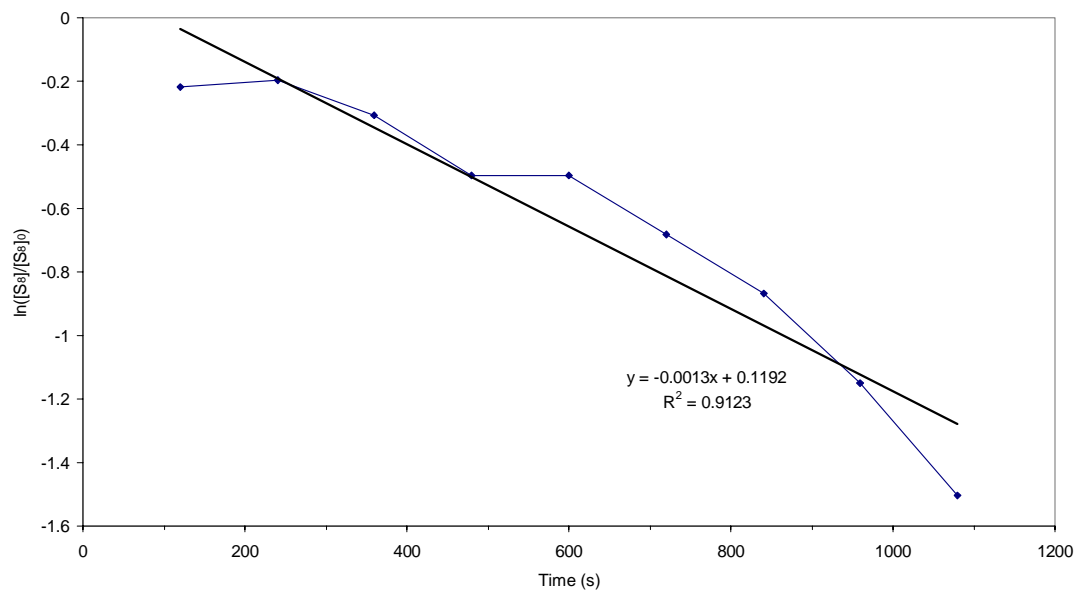
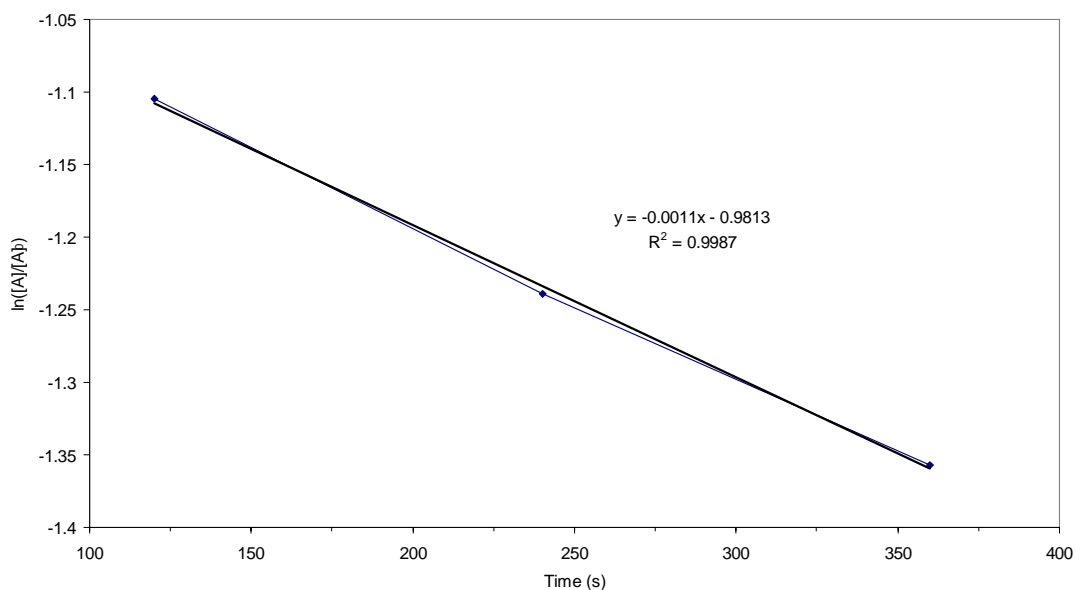


Figure F 5: Determination of relative rate using the initial slope method in relation to the N,N'-Bis(4-sec-Butylphenyl)thiuram disulfide concentration ( $[A]$ ) data



**Figure F 6:** Determination of the first order rate constant for the N,N'-Bis(4-sec-Butylphenyl)thiuram disulfide model compound reactions in relation to sulfur concentration data



**Figure F 7:** Determination of the first order rate constant in relation to N,N'-Bis(4-sec-Butylphenyl)thiuram disulfide concentration data (the accelerator is represented by the letter A in the above figure)

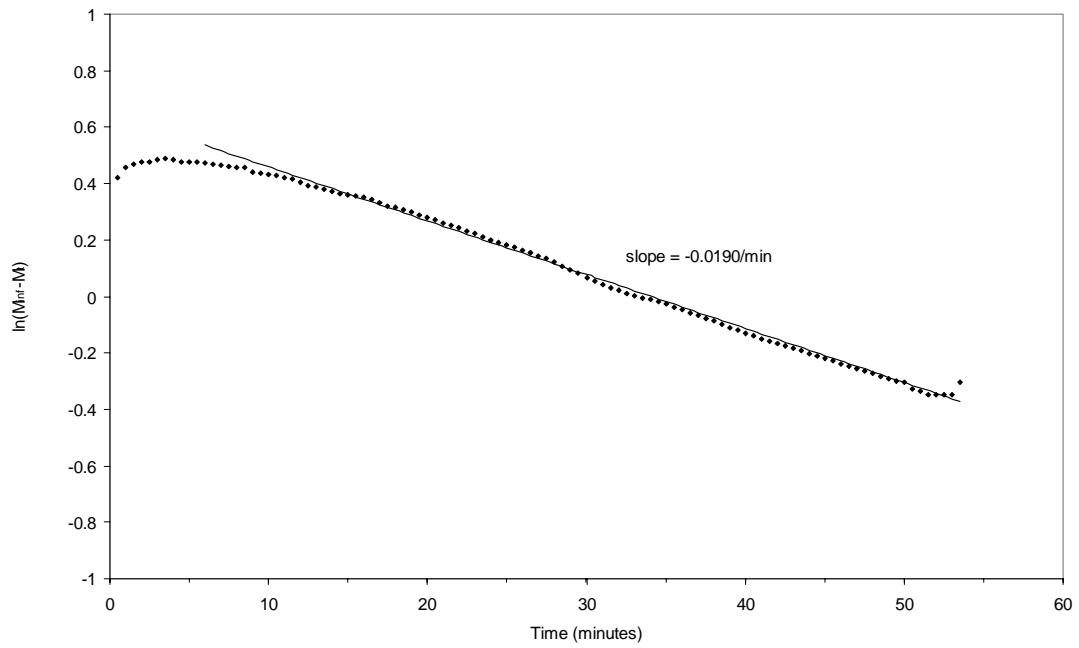


Figure F.8: Determination of the Coran rate constant ( $k_2$ ) constant from the rheometer data derived from the cure of N,N'-Bis(4-sec-butylphenyl)thiuram disulfide/S<sub>8</sub>/IR system

# Appendix G

## N,N'-dimorpholinethiuram disulfide

---

### List of figures

Figure G.1: $^1\text{H}$ -NMR spectrum for N,N'-dimorpholinethiuram disulfide.....	240
Figure G.2: $^{13}\text{C}$ -NMR spectrum for N,N'-dimorpholinethiuram disulfide.....	241
Figure G.3: IR spectrum for N,N'-dimorpholinethiuram disulfide.....	242
Figure G.4: Determination of relative rate using the initial slope method in the N,N'-dimorpholinethiuram disulfide model compound reactions in relation to the sulfur concentration data.....	243
Figure G.5: Determination of relative rate using the initial slope method in relation to the N,N'-dipmorpholinethiuram disulfide concentration data.....	243
Figure G.6: Determination of the first order rate constant for the N,N'-dimorpholinethiuram disulfide model compound reactions in relation to sulfur concentration data.....	244
Figure G.7: Determination of the first order rate constant in relation to N,N'-dimorpholinethiuram disulfide concentration data.....	244
Figure G.8: Determination of the Coran rate constant ( $k_2$ ) constant from the rheometer data derived from the cure of N,N'-dimorpholinethiuram disulfide/ $\text{S}_8$ /IR system.....	245

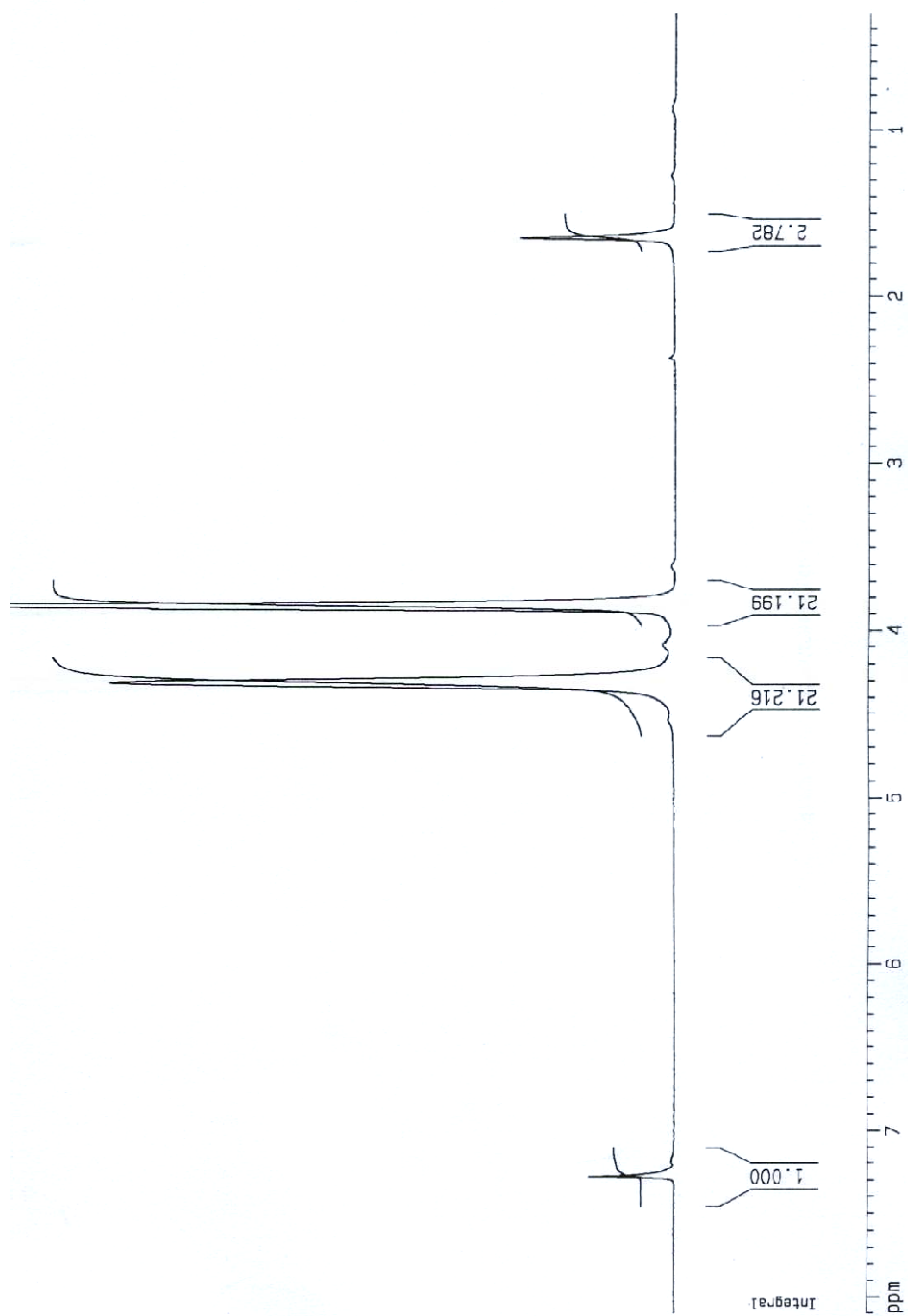


Figure G.1:  $^1\text{H-NMR}$  spectrum for  $\text{N,N}'\text{-dimorpholinethiuram disulfide}$

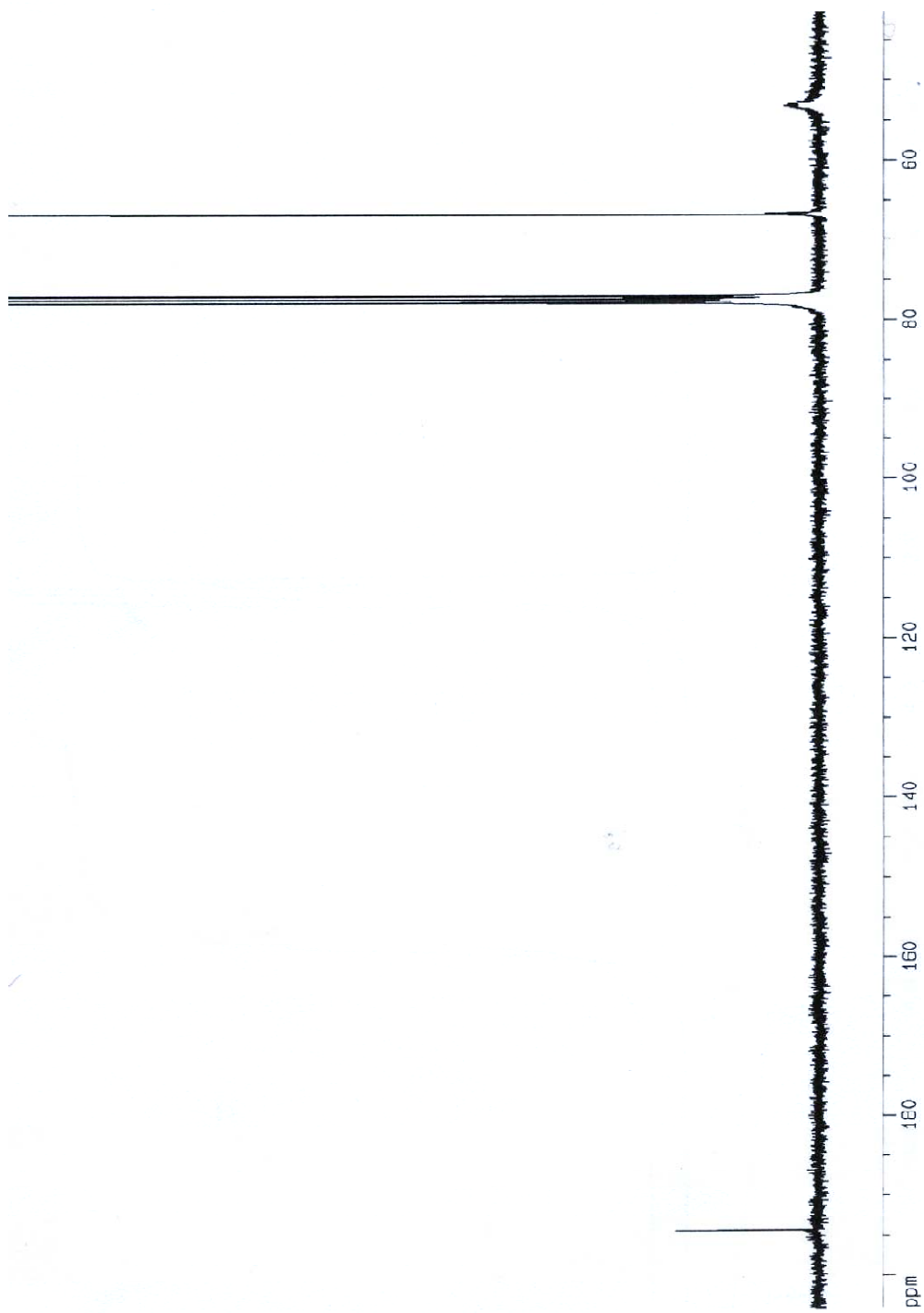


Figure G.2: <sup>13</sup>C-NMR spectrum for N,N'-dimorpholinethiuram disulfide

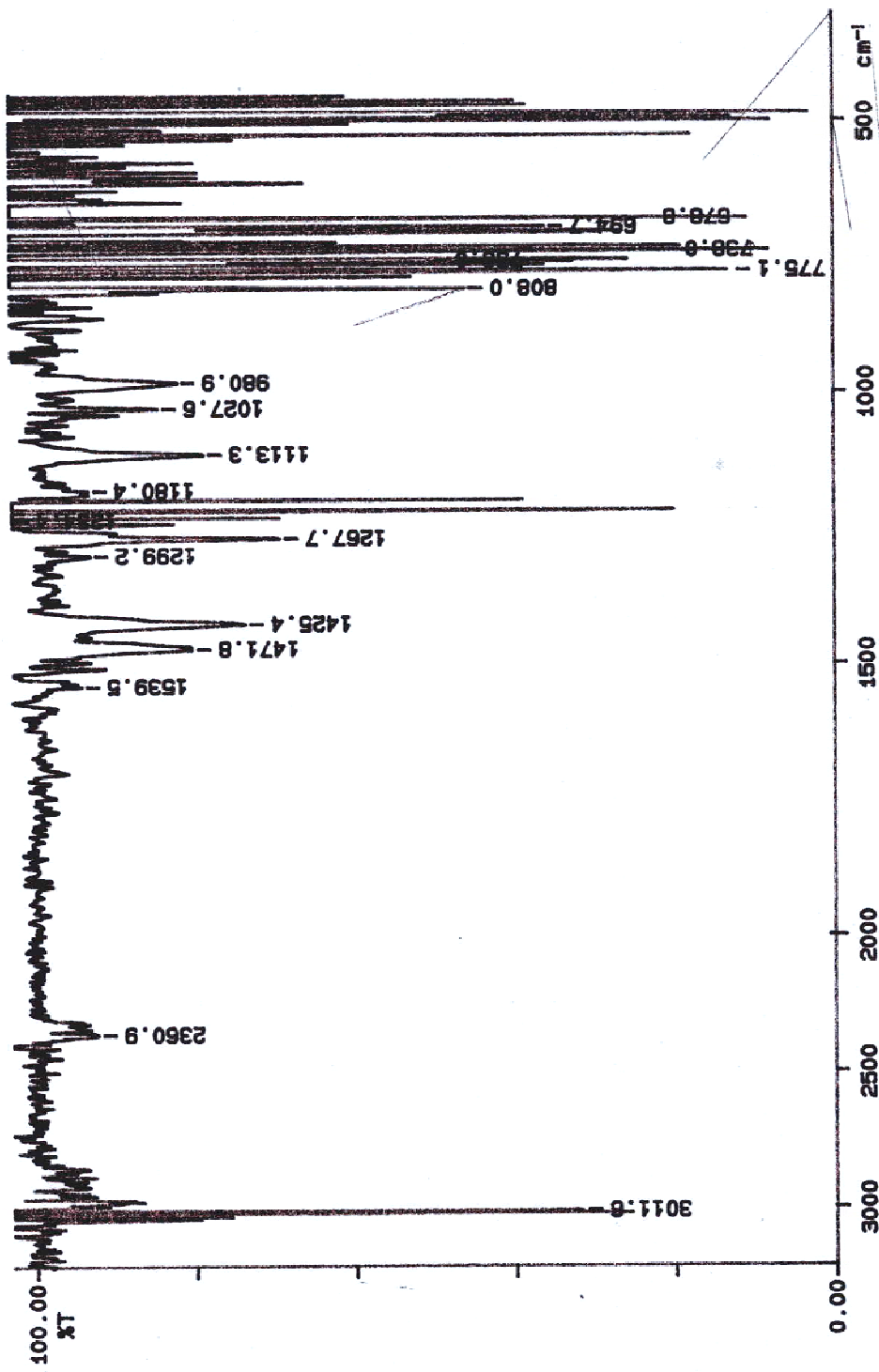
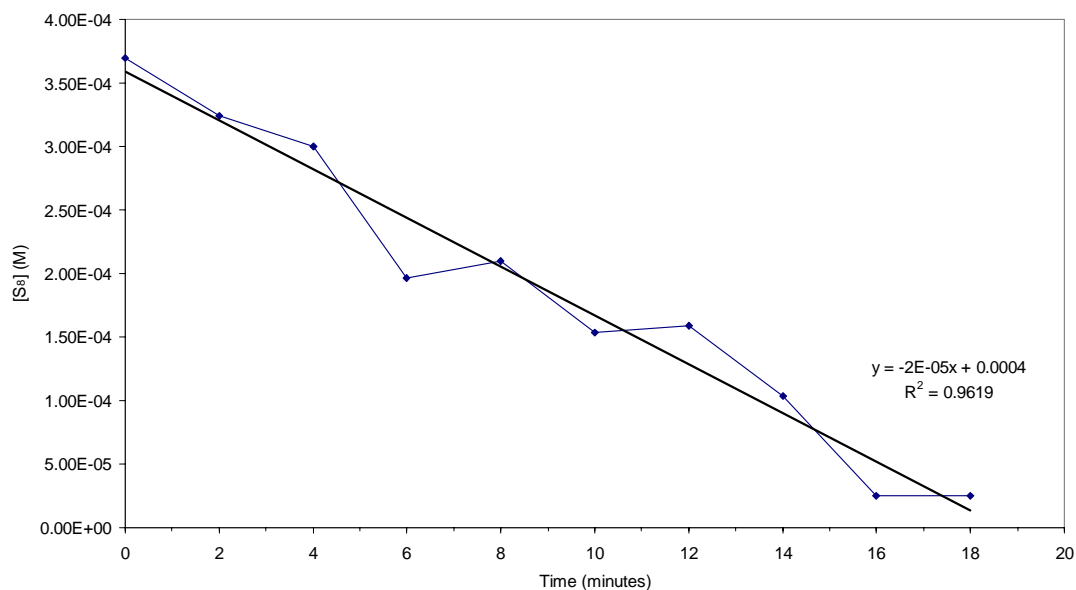
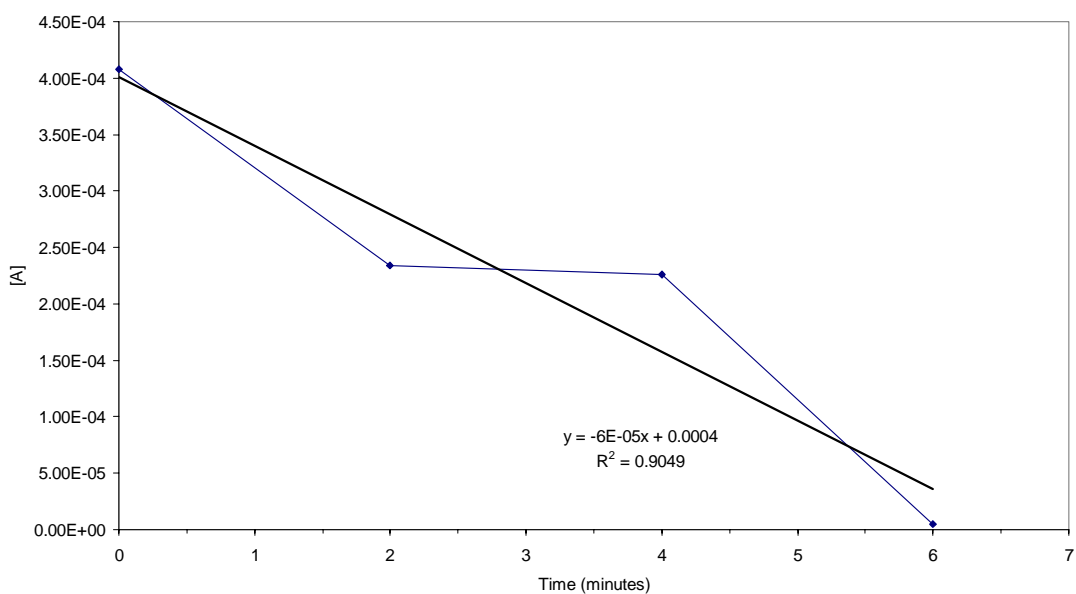


Figure G.3: IR spectrum for N,N'-dimorpholinethiuram disulfide



**Figure G.4:** Determination of relative rate using the initial slope method in the N,N'-dimorpholinethiuram disulfide model compound reactions in relation to the sulfur concentration data



**Figure G.5:** Determination of relative rate using the initial slope method in relation to the N,N'-dipmorpholinethiuram disulfide concentration ([A]) data



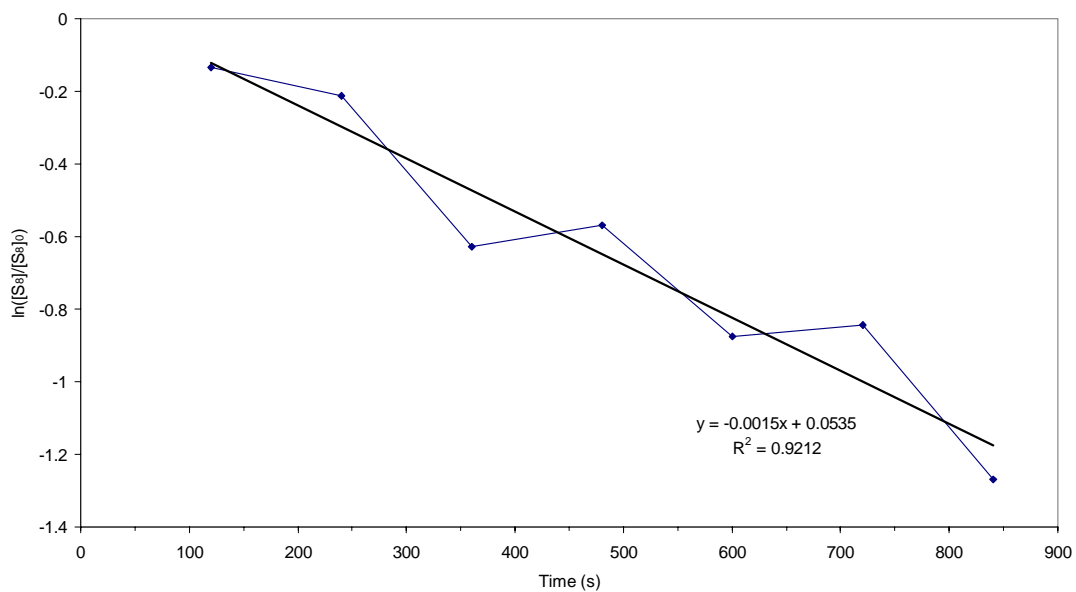


**Figure G.6:** Determination of the first order rate constant for the N,N'-dimorpholinethiuram disulfide model compound reactions in relation to sulfur concentration data

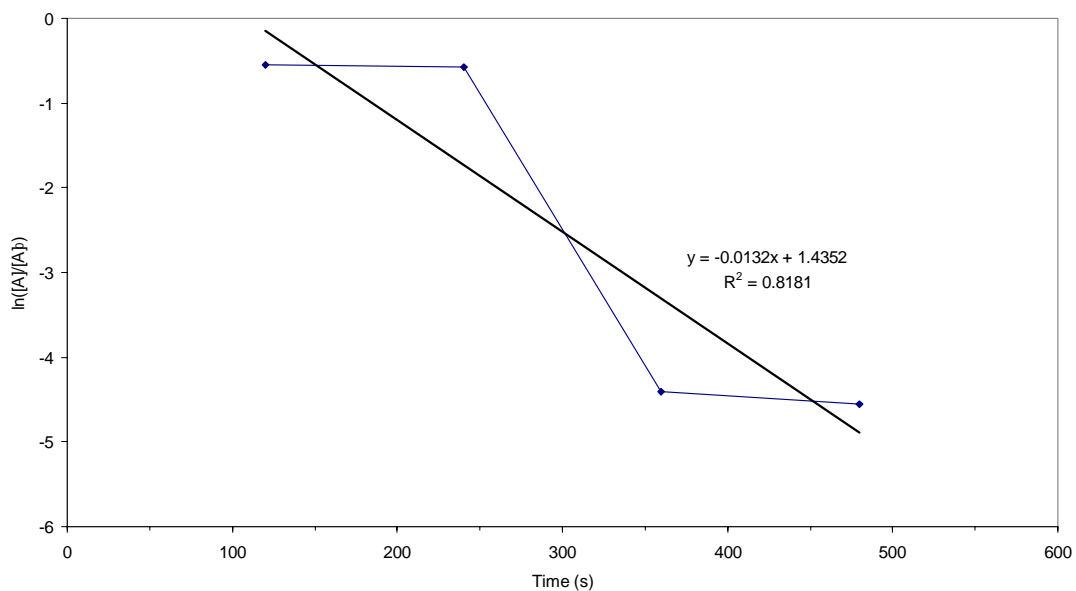


**Figure G.7:** Determination of the first order rate constant in relation to N,N'-dimorpholinethiuram disulfide concentration data (accelerator represented by the letter A)

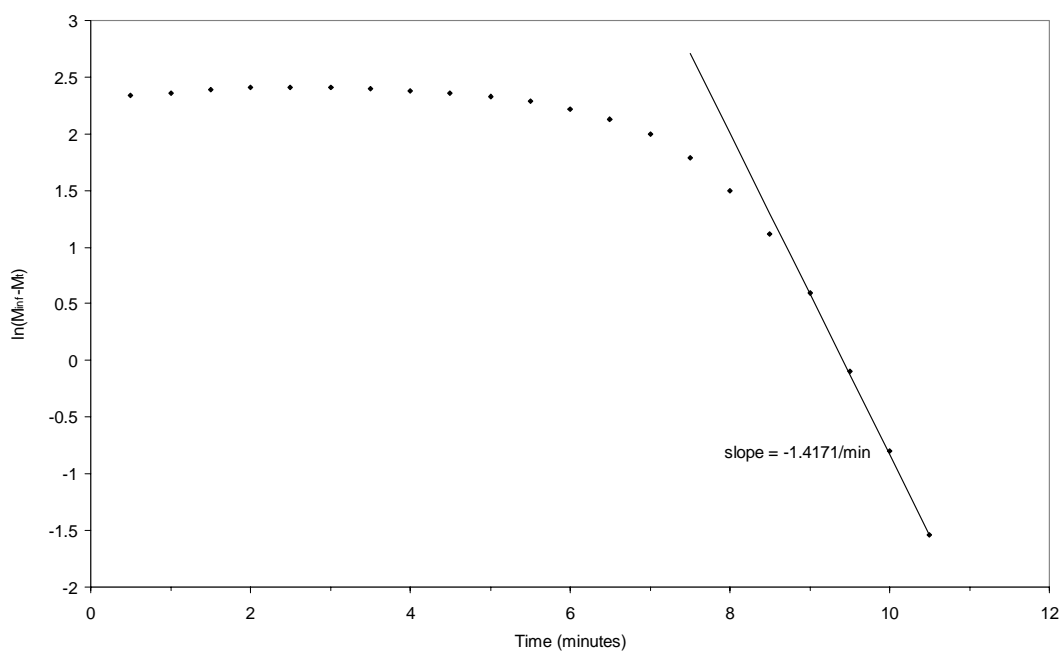


Figure G.8: Determination of the Coran rate constant ( $k_2$ ) constant from the rheometer data derived from the cure of N,N'-dimorpholinethiuram disulfide/S<sub>8</sub>/IR system